DOCTOR OF PHILOSOPHY

Identification and characterisation of novel cancer testis antigens in human cancer cells

Alsiwiehri, Naif

Award date:
2017

Awarding institution:
Bangor University

Identification and characterisation of novel cancer testis antigens in human cancer cells

Naif O. Alsiwiehri

PhD Thesis

2017

NWCRFI

School of Biological Sciences

Bangor University

Abstract

Carcinogenesis is a multi-step process which involves genomic instability and abnormal cellular growth over long period of time which eventually develop tumour. Cancer testis antigens consistently reported in many types of cancer which suggest its oncogenic role. But, it's functional role in cancer still unknown and need further investigation. Also, cancer testis antigens might be used as potential targets for cancer immunotherapy due to their main presence in normal testis cells and abnormally exist in several types of human cancer. Their aberrant expression in cancer makes them useful to target human malignancies by immunotherapy.

TEX19 one of the novel CT gene was identified in this study. *TEX19* show interesting expression pattern due to its confined in normal testis and expressed in many cancer tissues. This expression may indicate the oncogenic activity of *TEX19* gene in somatic tissue. Thus, the possible approach to use this gene as target for cancer immunotherapy and cancer prognosis and diagnosis.

In addition, *TEX19* might play a role in stemness state, this was observed in *TEX19* depleted cells, the stem cell markers genes such as *OCT$*, *NANOG*, *SOX2* were affected after the knockdown of *TEX19*. However, Tex19 was not affected after differentiating NT-2 cancer cells using Retinoic acid and HMBA.

We also studied the relation between *TEX19* and transposable genetic elements by knockdown *TEX19* in NT-2 and A2780 cancer cells. The qRT-PCR results show that human *ERVK* family gene expression was affected by *TEX19* depletion.

Moreover, our RNA sequencing data of *TEX19* depleted sample and qRT-PCR analysis reveal the influence of *TEX19* depletion on some differentially expressed genes. Interestingly, these genes were upregulated and down regulated after the depletion of *TEX19* in four types of human cancer cell lines.

Acknowledgment

This work undergoes in NWCRFI at School of Biological Sciences of Bangor University, and funded by Taif University, MOHE of Saudi Arabia.

My deep and sincere thanks to my supervisor Dr Ramsay MacFarlane for his help, continuous support and patient. This work couldn't be achieved without his help, guidance and enriched knowledge.

My thanks to all staff and colleagues within our group, for their help and support, thanks to Dr Khaled Alzeer for teaching me some techniques and methods in the laboratory. I would like to thank Mr Vicente Planells Palop for his help in RNA sequencing work. My thanks to Dr. Julia Feichtinger for her help in bioinformatics part of the work. My thanks to Dr Edgar Hartsuiker for helping me in DSB assay. Thanks to Dr Faisal Alzahrani for helping me with IPSCs.

I would like to thank the lovely people of Felinheli for the good time and lovely memories that I will carry it back home with me. Thank to our locals in Tafarn Fic. and Plas Hotel Dinorwic.

My great thanks and respect to my godfather Mr KennethWalker for all good times help and support.

Finally, I would like to thank my parents for their influence on my education and career since I was young. Special thanks to my family particularly my wife Ejlal for her patient, support and devotion through the last years of my study. In addition, to my little angels Judy, Wajed, Hala and Yusur you are the one keep me going.

Contents

Abbreviation list

AD	Alzheimer's disease
ALT	Alternative lengthening of telomeres
AML	Acute Myeloid Leukemia
APC	Antigen presenting cells
APL	Acute promyelocytic leukemia
ATCC	American Type Culture Collection
BBB	Blood brain barrier
BET	Bromodomain and extra-terminal
BTB	Blood-testis barrier
CML	Chronic myeloid leukemia
CT	Cancer Testis
CTA	Cancer-testis antigens
CTL	Cytotoxic T-lymphocytes
DF	Degrees of freedom
DSB	Double strand breaks
EC	Embryonal carcinoma
ECACC	European Collection of Cell Cultures
EG	Embryonic germ
ELDA	Extreme limiting dilution analysis
ESC	Embryonic Stem Cells
EST	Expression sequence tag
FBS	Foetal bovine serum
GCC	Germ cell cancers
HLA	Human leukocytes antigens
HPV	Human papilloma virus
HR	Homologous Recombination
IHCC	Intra-hepatic Cholagio-carcinoma

LE	Lateral elements
LFT	Liver function tests
LINE	Long interspersed transposable elements
LTR	Long terminal repeat
MBD	Methyl-CpG-binding domain
MLL	Mixed Lineage Leukemia
MPSS	Massively parallel signature sequencing
NRT	No reverse transcription
NTC	No template control
NVU	Neurovascular unit
PBS	Phosphate buffer saline
PCR	Polymerase chain reaction
PGC	Primordial germ cells
RA	Retinoic acid
RI	Refractive index
SAGE	Serial analysis of gene expression
SC	Synaptonemal complex
SINE	Short interspersed transposable elements
SNP	Single nucleotide polymorphisms
TE	Transposable elements
TGE	Transposable genetic elements
TSG	Tumour suppressor genes

1. Introduction

1.1 Human malignancies

Cancer is a disease characterized by abnormal and uncontrolled cell divisions leading to invasion of adjacent tissues and it is capable of metastasis to distant organs. Cancer is considered as one of the leading causes of death in many countries. In UK, approximately 162,000 people died of cancer in 2012 (Cancer Research UK, 2014). These facts emphasize the importance of understanding cancer genetics to find new and better methods for cancer diagnosis and treatment.

1.1.1 Carcinogenesis

Cancer is a disease where normal cells undergo a malignant transformation, leading to uncontrolled and abnormal cell division, which can result in invasion of the adjacent tissues. In addition, aggressive malignant tumours can undergo metastasis, in which, cancerous cells spread from the primary site, and infiltrate different sites of the body through haematogenous or lymphatic routes (Pitot, 2002).

The process of cancer spreading is referred to as carcinogenesis. It is a multi-step process in which a normal cell undertakes an abnormal cellular division and growth, achieving various levels of neoplastic phenotype. Cancerous cells are characterised by genomic instability and abnormal balance of chromosomes. The phenotypic features of the multi-step carcinogenesis include dysplasia, hyperplasia, anaplasia, abnormal cellular morphology, immortality, abnormal metabolism, significant growth, invasiveness, metastasis and drug resistance (Pitot, 2002).

In rodents, the kinetics of carcinogenesis is a slow and multi-step process in which, after exposure to an initiated dose of carcinogen, it takes several months for the normal cell to transform into a cancer cell and to develop cancerous phenotypes (Tani *et al*., 2016). However, most human carcinogenesis takes a lot more time, as much as decades are required to develop cancer after several occupational and accidental exposures to carcinogens.

1.1.2 Hallmarks of Cancer

The origin and progression of cancer is dependent on the cellular machinery and the genetic programming inside the cells. Out of 23,000 human genes present, approximately 3000-5000 genes encode for the production of proteins which are almost always disrupted in cancer, or become part of the biochemical pathway deregulated by cancer (IARC, 1999). The modified or dysfunctional gene in case of cancers may lead to a number of outcomes: increase the

production of its protein or decrease it, produce abnormal protein incapable of carrying out its function or completely eliminate it from the cell. Mutations of such types are most common in the genes responsible for modulating the cell growth signal and they are modified in such a way that they remain activated inside the cell and hence promote cell proliferation at all times. They are also referred to as oncogenes and the most common example of an oncogene is the mutated KRAS gene which is found to be present in colorectal cancers, lung adenocarcinomas (IARC, 1999). However, cancer development may also rely on the permanent inactivation of a gene inside the cell, as is the case with the TP53 gene. It is responsible for the production of the protein which modulates and represses inappropriate cell growth or stops cell proliferation. After loss-of-function mutation in the gene, the protein product formed is unable to carry out its function and hence cancer growth is unregulated. These type of genes are referred to as tumour suppressor genes, as their normal protein product would have suppressed the growth of tumour (IARC, 1999).

These disruptions in the genetic programming of the cells may contribute to the origin and progression of cancer from either one cell or from a small number of cells. In order to become cancerous in nature and spread to the later part of the cell, tissue, organ or body, the cell has to undergo genetic, phenotypic as well as biochemical changes. The origin is the series of changes in the oncogenes and the tumour suppressor genes that allow the cell to proliferate and form a cluster of cancerous cells (tumour). In the context where this tumour remains undisturbed and is not attacked by the body's immune system, it continues to grow and gather more and more genetic modifications. Eventually the most aggressive cancerous cells are able to take over the weaker cells part of the tumour and the tumour becomes malignant and ready to spread to other parts of the body. Because of the numerous and unpredictable genetic modifications in the cancer, it is very difficult to treat. Even if a drug is capable of clearing out the majority of the tumour cells, a few cancerous left over cells can relapse into a more aggressive form of the cancer, worse than before. Therefore, it is a progressive disease which starts as a small and inconspicuous ball of cells and after some period of time, turns into a malignant cancer. However, if it is detected when it is still in the inconspicuous phase of development, it may be easily removed and would not contribute to the development of a full-grown cancer (Petrovic, 2016).

The context of cancer development, however, is more complicated than as stated. Genetic modifications and conducive cellular environment are not the only precursors responsible for the development of cancer. Cancers can develop while hinging onto the cellular and

biochemical landscape established by other diseases in order to spread to other susceptible tissues or organs in the body. These diseases are often also referred to as precursor diseases of cancer and may include chronic inflammatory diseases such as liver cirrhosis, intestinal metaplasia etc. Using lymphatic and blood vessels, the cancerous cells can travel to neighbouring tissues to perturb their biochemical activities and transfer their malignancies through possible genetic modifications. The main reason that tumours can keep growing and facilitate their growth is tumour angiogenesis. They are capable of synthesizing new blood vessels to ensure constant supply of oxygen and essential nutrients to all cells in the tumour (Petrovic, 2016).

The mutagenesis of the tumours or spread of the tumour creates complications for the oncologists and the cancer pathologists in the identification and possible cure of cancer. The two mechanisms discussed above represent the hallmarks of cancer. These are 6 basic mechanisms which the cell must acquire changes within before becoming cancerous. As we saw earlier how sustained angiogenesis, limitless replicative potential and tissue invasion and metastasis helps in the origination and progression of cancer, the remaining mechanisms pertain to how cancerous cells evade apoptosis, become self-sufficient in growth signals and gather insensitivity to anti-growth signals (Hanahan and Weinberg, 2011).

1.1.3 Epigenetic origin of cancer

The term ‘epigenetic’ is used to describe the heritable alteration of gene expression and the structure of chromatin that does not affect the DNA sequence directly. In normal eukaryotic cells, modifications of the chromatin take place mainly by at least three epigenetic mechanisms of DNA methylation, histone modifications and silencing of non-coding RNAs (Bernstein *et al.* 2007).

In modern disease pathological studies, genetics and epigenetics both play a crucial part in determining the course of disease development. At cellular level, both epigenetics and genetics collaborate to manoeuvre transcriptional activities taking place and decide which genes are expressed and which stay in the repressed state. These epigenetic modifications represent stable changes of the epigenome that are inherited through phases of mitosis and do not include mutations of the DNA itself. Epigenetics has been, more than often, referred to being the study of these stable alterations of gene expression potential that is the result of development and cell proliferation and be outside conventional genetics (Shah and Allergrucci, 2013). These changes are not essentially inherited at the stage of embryogenesis

and can be present in mature humans by a random change or by the environmental stimuli. They can be incorporated as the posttranslational modifications of the DNA or the proteins associated with it. Therefore, the epigenetic regulation or modifications can arise through covalent modifications of the DNA (methylation, ubiquitylation, acetylation etc) and histone molecules, nucleosome rearrangement or positioning with respect to the DNA. These epigenetic changes have been found to be recurrent in tumours and participate in gene silencing. Therefore, studying the mechanism by which the three aspects of DNA methylation, Histone modifications and nucleosome remodeling bring about modifications in the gene expression profile of diseased individuals can give a head start at determining the sites that need to be regulated for controlling the progress of diseased states. Furthermore, the epigenetic modifications can also be assessed for their therapeutic potential against cancer development and progression since they have been recognized as the emerging hallmarks of cancer (Shah and Allergrucci, 2013).

1.1.3.1 DNA methylation:

In eukaryotes, gene expression homeostasis is regulated by DNA methylation and it is the addition of a methyl group covalently to the 5^{th} position of the cytosine ring of CpG dinucleotides and is the primary epigenetic mechanism for promoting or repressing expression of genes during the stages of development and embryogenesis. Therefore, it involves modifications at the 5' of cytosine within CpG (Wu and Zhang, 2010). CpG dinucleotides, are not evenly spread across the human genome and are found in high concentrations near the regions of high repetitive sequences, including centromeric repeats and retrotransposon elements often referred to as 'CpG islands'. Most of these sites have been reported to be methylated, however, majority of the CpG islands remain unmethylated during the stages of development and differentiation. In cases of long-term transcriptional inactivation, X-chromosome inactivation and imprinted genes, the promoters of CpG islands become methylated naturally at the time of development. Tissue-specific methylation has also been reported to occur, in cases of developmentally important genes, in a variety of somatic tissues (Wu and Zhang, 2010). In sharp contrast, the repetitive genomic sequences present across the human genome are found to be highly methylated and therefore, prevent chromosomal instabilities by silencing the non-coding DNA and transposable elements. DNA global hypomethylation and promoter-specific hypermethylation are known to be key role-players in cancer epigenome that lead to genomic instability and they largely target these repetitive elements along with intergenic regions and gene bodies. This loss of DNA methylation is followed by *de novo* hypermethylation of important tumour suppressor genes

(TSG) promoters and the genes that are localized in CpG islands to initiate permanent gene silencing. Of these two epigenetic mechanism, the hypermethylation of promoters in CpG islands are better characterized with respect to cancer development. The human genome contains approximately 29,000 CpG sequences and approximately 50–60% of gene promoters sites are located within CpG islands (Pradhan *et al.*, 2009). The research study by Frigola and colleagues in colorectal cancer showed how the entire chromosome band was remodeled epigenetically to cause gene repression and promote the growth of the cancer. Therefore, while we acknowledge the incidence of promoter-specific and cancer-specific DNA hypermethylations, we should also remain open to the fact that in more than one incidences, whole gene neighborhoods or entire chromosome bands have been affected. Another hallmark of cancer besides disruption of DNA methylation patterns in the recurring global loss of Histone H4 Lysine 16 (H4K16) acetylation and Histone H4 Lysine 20 (H4K20) trimethylation patterns along with increased expression of BMI1 and EZH2. BMI1 has been characterized as a component of Polycomb Repressive Complex 1 and EZH2 is part of Polycomb Repressive Complex 2 (PRC2) and both are involved in silencing gene expression (Sharma *et al*., 2010). These type of modifications have been credited with bearing high prognostic value in regards to cancer. Furthermore, in a series of recent studies it has been shown that the targets of or genes associated with PRC are likely to become methylated in cancer in Embryonic Stem Cells (ESC) and thereby linking other epigenetic silencing mechanism to bring about collective genome repression and progression of cancer (Ohm et al., 2007; Schlesinger et al., 2007; Widschwendter et al., 2007). The proteins responsible for causing these epigenetic modifications leading to cancer are those enzymes that catalyze DNA methylation, bind methylated DNA at promoters and cause gene silencing, catalyze histone acetylation, deacetylation, methylation and demethylation and are found to be targets of tumor initiation and progression pathways. These proteins help in identification of epigenetic genes that are being modified in the course of specific cancers and whether they are being altered through somatic or germ-line mutations. Furthermore, a detailed literature review was conducted to make sure that these epigenetic genes belonged to the families of DNMTs, MBD (methyl-CpG-binding domain), HAT (histone acetyltransferases), HDAC (histone deacetyltransferases), HMT (histone methyltransferases) and histone demethylases (Miremadi et al., 2007). These specific families were essentially chosen because they mediate epigenetic modifications in the genome and we can study each family in detail and elaborate on the different mutations they go through in different cancers.

DNA methyltransferases:

DNA methylation is achieved by DNA methyltransferases enzyme (DNMTs) which causes inactivation of the gene (Rodriguez-Paredes and Esteller, 2011). DNMTs enzymes are categorized into three main types, the first one is DNMT1, plays a role during the DNA methylation after DNA replication. The other two types of enzymes are DNMT3A and DNMT3B, which are highly expressed during embryogenesis and these enzymes are involved in DNA methylation directly on unmethylated CpGs (Burge *et al.*, 2009). Another family member of DNA methylation is known as DNMT-3L which lacks the intrinsic methyltransferase enzyme activity, but plays an important role in transposable elements methylation through interaction with DNMT3A and DNMT3B (Fuks *et al*., 2002). This process occurs in repetitive genomic regions such as satellite DNA and transposable genetic elements (TGE) which include long interspersed transposable elements (LINEs) and short interspersed transposable elements (SINEs), and this process is crucial for the maintainence of genomic integrity (Robertson, 2005).

CpG dinuleotides are covalently modified through DNMTs in order to suppress transposons ad repetitive DNA sequences to confer genomic stability (Yoder et al., 1997). These dinucleotides are enriched in stretches of DNA that range from 0.5 to several kilobases, CpG islands, and are often present along with promoter regions. The methylation laid out during early embryogenesis via DNMT1, DNMT3A and DNMT3B at these CpG islands controls the normal development of an organism. Targeted deletions of these genes in mouse models resulted in embryonic lethality and disrupted development. In human tumours, these DNMTs have been found to present moderate-high levels, representing their overexpression. DNMT1 has been reported for causing Fos-induced transformation of mouse fibroblast cells and maintaining repression of tumor-suppressor loci in human cancer cell lines, whereas, DNMT3A has also been reported in pathways mediating cancer cell's survival (Beaulieu et al., 2002; Robert et al., 2003). Somatic mutations in DNMT1 have been repeatedly reported in 2 types of colorectal cancers out of a total of 29 suggesting that the inactivation or repression of DNMT1 is involved in carcinogenesis. Due to a decrease in aberrant methylation of TSG, mice deficient in DNMT1 show a tumor resistant phenotype, whereas, reduced expression of DNMT1 result in a global DNA methylation level that is reflective of genomic instability. DNMT1-deficient mice were also reported to have developed sarcomas at an earlier age and the mice which were carrying hypomorphic and a

null allele for DNMT1 developed aggressive T cell lymphomas, displaying a high frequency of genomic rearrangements. Lastly, ESC deficient for DNMT1 displayed increased frequency of chromosomal rearrangements required for tumor formation.

Furthermore, DNMT3B germ-line mutations reveal that in cases where it is non-functional, we observe immunodeficiency, centromeric instability and facial abnormalities (Hansen et al., 1999; Xu et al., 1999). Mouse embryo fibroblasts which are deficient for DNMT3B also reveal resistance to being transformed by SV40 largeT and activated RAS oncogenes, meaning that epigenetic mechanisms work in collaboration with genetic mechanisms during cellular transformation (Soejima et al., 2003). Furthermore, germ-line SNPs (single nucleotide polymorphisms) in DNMT3B have been reported to be associated with breast cancer (Yamane et al., 2006), lung adenocarcinoma (Lee et al., 2005) and lung cancer (Shen et al., 2002) and all of these modifications have been found to be present in the promoter region of DNMT3B. However, the alteration in the DNA methylation levels of 6 suggested genes in CpG island (*RARβ2*, *CDH1*, *ER*, *BRCA1*, *CCND2*, *p16* and *TWIST*) were not confirmed in the study by Ceberian et al which used the biggest sample size and therefore modification of methylation at CpG island promoter is highly unlikely (Cebrian et al., 2006; Li et al., 2006).

Furthermore, gene expression's inhibition occurs directly by binding of specific transcription factors and indirectly by the involvement of methyl-CpG-binding domain (MBD) proteins. There are six members of methyl-CpG-binding proteins identified in mammals, including methylcytosine binding protein 2 (MECP2), MBD1, MBD2, MBD3, MBD4 and Kaiso (Bogdanovic and Veenstra, 2009). Their somatic as well as germline variants have been associated with multiple cancers either through their overexpression or deregulated mutations. Except for MBD4 which is involved in DNA mismatch repair, other MDB proteins are involved in transcriptional repression. Methyl-CpG-binding proteins have been reported to be associated with histone modifying enzymes to maintain the transcriptional silenced state and MBD proteins have been found to be associated with aberrantly methylated promoter regions of TSG (Nguyen et al., 2001) and DNA repair gene (MGMT) (Nakagawachi et al., 2003).

Three SNPs in MBD1 (634G>A, 501delT and Pro401Al) have been associated with the development of lung cancer (Jang et al., 2005) and the presence of these polymorphisms increases the overall risk for lung cancer and lung adenocarcinoma. MBD4's SNP has been suggested to regulate the risk of cancer. The neutral amino acid substitution has been reported

to lie in unknown functional domains of the protein, whereas, the Lys/Lys genotype has been reported in esophageal squamous cell carcinoma and subsequently increase its risk of incidence (Hao et al., 2004).

Moving on, although role of somatic changes in MBD proteins in cancer is still unclear, however, it has been shown that MBD2 binds to the aberrantly methylated promoter of TSG and represses its expression, as highlighted earlier. These TSG include p14/ARF and p16/Ink4A, which have been found to be associated with MBD2 in colon cancer lines (Magdinier and Wolffe, 2001). Since these alterations are not yet clear, they may as well be due to increased cell proliferation in these cancer cell lines. Furthermore, when the mice deficient in MBD2 were crossed to APCMin/+ background, they were found to be resistant to the development of intestinal tumours. Varying the dosage of MBD2 also was observed to resul in varying tumor resistant effects (Sansom et al., 2003). Moreover, MeCP2s overexpression and mutations have been observed in breast cancer and have been shown to be related to estrogen receptor positivity (Müller et al., 2003). However, there is evidence that MeCP2, MBD2 and MBD4 are down-regulated in cancers as shown here, however, no firm connections with cancer development for either one of them have been found as yet. MBD1 and MBD2 are present on chromosomal locus of 18q21, which is often found to be lost in cancer, however, mutation analysis of human lung and colon cancers reveal few changes in these proteins, thereby limiting their role in cancers (Bader et al., 2003).

Furthermore, DNA methylation can also be achieved by nucleosome remodeling complex (NuRD) interaction with DNA methylation binding protein MBD2, which directs the NuRD complex to methylate DNA (Bogdanovic and Veenstra, 2009; Lai and Wade, 2011). Table 1.1 shows a list of DNA methylation genes disorders in some types of human malignancies (Kanwal, and Gupta, 2012).

Table 1.1 DNA methylation gene changes in various human cancers (Kanwal, and Gupta, 2012).

DNA methyltransferase	Function	Alterations	Cancer type
DNMT 1	Maintenance of methylation, repression of transcription	Upregulation, mutation	Colorectal cancer, ovarian cancer
DNMT3a	*De novo* methylation during embryogenesis, imprint establishment, repression	Upregulation	Colorectal cancer, breast cancer, ovarian cancer, esophageal squamous cell carcinoma
DNMT3b	*De novo* methylation during embryogenesis, repeat methylation repression	Upregulation	Breast cancer, hepatocellular carcinoma, colorectal cancer,
DNMT3L	Interacts with DNMT3a &b and facilitate methylation	Upregulation	
MeCP2	Transcription repression	Upregulation, Mutation	Prostate cancer, Rett syndrome,
MBD1	Transcription repression	Upregulation, Mutation	Prostate cancer, colon cancer, lung cancer
MBD2	Transcription repression	Upregulation, Mutation	Prostate cancer, colon cancer, lung cancer
MBD3	Transcription repression	Upregulation, Mutation	Colon cancer, lung cancer
MBD4	DNA repair, glycosylase domain, repair of deaminated 5-methylC	Upregulation, Mutation	Colon cancer, gastric cancer, endometrial cancer
Kaiso	Transcription repression	Upregulation	Colon, intestinal, lung cancer

However, in cancer, hypermethylation of CpG island promoters leads to inactivation of transcription and hypomethylation of the genome are observed which involved in various types of cancer (Sincic and Herceg 2011). The cellular pathways affected by transcription inactivation include *BRCA1* (breast cancer 1)], Ras signaling {*RASSF1A* [Ras association (RalGDS/AF-6) domain family member 1], *NOREIA*}, and p53 network [$p14^{ARF}$, *p73* (also known as *TP73*) (Kanwal, and Gupta, 2012).

1.1.3.2 Histone Modifications:

Another process play a role in malignancy and epigenetic regulation is histone modifications, which influence the chromatin structure (Cedar and Bergman, 2009). In eukaryotes, the highly condensed chromatin structure consists of two strands of DNA sequences wrapped around core histones, H2A, H2B, H3 and H4 which form nucleosomes (Luger *et al.* 1997). This composition gives the chromatin the ability to condense, protect, preserve and control the genetic information and gene expression (Fyodorov and Kadonaga 2001). The molecular function of chromatin is regulated by histones, which undergo numerous posttranslational modification including acetylation, methylation, phosphorylation, ubiquitination and poly (ADP) ribosylation (Margueron *et al.* 2005). Some epigenetics changes happened during the generation of DNA double strand breaks (DSBs) in both mitosis and meiosis. For example, the induction of DSBs leads to a changes in the chromatin through phosphorylation of the histone H2AX (Mahadevaiah *et al*. 2001).

Although a number of histone modifications have been found to be associated with epigenetic deregulations, however, acetylation and methylation are the most important with regards to having been found recurrently in pathological samples from cancer cells. In human cancer, an alteration of histone modification processes has been observed in some studies. A change of the histone modification levels reflects alteration of gene expression. High levels of H3K4me3, H3K27ac, H2BK5ac and H4K20me1 in the promoter and H3K79me1 and H4K20me1 of the gene were observed in the active transcribed genes (Karlic *et al.,* 2010). Therefore, specific loss of acetylation and methylation of specific residue present on core histones of H3 and H4 have been identified as markers for tumor cells (Fraga et al., 2005; Seligson et al., 2005).

Histone Acetyltransferases (HATs), Histone Deacetyltransferases (HDACs) and Histone Methyltransferases (HMTs):

The acetylation on these core histones of H3 and H4 controls and regulates chromatin assembly, transcription and gene expression. This acetyl mark is introduced by the opposing activities of HATs and HDACs. There are around 3 main families of HATs that introduce acetyl marks on the lysine residues of the nucleosome core histones which include the MYST family, GNAT family and CBP/p300 family (Inche and La Thangue, 2006; Wang et al.,

2007). They are recruited by the transcription factors as co-activators of transcription for large chromatin complexes' remodeling. CBP, p300 and PCAF also acetylate multiple non-histone proteins which play an active role in oncogenesis (Davis and Brachmann, 2003; Glozak et al., 2005; Kouzarides, 2007; Wang et al., 2007). When hematological and solid cancers were analyzed, altered activity for HATs was reported which had been caused by either inactivation of HAT through gene mutation or deregulation by viral oncoproteins involved in cellular transformation (eg E1A and SV40 T antigen proteins targeting p300/CBP) (Rasti et al., 2005). These viral oncoproteins cause global hypoacetylation of H3K18, relocalization of p300/CBP HATs to promoter of specific genes that regulate cell growth and division, hyperacetylation of H3K18 and transcriptional activation of specific genes (Ferrari et al., 2008). Therefore, cellular transformation is undertaken by reprogramming epigenetic landscape of the cell, especially through interaction of the viral oncoproteins with HATs. Missense mutations of p300 have been reported in colorectal, gastric, breast and pancreatic cancers (Davis and Brachmann, 2003). Furthermore, Tip60, that participates in regulating tumorigenesis, when expressed less than its threshold results in hypoacetylation of p53 and consequently, defective apoptic signaling cascade and thereby increasing the risk for malignant transformation. Mono-allelic loss of Tip60 has been widely reported in lymphomas, mammary carcinomas, and head and neck tumours (Gorrini et al., 2007). Moreover, chromosomal translocations taking place in regard to HATs and their subsequent fusion proteins have been reported in the development and progression of acute leukemia (Davis and Brachmann, 2003). MLL-CBP is a fusion protein caused by the translocation t(11;16)(q23;p13) results in combination of Mixed Lineage Leukemia (MLL) protein and CBP (HAT) and is present in Acute Myeloid Leukemia (AML) and Acute Lymphoblastic Leukemia (ALL) (Ayton and Cleary, 2001). More examples of chromosomal translocations leading to the formation of fusion proteins including MOZ-CBP and TIF2-MOZ have been reported in hematological malignancies (Cairns, 2001; Panagopoulos et al., 2001) and cause the onset of acute leukemia (AML and ALL).

Moving on, the main role of HDACs is to oppose the activity of HATs thereby causing transcriptional activation by removing acetyl marks from the lysine resides of the core histones H3 and H4 and through deacetylation of non-histone substrates (Bolden et al., 2006). There are four classes of HDACS that are present in different compartments of the cell, operating in a context-dependent manner. Class I HDACs consists of HDAC 1, 2, 3 and 8 and are localized in the nucleus, class II consists of HDACs 4, 5, 6, 7, 9 and 10 that are

present both in the cytoplasm and the nucleus, class III consists of sirtuins 1-7 and lastly, class IV consists of HDAC 11 that resembles the first two classes of HDACs (Glozak and Seto, 2007). Even within the classes of HDACs, the different deacetyltransferases do not operate in a similar fashion and are part of distinct repressor complexes. Deleting or knocking down these HDACs would result in a variety of cellular responses and effects (Witt et al., 2009). Knockdown of HDAC1 and HDAC2 result in suppression of proliferation of colon carcinoma cells in vitro (Weichert et al., 2008) and sensitized the chronic lymphocytic leukemia cells to TRAIL-induced apoptosis (Inoue et al., 2006). Knockdown of HDAC3, on the other hand, resulted in more effective inhibition of the growth of different set of colon carcinoma cells as compared to HDAC1 and HDAC2 (Wilson et al., 2006). Moreover, knockdown of both HDAC3 and HDAC2 did result in inducing DNA damage and consequently, apoptosis (Bhaskara et al., 2008). Knockdown of HDAC4 also resulted in inhibition of cell proliferation and apoptosis was induced in the cells, which means that it helps in the growth of colon cancer cells (Wilson et al., 2008). Knockdown of HDAC7 on the other hand did not affect cell growth or survival, however, it did inhibit the capacity of the cells to migrate and form capillary tube-like structures which is an important step in angiogenesis (Mottet et al., 2007). Like HATs, the chromosomal translocations of HDACs have also been implicated in promoting tumorigenesis in leukemias and is most evident in the case of APL (acute promyelocytic leukemia). In APL, due to chromosomal translocations of t(15;17) and t(11;17) results in the formation of a fusion protein RARα-PML and RARα-PLZF resulting in transcriptional silencing of RAR-targeted genes and repression of cell differentiation (Cress and Seto, 2000; Lin et al., 2001; Pandolfi, 2001; Zelent, 1994). In addition to their aberrant transcriptional pathways, the alteration in their expression profiles have also been widely reported. HDAC1 has been found to be overexpressed in prostate, gastric, colon and breast carcinomas (Choi et al., 2001; Halkidou et al., 2004; Wilson et al., 2006; Zhang et al., 2005). HDAC2 is overexpressed in colorectal (Zhu et al., 2004), cervical (Huang et al., 2005) and gastric (Song et al., 2005) cancer. HDAC6 is overexpressed in breast cancer (Zhang et al., 2004) . Therefore, we can observe that aberrant expression of HDACs can result in tumorigenesis and they can provide a molecular model for targeting HDAC activity in tumours.

Lastly histone methylation can be found in mono, di or tri state on lysine and arginine residues and has been reported to be an enzymatically dynamic process (Lan et al., 2008). Methylation at H3K4, H3K36 and H3K79 resides leads to transcriptional activation and the

methylation marks at H3K9, H3K27 and H3K20 are transcriptional repressor marks (Kouzarides, 2007). There is limited information present with respect to how the methylations vary across different cancers, however, evidence does exist that they are related to the onset and growth of tumours. Cell-specific loss of trimethylation of H4K20 in tumours (Fraga et al., 2005) and knockout of HMT SUV39H makes the cells susceptible to tumorigenesis, as experimented in mice (Peters et al., 2001). The development of new techniques and methods is required to study the epigenomic landscape of cells in tumours to understand the changes in the methylation levels with the progression of diseased state.

Therefore, what we can clearly see is that how epigenetics along with genetics controls the progression of the cells from normal to tumorigenic states. Since these states are heritable and reversible, they are strong candidates for cancer therapeutics and aiding in reversing the diseased phenotype to normal through inhibitory drugs.

1.2.1 Meiotic homologous recombination

Meiosis is a unique cell division required for sexual reproduction among eukaryotes, during which four haploid gametes are formed from a diploid progenitor cell. It involves two chromosomal segregation events preceded by one round of DNA replication. Following pre-meiotic DNA replication, meiosis I (MI) and meiosis II (MII) both occur in four sequential steps; Prophase, Metaphase, Anaphase and Telophase. Homologous Recombination (HR) is fundamental in maintaining genomic stability, and ensures proper distribution of the genetic information (Loidl, 1990).

The reductional segregation of the homologous chromosomes takes place in MI. It is initiated during prophase I by homologous chromosomes aligning, pairing and conjoining via the establishment of homologue recombination events; these ultimately become chiasmata, which play a critical role in bivalent alignment of the metaphase I plate. Meiotic recombination events are initiated by the programmed formation of DNA double stranded breaks (DSBs), which are generated by the conserved meiosis-specific protein Spo11 (Keeney and Kleckner, 1995). Repairing the DSBs in most eukaryotes is associated with synapsis. Synapsis of homologous chromosomes relies on the formation of a complex proteinacious structure called the synaptonemal complex (SC). The SC is a scaffold protein structure which consists of lateral elements (LEs) connected by transverse filaments (Figure 1.1). In mammals there are a number of known meiosis-specific proteins which are components of the SC, SYCP2, SYCP3, which are attached to LEs, and central element proteins, including SYCE1, SYCE2

and TEX12. SYCP1 is an additional SC protein which serves to form the transverse filaments (Figure 1) (Hamer *et al*., 2008).

In meiosis, cohesion is established between the two sister chromatids during pre-meiotic DNA replication (Figure 2). This is generated by a protein complex called the cohesin complex (Winters *et al*., 2014). The meiotic cohesin complex differs from the mitotic cohesin complex majorly in the proteins involved in the processes respectively. In budding yeast, the difference lies in the existence of meiosis specific Rec8 instead of Scc1 (Klein et al., 1999). In addition, in mammals, the meiosis-specific variant Smc1β replaces Smc1 in some complexes (Revenkova et al., 2001). Scc1 is also replaced by the meiosis-specific Rec8, and the Scc3 orthologues, SA1 and SA2, are replaced by the meiosis-specific variant STAG3 (Prieto *et al.*, 2001). In *Caenorhabditis elegans*, depletion of the Rec8 orthologue causes separation of the two sister chromatids in the first meiotic prophase indicating Rec8 is centrally important for sister chromatid cohesion (Spike *et al*., 2014).

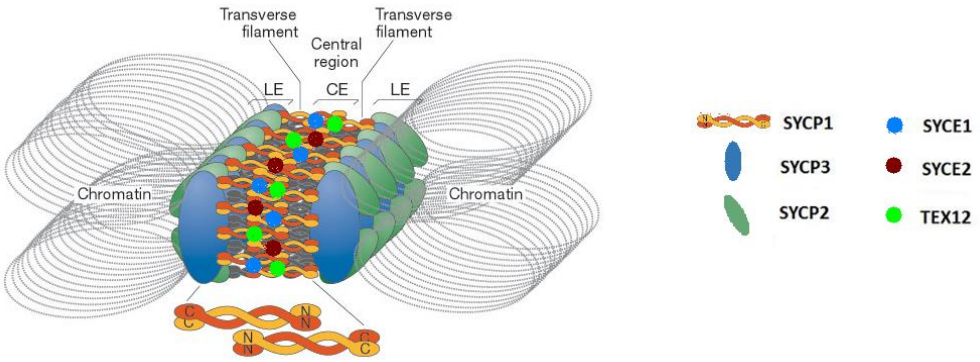

Figure 1.1 Synaptonemal complex illustrating central (CE) and lateral (LE) elements connected by transverse filaments (Hamer *et al*., 2008).

In fission yeast, the deletion of the *Rec8* gene leads to cohesin loss (Watanabe and Nurse, 1999). Moreover, in *Saccharomyces cerevisiae*, the deletion of *Rec8* gene again causes the loss of cohesin between the two sister chromatids leading to aneuploid gametes formation (Klein et al., 1999). When the programme of genetic recombination and/or synapsis fails, chromosome mis-segregation occurs which can result in aneuploidy in the meiotic daughter cells; this in turn can result in genetic diseases, such as Down syndrome, stillbirths and infertility in humans (Fledel-Alon, 2009). In MII, sister chromatids are segregated into four

haploid nuclei via a segregation event similar to mitotic sister chromatid separation (Uroz and Templado, 2012).

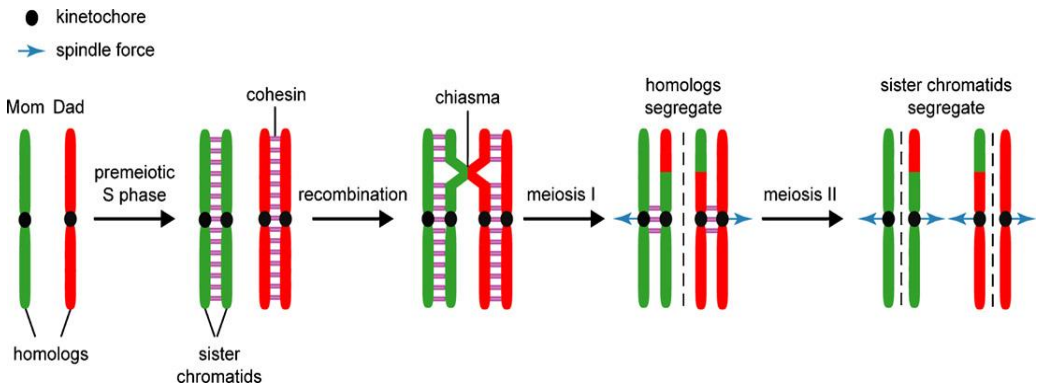

Figure 1.2 Meiotic recombination mechanism show creation of cohesin between sister chromatids and pairing between homologous maternal and paternal chromosomes generates chiasmata (Longhese *et al*., 2009)

Initiation and repair of meiotic DSBs

In humans, it is estimated that ten spontaneous DSBs take place within the cell in every cell cycle, mainly during DNA replication. This damage is caused by either endogenous agents such as free radicals or exogenous agent such as ionizing radiation (Van Gent *et al.*, 2001). However, in meiosis, meiotic DSBs are initiated by the meiotic-specific protein Spo11 that is encoded by a gene that is conserved from yeast to mammals (Keeney, 2001).

In budding yeast DSB location is influenced by promoter regions, which are enriched with GC content (Baudat and Nicolas, 1997; Keeney, 2001). DSBs are initiated by meiotic recombination protein Rec12 in *Schizosaccharomyces pombe,* and Mei-W68 in *Drosophila,* the respective orthologues of Spo11 (McKim and Hayashi-Hagihara, 1998). DNA DSBs are generated by a Spo11 homodimer (Keeney, 2008); upon break formation, one Spo11 subunit remains attached to each side of the break by generating a phosphodiester link between its catalytic tyrosine residue and the newly created DNA 5' ends (Keeney, 2001). Spo11 is removed from the DNA strand and then the 5'ends are resected by exonucleases, forming a single stranded 3' overhang either side of the DSB. Thus, one 3' overhang strand invades a homologous non-sister, which is vital for generating chiasmata (Hunter and Kleckner, 2001) (Figure 1.3).

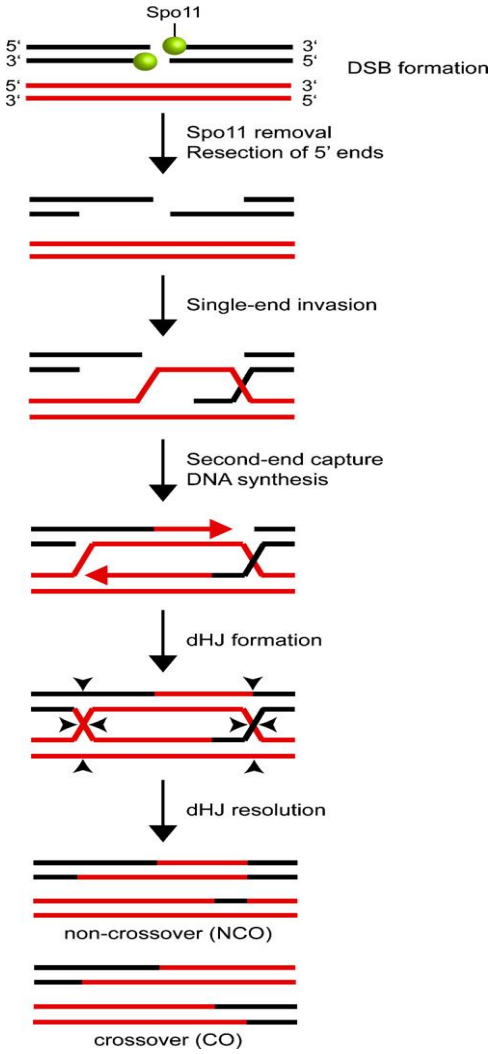

Figure 1.3 Mechanism of DSB repair in meiotic recombination shows how Spo11 initiates DSBs in DNA duplex. After Spo11 removal, DSB ends are resected to generate 3'ended ssDNA tails. One 3' ended ssDNA tail invades the duplex homologous DNA sequence (red lines). Capture of the second ssDNA end and DNA synthesis create a double Holliday junction (dHJ), whose resolution can occur in either plane at both junctions (triangles) to generate crossover or non-crossover products. Red arrows indicate the 3' ends of the newly synthesized strands (Longhese *et al.*, 2009)

Spo11 null mutants in yeast do not generate DSBs and as a result block recombination initiation and synapsis leading to the formation of aneuploid spores (Klapholz *et al.*, 1985). Mouse *Spo11* null mutants cause cell arrest and create infertile, mutant spermatocytes that show many meiotic pairing, synapsis and recombination defects (Romanienko and Camerini-Otero, 2000). Furthermore, mammalian SPO11$^{-/-}$ spermatocytes and oocytes undergo high level of apoptosis (Scott and Pandita, 2006). These mutant models consistently prove that

Spo11 play an important role in the initiation of the DSBs in meiotic homologous recombination. However, in *S. cerevisiae*, Spo11 alone is not sufficient to cause DSB formation and requires at least nine additional proteins to create DSBs, including Mei4, Mer2, Rec102, Rec104, Rec114, Ski8, Mre11, Rad50 and Xrs2 (Borde, 2007).

Whilst homologous recombination is important in the creation of genetic variation and diversity, it is also a potential hazard for genome stability because chromosomal breaks need to be faithfully repaired. Inaccurate repair or failure to repair may force the cell to undergo apoptosis or drive tumourgenesis. In humans, there are some genetic diseases characterised by an insufficient response to repair the DSB which commonly share typical characteristics such as development and immunodeficiency and cancer predisposition (Scott and Pandita, 2006; Segurel, 2013).

An early response for the DNA DSBs is the Mre11–Rad50–Nbs1 (MRN) complex which is composed of Mre11 (Rad32 in *S.pombe*), Rad50 which is a member of the Rad52 epistasis group and Nbs1 (Xrs2 in *S. cerevisiae*). It is a highly conserved complex, which plays an important role in both homologous recombination (HR) in meiotic cells and mitotic DNA damage repair (Lamarche *et al*., 2010).

1.3 Cancer Testis (CT) antigens

1.3.1 Overview

Extensive research has been carried out to investigate the possible use of tumour antigens as targets in cancer immunotherapy and cancer vaccination (Sharpeand Mount, 2015; Adelmann et al., 2008). The main requirement for tumour antigens to be considered as potential targets for immunotherapy is to have restricted or limited expression in normal tissues. Some antigens are found to fulfill this requirement, such as viral antigens [e.g., human papilloma virus (HPV) antigens in cervical cancer], and differentiation antigens (e.g., CD20 in B-cell lymphoma (Tay, 2012).

In the last decade, an emerging category of antigens known as cancer testis (CT) antigens have been uniquely defined as a group of potential antigen targets for cancer immunotherapy due to their presence in normal testicular cells and in some types of human malignancies, including breast cancer, ovarian cancer, and lung cancer. These Antigens are a group of protein antigens transcribed by testis-specific genes and characterized by their restricted expressed in gametogenic tissue, but abnormally activated and expressed in some types of

human neoplastic tissues (Caballero and Chen, 2009). Number of studies suggest that CT antigens could potentially be employed in cancer specific immunotherapy and novel biomarker tools for cancer diagnosis and prognosis (Kulkarni, *et al*., 2012). Some CT genes are meiosis-specific genes, which have a role in meiotic cell division, including *SPO11* gene, Synaptonemal Complex genes such as *SYCP1* and *SYCP2* which both contribute and facilitate sister chromatids pairing and meiotic chromosomal recombination. However, their aberrant expression in some types of cancer is currently poorly understood (Handel and Schimenti, 2010). Their confined expression in normal somatic cells and aberrant occurrence in some types of cancerous tissues makes them interesting candidates as CTA genes (Koslowski et al., 2002) and (Tureci et al., 1998).

The first CT antigen was identified by van der Bruggen's group in 1991 who used the melanoma cell line MZ2-MEL and autologous CTL clones cytolytic to this line. The tumour antigen discovered by host cytotoxic T-lymphocytes (CTL) resulted in the molecular cloning of *MAGE-1* (Kawakami et al., 1994). Further research which followed by several groups identified more CT antigen family members including *MAGE-A3, MAGE* and *GAGE* (Van der Bruggen *et al.,* 1991).

1.3.2 Identification of CTAs

Several approaches have been used to identify and characterized CT antigens, one of these approaches is T-cell epitope cloning by cloning epitopes recognized by cytotoxic T-lymphocytes. This method was helpful in discovering multiple CT antigens including the first CT antigen MAGE-1 (Van der Bruggen *et al.,* 1991; Boon *et al.,* 1994). Another approach used to identify new CT antigens is the serological analysis of recombinant cDNA expression library, termed as SEREX. This is carried out by immunological screening of tumour cDNA expression library from the sera from autologous patients. This method identified many CT antigens including SSX-2 (Gure *et al.,* 1997), SCP-1 (Tureci *et al.,* 1998) and NY-ESO-1 (Chen *et al*., 1997). Furthermore, another powerful tool used in detection of new CT antigens is differential gene expression analysis. This method identified CT antigens based on their mRNA expression profile by comparing the mRNA expression profile of tumours versus normal tissues, or comparing the mRNA expression profile between testicular and other non-germ tissue. Using this approach, many new CTA genes have been identified such as MAGE-C1^{CT7} (Lucas *et al.,* 1998), PAGE-1 (Chen *et al.,* 1998), LAGE-1 (Lethe *et al.,* 1998). Recently testis expressed meiosis specific gene *TEX19* was identified as potential CTA gene (Feichtinger *et al.,* 2012) by this method.

Finally, bioinformatics using numerous public gene expression data such as serial analysis of gene expression (SAGE) and expression sequence tag (ESTs) can be used for detecting many new CTA genes. New CTA genes identified by applying this approach included *PAGE-4* (Brinkmann *et al.*, 1998) and *CT9* (Scanlan *et al.,* 2000). In addition, using millions of short sequence tags of different RNA preparation are compared between the normal testicular tissue and variety of tumours to the massively parallel signature sequencing data (MPSS). Using this approach the CTA CT45 was found repeatedly in lung cancers (Chen *et al.,* 2005). Recently, several CTA candidate genes were identified using this application tool (Feichtinger et al., 2012).

Recent research was able to identify and characterize CTAs present in the non-small-cell lung cancer. The RNAseq data from around 1999 NSCLC tissues was collected and compared with normal transcriptional information from 142 samples, from a variety of 32 samples of the normal, non-cancerous organs (Djureinovic et al., 2016). Of all the CTAs identified, 232 were already confirmed agents and present in the Cancer Testis Database and 96 new CTAs were identified as potential biomarkers, even after strict conditions were applied on the RNAseq data. Of these identified agents, 55 genes were not annotated in the database and directly represented the newly identified CTA agents, including, TKTL-1, TGIF2LX, VCX and CXORF67. Moreover, another important finding of this research study was methylation as the regulatory mechanism controlling the expression of the cancer testis antigens.

1.3.3 Classification and expression of CTAs

CT genes are characterized by their X chromosome localisation. generally, most of the well-characterized CT antigens, such as MAGE-1, NY-ESO-1, CT7/MAGE-C1, CT10 and SAGE, are encoded by multigene family located on the chromosome X between Xq24 to Xq28. Moreover, some CT antigens genes are located in the centromeric position of the X chromosome, Xp11.2-11.4, such as SSX and GAGE (Caballero and Chen, 2009). Moreover, most of the CT genes located on chromosome X are encoding approximately 10% of the protein (Ross *et al.,* 2005). This noticeable clustering of CTA genes on the X chromosome lead to the classification of the CT antigen into two categories according to their location, they are termed as CT-X and non-X CTA genes (Simpson *et al*., 2005). One characteristic of CT-X genes includes the fact that they are mainly multi-copy paralogues which are formed due to gene duplications. However, most of the non-X CTA genes are genes with a single copy and show no chromosomal clustering as in CT-X genes. Thus, these differences support the CT-X antigens as a target in the promising cancer immunotherapy (Mueller *et al.,* 2008).

The expression pattern of CTA genes is restricted to the germ cell tissue, where they are negative in the other testicular tubular cells such as Leydig and Sertoli cells. This explains the high expression of CTA genes in the seminomas germ cell cancer compared to the non-seminomas (Yuasa *et al.,* 2001). In contrast, some other CTA genes including NY-ESO1 and MAGE show low level of expression in normal non-germ cell tissue such as placenta (Jungbluth *et al.,* 2001).

Furthermore, recent studies suggest the useful correlation between the level of expression of CTA and prognosis (Rousseaux *et al.,* 2013). In a research study which was conducted on 89 patients with Intra-hepatic Cholagio-carcinoma (IHCC), high expression levels of CTA genes MAGEA3/A4 were correlated with large tumour size, of more than 5cm (Zhou *et al.,* 2011).

1.3.4 Function of CT genes

The functional role of CT-X genes in normal testicular tissue and their aberrant expression in some tumours is still poorly understood. Some proteins identified as CT antigens play a vital role in meiosis such as SYCE which is part of the LE and CE of the SC, and HORMAD1/ CT46 (Hamer *et al.,* 2006). However, *HORMAD1* expression have been observed in human epithelial ovarian carcinoma (Shahzad, *et al.,* 2013). During meiotic recombination, some CTA genes functions are described, such as the CTA SYCP-1 is part of SC and forms a transverse filament that plays an important role in chromosomal synapsis in meiosis (Tureci *et al.,* 1998). In addition, the induction of DSB in meiosis is carried out by the endonuclease activity of the conserved meiotic-specific protein Spo11 where has been reported to be a CT antigen (Romanienko and Camerini-Otero, 1999).

In cancer, recent studies demonstrate the potential role of CTA genes in human tumorigenesis such as the over expression of *MAGE-A4* in human embryonic kidney cells which influences the activation of apoptosis. But, it shows a different effect in squamous lung cancer through inhibition of Caspase-3 activity (Peikert *et al.,* 2006). Also, CTA MAGE-A11 plays a role in maintaining the function of the nuclear androgen receptors (Bai *et al.,* 2005). MAGE-A2 plays an important role in down-regulating the activation function of P53, which is a tumor suppression protein (Monte et al., 2006). Similarly, the CT antigen GAGE-7 show anti-apoptotic activity and prevent the cells to undertake apoptosis by the influence of IFN-γ or Fas (Cilensek *et al.,* 2002). These anti-apoptotic activities that drive the cells to resist the clinically induced apoptosis agents lead to correlate between the expression of GAGE and poor prognosis. Moreover, recent clinical and research studies suggest that CT antigens are

potential target for cancer immunotherapy and vaccination. This study revealed through a clinical treatment of recurrent melanoma patient showed that the development of CD4+ T-cells were specific to the tumor-associated antigen melanoma-associated antigen NY-ESO-1, leading to tumor regression and the patient start to produce its own T cells against the tumor antigens. This study support further medical and clinical application approaches for antigen-specific CD4+ T cells in the treatment of some malignancies (Hunder *et al.*, 2008). Furthermore, in one of the recent research studies, photodynamic therapy (PDT) was used to measure its efficacy against the expression of cancer/testis antigens in squamous cell carcinoma, normally present in the head or the neck (Theodoraki et al., 2016). PDT represents a form of palliative treatment technique against cancer and it induces inflammatory responses which are the basis of antitumor immunity. Even though they have proved to markers for tumurs in the body, however, CTA are still responsible for poor prediction of multiple cancer types, for example, head and neck squamous cell carcinoma. This study analyzed the samples of tumor tissue before and after the treatment by PDT, using four distinct CTAs for measuring the effects on their expression patterns. It was observed that the expression levels for MAGEs decreased, whereas, NY-ESO-1 increased slightly due to epigenetic regulation of CTA expression or immunological pressure (Theodoraki et al., 2016).

Moreover, the role of CTA genes is still under a great amount of investigation and new researches are helping in the assessment of how they might be able to help in the control and treatment of cancer. Nettersheim and colleagues were able to prove in their recent study that the CTA agent, PRAME, supports the pluripotency network and it also plays an essential role in the repression of somatic and germ cell differentiation programs in seminomas (Nettersheim et al., 2016). To reinforce, CTAs play an important function of acting as regulators of gene expression, cell cycle and spermatogenesis. Therefore, they are popular targets for immune-based therapies. CTA PRAME is specifically produced in various cancers where it antagonizes retinoic acid signaling and is specifically regulated by the DNA methylation and histone acetylation processes. It is the master regulator of PGCs SOX17.The molecular function of the gene was analyzed in the PGC (primordial germ cells) and the testicular GCC (germ cell cancers). In this study, the own regulation of PRAME in seminomatous TCam-2 cells had no influence on the levels of SOX17 levels, however, resulted in the down regulation of LIN28, PRD14 and ZSCAN10. The somatic and germ cell differentiation markers were observed to be upregulated. Therefore, PRAME acts downstream SOX17 and regulates the germ cell differentiation and pluripotency chemical

pathways. The interesting finding of the study was also that PRAME in these cell lines did not make them susceptible to retinoic acid where it has been already established to antagonize retinoic acid signaling.

1.4 Cancer immunotherapy

1.4.1 Overview

The introduction of the cancer immuno-surveillance hypothesis by Frank MacFarlane Burnet and Lewis Thomas in 1957, raised hope for cancer immunology (Burnet, 1957). Later in 1990s, some studies promoted the concept of immune-surveillance through new technological application such as monoclonal antibodies and mouse genetics (Dunn *et al.* 2002; Dunn *et al.* 2004a). Some studies showed different aspects of the tumor escaping capabilities from immune system, and sometimes the involvement of the immune system in immunogenicity and cancer occurrence (Shankaran *et al.*, 2001).

Consequently, the whole picture of cancer immunology focused on the cancer immune-editing theory that concludes that three consecutive phases of elimination, equilibrium and escape determine the efficacy of cancer immunotherapy (Dunn *et al.* 2004a). The first phase of elimination represents the hypothesis of cancer immune-surveillance and after the successful inactivation of the immune mediation in the tumor, it resembles the equilibrium phase. Eventually, they are followed by the escape phase, which features the expansion of the tumor and breaks the immunological restrain during the equilibrium phase (Figure 1.4) (Dunn *et al.* 2004b).

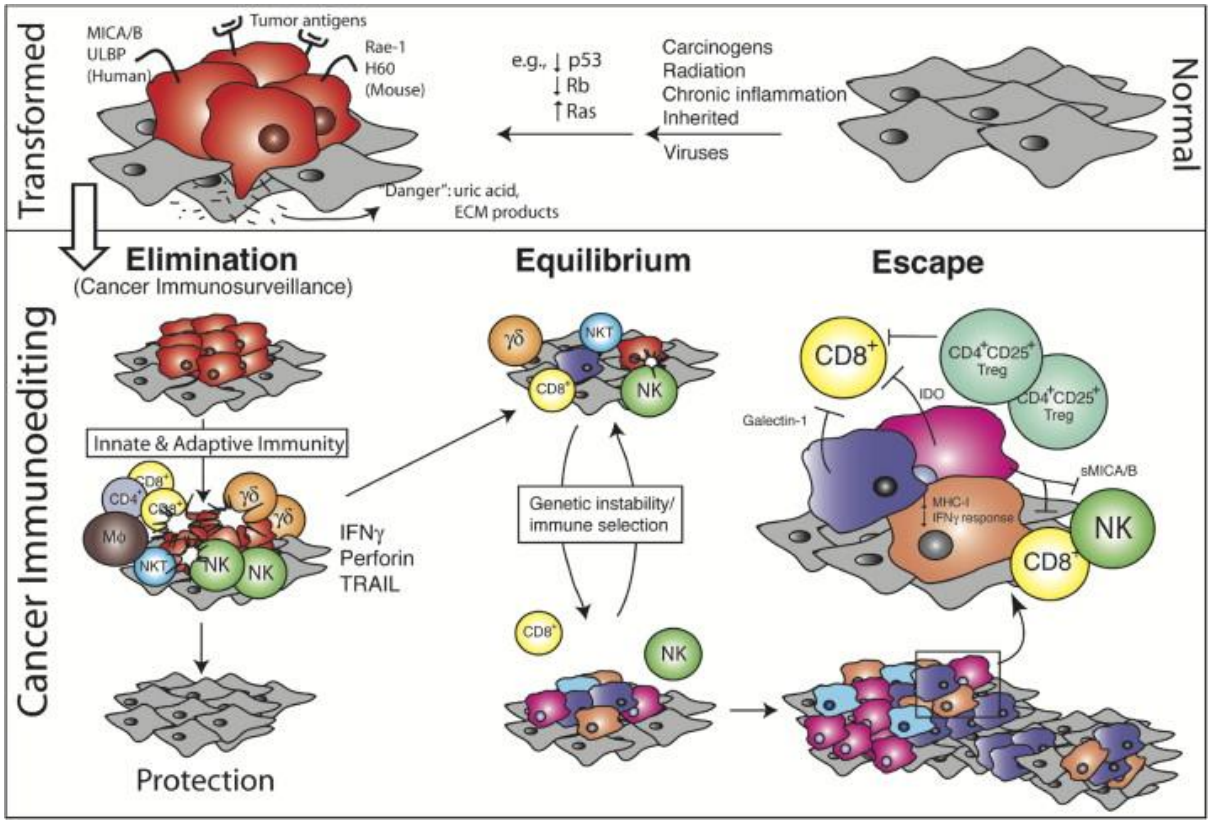

Figure 1.4 The Cancer Immuno-editing three phases including elimination, equilibrium and escape. The normal cells in (gray) under the process of transformation to become tumor cells (red).the initiation of cancer immune-editing (bottom). In the first phase of elimination, cellular and immunological interaction represent the cancer immune-surveillance. Later, transformed cells may enter the equilibrium phase. Later the escape phase feature the immune evasion (Dunn *et al.* 2004b).

The evolution of anti-cancer monoclonal antibody engineering and bone marrow transplantation shows positive results in the treatment of some types of cancers including hematologic and solid malignancies (Dougan and Dranoff , 2009). In these instances, the donating cells and antibodies play a passive immune role to induce endogenous immune reaction against the malignant cells (Dougan and Dranoff , 2009). Thus, several anti-cancer monoclonal antibodies were engineered and approved to target some proteins associated with hematological and solid cancer including Anti- EGFR, Her-2/neu, CD20, CD33 CD52 and VEGF (Mellman *et al*., 2011).

Several research groups have been suggesting the use of cancer antigens as potential targets in cancer immunotherapy by generating an immune response through cytotoxic T-cell lymphocyte (CTL) which is specifically directed against the tumour cells. This is achieved by

presenting antigenic protein fragment on the surface of the tumour cells by human leukocytes antigens (HLA) class II, present on the surface of antigen presenting cells (APCs) that mediate the immune-response. Thus, identification of these epitopes by the immune system is crucial for the production of tumour specific vaccine (Dalerba *et al.*, 1998)

Since the main objective of the cancer immunotherapy is to suppress the environment which allow for the growth of the tumours and thereby use it to produce anti-tumour specific-immune responses. However, due to the complexity of the immune-inhibitory mechanism of tumours in humans, anti-tumour specific vaccines are unable to produce positive results in abundance (Berrong, 2016). Therefore, a revision of the research techniques now focuses on the increased therapeutic efficacy of tumour vaccination. This is done by combing different immunological approaches that target multiple immunosuppressive pathways and hence enhance the efficacy of the vaccines by T cell agonists. For example, OX0 is a co-stimulatory receptor which is expressed on the surface of the T cells and plays an important role in the proliferation and enhancement of the T cell effector function in presence of its ligand. It can also be induced to carry out its function when targeted with agonist antibody.

All in all, in cancer treatment, tumour antigens have been employed as a potential approach for cancer immunotherapy. CTAs are a potential target for cancer immunotherapy due to their restricted or limited expression in normal tissues and hence they are only confined in the germ cell tissues. Thus, because of the nature of the testis blood barrier, the germ cell tissues show no expression of HLA Class I molecule thereby making the CT antigens potential targets for cancer immunotherapy (Bart *et al.*, 2002).

1.4.2 Ipilimumab and melanoma

Several developments in the field of cancer immunotherapy emerged in the last few years such as the recent trials data of the Ipilimumab Phase III that was used in the late stage metastatic melanoma cases. Due to its activating mechanism towards T cells in order to initiate endogenous response of T cells against malignant melanoma cells, the survival rate of the metastatic melanoma patients was greatly enhanced (Mellman et al., 2011; Delyon *et al.*, 2015).

Ipilimumab is a monoclonal antibody against CTLA4 (cytotoxic T-lymphocyte-associated protein 4), which plays an important role in T cell regulation and function. CTLA4 is member of the immunoglobulin family and is normally expressed on the surface of the T helper cells and play a negative inhibitory role towards the T cells (Chambers *et al*., 2001) (Figure

5). The ligation of CTLA4 consequently inhibits the immune response against the malignant cells. Furthermore, CTLA4 reflects its important role in controlling T cell function which was successfully described in studies involving the knockout mice CTLA4-/-. These changes caused mortality in young age due to aggressive lymphoproliferative disorder (Waterhouse *et al.*, 1995). The implementation of Ipilimumab monoclonal antibody to melanoma patient block the negative regulatory effect of CTLA4 and activate the immune response against the malignant cells in melanoma patients (Mellman et al., 2011).

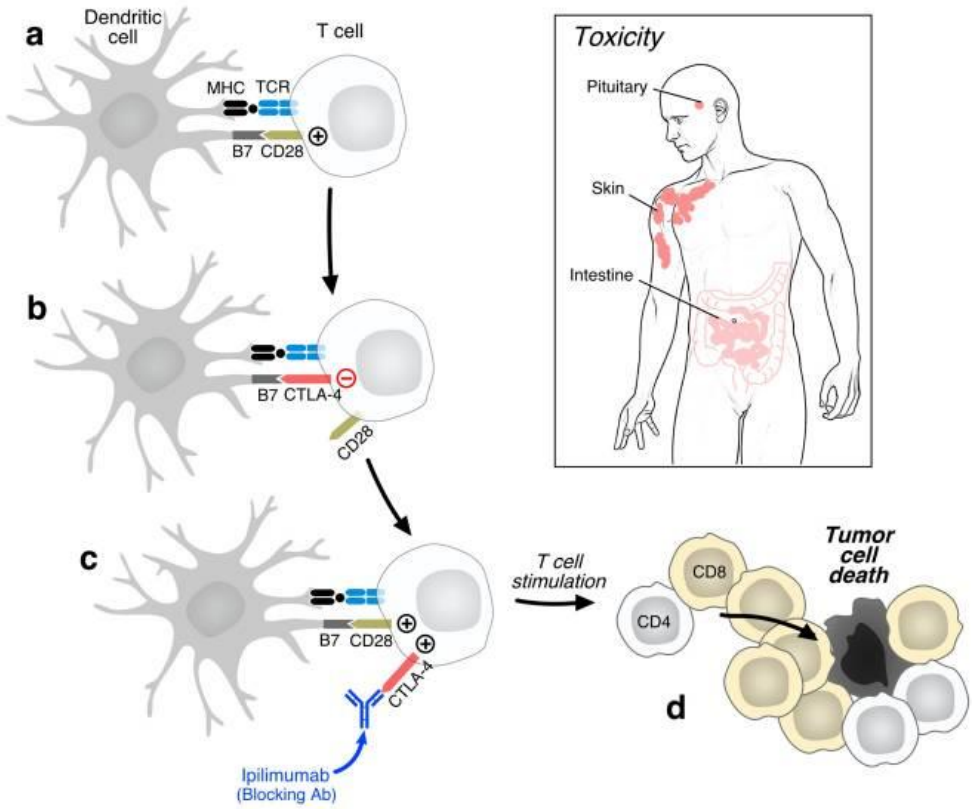

Figure 1.5 the biological role of CTLA4 and Ipilimumab (Mellman et al., 2011).

In contrast, many chemotherapeutic cytotoxic agents initiate a direct response against malignant cells leading to cancer shrinkage and death. The activation of T cells by Ipilimumab in order to kill malignant cells may take several months to show results. Meanwhile, cancerous melanoma cells may keep growing in size and expand, which is an important challenge to treat melanoma with monoclonal antibody Ipilimumab (Hodi *et al.*, 2010; Sharma and Allison, 2015).

As most cancer therapeutic agents are toxic, Ipilimumab show relatively low toxicity in few patients due to the inflammation that could be the autoimmune response such as colitis and hypophysitis, occurring in 23% of all patients treated by Ipilimumab (Mellman et al., 2011). Moreover, 20% of the patients treated with Ipilimumab in conjugation with dacarbazine, showed significant raises of the liver function tests (LFT). These inflammatory effects may occur due to the blockage of CTLA4 as we mentioned previously in the research study conducted on mice (Mellman et al., 2011; Sharma and Allison, 2015).

Regardless of these challenges and limitations, Ipilimumab is a reliable treatment that provides hope for many melanoma patients, especially in the later stages of the disease. Also, Ipilimumab and its activity against CTLA4 has opened doors towards further research that can help in finding new antibodies for activation of T cell response against malignant cells (Mellman et al., 2011; Sharma and Allison, 2015).

1.5 Transposable genetic elements

1.5.1 Overview

Transposable genetic elements or transposons (TEs) are non-coding DNA sequences that are mobilized and move their positions within the human genome through RNA copy and paste mechanism. The prevalence of TEs vary between plants, animals, and human. In mammalian genome, TEs fragments represent up to 50% of the entire genome sequence. However, in some plants, they represent up to 90% of the genome as well (SanMiguel *et al.*, 1996). In eukaryotes, TEs cause genomic instability due to their mobility and this may lead to genetic mutation or disruption of several protein products if they transpose between their gene sequences (Ayarpadikannan, and Kim, 2014).

Previously, the mobile genetic elements were considered as 'junk DNA'. Nevertheless, after the discovery of TEs by Barbara McClintock (1950) for the first time, the importance of these elements has increasingly been recognized. TEs modify both gene structure and expression (McClintock, 1950). By the process of mobilization, transposons promote ectopic rearrangement, reshuffle sequences and create novel genes. Unlike common belief, it is very rare that TE insertions result in conditions leading to a genetic disease (Beck *et al*., 2011).

1.5.2 Classification of TEs

There are two main classes of TEs, DNA transposons and Retrotransposons. DNA transposons, are inactive in the human genome now, but were mobilize within the genome by changing its location to new site tens of millions years ago (Craig *et al*., 2002; Pace and

Feschotte, 2007). On the other hand, Retrotransposons are the active type of TEs that undergo replication by forming RNA intermediates through reverse-transcription, generating DNA sequences that mobilize and insert sequences into new genomic locations accordingly (Pace and Feschotte, 2007). Retroelements are sub-categorized into two classes based on the existence of long terminal repeats as LTR transposons and non-LTR transposons (Figure 1.6). In human genome, LTR transposons are referred to as human endogenous retroviruses (HERVs) and they have been estimated to have been inserted into the human genome more than 25 million years ago (Lander *et al.*, 2001). The second group of non-LTR retrotransposons represent the active form within the genome and include LINE-1, Alu, and SVA elements (Belancio *et al.*, 2008).

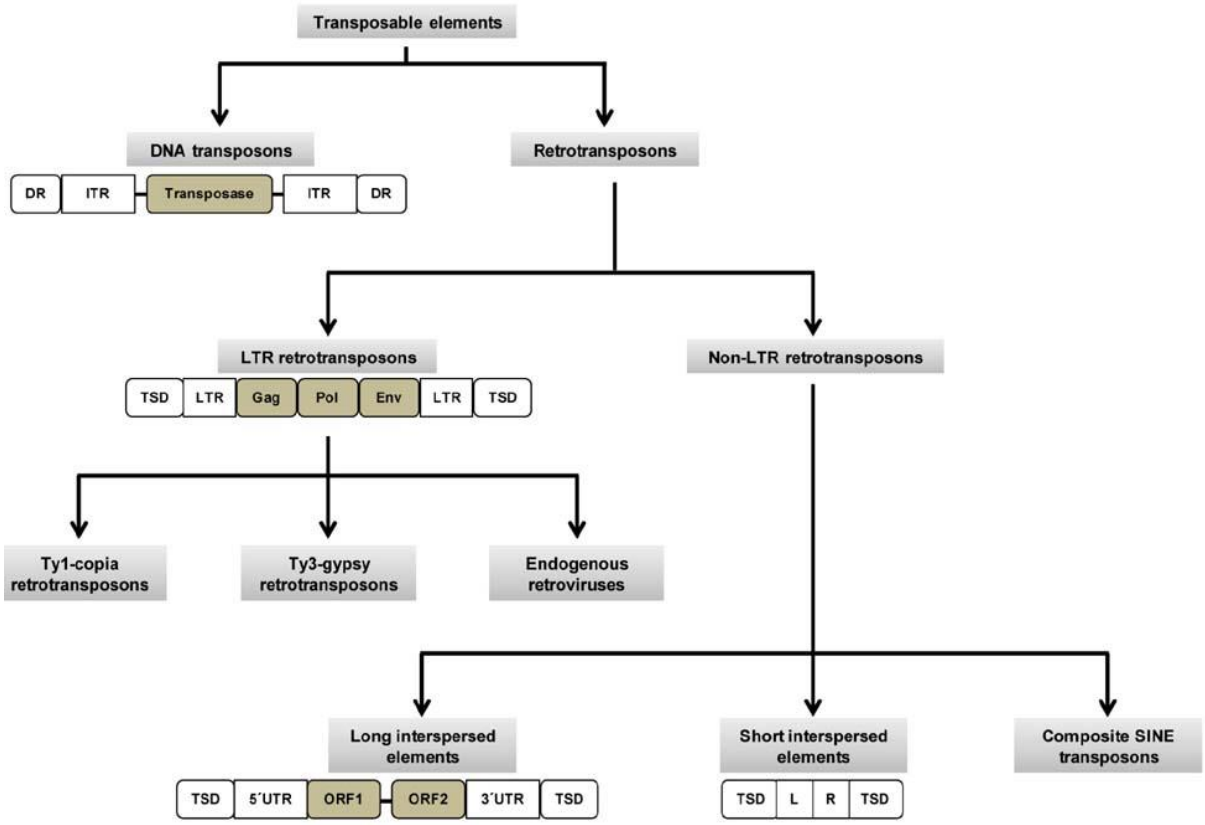

Figure 1.6 The structural classification of transposable genetic elements. DRs, direct repeats; ITRs, inverted terminal repeats; TSD, tandem site duplication; LTRs, long terminal repeats; UTRs, untranslated region; ORF, open reading frame; L, left; R, right; SINE, short interspersed nuclear element (Ayarpadikannan, and Kim, 2014).

1.5.3 Retrotransposons in cancer

There are many tumor antigens including those which are presented to human cytotoxic T lymphocytes (CTL) by human leukocyte antigen (HLA) class I molecules have emerged as safe immunotherapy targets, due to their absence in normal tissues. Amongst such tumor specific antigens an important category is that of CTA genes which include BAGE, CAGE, GAGE, HAGE, LAGE, MAGE, PAGE, NY-ESO-1, SCP and SSX gene families (Simpson *et al.*, 2005). Expression of these genes has been found in many types of tumours except for adult tissues including spermatogonia. The normal adult cells are devoid of HLA molecules and thus are unable to present the antigens to T cells. Although these antigens are generally expressed in many types of human tumours, but a few CTA genes have also been found to be expressed in different hematological malignancies related to blood cells (Roman-Gomez *et al*., 2007). Expression of CTA in cancer cells involves a unique mechanism through epigenetic regulations. Amongst these epigenetic events, DNA methylation has been found to have a crucial role in gene expression and correlating with hypomethylated CpG dinucleotides in CTA promoters. Moreover, the expression of CTA antigens has been evident in neoplastic tissues and cell lines (Cho et al., 2003; Grunau et al., 2005; Lim et al., 2005; Wang et al., 2006). Therefore, it is evident that the CTA genes expressed in different tumor conditions can be induced by DNA demethylation or by inhibiting deacetylation of histone documented for cutaneous melanoma (Sigalotti et al., 2004). It has also been documented that in case of chronic myeloid leukemia (CML), the promotor hypomethylation of CTA genes results in activation of the LINE1 retrotransposon and disease progression from the nascent to the advanced phase (Roman-Gomez *et al*., 2007).

1.6 Stem Cells

1.6.1 Background

Stem cells are undifferentiated cells that have the capability to differentiate into different types of specialised cells. These cells are present in embryos and in adult tissues and are therefore named as embryonic and adult (or somatic) stem cells respectively.

Embryonic stem cells (ESCs) are derived from inner blastocyst cell mass of the gastrula containing totipotent cells (Donovan and Gearhart, 2001). If we separate these ESCs from the developing embryo/blastocyst, followed by inducing the arrest for further embryonic development, the majority of ESCs of this mass can be maintained in an undifferentiated state. However, evidence still exists where some of these ESCs still undergo early embryonic

development, differentiating into different cell lineages forming embryoid bodies (Donovan and Gearhart, 2001; Surani, 2001). Thus ESCs are a potential source of the cells possessing a capability for diverse differentiation and self-renewal. In fact, these cells are "uncommitted" progenitors of three embryonic germ layers; ectoderm, mesoderm and endoderm. Therefore, they possess the ability to develop into any type of somatic or germ line cells (Donovan and Gearhart, 2001; Lovell-Badge, 2001; Spradling et al., 2001; Surani, 2001; Fonseca *et al.,* 2015).

Furthermore, adult stem cells can be derived from different organs throughout the body in animals and humans. They also possess the capability to differentiate into specific types of cells they were originally derived from and therefore have the potential to regenerate the complete organ. They can be potentially used in different medical therapies, such as in bone marrow transplantation. Currently the research on stem cells involves their artificial growth and differentiation or transformation into specific types of cells such as nerves, muscles etc. (Mariano *et al*., 2015). Moreover, ESCs and autologous ESCs (developed by transfer of somatic cell nucleus) have been recognized as the potential candidates for future therapies, in part due to their associated biomarkers (Tuch, 2006).

1.6.2 Stem Cells Markers

Recently, a number of different types of molecular and surface markers have been reported as important characteristic feature of undifferentiated ESCs, particularly in humans (Zhao et al., 2012). The cell fate decision functions have also been described to be performed by different proteins involved in signaling pathways (Zhao et al., 2012). Amongst these proteins, lectins are most prominent along with other similar proteins and peptides which can specifically bind to ESCs, thereby, helping in the identification of the markers. However, there are common markers expressed both in ESC and tumour stem cells, making the distinction between the teo type difficult and complicated. Therefore, identification of more specific and unique markers is necessary the isolation of ESCs.

Moreover, explaining the underlying mechanisms regulating the pluripotency of human ESCs (hESCs) remains a challenge for the scientific community. ESCs in humans differ from mouse ESCs in many aspects including cellular morphology, growth factor signaling and chromosome X's epigenetic state (Prowse *et al*., 2007; Fonseca *et al.*, 2015). Therefore,

specific studies on human ESCs for their mechanisms of pluripotency and self-renewal potential are necessary despite the amenability of mouse ESCs.

Moving on, stem cell markers belong to different types of functional proteins/molecules including surface antigens (such as SSEA-1, SSEA-3, and SSEA-4, CD9, CD24, and CD133, TRA-1-60 and TRA-1-81), transcription factors (including Oct4, c-Myc, Sox2, and Klf4) (Brimble *et al*., 2007), signal pathway related intracellular markers (examples are; LIF-STAT3, BMP-SMAD, TGF- β /Activin/Nodal, IGF-IR, FGFR and Wnt-β-catenin) (Hao *et al*., 2011), enzymatic markers (ESCs express high levels of alkaline phosphatase and telomerase) and some other markers (lectins and short peptides) belonging to different categories (Huang *et al*., 2014). These markers are present on ESCs, CSCs and other adult stem like cells and are therefore potential molecules for their identification. They can also serve to be potential therapeutic targets for diagnosis of the disease implicated by those specific cells.

1.6.3 Stem Cells Differentiation Therapy

Stem cell differentiation therapy has been associated with the establishment of human embryonic germ (EG) cells and embryonic stem cells (Shamblott et al., 1998; Thomson et al., 1998), resulting in the development of a major area of research in medicine for studying the potential of pluripotency of different cells including ESCs. Due to pluripotency and self-renewal characteristics of ESCs, these cells have become promising tools in cell replacement therapy. The basic scheme of these therapeutic treatments includes *in vitro* production of particular types of cells followed by transplantation into the patient with a functional disorder. These transplanted cells can restore the normal functions of these cells in case of diseases including Parkinson disease, Huntington disease, and heart failure. Although the efficacy of these diseases seems to be all-so-gold, however, the above-mentioned strategies face the challenge of tissue rejection in cases of organ transplants. A possible solution of this problem is producing the tissue from autologous ES cells or ES-like cells, which results in the growth of patient-histo-compatible tissue (Ramesh et al., 2009) and hence stands a chance against the immune system of the human body. Production of such histo-compatible tissues can be carried out by one of the three methods for reprogramming of differentiated cells; transfer of the nucleus of differentiated cell to enucleated oocyte exploiting their reprogramming capabilities, fusing the pluripotent cells with somatic/adult cells and reprogramming the fibroblasts by transfecting four transcription factors including Oct4, c-Myc, Sox2, and Klf4 (Takahashi and Yamanaka, 2006; Maherali *et al*., 2007; Okita *et al*.,

2007; Henzler, *et al.*, 2013; Wernig *et al.*, 2007; Ramesh *et al.*, 2009). Differentiation of the reprogrammed cells can be initiated by any of the above described mechanisms, but these differentiation events of reprogrammed cells are initiated through a regulatory cascade of reactions involving a stimulus/trigger of a specific cascade by different stimulating agents including certain chemicals such as retinoic acid (RA) and hexamethylene bisacetamide (HMBA) (Andrews et al., 1990).

1.7 Aims and objectives

CTA genes and their products may possibly be a target for cancer diagnosis, prognosis and immunotherapy due to their restricted expression in germ cells and some types of cancer. In addition, CTAs may be involved in oncogenesis. In this study, all these techniques with possible regenerative potential against cancer will be assessed and their efficacies will be quantified using different molecular assays. We aim:

1. To identify novel CT genes by RT-PCR validation of an *in-silico* pipeline.
2. To study the stem-like role of *TEX19:*

- By knockdown *TEX19* in NTERA2 cancer cell line and quantifying stem cell marker genes expression profile.
- Differentiate NTERA2 cells using HMBA and RA, and observe the proteins of stem cell markers including Oct4, Sox2 and Nanog by western blot.

3. Evaluate the influence of *TEX19* on TE in NTERA2 and A2780 cells

- Knockdown *TEX19* in A2780 and NTERA2 cancer cell-lines, and validate the expression using qRT-PCR.

4. To investigate the effect of TEX19 on differential gene expression in cancer.

- By *TEX19* knockdown in A2780, SW480, NTERA2 and H460 cancer cell-lines. Then, based on RNA sequencing data, quantifying the expression of 20 dysregulated genes by qRT-PCR.

5. To detect Spo11-DNA covalent bounding in SW480 cells by DSB assay.

2. Material and methods

2.1 Human cancer cell-lines source

Most of cancer cell-lines were acquired from the European Collection of Cell Cultures (ECACC) including 1321N1, COLO800, COLO857, G-361, SW480, HCT116, HT29, LoVo, MCF7, MM127, and T84 cell lines. Professor P.W. Andrews (Sheffield University) kindly provided the testicular carcinoma NTERA-2 cell-line. Professor P. Workman of Cancer Research UK, Surrey UK generously gifted the A2780 ovarian carcinoma cell-line. The lung cancer cell-line H460 and the breast cancer cell-line MDA-MB-453 were obtained from the American Type Culture Collection (ATCC). The ovarian carcinoma cell-lines PE014 and T014 were obtained from Cancer Research Technology Ltd. All cell-line checked upon received and regularly for contamination including mycoplasma.

2.2 Storage of cancer cell-lines

Cells were culture in T75 tissue culture flasks, the confluent cells were washed twice using 1x PBS (Phosphate buffer saline) and then trypsinised with 1x trypsin – EDTA (Invitrogen, GIBCO 1370163). The number of cells were counted using a haemocytometer slide. Cells were centrifuged at 100 x g for 5 minutes. The pellet of cells was suspended in a freezing media, which contain a 1 to 9 ratio of DMSO (Dimethyl sulfoxide) and FBS (foetal bovine serum) (Invitrogen; GIBCO 10270). The cells were transferred to the sterile, labelled cryotube with the required information (such as the identity of cell-line, number of cells). Initially the cryotube was stored at -80°C for 24 hours. Then cells were transferred into a liquid nitrogen cell bank. For any recently received cancer cell-lines a series of morphological and microbial check such as mycoplasma test taken before banking.

2.3 Thawing of frozen cell-line storage

Before removing any banked cells, updating the data sheet of tissue culture needed by removing the number and identity of cell-line going to used. The cryotube was obtained from liquid nitrogen and immediately placed into a 37°C water bath until defrosted. Then transferred into 5 ml of suitable warm media and mix gently. Cells were then centrifuged for 5 minutes at 100 x g. After aspiration of the media, 10 ml of the required media was added and the cell suspension was split into two T25 flasks and incubated overnight according to CO_2 requirement. Growing and maintaining the cancer cell-line was undertaken according to the supplier's protocols.

2.4.1 Western blot

2.4.2 Whole cell protein extraction

After harvesting the cells and washing using PBS, the cells were added to the media and cell counted using a haemocytometer to standardised the number of cells used for each well during the running of western blot; approximately 65,000 cells applied per well were needed. Whole cell protein lysates were obtained from the cell lines using the lysis buffer (50 mM Tris HCl pH 7.4, 200 mM NaCl, 0.5% Triton X-100, 1 mM AEBSF [4-(2-aminoethyl) benzenesulfonyl fluoride] (Sigma-Aldrich; A8456) with complete, mini, EDTA-free protease inhibitor cocktail (Roche Applied Science; 11836170001)) and an equal volume of 2x Laemmli buffer (Sigma-Aldrich; S3401). The protein lysate was then boiled at 100˚C until the cell pellet dissolved, with vortexing.

2.4.3 Nuclear and cytoplasmic protein extraction

Two fractions of protein were prepared, the cytoplasmic fraction was extracted by re-suspending the cells in hypotonic buffer (50 mM Tris-HCl pH 7.4, 0.1 M sucrose, 1 mM AEBSF, Roche complete protease inhibitor) and an equal volume of lysis buffer C (1% Triton-X-100, 10 mM MgCl, 1 mM AEBSF, Roche complete protease inhibitor cocktail). Cells were incubated on ice for 30 minutes and centrifuged at 6,000 g for 2 minutes. The supernatant were transferred to a clean Eppendorf tube and an equal volume of Laemmli buffer was added.

Then, the nuclear fraction were obtained re-suspended the pellet in the lysis buffer N (50 mM Tris-HCl pH 7.4, 100 mM KAc, 1 mM AEBSF, Roche complete protease inhibitor cocktail) and an equal volume of Laemmli buffer was added.

2.4.4 Western blotting protocol

Protein samples were loaded in pre-cast NuPAGE® 4-12% Bis-Tris gel (Invitrogen; NP0322) together with protein marker Precision Plus Protein Dual Color Standards (Bio-Rad; 161-0374). The gel was run for 1.45 hours at 120 Volt using (1x) MOPS running buffer (Invitrogen; NP0001). After running, the gel was transferred to an activated Immobilon-P (PVDF) membrane (Millipore; IPVH00010) at 400 mA for 3-4 hours using (1x) transfer buffer (380 mM glycine, 50 mM Tris). The membrane was incubated for one hour in 5% dry skimmed milk (1x) PBS/Tween (0.3%) buffer. then incubated overnight in the optimum concentration of the required primary antibody at 4˚C in the rotator. Then, the non-specific binding of the antibody was removed by washing the membranes three times using blocking buffer (1x) PBS/Tween (containing 5% of milk) for 10 minutes each. The membrane were

placed in the secondary antibody for one hour at room temperature. To reduce non-specific binding the membranes washed three times, 10 minutes each using the blocking buffer. To detect the signal Enhanced chemiluminescence (ECL; Thermo Scientific; 34087) used to detect the protein. Signal was visualise by exposing the membrane to X-Ray film (Thermo Scientific; 34091).

Table 2.1 list of primary and secondary antibodies used.

Antibody	**Source**	**Dilution**
Mouse polyclonal Anti-Spo11	Abnova Cat. No. H00023626-A01	1/500
Mouse monoclonal Anti-Tubulin	Sigma T6074	1/5000
Goat polyclonal Anti-Lamin	Santa cruz sc-7292	1/1000
Polyclonal Anti-Tex19	R and D Catalog # AF6319	1/500
Rabbit polyclonal Anti-Oct-4	Abcam ab19857	1/1000
Donkey anti-rabbit	Jackson Immunoresearch 711-035-152	1/40000
Donkey anti-mouse	Jackson Immunoresearch 711-035-150	1/40000
Rabbit Anti-goat	Sigma A5420	1/40000

2.5 RNA isolation

RNA isolation was carried out using the traditional Trizol (Invitrogen; 15596-026) protocol by homogenise the cells in 1 ml of Trizol per 5 x 10^6 cells at room temperature for 5 minutes. Then 200 µl of Chloroform was added to each sample followed by vigorous shaking for 15 seconds and incubated for 5 minutes at room temperature. The sample were centrifuge at 12,000 g for 15 minutes at 4°C. The top aqueous layer was transferred to a new Eppendorf

tube and mix with 0.5 ml of isopropanol and incubate at room temperature for 10 minutes. The samples were centrifuged at 12,000 g for 20 minutes. Sample were then the supernatant was aspirated and the pellet was washed with 70% ethanol and re-centrifuged at 7,500 g for 5 minutes at 4°C. The supernatant was aspirated again and the cell pellet was left to dry at RT for 5-10 minutes until the alcohol residue evaporate and then 100 µl RNase free water containing 2 µl DNase I (Sigma; D5319) was added to each RNA sample. The samples were incubated at 37°C for 10 minutes and then at 75°C for 10 minutes. RNA yielded was measured by a NanoDrop (ND_1000) spectrophotometer and qualityof the ribosomal bands was checked on agarose gel.

2.6 cDNA synthesis

Total RNA was used to synthesise cDNA using SuperScript III First Strand Synthesis Kit (Invitrogen; 18080-051) according to the manufacture's instructions. Positive control housekeeping gene *β- Actin* were used.

2.7 Polymerase chain reaction (PCR)

Primers were designed manually and the oligonucleotide properties calculated (http://www.basic.northwestern.edu/biotools/oligocalc.html). The primers design was based on the gene sequences obtained from the National Center for Biotechnology (NCBI;http://www.ncbi.nlm.nih.gov/). 2 µL of diluted cDNA (approximately 150 ng/µl) was used for PCR along with 1µl of both forward and reverse primers mixed with 25 µl of BioMixTM Red (Bioline; BIO-25006), and distilled water was added to 50 µl final volume.

Samples amplification starting with a pre-cycling melt at 96°C for 5 minutes, followed by 40 cycles of denaturing at 96°C for 30 seconds. The annealing step temperature vary between 58-62°C for 30 seconds according to the primers in use and extension step at 72°C for 40 seconds followed by a final extension step at 72°C for 5 minutes. PCR product were analysed by agarose gel electrophoresis.

Table 2.2 List of primers used in RT PCR and qRT PCR

Gene	Primer	Sequence 5'-3'	Annealing Tm (°C)	Amplicon Size (bp)
C16orf46	F	GTCTTCTCGATGTCAGTGAC	58.4	591
	R	CCTTCTCTTCTGACTGCAAG		
GLIPR1L1	F	CTTGGGTCTGTGTTTGGTAG	58.4	630
	R	GGATTAAAGGCTGTCTGCTG		
FTMT	F	CTACGTGTACTTGTCCATGG	58.4	423
	R	GTGTCAAAAAGGTACTCCGC		
TCTE3	F	CTAGCATGTTCGAGAAGGAG	58.4	417
	R	CAATGTCCCAGATCCATCTG		
CXorf27	F	CAGACTCAAGACCCTTCTAG	58.4	304
	R	CATTCTTCCTGGATT TGGGC		
FAM166A	F	GAAACACGATCTCTTCACGC	58.4	624
	R	CGTTGGATTAGGTTAGGGTG		
C5orf48	F	CCTACTTTGCCTAAACTCAC	56.4	356
	R	TGGGAAATCACAGTGCTTTG		
SYNGR4	F	GTCTGGTTCATGGGTTTCTG	58.4	476
	R	AGCATAACTCAGGCTGTTGG		
C12orf70	F	CAAGGGTATGTTGGAGCTAG	58.4	512
	R	CAGAACTGTGAGAGTCAGTG		
CCDC54	F	CAACTGGATATCCCACTGTG	58.4	681
	R	CTAACTTGGTAGCACTGAGG		
CCDC105	F	GCTTATTAACCAGCAGAGCG	58.4	782
	R	GGTTCTTTTCCAGGTACGTG		
TEX19	F	GCTTCAACATGGAGATCAGC	58.4	386
	R	GAAGCTCCTCAAATCTCCAG		
BRDT	F	GAACCTGTTGAGAGTATGCC	58.4	691
	R	CATCCAGTAACCGCTTTTCC		
SHCBP1L	F	GGACTGTAAGGCAGAAGATG	58.4	720
	R	CTACGCCTCAGAATTCTTGG		

C20orf70	F	TCAAGTACTTCCAGGACCAC	58.4	371
	R	GGCTAGTCTTAAAAGGTGCC		
TRIML1	F	GAAGCTCAGGCTGTACTAAC	58.4	520
	R	CAAATCTTTCCGGGTTGTCG		
IL31	F	CCGTTTACTACGACCAAGTG	58,4	362
	R	GGTCCATGCACTCTGAAAAC		
PAPOLB	F	CACAGCAGAACTCCACATAC	58.4	577
	R	CTACCTTCTGTTGAGTGTGC		
FAM166A	F	CCATGTCCAAACCCAAGTTC	58.4	468
	R	TGCGTTGGATTAGGTTAGGG		
C5orf48	F	CAACTGCTCTGATGAGAGTC	58.4	389
	R	CTGAAGCCATGGGAAATCAC		
SOX2	F	GCAACCAGAAAAACAGCCCG	58.4	590
	R	CGAGTAGGACATGCTGTAGG		
NANOG	F	CTGCTGAGATGCCTCACACG	58.4	497
	R	GCTCCAGGTTGAATTGTTCC		
OCT4	F	CTGGAGAAGGAGAAGCTGGA	58.4	509
	R	GCATAGTCGCTGCTTGATCG		

*F: Forward; R: Reverse

2.8 DNA purification and sequencing

The purification of PCR product varies depending on the gene show one clear band in the expected size or show multiple bands. There was clear band the purification using the PCR product according to the manufacturer protocol using High Pure PCR Product Purification Kit (Roche Applied Science; 11732676001). However, in the multiple bands, cutting the specific band fragment out of the gel using sterile scalpel needed to undertake the purification process. Then, the purified DNA sample was sent for sequencing along with forward primers to the Eurofins MWG Company (Germany). The DNA sequencing results were analysed through BLAST (http://blast.ncbi.nlm.nih.gov/Blast.cgi) and EMBL European Bioinformatics Institute (http://www.ebi.ac.uk/).

2.9 Quantitative real time PCR

RNA was isolated using the RNeasy Plus Mini kit (Qiagen; 74134) and according to the manufacture's protocol. The synthesis of the cDNA was done using a SuperScript III First Strand Synthesis Kit (see above). The primers were designed manually, however, primers for the reference genes were ordered from Qiagen. The master mix qRT-PCR carried out using The Go Taq qPCR Master Mix (Promega; A6001) following the manufacturers protocol. Each well of a Hard-Shell® 96 well plate (BioRad; 9655) contained 1.5 µl cDNA in a final reaction volume of 20 µl, and in each reaction triplet repeat were done.

The reaction were amplified with a pre-cycling step at 95°C for 3 minutes, followed by 40 cycles of 95°C for 10 seconds. Annealing temperature setting at 60°C for 30 seconds, followed by 95°C for 10 seconds. A quantitative Bio-Rad CFX machine was used to do this analysis and the data was measured after normalising against the reference genes with Bio-Rad CFX Manager Software (version 2).

2.10 Knockdown gene by RNA interference

Approximately 200,000 cells per well were seeded into each six wells plate and incubated overnight. 100 µl of serum free media was used to make the transfection complex of 10 nM siRNA approximately 1.2 µl (Qiagen) and 6 µl HiPerfect reagent (Qiagen; 301705). The complex was incubated for 40 minutes at room temperature. The complex was applied to the cells drop wise with gentle agitation. Non-interfering RNA was used as negative control (Qiagen; 1022076) which was prepared the same way. The plate were incubated overnight, the cells were wash using PBS, refreshed with new media, and a second and third hit was applied consecutively as described before.

Table 2.3 list of siRNA used for gene knockdown.

Gene	siRNA	Qiagen cat. No.	Target sequence (5' -3 ')
SPO11	Hs_SPO11_1 FlexiTube siRNA	SI00100366	CAGAGTGTACTTACCTAA CAA
	Hs_SPO11_2 FlexiTube siRNA	SI00100373	ACAACTAATGTTAACGCA TAA
	Hs_SPO11_4 FlexiTube siRNA	SI00100387	TACCTTCTACGATACAAC TAA
	Hs_SPO11_6 FlexiTube siRNA	SI03024049	CCACACAGCCGTAATGAC AAA

TEX19	Hs_FLJ35767_1 FlexiTube siRNA	SI00409444	
	Hs_FLJ35767_6 FlexiTube siRNA	SI04215176	AGGATTCACCATAGTCTCTTA
	Hs_FLJ35767_7 FlexiTube siRNA	SI04247705	TTCAACATGGAGATCAGCTAA
	Hs_FLJ35767_8 FlexiTube siRNA	SI04276937	
NI	Non-interference RNA	1022076	AATTCTCCGAACGTGTCA CGT

2.11 Extreme limiting dilution analysis (ELDA)

12 well repeats were used for untreated cells, non-interference control siRNA, Hiperfect treated cells and gene small interference siRNA treated cells. The transfection complex made by adding 0.1 nM siRNA (Qiagen) containing 0.3 µl HiPerfect reagent (Qiagen; 301705) to 4.7 µl serum free medium and incubating for 45 minutes at room temperature. In addition, non-interference siRNA (Qiagen; 1022076) was prepared in the same way. The siRNA transfection mixture, negative control siRNA and Hiperfect were added drop-wise to the cells in the 12 well repetitions for each condition. Then, the plate incubated for 10 days in a humidified incubator at 37°C with required CO_2. On day 3 and 6, the Cells were supplemented with 50µl serum free medium and the transfection mixture as previously

After 10 days of incubation, the analysis of number of cells observed by light microscope and the data analysis done using ELDA web tool to carry out the statistical analysis. (http://bioinf.wehi.edu.au/software/elda/). In addition, images of cells were taken from first day of seeding and day 10.

2.12 Detection of SPO11 covalent bound to DNA Adapted from (Hartsuiker, 2011).

Confluent SW480 cells were trypsinised and washed twice using PBS. Using a haemocytometer, approximately 2,500,000 cells were lysis in freshly prepared 1.1 ml lysis buffer (8 M guanidine HCl, 30 mM Tris pH 7.5, 10 mM EDTA, 1 % Sarcosyl, adjusted to pH 7.5 with 10 M NaOH). The cell lysate were incubated at 65ºC for 15 minutes and then centrifuged at 16,000 g for 5 minutes.

Different density of CsCl gradients were prepared (1.45 g/ml density: 60.90 g CsCl dissolved in 100 ml distilled water. The refractive index (RI) was 1.3764; 1.50 g/ml density: 68.48 g CsCl in 100 ml distilled water, RI 1.3815; 1.72 g/ml density: 98.04 g CsCl in 100 ml distilled water, RI 1.4012; 1.82 g/ml density: 111.94 g CsCl in 100 ml distilled water, RI 1.4104) were loaded into polyallomer ultra-centrifuge tubes (Beckman Coulter Cat. No. 326819) beginning with CsCl 1.82 g/ml then very carefully layering 1 ml of CsCl 1.72 g/ml on top of the first layer; repeating this for the 1.50 g/ml and 1.45 g/ml CsCl solutions. A 1 ml sample of the lysed cells was then loaded as the top layer. The gradients were centrifuged for 24 hours at 30,000 r.p.m. at 25ºC in ultra-centrifuge Beckman SW55Ti rotor.

The remainder of the lysed cells were used for DNA quantification. The remaining cell lysate was incubated at 65ºC for 5 mins and centrifuged for 2 mins at 16,000 xg, then 10 µl of the supernatant was added to 90 µl of TE containing 0.5 µg/ml Rnase A (Sigma, Cat No. R6513) and incubated for 3 hours at 37ºC. The mix was centrifuged for 2 minutes at 16,000 g to remove any insoluble material, and then 50 µl of the supernatant was added to 50 µl of a 1:200 dilution of Quant-iT PicoGreen dsDNA reagent (Invitrogen, Cat. No. P7581)

Mixed in TE buffer, and incubated for 5 minutes at room temperature. A blank control (50 µl TE) and DNA standard (50 µl 100 ng/ml Lambda DNA [NEB, N3011] in TE) was prepared as well. An Invitrogen Qubit were calibrated using the blank control and DNA standard and then the DNA concentration in the samples was measured.

After 24 hours, the tubes were taken from the ultracentrifuge. A centrifuge tube containing the gradient was clamped in a retort stand. Silicone tubing was fitted into a peristaltic pump and the end silicone tubing was attached to a needle. The needle was inserted into the bottom of centrifuge tube at a 45º angle. Using the peristaltic pump, the gradient was slowly pumped out of the tube and 0.5 ml fraction were collected in each tube.

A nitrocellulose membrane (Whatman, Cat. No. 10402096) were immerse in 1X PBS and applied to a slot blotter (Hoefer PR648 slot blot filtration manifold unit). The fractions were loaded onto the slot blot for each sample equally, based on DNA concentration; the loadings for the slot blot were calculated as 150 ng for each sample. Once the samples were vacum extracted through the membrane, the membrane then dried face up on a piece of paper. Then, DNA was cross-linked to the membrane using a stratalinker (auto-crosslink, 120,000 microjoules).

The membrane was blocked in milk solution (3% non-fat dry milk, 0.1% Tween 20 in PBS) for 30 minutes on a shaker and then incubated overnight at 4°C in anti-SPO11 antibody (Abnova, Cat. No. H00023626-A01), which was diluted 1/500 in milk solution. The membrane was then washed in milk solution twice for 10 minutes each time and then incubated for 1 hour at room temperature in Donkey anti-mouse secondary antibody (Jackson Immunoresearch, Cat. No. 711-035-150, also diluted in milk solution). The membrane was washed twice for 5 minutes in milk solution and three times for 5 minutes in PBS/Tween 20 (0.3% w/v). Pierce ECL Plus Western Blotting Substrate (Pierce 32132) was used to detect SPO11 after exposure for 15 minutes to CL-XPosure Film (Thermo scientific, 34088).

2.13 Statistical analysis

In this project, several statistical approaches were employed regardless the fact of majority of data obtained were qualitative results. However, in ELDA assay we used a web page tool: (http://bioinf.wehi.edu.au/software/elda/).

Densitometry was performed using Image J software to quantify the intensity of protein bands. and some statistical data were analysed using Excel statistical analysis tools to calculate p value.

3. Identification and validation of novel CT genes using bioinformatics tools

3.1 Overview

Tumour antigens have been employed as targets for cancer immunotherapy. The main requirement for tumour antigens to be considered as potential targets for immunotherapy is to have no presence in normal tissues. CTA (see introduction) have been defined as a group of potential antigen targets for cancer immunotherapy due to their presence in normal testicular cells and in several types of human malignancies (Caballero and Chen, 2009). A number of studies also suggest that CT antigens could potentially be employed as novel biomarker tools for cancer diagnosis and prognosis. A recent study on 142 patients suffering from hepatocellular carcinoma showed correlation between the expression of CT genes and poor prognosis. This suggest the possible use of CT genes to evaluate hepatocellular carcinoma outcomes. In addition, it might be a potential target for hepatocellular carcinoma immunotherapy (Wang *et al*., 2015). Previous work reveal the possible involvement of CT genes in cancer, such as possible role for *MAGE-A2* influence on *P53* tumour suppressor gene down regulation (Monte *et al*., 2006). Additionally, another study on multiple myeloma and CT gene *SLLP1* expression, suggest *SLLP1* as potential target for immunotherapy in multiple myeloma (Yousef, *et al*., 2015).

Meiosis requires the expression of a number of specific genes that encode meiosis-specific functions. Some of these genes show significant expression in various types of cancer, such as the *SPO11* gene, which is responsible for encoding the initiator of the meiotic recombination (Keeney, 2008). Other examples including *SYCP1* and *SYCP2*, which make up parts of the meiosis-specific synaptonemal complex (see introduction). There confined expression in normal somatic cells and aberrant occurrence in some types of cancerous tissues, which is poorly understood, make meiotic genes potential candidate for CT genes (Koslowski et al., 2002; Tureci et al., 1998; Whitehurst, 2014).

A subgroup of CT genes, are not affected by chromosome X-inactivation as they are autosomalic encoded. Meiosis-specific genes have been hypothised to be in this class as their activation must correlate with meiotic X inactivation. Identification and validation of these genes reveal understanding of oncogenic involvement of these genes (Feichtinger *et al*., 2012). In addition, the expression of these meiosis-specific genes in some types of cancer might reveal a new sub-category of testis restricted CT genes (Feichtinger *et al*., 2012). The

potential use of meiosis-specific CT genes as cancer biomarkers and immunotherapy are increasing due to their immunogenicity and localized confined expression (Seoane and De Mattos-Arruda, 2014).

Here we aim to identify novel CT genes by applying two approaches. Firstly, through manual literature searches we identified meiosis-specific genes known to have expression restricted to the testis. Secondly, we used *in-silico* analysis of EST data sets (done by my colleague Dr. Julia Feichtinger) that will be discussed in the results to identify novel CT genes. (Feichtinger *et al*., 2012).

3.2 Results

Initially a group of meiosis-specific genes was selected by a manual search of the literature. This list proved to be relatively small and so we took a more systemic approach. 744 mouse genes have previously been identified (Chalmel *et al*., 2007) that were reported to be specific to meiotic spermatocytes. 408 human orthologues of these genes were identified (Feichtinger *et al*., 2012). Then, validating these genes against human genes involved in mitosis (Mitocheck) and excluding possible non-testis specific genes (a schematic is shown in Figure 3.1). 375 genes fit the requirements and these were fed into an express sequence tag (EST) analysis pipeline which search the gene list against ESTs for normal human and cancerous tissues , from this we identified 105 genes with predicted restricted expression and cancer tissue expression (Feichtinger *et al*., 2012). 9 genes were cancer/testis only restricted, 75 genes were testis restricted (no cancer EST footprint) and 21 genes were cancer/testis/CNS restricted. These 105 genes were validated by RT-PCT screening in various normal and cancer human tissue (Feichtinger et al., 2012). 21 genes were assaigned randomly to me for RT-PCR validation (Table 3.1).

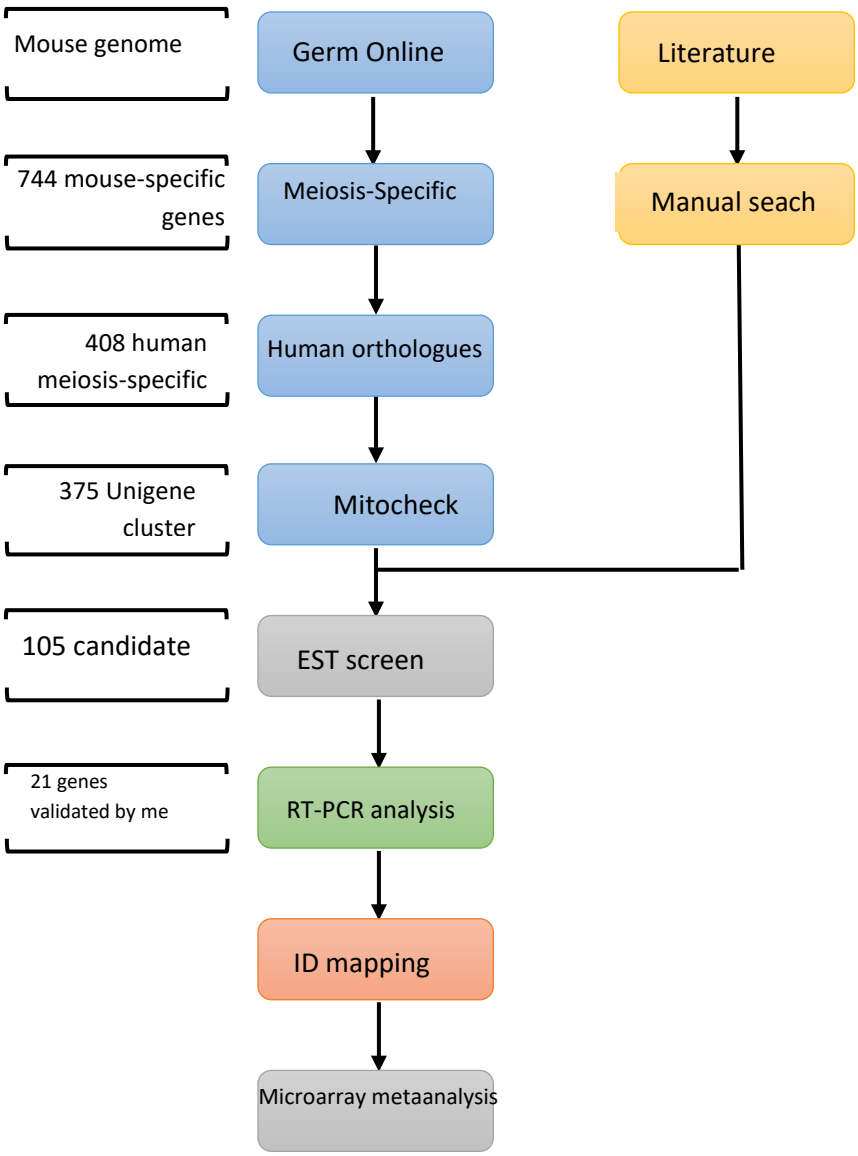

Figure 3.1 Illustrated flow diagram show step-wise approach applied for the candidate meiCT genes. 744 mouse meiosis-specific genes were starting with. Then, 408 human orthologues were identified and 375 human meiosis-specific genes remain after Mitocheck. All 375 candidates as well as 3 controls (*MAGE-A1, GAGE1* and *SSX2*) were fed into the EST analysis. Afinal 105 candidate genes were validated by RT-PCR /microarray meta-analysis (Feichtinger *et al*., 2012), of which I was allocated 21 genes at random.

Intron-spanning primers were designed using Primer3 software as possible (www.genome.wi.mit.edu/cgi-bin/primer/primer3www.cgi). cDNA were constructed from isolated RNA according to manufacturers protocol. RT-PCR were performed using 2µL of diluted cDNA (approximately 150 ng/µl), distilled water and BioMix™ Red (Bioline™) were used for PCR amplification of total volume 50 µL. RT-PCR run for 40 cycles and PCR product were separated and visualised using on 1% agarose gels containing ethidium bromide (Feichtinger et al., 2012a).

The candidate genes were subjected to RT-PCR using RNA obtained from 21 human normal tissue, which included testis as a positive control sample. Candidate gene which show restricted expression to the testis and/or CNS/ one or two other normal tissues, were screened for expression in 33 different types of human cancer cells obtained from tumour biopsies or cancer cell-lines. Then, all PCR product were validated by DNA sequencing.

3.2.1 Evaluation and validation of meiosis-specific *TEX19* as potential CT gene

Our fist approach was to search the literature manually for meiosis-specific genes; *TEX19* was one of the genes selected in this approach. Two sets of *TEX19* primers were designed. The first set were designed from the one translated exon and the second set were designed intron-spanning primers where the first exon is the untranslated exon.

RT-PCR results for RNA from normal human tissue using exon internal primers shows a clear band of *TEX19* at the expected size (386 bp) (Figure 3.2) for the testis and a faint band in the thymus. However, using the intron-spanning primers, a clear band at the expected size (757 bp) was observed in testis only (Figure 3.2). The PCR product were purified and sequenced and gene identity were confirmed (Table 3.2) RT-PCR amplification of *β-ACTIN* using intron spanning primers was used to quality control the cDNA.

Because of the restricted testis expression of *TEX19*, a panel of cancer cell RNA was used, RT-PCR show *TEX19* band was detected in several types of cancer including colon cancer cells SW480 and HT29, lung cancer cells H460, breast cancer cells MCF-7, ovarian cancer cells PE014 and A2780, leukaemia cells K562, melanoma cells COLO857 and liver carcinoma cells HEP-G2 cancer cell-lines. Both sets of primers were used show similar bands in these cancer tissue (Figure 3.3). DNA sequencing of *TEX19* band in SW480 reveal gene identity (Table 3.2).

Table 3.1 Functional role of predicted CT genes in EST analysis

Gene	function	Reference
C16orf46	Unknown	
GLIPR1L1	Involve in spermatogenesis	Caballero *et al*. (2013)
FTMT	encodes Mitochondrial ferritin (FtMt) protein	Drysdale *et al*., (2002)
TCTE3	Involve in sperm motility	Harrison *et al.,* (1998).
CXorf27	Involve in Huntington's disease	Butland *et al.,* (2014)
FAM166A	Unknown	
SYNGR4	Unknown	
C12orf70	Unknown	
CCDC54	Unknown	
CCDC105	Unknown	
TEX19	Meiotic upregulated and involve in spermatogenesis	Kuntz *et al*. (2008) Ollinger *et al*. (2008)
BRDT	encode Bromodomain testis-specific protein	Shi and Vakoc (2014)
SHCBP1L	Involve in spermatogenesis	Liu *et al.,* (2014)
C20orf70	Encode salivary protein parotid secretory	Abdolhosseini, *et al.,* (2012).
TRIML1	Play a role in protein ubiquitin	Marín, (2012)
IL31	Involve in immune reaction	Zhang *et al*., (2008).
PAPOLB	Involve in spermiogenesis	Matzuk *et al.,* (2012).

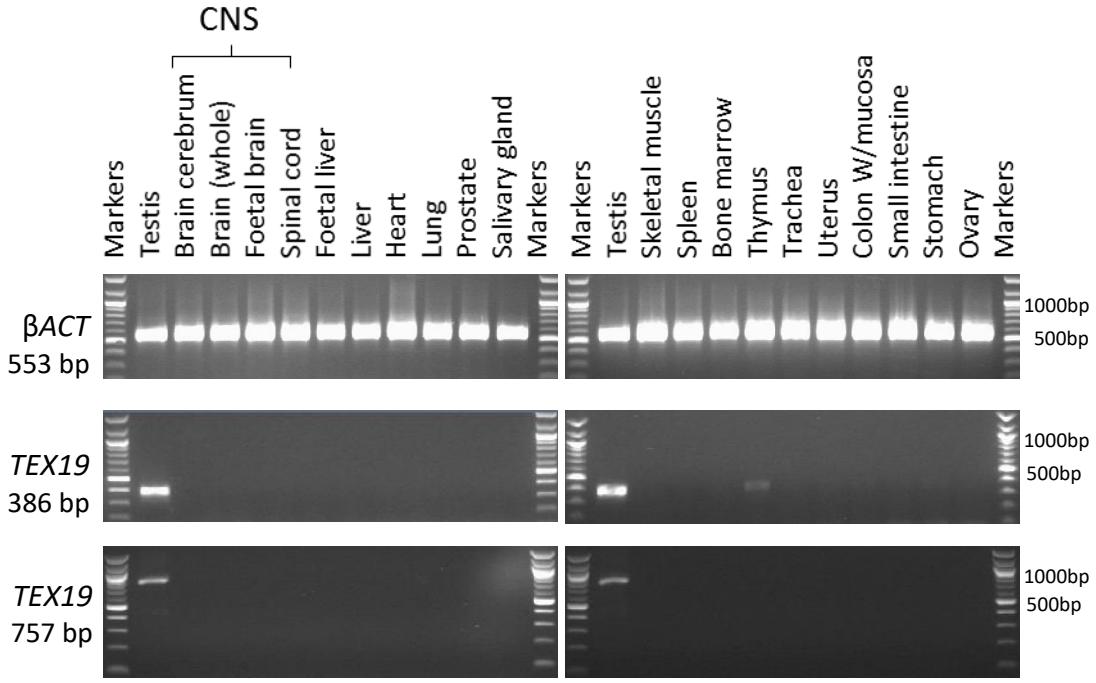

Figure 3.2 RT-PCR of potential CTA gene *TEX19* using human normal tissues. PCR product of *TEX19* gene observed on the agarose gel at the expected size. β*ACT* was used as a control for the cDNA quality.

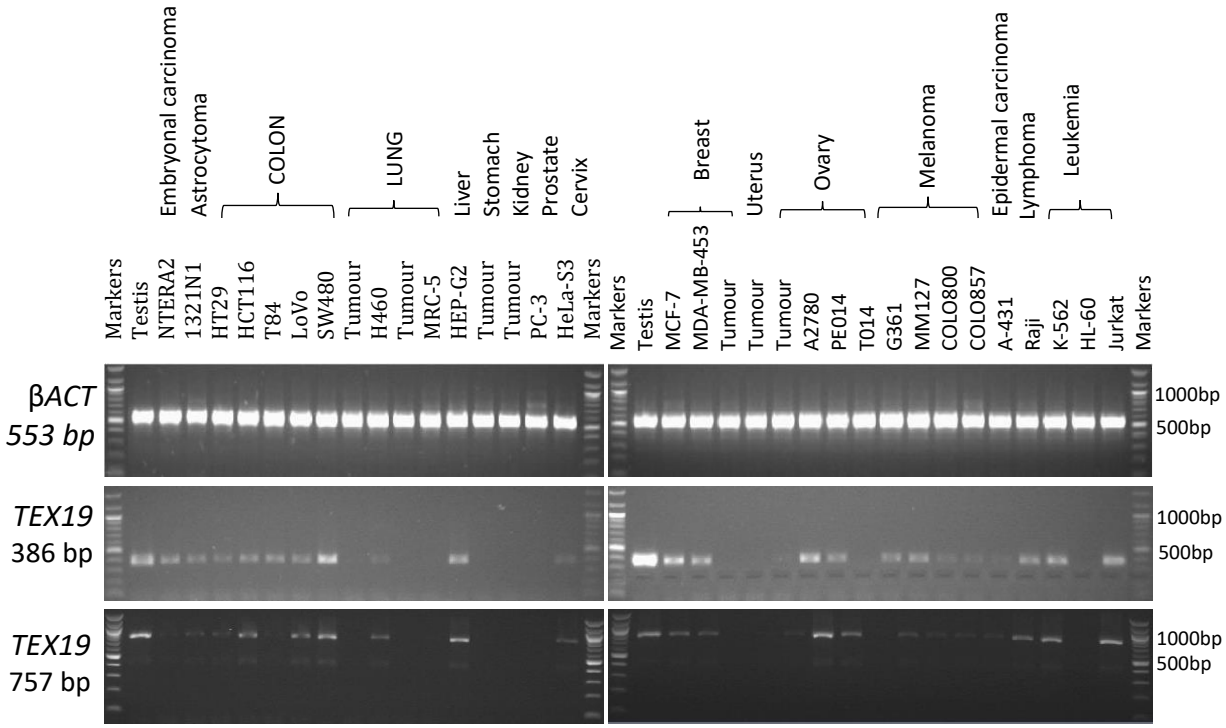

Figure 3.3 RT-PCR of potential CTA gene *TEX19* using human normal tissues. PCR product of *TEX19* gene observed on the agarose gel in the expected size. β*ACT* was used as a control for the cDNA quality.

3.2.2 Evaluation and validation of candidate CT genes in normal tissues using RT-PCR analysis

Candidate genes were analysed using RT-PCR on RNA extracted from 21 normal human tissues to assess their expression profile. According to RT-PCR results, some of these genes show multiple bands in many normal human tissues and therefore, they were classified as dismissed genes including *C20orf70*, *FAM166A*, *GLPRIL*, *SCHCP1* and *SYNGR-4* (Figure 3.4). The RT-PCR analysis show clear bands at the expected size (512 bp) of *C20orf70* in many normal tissues including testis, foetal brain, spinal cord, heart, lung etc. (Figure 3.4). DNA sequencing were performed from purified PCR product and confirm the identity of the gene in testis (Table 3.2) A band for *FAM166A* was observed at the expected size (468 bp) and multiple bands were detected in some normal tissues including testis, brain, foetal brain, spinal cord, heart, lung, thymus and trachea (Figure 3.4). DNA sequencing were performed and the identity of the gene confirmed in testis. However, DNA sequencing of lung sample did not confirm the gene identity (Table 3.2). Analysis of *SCHCP1* showed multiple bands, one at the expected size (720 bp) and others lower than the expected size (Figure 3.4). These bands were observed in some normal tissues including testis, brain, prostate, liver, skeletal muscle, uterus and ovary. Purified PCR product from testis and skeletal muscle samples were used for DNA sequencing and did not confirm the gene identity (Table 3.2).In addition, *SYNGR-4* analysis shows clear band in testis and multiple faint band in normal tissue in expected size (476 bp) including cerebrum, brain, spinal cord, prostate, bone marrow and skeletal muscle (Figure 3.4). DNA sequencing was performed from PCR purified product of testis confirm the identity of the gene. However, DNA sequencing of lung sample did not confirm the gene identity (Table 3.2). Finally, *GLPRIL* show several bands in many normal tissues including testis, cerebrum, brain, foetal brain, spinal cord, lung, prostate, skeletal muscle, uterus etc., some were detected in expected size (424 bp) and others were lower than expected size (Figure 3.4). The DNA sequencing from testis PCR product reveal the identity of the gene. However, DNA sequencing of skeletal muscle sample did not confirm the gene identity (Table 3.2).

RT-PCR analysis defined some candidate CT genes as testis-restricted genes including *BRDT, C5orf48, CCDC105, TCTE-3* and *TRIML-1* due to their confined expression in testis only. Analysis of *BRDT* expression show clear band in testis detected at the expected size

(691 bp) (Figure 3.5). In addition, *C5orf48* also show clear band in testis observed in expected size (389 bp) (Figure 3.5). Moreover, analysis of *CCDC105* expression show clear band in testis detected at the expected size (782 bp) and no expression was detected in somatic tissue (Figure 3.5). Moreover, *TRIML-1* show clear band in testis detected of the expected size (807 bp) and no band detected in the rest of normal tissue (Figure 3.5). Finally, analysis of *TCTE-3* show clear band in testis detected at the expected size (417 bp) (Figure 3.5). Purified PCR product from testis were used for DNA sequencing which confirm the identity of these genes (Table 3.2).

Based on RT-PCR analysis, some candidate CT genes were classified as testis-selective genes including *FTMT* and *IL-31* were expressed in testis and one somatic tissue. *FTMT* strong clear band in the testis and a faint band was detected in skeletal muscle and trachea (Figure 3.6) the observed band were at the expected size (423 bp) and DNA sequencing performed from testis sample confirm the gene identity (Table 3.2). In addition, *IL-31* show clear and strong band in testis and faint band in thymus (Figure 3.6) the observed band was detected at the expected size (362bp) and DNA sequencing of purified PCR product of testis did not confirm the gene identity (Table 3.2).

The expression of *PAPOLB* gene were analysed by RT-PCR and classed as testis-CNS restricted gene due to its confined expression observed in testis and cerebrum. The detected band was at the expected size (577 bp) for the testis. In addition, a faint expected size band were detected in cerebrum (Figure 3.7). PCR product were purified and DNA sequencing confirm the gene identity of testis sample (Table 3.2).

However, two candidate CT genes were classed as testis-CNS selective genes according to their expression profile assessed by RT-PCR including *CXorf27* and *CCDC54*. RT PCR analysis of *CXorf27* show clear band in testis were detected in expected size (304 bp) and faint band were at expected size in the brain, foetal brain, spinal cord and uterus (Figure 3.8). DNA sequencing confirm the identity of the gene (Table 3.2). In addition, RT PCR analysis for *CCDC54* showed a clear band for the testis at the expected size (681 bp) and a faint band in cerebrum, spinal cord, uterus and prostate were detected at the expected size (Figure 3.8). RT-PCR product were purified and DNA sequencing confirm the gene identity (Table 3.2)

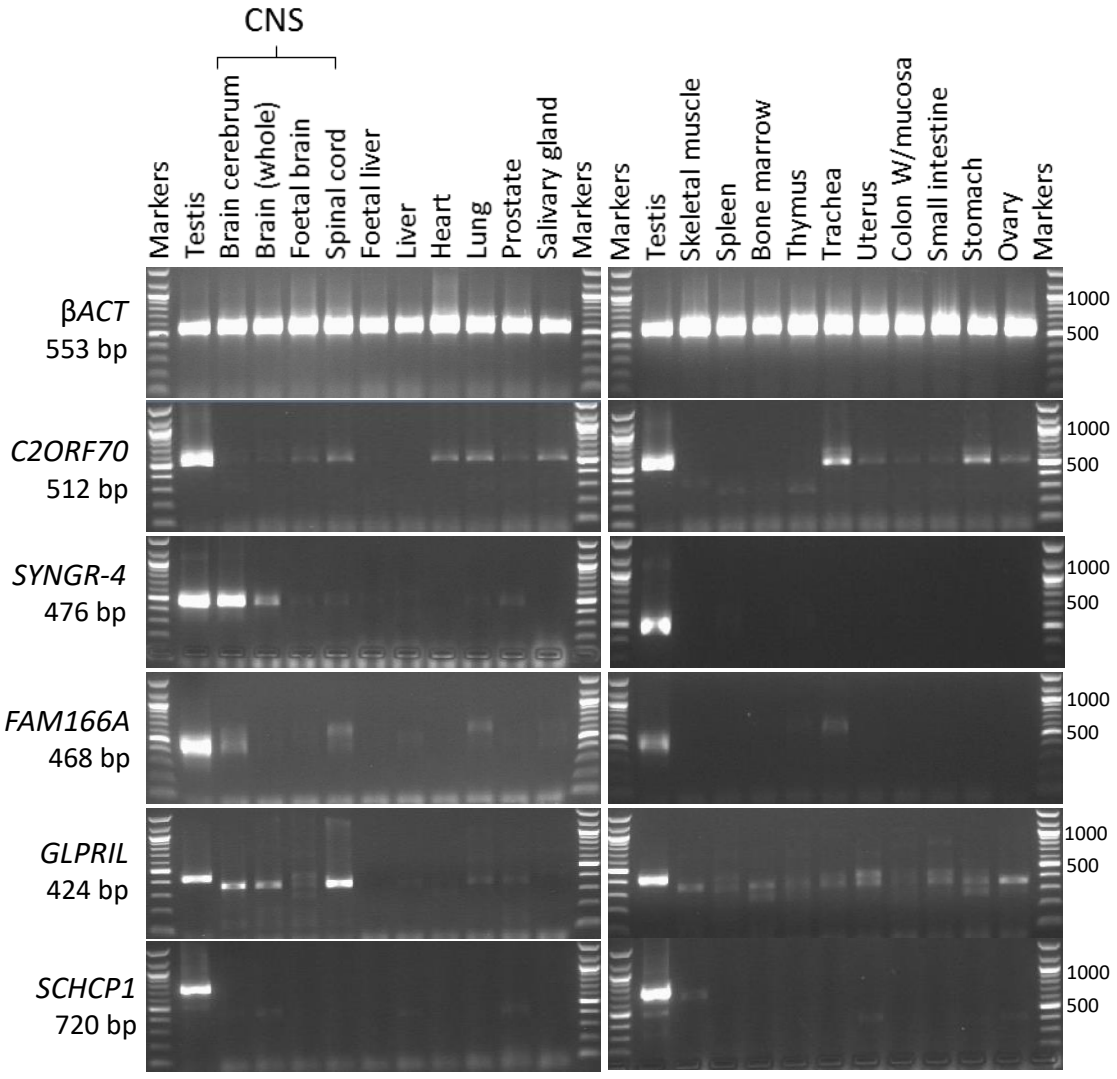

Figure 3.4 RT-PCR of excluded genes using human normal tissues. PCR product of *C20orf70, FAM166A, GLPRIL, SCHCP1*and *SYNGR-4* genes observed on the agarose gel at the expected size. β*ACT* was used as a control for the cDNA quality.

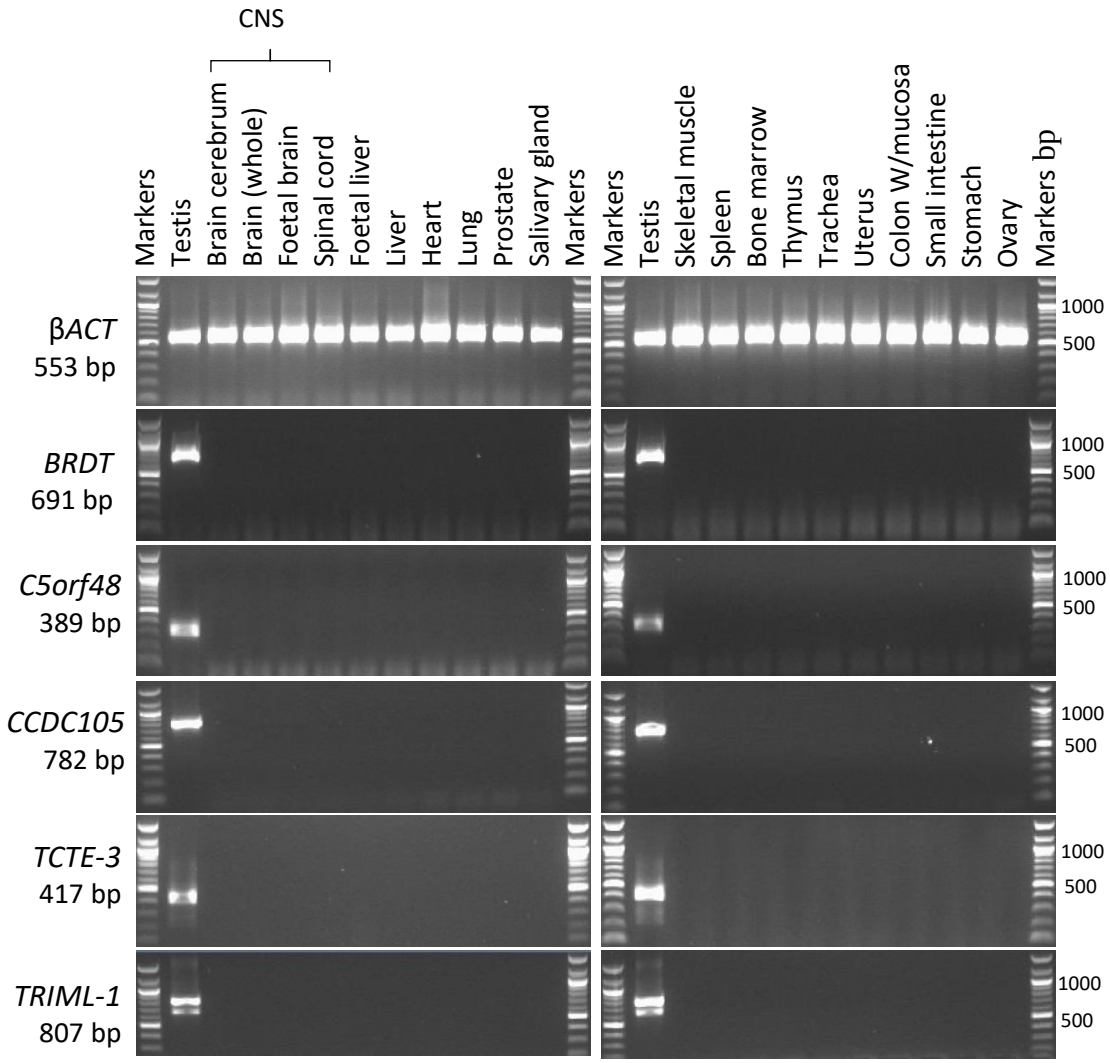

Figure 3.5 RT-PCR of predicted testis-restricted genes using human normal tissues. PCR product of *BRDT, C5orf48, CCDC105, TCTE-3* and *TRIML-1* genes observed on the agarose gel at the expected size. β*ACT* was used as a control for the cDNA quality.

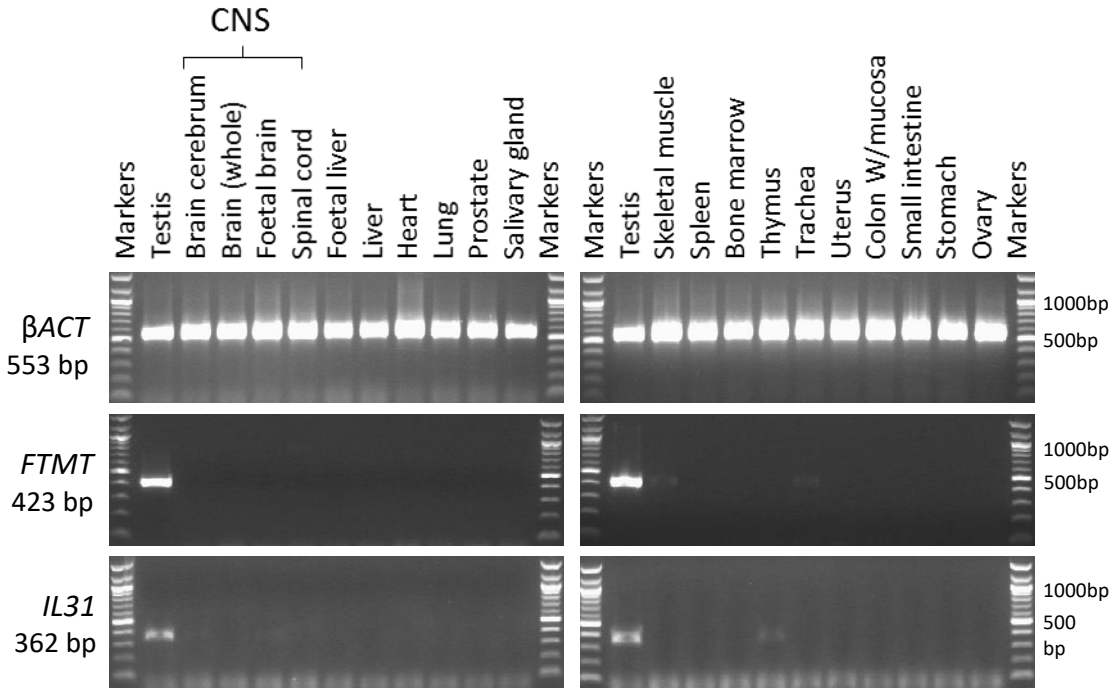

Figure 3.6 RT-PCR of some testis-selective genes using human normal tissues. PCR product of *FTMT* and *IL31* genes observed on the agarose gel at the expected size. β*ACT* was used as a control for the cDNA quality.

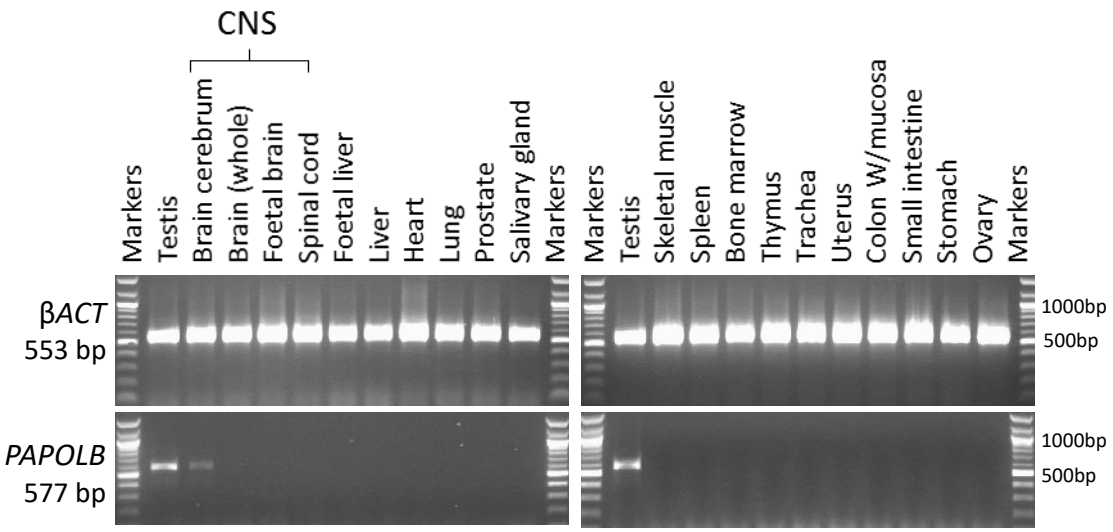

Figure 3.7 RT-PCR of testis-CNS restricted genes using human normal tissues. PCR product of *PAPOLB* gene observed on the agarose gel at the expected size. β*ACT* was used as a control for the cDNA quality.

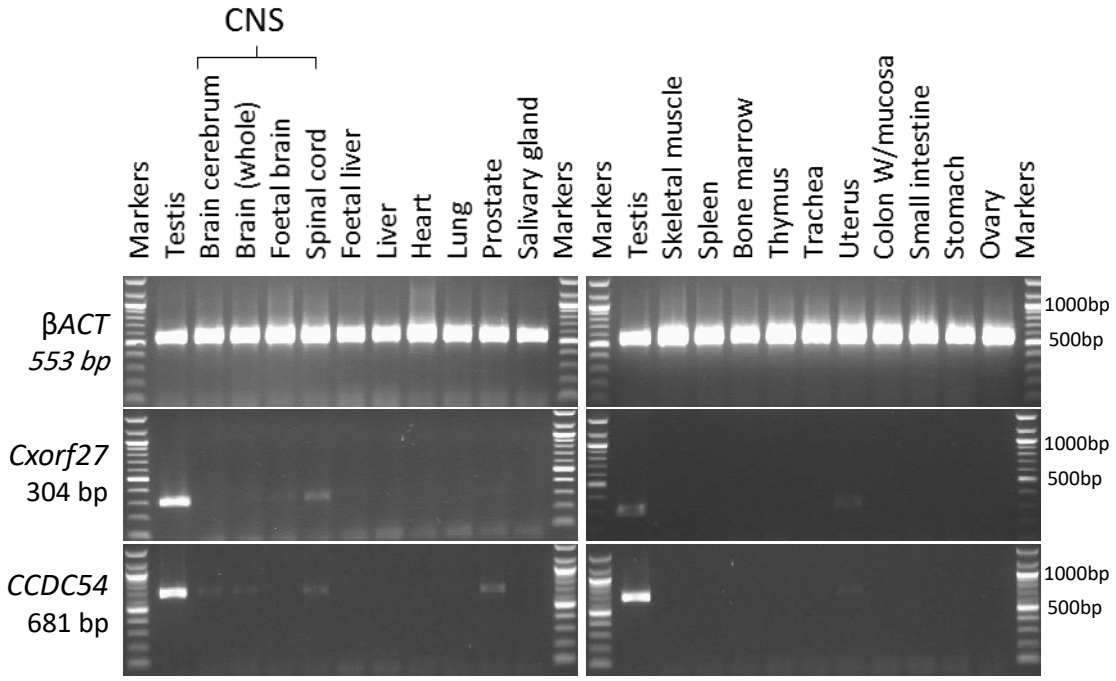

Figure 3.8 RT-PCR of testis-CNS selective genes using human normal tissues. PCR product of *CXorf27* and *CCDC54* genes observed on the agarose gel at the expected size. β*ACT* was used as a control for the cDNA quality.

3.2.3 Evaluation and validation of candidate CT genes in cancer cell-lines and tissues using RT-PCR analysis

RT-PCR analysis of testis-restricted genes including *BRDT, C5orf48, CCDC105, TCTE-3* and *TRIML-1* showed that no expression was detected in cancer tissues and cell-lines and although a clear band was detected for the testis.

The analysis of testis-selective genes including *FTMT* and *IL-31* in cancer tissues, show interesting result compared to normal tissue screening. RT-PCR analysis of *FTMT* showed a clear band was detected at the expected size (423 bp) in the testis and a faint band was detected in several types of cancer tissue panel such as colorectal cancer SW480, NTERA2, TO14 and astrocytoma cell-line 1321N1 (Figure 3.10). DNA sequencing performed from SW480 sample confirm the gene identity. However, RT-PCR analysis of *IL-31* showed a faint band for the prostate cancer cell-line PC-3 and SW480 at the expected size (362 bp) (Figure 3.10). DNA sequencing of purified PCR product from testis, PC-3 and SW480 failed to confirm gene identity (Table 3.2).

Based on RT-PCR analysis, *PAPOLB* was categorised as testis-CNS restricted gene. Expression analysis of *PAPOLB* showed a clear band in the testis was observed at the expected size (577 bp) While, in the cancer tissue, a faint band was observed at the expected size in testicular cancer NTERA-2 cell-line (Figure 3.11).

Interestingly, *CXorf27* was classed as testis-CNS selective gene according to RT-PCR analysis, which showed a clear band for the testis and some cancer tissues including breast cancer cell-line MCF-7, melanoma cell-line COLO857, lung cancer cell-line H460 and ovarian cancer cell-line PE014 (Figure 3.12).The band were detected at the expected size (304 bp). In addition, RT-PCR of *CXorf27* showed a faint band in some cancer tissues including NTERA2, colon cancer HT29, kidney tumour, liver cancer HEP-G2, lung cancer MRC-5, leukaemia K-562 and ovarian cancer T014. RT-PCR results show the band was at the expected size (304 bp) (Figure 3.12). DNA sequencing confirm the gene identity in testis. However, purified PCR product from HT29 were used for DNA sequencing did not confirm the gene identity.

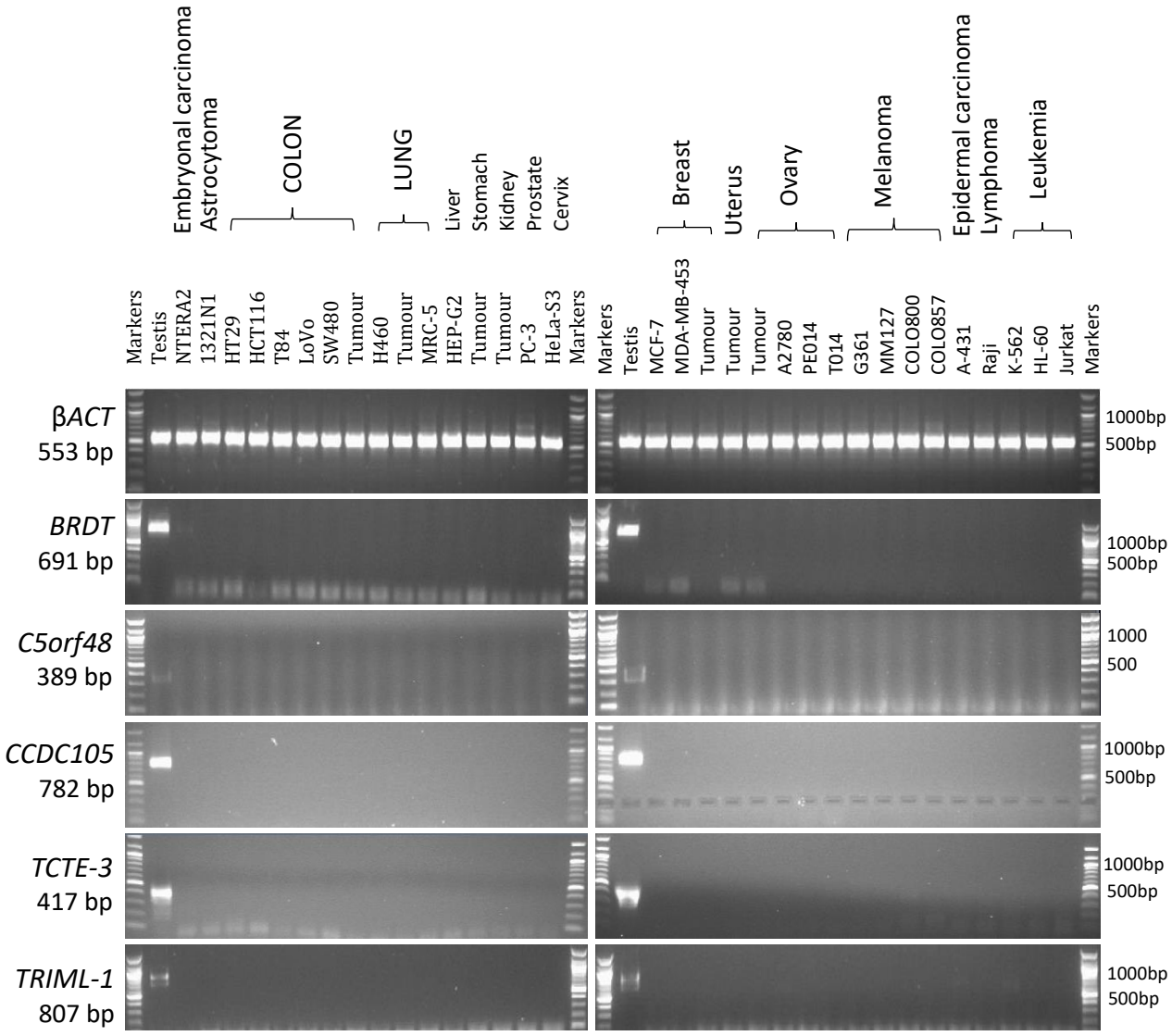

Figure 3.9 RT-PCR of some testis-restricted genes using human cancer tissues. PCR product of *BRDT, C5orf48, CCDC105, TCTE-3 and TRIML-1* genes observed on the agarose gel at the expected size. β*ACT* was used as a control for the cDNA quality.

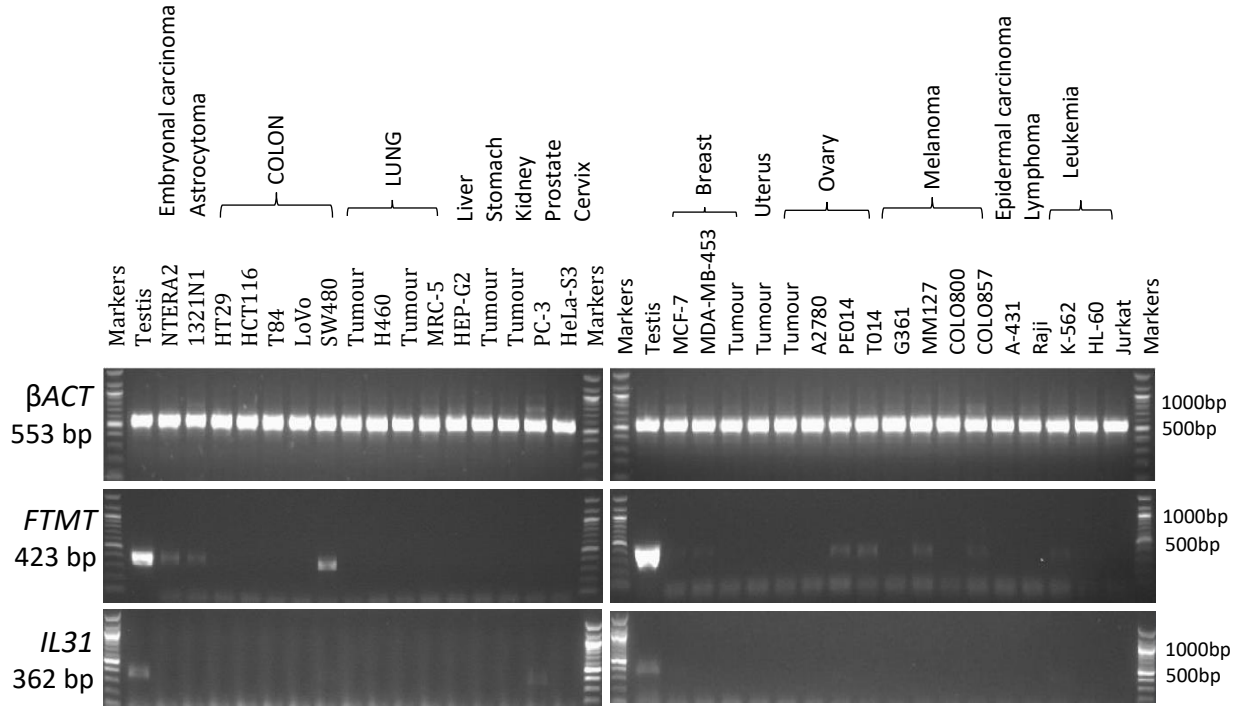

Figure 3.10 RT-PCR of some testis-selective genes using human cancer tissues. PCR product of *FTMT* and *IL31* genes observed on the agarose gel at the expected size. β*ACT* was used as a control for the cDNA quality.

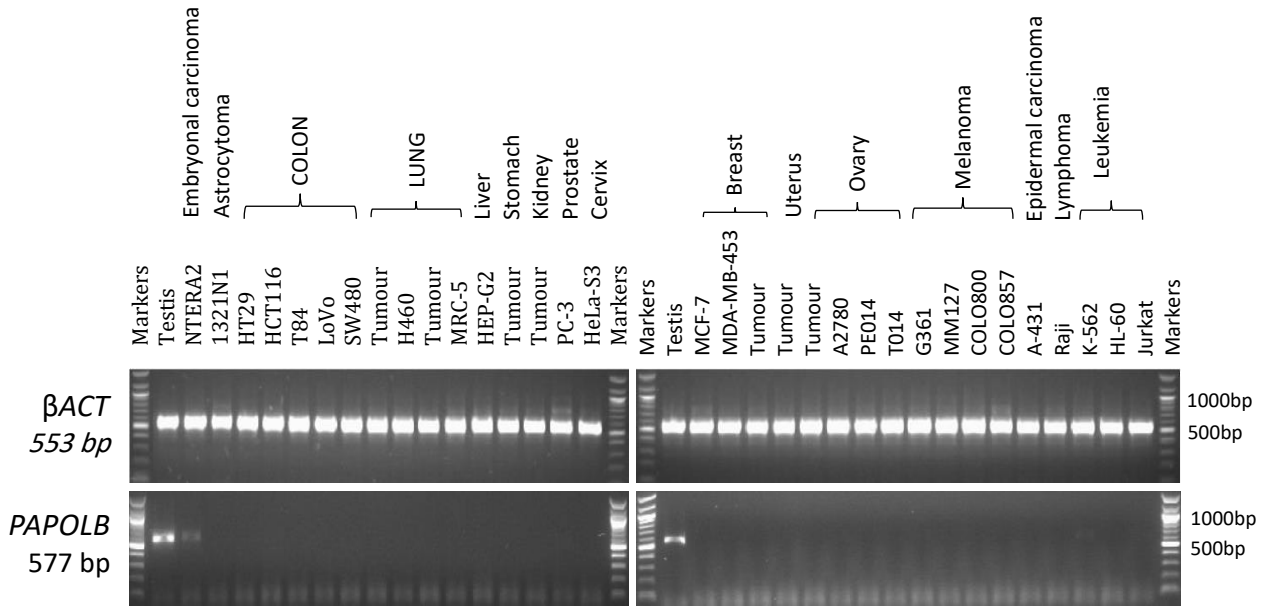

Figure 3.11 RT-PCR of testis-CNS restricted genes using human cancer tissues. PCR product of *PAPOLB* gene observed on the agarose gel at the expected size. β*ACT* was used as a control for the cDNA.

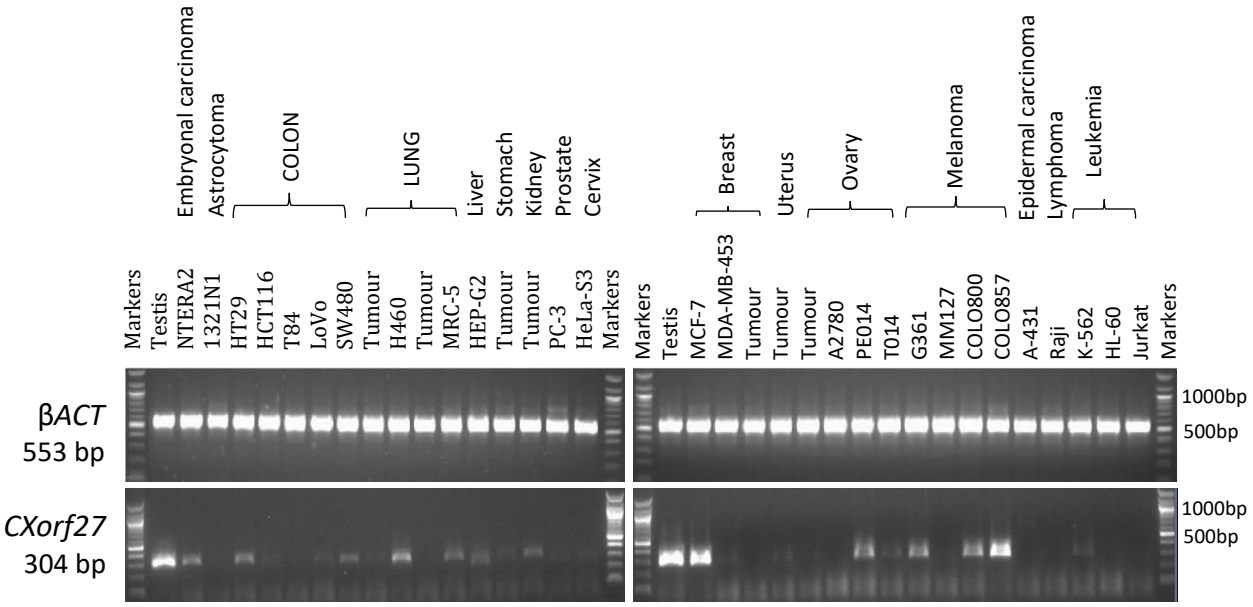

Figure 3.12 RT-PCR of testis-CNS selective genes using human cancer tissues. PCR product of *CXOFR27* gene observed on the agarose gel at the expected size. β*ACT* was used as a control for the cDNA quality.

Table 3.2 DNA sequencing of purified RT-PCR product of candidate CT genes from different human tissues.

GENE	TISSUE SOURCE	EXPECTED SIZE	APPROXIMATE OBSERVED SIZE	PRIMER	MWG RESULT	NCBI Blast Result
FTMT	testis	423	420	F	PASSED	Confirmed (**Query ID:** lcl|1223)
CXorf27	testis	304	300	F	PASSED	Confirmed (**Query ID:** lcl|2191)
CCDC54	testis	681	680	F	PASSED	Confirmed (**Query ID:** lcl|46537)
CCDC105	testis	782	780	F	PASSED	Confirmed (**Query ID:** lcl|49241)
TEX19	testis	386	385	F	PASSED	Confirmed (**Query ID:** lcl|56117)
PAPOLB	testis	577	580	F	PASSED	Confirmed (**Query ID:** lcl|58421)
SYNGR4	testis	476	475	F	PASSED	Confirmed (**Query ID:** lcl|39559)
TRIML1	testis	807	810	F	PASSED	Confirmed (**Query ID:** lcl|5389)
FAM166A	testis	468	470	F	PASSED	Confirmed (**Query ID:** lcl|60873)
C5orf48	testis	389	390	F	PASSED	Confirmed (**Query ID:** lcl|29855)
BRDT	testis	691	690	F1	PASSED	Confirmed (**Query ID:** lcl|12139)
IL31	testis	362	360	F	FAILED	Uncertain (**Query ID:** lcl|21455)
C2orf70	testis	512	510	F	PASSED	Confirmed (**Query ID:** lcl|55305)
GLIPR1L1	testis	424	425	F	PASSED	Confirmed (**Query ID:** lcl|62295)
TCTE3	testis	417	420	F	PASSED	Confirmed (**Query ID:** lcl|14837)
SHCBP1L	testis	720	720	F	FAILED	Uncertain (**Query ID:** lcl|1837)
FTMT	SW480	423	420	F	PASSED	Confirmed (**Query ID:** lcl|48449)
CXorf27	HT-29	304	305	F	FAILED	Uncertain (**Query ID:** lcl|10649)
GLIPR1L1	Skeletal muscle	424	425	F	FAILED	Uncertain (**Query ID:** lcl|18635)
SYNGR4	Lung	476	480	F	FAILED	Uncertain (**Query ID:** lcl|45731)
TEX19	SW480	386	390	F	PASSED	Confirmed (**Query ID:** lcl|29373)
FAM166A	Lung	468	470	F	FAILED	Uncertain (**Query ID:** lcl|38065)
SHCBP1L	Skeletal muscle	720	720	F	FAILED	Uncertain (**Query ID:** lcl|4003)
IL31	SW480	362	360	F	FAILED	Uncertain (**Query ID:** lcl|19989)
IL31	PC-3	362	360	F	FAILED	Uncertain (**Query ID:** lcl|52703)

3.3 Discussion

The expression profile of CT genes and their antigen association with some types of cancer indicate their oncogenic contribution. Therefore, further CTA classification and validation might enhance our understanding to approach cancer treatment.

3.3.1 Testis-restricted genes

Based on RT-PCR analysis and DNA sequencing data of testis-restricted genes, there expression was observed only in the testis and no detection was found in the normal and cancer tissue, which refer them as testis-specific genes including *BRDT, C5orf48, CCDC105, TCTE-3 and TRIML-1* (Figure 3.13 and Figure 3.13). *BRDT* gene is responsible for encode Bromodomain testis-specific protein, which plays an important role in mammalian transcription regulation and modification in normal tissue along with three other proteins including BRD2, BRD3 and BRD4 which collectively known as Bromodomain and extra-terminal (BET) (Lovén et al., 2013). However, recent study reveal oncogenic role of BET in some types of cancer. BET is involve in oncogenic activity through regulation of some oncogenes (Shi and Vakoc, 2014). In our study, BRDT expression was observed in testis only and no expression was observed in other normal and cancer tissue.

The importance of this class is their confined expression in testis, which resides in immune privilege through blood-testis barrier (BTB), where sertoli cells (SC) control and prevent immune cells and antibodies entry into testis lumen (Mital *et al*., 2011). Therefore, the possible use of testis-restricted genes to target some types of cancer through immunotherapy can be achievable due to testicular immune-privilege.

3.3.2 Testis-selective genes

In the testis-selective gene category, *FTMT* observed in the testis, skeletal muscle and trachea of the normal tissue (Figure 3.13) but show expression in various types of cancer tissue such as colon cancer cell-line SW480, ovarian cancer cell-line TO14 and brain cancer cell-line 1321N1 (Figure 3.14). The *FTMT* gene encodes Mitochondrial ferritin (FtMt) protein which is restricted in few human organs including the brain and testis (Drysdale et al., 2002). Overexpression of *FTMT* is observed in some neuro-degenerative diseases such as Alzheimer's disease (AD) (Altamura and Muckenthaler, 2009) and neuronal tumour cells, which involve in the inhibition of tumour growth without initiation of apoptosis (Shi et al., 2015).

The other gene in this category is *IL-31* show clear band in the testis and faint band in the thymus, cerebrum and foetal brain of normal tissue (Figure 3.13). While in cancer tissue a faint band for the prostate cancer cell-lines PC-3 and SW480 was observed (Figure 3.14). Based on DNA sequencing of *IL-31*from testis, PC-3 and SW480 tissues. The CT classification of *IL-31* is uncertain and its expression were inconclusive.

3.3.3 Testis-CNS restricted genes

The testis-CNS restricted gene *PAPOLB* show clear band in the testis and brain cerebrum of normal tissue (Figure 3.13). However, in the cancer tissue panel a faint band was observed in the NTERA-2 cancer cell-line (Figure 3.14). The significance of this class is the capability to target cancer via immunotherapy with least harm consequences for cancer patient. Because, CNS is protected by blood brain barrier (BBB) which consist of lining of endothelial cells forming tight junction to implement selective permeability and mediate the entry of immune cells and antibodies into the CNS (Neuwelt *et al*., 2011). In addition, there are supporting cells including astrocytes, neurons and pericytes which collectively forming neurovascular unit (NVU) to control the permeability to CNS (Muldoon *et al*., 2013). Moreover, deficiency of pericytes cause BBB failure, which consequently lead to neurodegeneration of the brain cells (Winkler *et al*., 2011). Therefore, the immune privilege feature of CNS allow to target some types of cancer using testis-CNS restricted genes, such as *PAPOLB,* without causing auto immunological damage to CNS.

3.3.4 Testis-CNS selective genes

In the category of testis-CNS selective gene *CXorf27* show a clear band in the testis and spinal cord, and show faint band in the whole brain, foetal brain and uterus of the normal tissue (Figure 3.13). In addition, expression was apparent in variety of cancer tissue such as testicular cancer NTERA-2, lung cancer H460, breast cancer MCF-7, ovarian cancer PE014 and melanoma COLO857 cancer cell-lines (Figure 3.14). These finding suggest the oncogenic role of *CXorf27* that may play. Therefore, these findings make this gene interesting as a potential biomarker and for gene therapy applications due to its relatively confined expression in the testis and CNS which characterised by their immune-privilege through blood brain barrier (BBB) of the CNS. However, the expression detected in the

uterus can be intervened surgically by hysterectomy as selective option in female patient in case gene therapy applicable.

3.3.4 Excluded genes

The excluded genes category as its name suggests, the RT-PCR analysis of *C2orf70, FAM166A, GLPRIL, SCHCP1*and *SYNGR-4* genes observed many signals in different normal tissue (Figure 3.13). Therefore, the RT-PCR analysis and validation of these genes in the human cancer tissue and cell-lines was not performed due to their expression profile in somatic tissues.

3.3.4 Meiosis-specific genes

The meiosis-specific gene *TEX19* showed clear expression in the normal testis and thymus, while repetition of the RT-PCR using intron-spanning primers showed clear expression only in the testis. Therefore, according to RT-PCR analysis, *TEX19* is testis-restricted/cancer CT gene (Figure 3.13). The RT-PCR analysis of *TEX19* in the cancer tissue show clear expression in different cancer tissue such as colon cancer SW480 and HT29, lung cancer H460, breast cancer MCF-7, ovarian cancer PE014 and A2780, leukaemia K562, melanoma COLO857 and liver carcinoma HEP-G2 cancer cell-lines (Figure 3.14). The activation of *TEX19* gene in many types of cancer tissue and its expression pattern make it a good candidate as CT gene according to the RT-PCR results and the DNA sequencing data.

The genetic expression of somatic cells to germline transition may involve stimulating oncogenic activity lead to continuous, numerous and uncontrolled mitotic cell divisions. This suggest a possible oncogenic contribution of one or more CTA genes in the absence of the whole germline genetic environment. The expression of some CT genes in cancer may suggest other different functions of these genes in somatic tissue. Moreover, they might contribute in tumour initiation/ progression (McFarlane et al., 2014).

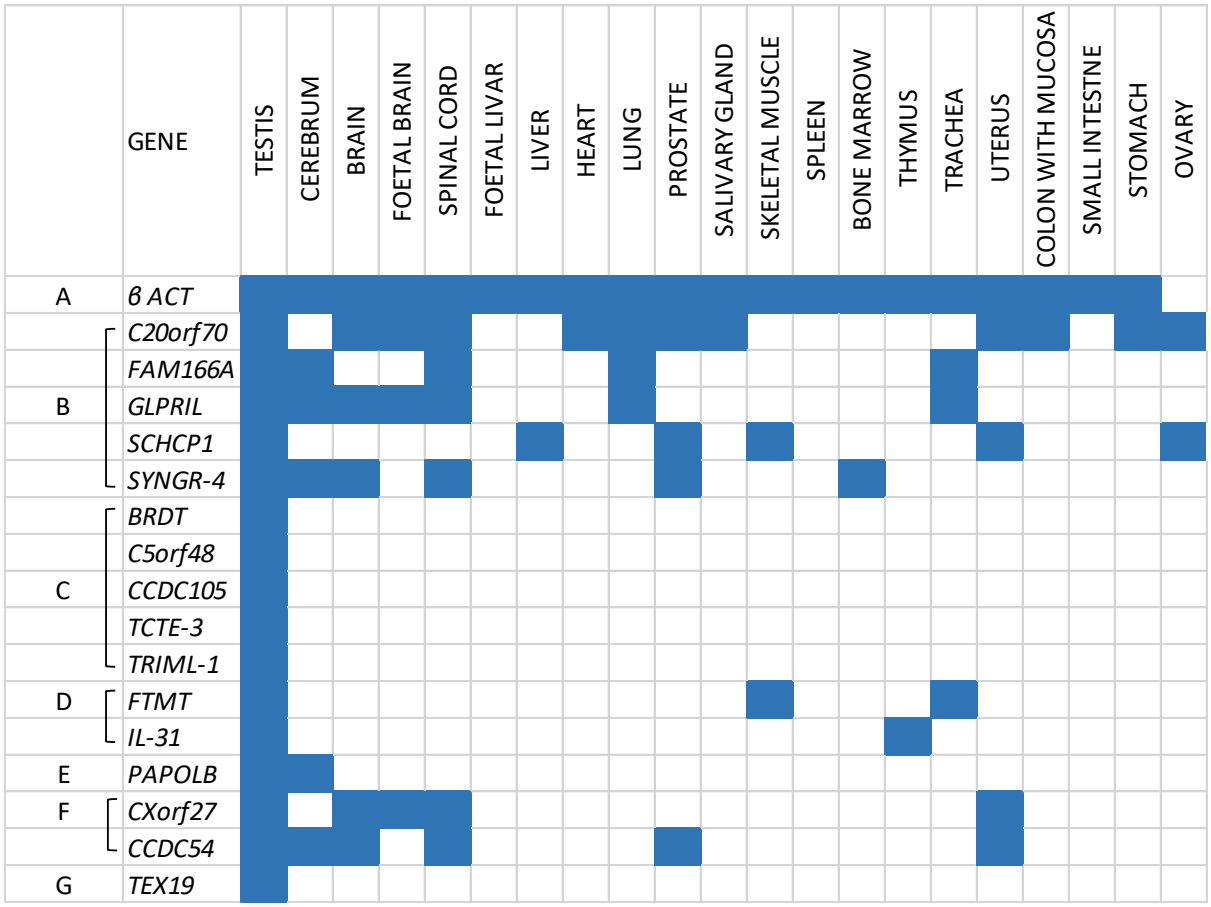

Figure 3.13 representation of RT-PCR analysis of tested genes in normal human tissue. The dark square reflect expression of the gene. (A) β Actin used as control for cDNA quality. (B) Excluded genes. (C) testis-restricted genes. (D) testis-selective genes. (E) testis-CNS restricted genes. (F) testis-CNS selective genes. (G) meiosis-specific gene.(*TEX19*)

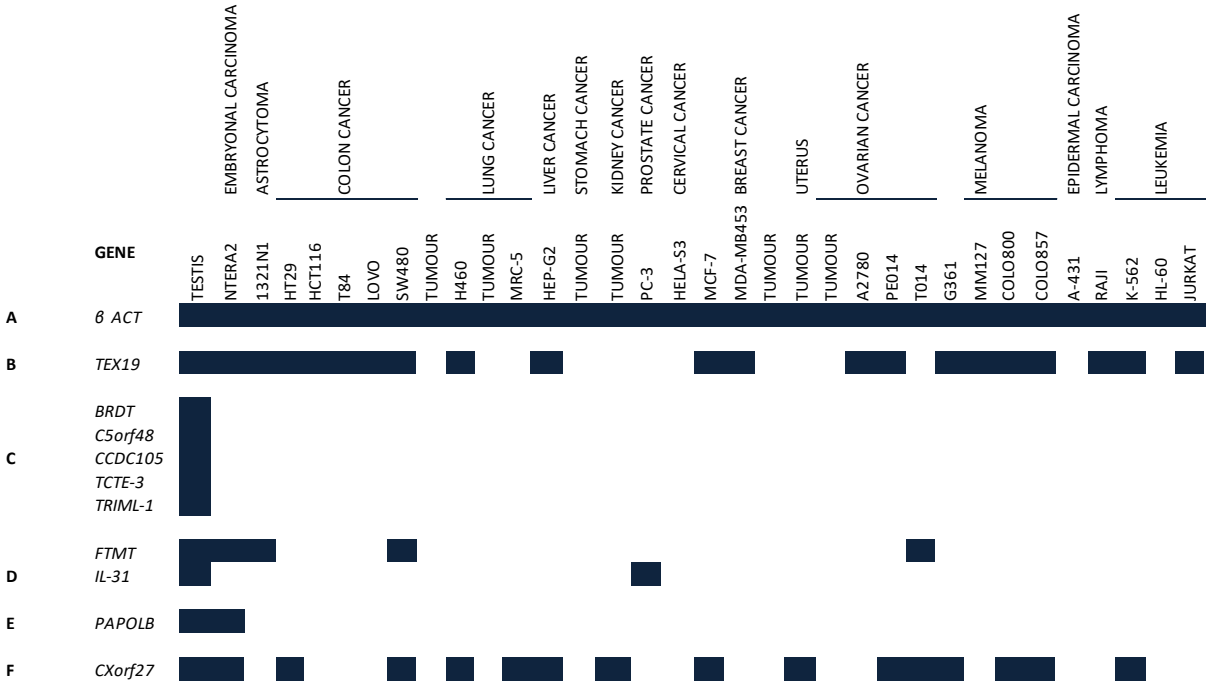

Figure 3.14 representation of RT-PCR analysis of tested genes in human cancer tissue. The dark square reflect expression of the gene. (A) β Actin used as control for cDNA quality. (B) meiosis-specific gene (C) testis-restricted genes. (D) testis-selective genes. (E) testis-CNS restricted genes. (F) testis-CNS selective genes.

3.4 Conclusion

The bioinformatics analysis pipeline tool provide us with a reliable interface platform to identify novel CTA genes and determine their precise expression in tissues. In addition, the identification and validation of these novel cancer biomarkers rises the questions of the function of these genes in normal and cancer cells, and suggest the unknown role of some of these genes that might play in some types of cancer. Moreover, the possible approach to use these genes in many clinical and research applications including cancer specific gene therapy, diagnosis and prognosis.

In this chapter, a new class of CTA named as mei-CT genes, show high immunological privilege rather than testis-restricted (Feichtinger *et al*., 2012). *TEX19* one of the novel meiCT gene show interesting expression pattern. This expression may indicate the oncogenic activity of *TEX19* gene in somatic tissue. Consequently, the possible approach to employ these genes as a target for cancer immunotherapy and their possible use in cancer prognosis and diagnosis.

Testis-CNS selective *CXORF27* gene, might be promising as target for diagnosis, prognosis and immunotherapy of cancer based on RT-PCR results and DNA sequencing data regardless its expression in uterus.

Chapter 4 A potential role for *TEX19* in regulation of stemness

4.1 Overview

The human teratocarcinoma-derived cell line NTERA2 consists of EC stem cells with property of pluripotency possessing the capability of differentiation induced by retinoic acid, forming different types of cells such as post-mitotic neurons (Andrews *et al.* 1984b; Andrews, 1984; Rend *et al.*, 1989; Pleasure *et al.*, 1992; Squires *et al.* 1996). In fact, the induction of differentiation of EC stem cells has been described for the association of specific changes in gene expression of cell surface antigens (Ackerman et al. 1994). The differential expression of surface antigens serves as an effective method for monitoring cell differentiation (Fenderson *et al*. 1987). In this context, for example, NTERA2 cells have the characteristic expression of surface antigens including SSEA3 and SSEA4, but lacking expression of SSEA1 (Andrews *et al*., 1996). Moreover, these cells also show the expression of antigens TRA-1-60 and TRA-1-81 (Andrews *et al*. 1984a; Badcock *et al.* 1999) along with other antigens TRA-2-49 and TRA-2-54 (Andrews *et al*. 1984c). In case of retinoic acid as differentiation inducer all the expressed antigens described above are down regulated coupled with the expression of other silent genes such as SSEA1 and many other gangliosides glycolipid antigens, playing important role in differentiating different subsets of cells (Fenderson *et al.* 1987). Differentiation induced by HMBA also results in downregulation of the antigens induced HMBA are different by those induced by retinoic acid do which strengthens the view that HMBA and retinoic acid induce differentiation in distinct cell lineages (Andrews *et al.* 1990). Therefore, retinoic acid and HMBA holds much potential for cancer therapy by inducing reprogramming of EC stem cell lines in controlling tumour growth.

4.1.1 Cancer-testis antigens (CTAs) and Stem Cells

The expression of CTA genes has also been described in some types of stem cells such as CD34+ hematopoietic stem cells (Steinbach *et al.*, 2002), *Mesenchymal stem* cells (MSCs) of different fetal and adult tissues (Cronwright *et al.*, 2005; Saldanha-Araujo et al., 2010) and different ES cell lines (Lifantseva *et al*., 2011). However, the functional role of these CTAs in the stem cells remains to be defined yet, but some evidences suggests a potential role of

some CTA in self-renewal capability of stem cells during the early phases of embryonic development. In addition, it has been postulated that the expression of CTAs is limited only to the cells of a cancer tissue which possess stem cell properties (Ghafouri-Fard and Modarressi, 2009; Ghafouri-Fard *et al.*, 2012a).

Evidence of a higher expression of CTA genes in CSCs compared to differentiated cells were revealed from epigenetic studies, shows promoters hypomethylation of CTA genes and higher acetylation of histones in CSCs compared with differentiated cells (Yawata *et al.*, 2010). Therefore the CSCs with a higher expression of CT genes possess great potential in providing special therapeutic targets for treatment of cancer recurrences and metastasis (Ghafouri-Fard, 2012a; Ghafouri-Fard and Modarressi, 2012). Moreover, in certain tumour types, the CTA genes have been investigated as immunotherapy targets against CSCs (Yawata *et al*., 2010). However, it will be of much significance that the MSCs potential for possessing CTA genes as target for such therapies could be established.

A study on mouse suggest that *TEX19.1* (one of two isoforms in mouse and related to human *TEX19* gene) may play a role in the self-renewal of pluripotent stem cells self-renewal. This proposal based on localisation of Tex19 protein in mouse ES cell nucleus using immunofluorescence technique (Kuntz *et al*., 2008). Moreover, our data show a link between some CTAs genes such as *TEX19* and stem cells in human cancer tissue, but the functional role and more characterisation are yet achieved.

4.2 Results

4.2.1 Correlation of stem cell markers with TEX19 knockdown

Based on *TEX19* expression profile in cancer cells (Chapter 3)

We validate Tex19 antibody used by knockdown of *TEX19* in SW480 cancer cell-line using four different siRNAs. The protein level of Tex19 were observed in the untreated cells along with the non-interference RNA, which serves as negative control. However, no (or low) protein signals of Tex19 protein were detected in the four *TEX19* siRNAs that were used to knockdown protein level. And, the detected protein signals of Tubulin were similar in all samples (Figure 4.1) consistent three experiments were performed.

To determine whether there was a correlation between *TEX19* and stem cell marker expression in NTERA2 cells we knockdown Tex19 with one of the of *TEX19* siRNAs, (HS_FL35767_6) in NTERA2 cancer cell-line and quantify the expression of stem cells markers using qRT PCR.. *TEX19* expression was significantly decreased in the siRNA treated cells compared to both untreated and non-interference RNA samples. With *TEX19* knockdown, a significant decrease of *OCT4* expression was observed compared to untreated and non-interfering samples. This finding was consistent with the analysis of further stemness markers, *SOX2, NANOG, PIWIL1 and PIWIL2* (Figure 4.2) The experiment were done once for *PIWIL1 and PIWIL2*. Therefore, based on qRT-PCR results, there might be a correlated expression between *TEX19* and stem cell markers such as *OCT4*, *SOX2* and *NANOG*.

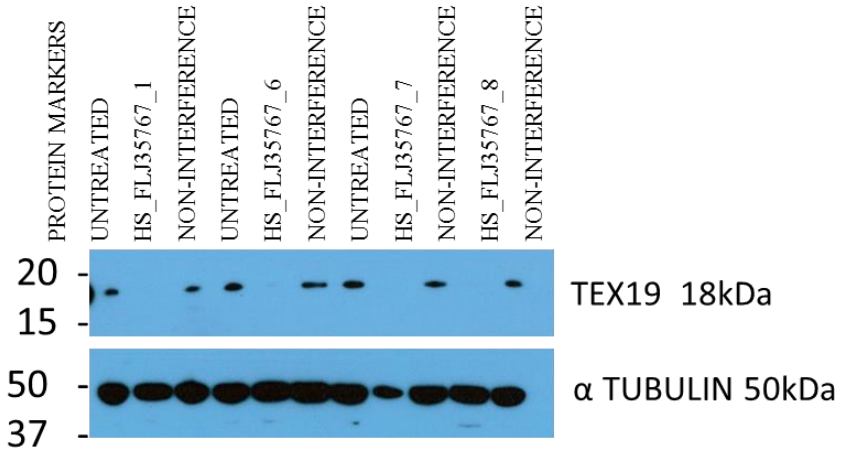

Figure 4.1 Knockdown of *TEX19* in SW480 cancer cell-line using four siRNAs. It shows all siRNA work to knockdown Tex19 in SW480 cells. Untreated and Non-interference samples work as negative control. α tubulin was used as a loading control for our western blot. Protein markers (kDa).

Table 4.1: quantification of western blot bands of Figure 4.1 including 4 *TEX19* siRNA, Non-interference RNA and Untreated samples. P value <0.01

Sample	Tubulin Density	Tubulin Peaks	Tex19 Density	Tex19 Peaks	p value
HS-1	10051.775	13.948	28.243	0.013	0.005271924
HS-6	10012.534	13.587	74.607	0.015	0.004455708
HS-7	4144.861	5.573	14.536	0.007	0.005792518
HS-8	9472.3	12.676	5.799	0.003	0.001108174
Ni-1	9864.802	11.901	4472.82	2.104	
Ni-6	10201.332	13.012	6852.941	3.224	
Ni-7	9450.001	12.802	5901.113	2.776	
Ni-8	9420.321	12.001	5448.527	2.563	
Un-1	9650.832	11.335	4113.426	1.935	
UN-6	10123.666	12.922	7094.698	3.337	
UN-7	10113.121	13.202	7743.941	3.643	

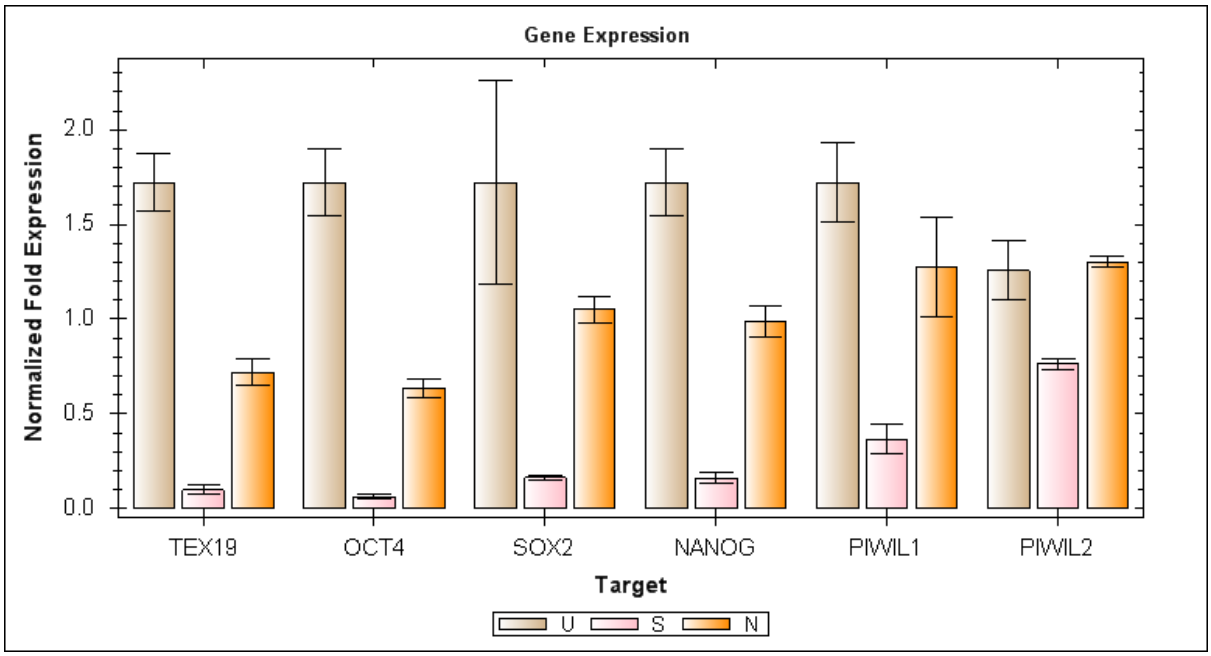

Figure 4.2 qRT-PCR of *TEX19* knockdown (S) in NTERA2 cancer cell-line with quantification of expression of some stem cell marker genes including *OCT4, SOX2, NANOG*. Untreated (U) and non-interfering (N) samples work as a control

Table 4.2 qRT-PCR of *TEX19* knockdown (S) in NTERA2 cancer cell-line with quantification of expression of some stem cell marker genes including *OCT4, SOX2, NANOG*. showing quantification cycle reading (Cq) and standard deviation reading (SEM). The readings were normalised against *TUBULIN* and *LAMIN*. siRNA sample (S), untreated sample (U) and non-interfering sample (N)

Target	Sample	Expression	Expression SEM	Corrected Expression SEM	Mean Cq	Cq SEM
LAMIN	N				21.93	0.03062
LAMIN	S				21.24	0.00951
LAMIN	U				24.09	1.45737
NANOG	N	0.84918	0.07009	0.07009	24.83	0.11586
NANOG	S	0.14750	0.02735	0.02735	27.06	0.25442
NANOG	U	2.73833	1.42665	1.42665	24.25	0.18320
OCT4	N	0.71308	0.05378	0.05378	23.52	0.10526
OCT4	S	0.07489	0.01414	0.01414	26.47	0.25956
OCT4	U	2.73833	1.43723	1.43723	22.69	0.20488
PIWIL1	N	0.90584	0.15618	0.15618	33.86	0.24721
PIWIL1	S	0.31215	0.07112	0.07112	35.10	0.31817
PIWIL1	U	2.73833	1.48543	1.48543	33.37	0.28474
PIWIL2	N	1.26848	0.02992	0.02992	25.06	0.02003
PIWIL2	S	0.78967	0.04974	0.04974	25.44	0.03795
PIWIL2	U	1.70924	0.91043	0.91043	25.74	0.24318
SOX2	N	1.10442	0.07606	0.07606	28.90	0.09547
SOX2	S	0.18206	0.01731	0.01731	31.20	0.10956
SOX2	U	2.73833	1.47477	1.47477	28.70	0.26892
TEX19	N	0.70285	0.06602	0.06602	34.02	0.13270
TEX19	S	0.10060	0.02602	0.02602	36.52	0.36384
TEX19	U	2.73833	1.38945	1.38945	33.17	0.06697
TUBULIN	N				18.41	0.04572
TUBULIN	S				18.50	0.16485
TUBULIN	U				18.47	0.04023

4.2.2 Evaluation of TEX19 in differentiated NTERA2 cells using RA and HMBA

With *TEX19* knockdown in NTERA2 cancer cells, we observe consequential reduction of *OCT4* expression in our previous experiment. This suggest a functional association between *TEX19* and stemness. To determine if Tex19 protein is correlated with Oct4, we carried out differentiation of NTERA2 using HMBA and RA conditions. Undifferentiated and DMSO conditions were used as a control in this experiment.

After differentiating NTERA2 using HMBA and RA, the protein level of Tex19 was similar and no changes were observed during the differentiation over 6 days in the four conditions including untreated, DMSO, RA and HMBA protein lysate of cells (Figure 4.3). Similar results were observed for the Tubulin protein, where the level of tubulin protein signals were detected in all conditions from day 1 to day 6, which is consistent with the number of cells, acquired for the extraction of protein lysate of the samples (Figure 4.5). However, a gradual decrease in the protein level of OCT4 were observed throughout the differentiation of NTERA2 with RA and HMBA indicating successful differentiation had been induced. After four days of the differentiation, no Oct4 protein could be detected in both differentiated samples (Figure 4.4).

The effect of the differentiation process on the growth rate of NTERA2 cells was noted due to the reduction of cell proliferation and driving the cells to differentiate. The proliferation rate of the untreated cells and DMSO was high compared to the cells differentiated with RA and HMBA (Figure 4.6) The experiment was repeated three times for reproducibility of the results.

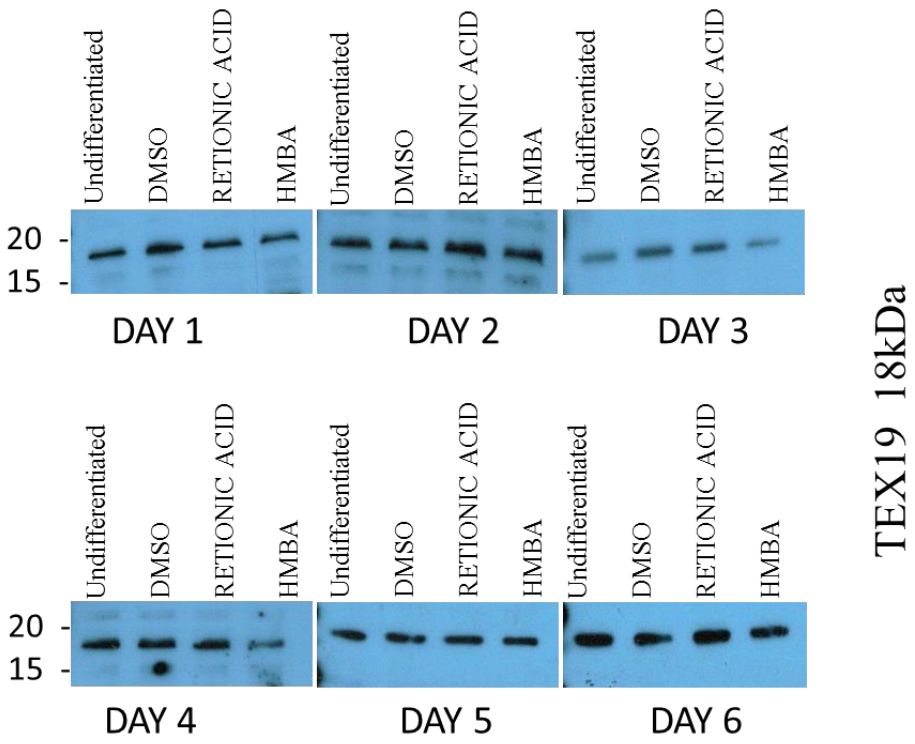

Figure 4.3 differentiation of NTERA2 cancer cell-line using RA and HMBA over six days show Tex19 unaffected after the differentiation. Undifferentiated samples work as a control and DMSO work as a control for the differentiated RA samples. Protein markers (kDa) and Undifferentiated sample work as loading control.

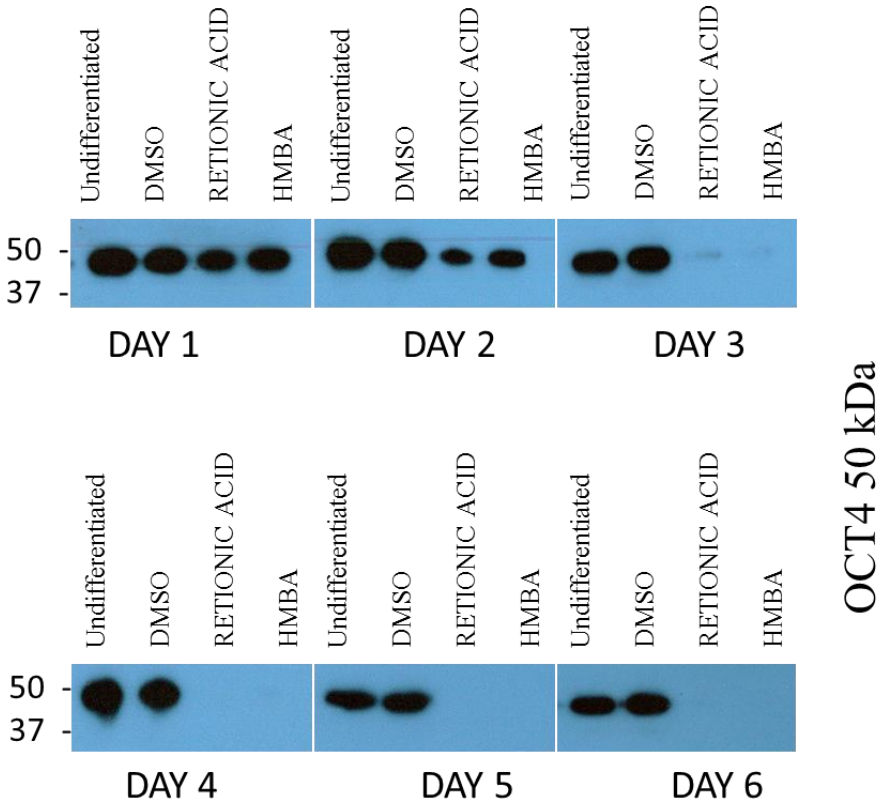

Figure 4.4 Differentiation of NTERA2 cancer cell-line using RA and HMBA over six days show Oct4 decreased from day 2 and no signals observed after day 4 of the differentiation. Undifferentiated samples work as a control and DMSO work as a control for the differentiated RA samples. Protein markers (kDa)

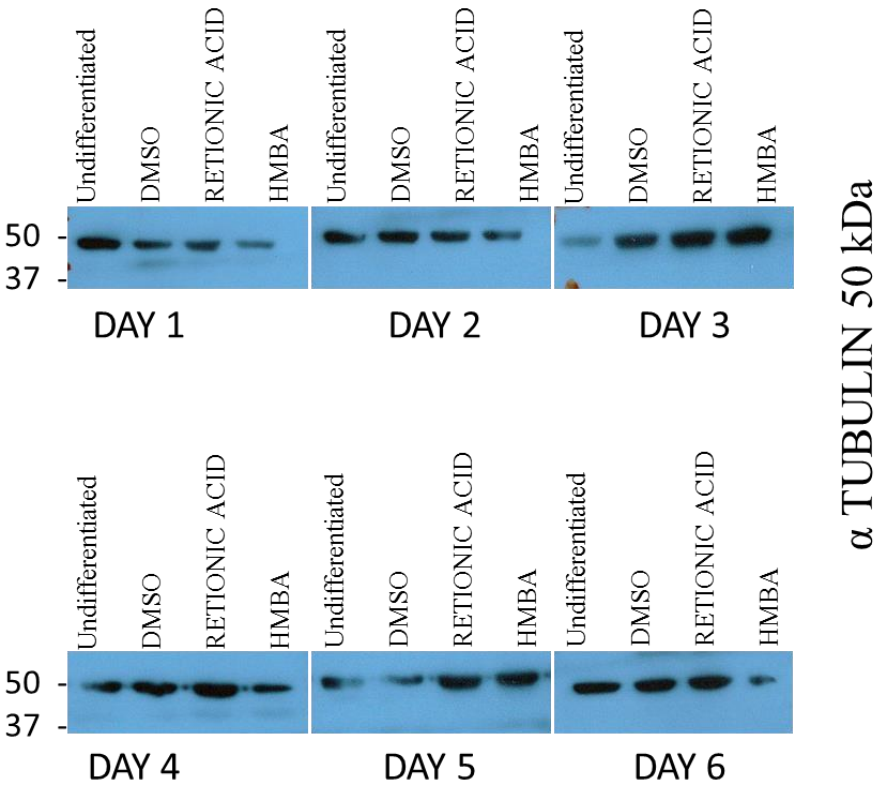

Figure 4.5 Differentiation of NTERA2 cancer cell-line using RA and HMBA over six days show αTubulin signals consistence through the course of differentiation indication level of protein loading. Undifferentiated samples work as a control and DMSO work as a control for the RA samples. Protein markers (kDa)

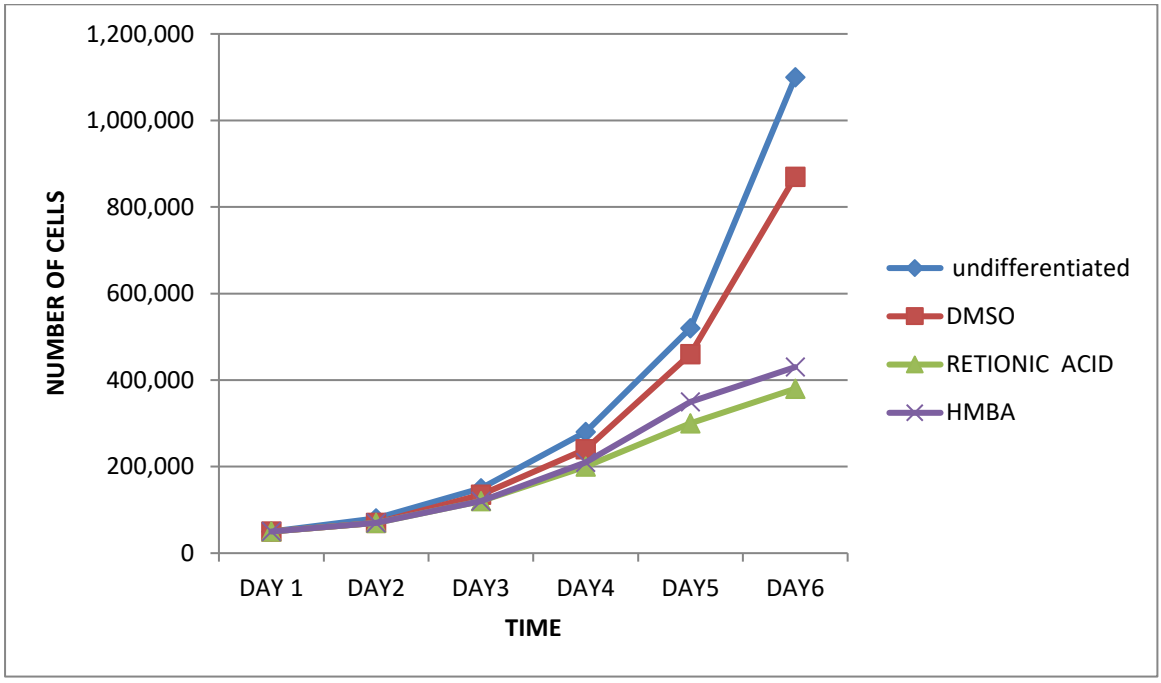

Figure 4.6 Graph show the proliferation rate of NTERA2 cancer cell-line during the differentiation using RA and HMBA over six days. Undifferentiated samples work as a control and DMSO work as a control for the RA samples.

4.2.3 Influence of *TEX19* on NTERA2 differentiation

To determine whether TEX19 control the ability of stem-like cells to undergo differentiation, we depleted TEX19 in NTERA2 cells followed by induction of differentiation. This achieved by siRNA-mediated depletion of *TEX19* in NTERA2 cells followed by differentiation using HMBA and RA for six days. Protein lysate were extracted for western blot and total RNA isolated to synthesis cDNA for qRT-PCR.

The expression level of stem cell marker genes such as *OCT4, NANOG* and *SOX2* declines with differentiation of cells with HMBA after *TEX19* knockdown compared to the untreated sample. This result was similar in all markers used including *OCT4, NANOG* and *SOX2*. Whereas, *TEX19* expression was decrease with differentiation using HMBA after *TEX19* knockdown comparing with the untreated sample (Figure 4.7) The experiment were repeated three times for reproducibility of the results. However, the Tex19 protein were detected in the HMBA differentiated sample after the knockdown and show no significant changes in the protein levels in both sample and the protein signals of HMBA treated cells were similar to the untreated one (Figure 4.9). In addition, Oct4 protein decreased in HMBA treated cells compared to the untreated cells. Similar tubulin protein levels were detected in both HMBA and untreated sample which as consistent with the number of cells used for protein lysate (Figure 4.9)

In contract, the differentiation of NTERA2 using RA after knockdown *TEX19* (were repeated three times for reproducibility) show an increasing level of *TEX19* expression comparing to the DMSO. While, stem cell markers expression were decreased in the differentiated cells using RA after *TEX19* knockdown comparing to DMSO treated cells. Expression of stem cell markers decreased including *OCT4, NANOG and SOX2* (figure 4.8). Interestingly, Tex19

protein was not detected in RA induced differentiation after *TEX19* knockdown compared to the DMSO treated cells regardless the overexpression detection of *TEX19* using qRT-PCR. Similarly, Oct4 protein was not detected in RA induced differentiation after *TEX19* knockdown (Figure 4.9). In addition, Tubulin protein levels were similar in both RA and DMSO samples.

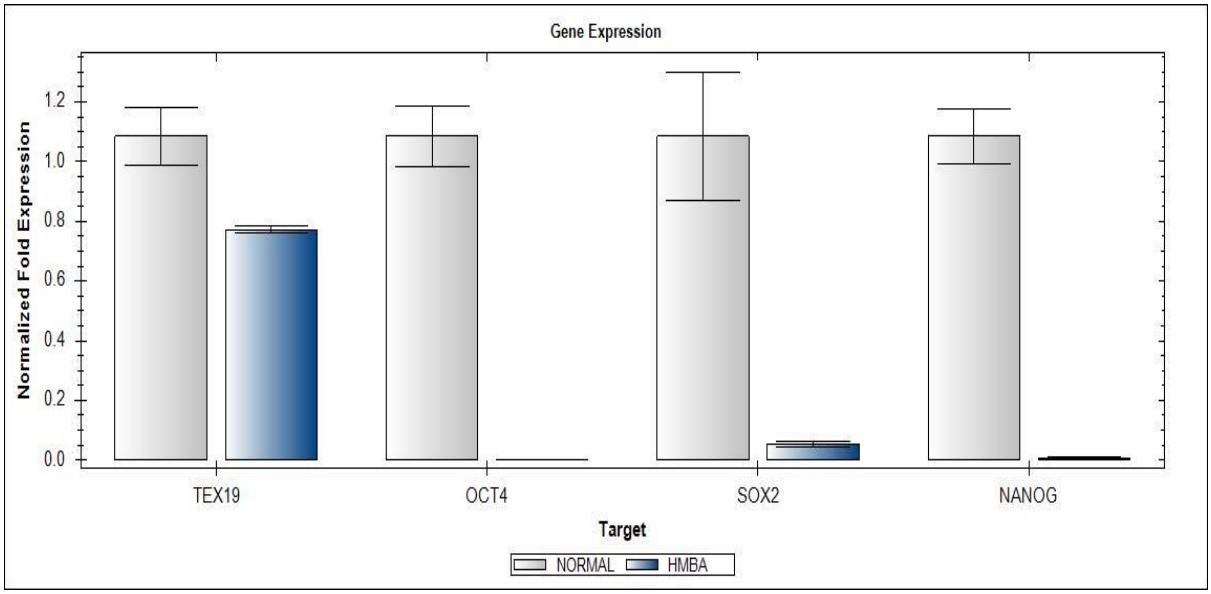

Figure 4.7: qRT-PCR results of differentiated NTERA2 cancer cell-line using HMBA after knockdown of *TEX19* and quantification of some stem cell markers including *OCT4, SOX2, NANOG*. Undifferentiated samples provide a control.

Table 4.3 *TEX19* knockdown followed by HMBA differentiation of NTERA2 cells. qRT PCR of some stem cell markers including *OCT4, SOX2, NANOG*. show quantification cycle reading (Cq) and standard deviation reading (SEM). The readings were normalised against *TUBULIN* and *LAMIN*. siRNA sample (S), untreated sample (U) and non-interfering sample (N)

Target	Sample	Expression	Expression SEM	Corrected Expression SEM	Mean Cq	Cq SEM
LAMIN	HMBA				25.04	0.02707
LAMIN	NORMAL				24.75	0.05291
NANOG	HMBA	0.00642	0.00221	0.00221	34.65	0.49508
NANOG	NORMAL	1.08468	0.09070	0.09070	27.22	0.03048
OCT4	HMBA	0.00172	0.00009	0.00009	32.75	0.07089
OCT4	NORMAL	1.08468	0.10179	0.10179	23.42	0.06861
SOX2	HMBA	0.05487	0.00914	0.00914	31.18	0.23941
SOX2	NORMAL	1.08468	0.21321	0.21321	26.85	0.25844
TEX19	HMBA	0.77171	0.01197	0.01197	30.07	0.01080
TEX19	NORMAL	1.08468	0.09500	0.09500	29.55	0.04838
TUBULIN	HMBA				20.06	0.02837
TUBULIN	NORMAL				20.30	0.22737

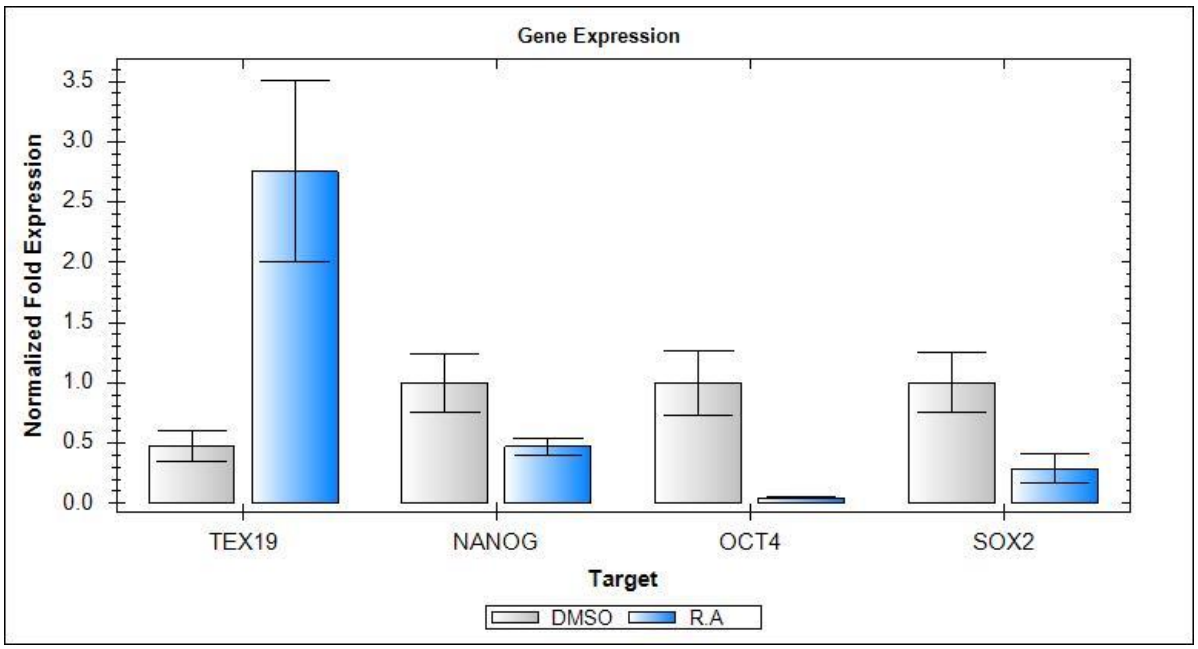

Figure 4.8: qRT-PCR results of differentiated NTERA2 cancer cell-line using RA after knockdown of *TEX19* and quantify some stem cell markers including *OCT4, SOX2, NANOG*. DMSO treated sample provide a control.

Table 4.4 show quantification cycle reading (Cq) and standard deviation reading (SEM). The readings were normalised against *TUBULIN* and *LAMIN*. siRNA sample (S), untreated sample (U) and non-interfering sample (N)

Target	Sample	Expression	Expression SEM	Corrected Expression SEM	Mean Cq	Cq SEM
LAMIN	DMSO				26.39	0.04243
LAMIN	R.A				28.40	0.37825
NANOG	DMSO	1.00000	0.24413	0.24413	27.03	0.02389
NANOG	R.A	0.47226	0.06813	0.06813	29.58	0.08539
OCT4	DMSO	1.00000	0.26571	0.26571	25.58	0.15321
OCT4	R.A	0.04446	0.00632	0.00632	31.53	0.07742
SOX2	DMSO	1.00000	0.25086	0.25086	29.60	0.08664
SOX2	R.A	0.28848	0.12302	0.12302	32.85	0.58519
TEX19	DMSO	0.47802	0.12911	0.12911	31.15	0.16841
TEX19	R.A	2.75489	0.74902	0.74902	30.09	0.31595
TUBULIN	DMSO				20.91	0.70151
TUBULIN	R.A				21.83	0.03200

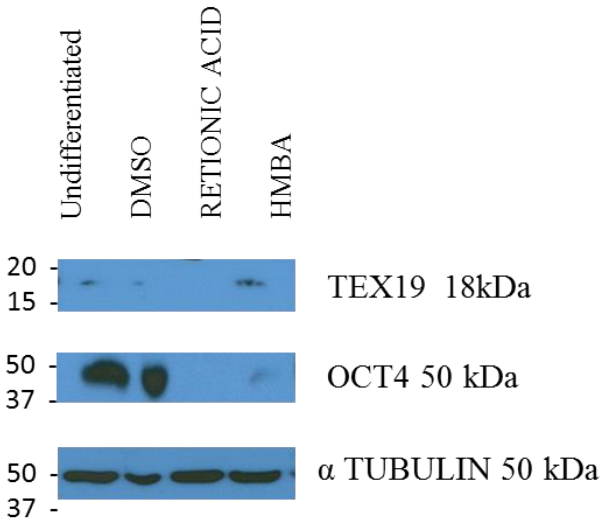

Figure 4.9 differentiation of NTERA2 cancer cell-line using RA and HMBA after knockdown of *TEX19*. Oct4 protein was detected in undifferentiated and DMSO samples. Tex19 was observed in undifferentiated and DMSO and HMBA treated samples. Undifferentiated samples provide a control and DMSO provide a control for the RA treated cells. Tubulin was used as control for loading.

Table 4.5: densitometry data of figure 4.9 shows reduction of Oct-4 in RA and HMBA compared with UT and DMSO p value <0.05 which reveal the significance of the Oct-4 reduction after differentiation. However, no significance of Tex19 in RA and HMBA samples compared with UT and DMSO p value <0.899

Sample	Tubulin density	Tubulin peaks	Oct-4 density	Oct-4 peaks	Tex19 density	Tex19 peaks
UT	31030.288	29.313	36704.874	64.996	4312.548	54.8
DMDO	16781.368	15.853	18664.811	33.051	749.163	9.52
RA	31716.158	29.961	0	0	0	0
HMBA	26330.459	24.873	1103.062	1.953	2807.941	35.681

4.2.4 Evaluate *TEX19* expression in IPSCs

In this experiment, IPSCs was prepared by Dr. Faisal Alzahrani, we carry out the knockdown of *TEX19* in IPSCs. The stem cell marker genes expression were uncorrelated with *TEX19* expression despite the previous experiment results using NTERA2 cell. Here, all stem cell marker genes including *OCT4, NANOG* and *SOX2* show high expression in the *TEX19* knockdown sample compared to the non-interference treated sample (Figure 4.10).

However, differentiate the IPSCs using RA show clear decline in stem cell marker genes expression including *OCT4, SOX2* and *NANOG* compared to the undifferentiated sample. Interestingly, the expression of *TEX19* was correlated with the inhibition of stem cell marker genes and show a decreasing of its expression compared to the undifferentiated sample (Figure 4.11)

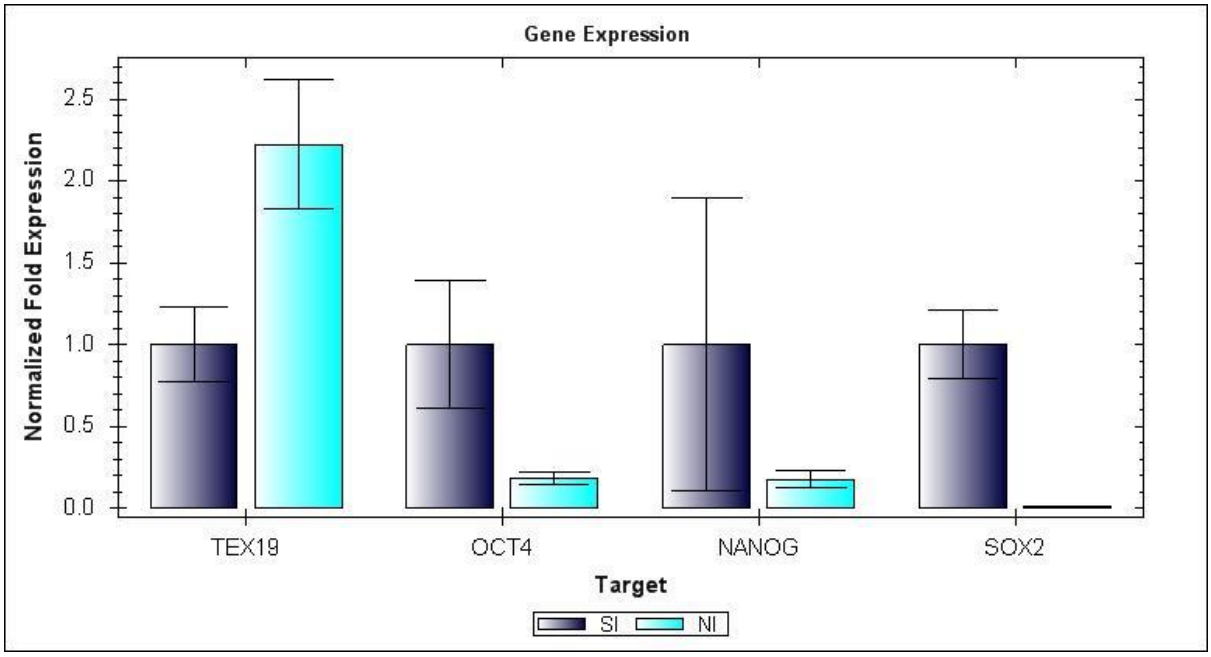

Figure 4.10: qRT-PCR of *TEX19* knockdown in IPSCs and quantification of stem cell marker genes *OCT4, SOX2* AND *NANOG*. Non-interfering sample was used as a control.

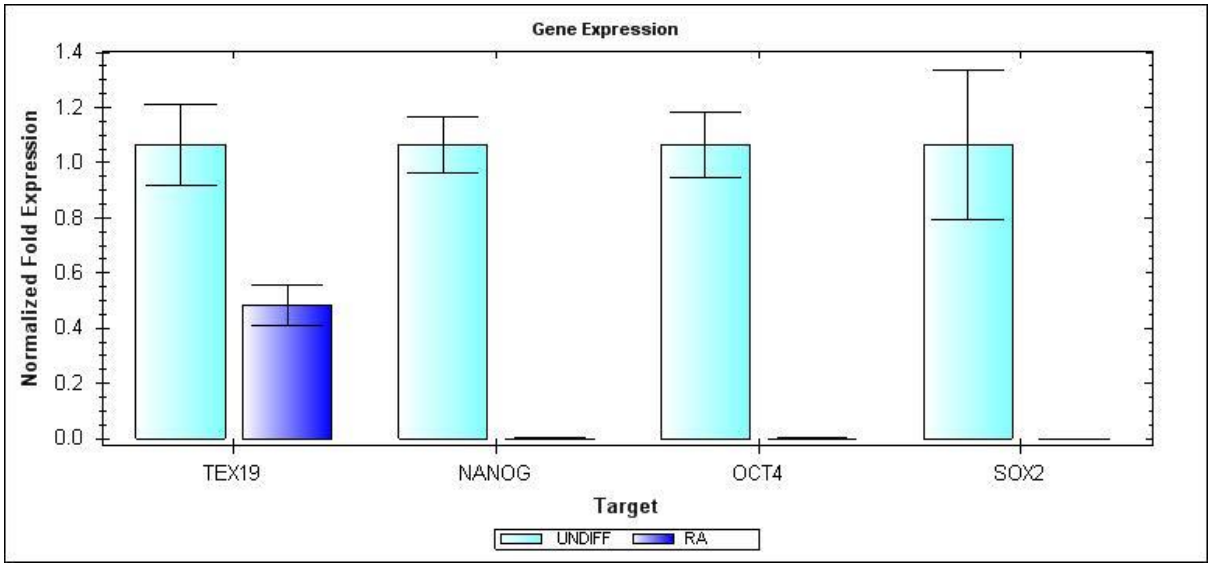

Figure 4.11: qRT-PCR of *TEX19* expression after differentiate IPSCs using RA over 6 days and quantification of stem cell marker genes *OCT4, SOX2* and *NANOG*. Undifferentiated sample was used as a control

Table 4.6 qRT-PCR of *TEX19* expression after differentiating IPSCs using RA over 6 days and quantification of stem cell marker genes *OCT4, SOX2* and *NANOG*. Quantification cycle reading (Cq) and standard deviation reading (SEM). The readings normalised against *TUBULIN* and *GAPDH*. siRNA sample (S), untreated sample (U) and non-interfering sample (N)

Target	Sample	Expression	Expression SEM	Corrected Expression SEM	Mean Cq	Cq SEM
GAPDH	RA				19.96	0.29670
GAPDH	UNDIFF				20.14	0.26976
NANOG	RA	0.00050	0.00019	0.00019	35.68	0.50452
NANOG	UNDIFF	1.06544	0.10007	0.10007	24.05	0.00277
OCT4	RA	0.00064	0.00009	0.00009	31.30	0.08560
OCT4	UNDIFF	1.06544	0.11654	0.11654	20.01	0.08094
SOX2	RA					
SOX2	UNDIFF	1.06544	0.27225	0.27225	27.39	0.34286
TEX19	RA	0.48237	0.07489	0.07489	33.92	0.13838
TEX19	UNDIFF	1.06544	0.14547	0.14547	32.19	0.14300
TUBULIN	RA				21.15	0.18994
TUBULIN	UNDIFF				19.79	0.02525

4.3 Discussion

An essential step for studying *TEX19* is to test and validate the antibodies in use. For this reason, we applied four different small interfering RNA including (HS_FL35767_1, HS_FL35767_6, HS_FL35767_7 and HS_FL35767_8) to knockdown *TEX19* to validate the specificity of our anti-Tex19 antibody (figure 4.1). Densitometry performed and reveal a significant knockdown of Tex19 in all four siRNA samples compared with untreated and non-interference samples with p value < 0.01.

Another important step in the characterisation of *TEX19* is applying different conditions and treatments including differentiated cells using HMBA and RA, and undifferentiated sample and DMSO sample control. In addition, we used non-interfering and untreated cells as a control for *TEX19* depletion.

Some research studies, investigate the relationship between *TEX19* and pluripotency in mice. One study carried out on *TEX19.1* knockout mice and observed no effect of *TEX19.1* deletion on the ability to grow unaffected ES cells. In addition, the stem cell marker genes were unaffected as well including Oct4, Nanog and Sox2 (Tarabay, *et al*., 2013). However, another study carried out in mouse pluripotent stem cells suggests a similar expression pattern between Tex19.1 and the stem cell marker Oct4 (Kuntz *et al.*, 2008). Therefore, to study the correlation of *TEX19* expression and stem cell markers in NTERA2, which represent a human cancer cell-line model that possess stem cell-like features; is important to understand this expression pattern.

The knockdown of *TEX19* in NTERA2 consequently affected expression level all stem cell marker genes including *OCT4, SOX2* and *NANOG*. This may suggest that expression of these genes in NTERA2 requires *TEX19*. In contrast, the expression of stem cell marker genes was

unaffected after *TEX19* knockdown in IPSCs, which suggests an independency of stem cells marker genes in the IPSCs from *TEX19* interaction, which is unlike the NTERA2 model.

The expression of *TEX19* was linked with stem cell markers after differentiation using RA in IPSCs. In which, the depletion of *TEX19* expression affected those markers; which may suggest a pluripotency regulation role for *TEX19* in IPSCs (Figure 4.11). However, Tex19 protein was detected after NTERA2 was differentiated with RA and HMBA (Figure 4.3) and the differentiation were succeeded and gradual decrease of Oct4 protein were observed after 24 hours of the treatment and no Oct4 detected from day 4 of western blot result (Figure 4.4).

While, in the NTERA2 model the differentiation with RA after knockdown *TEX19* show different result; where an increasing level of *TEX19* expression accompanied by decreasing expression of stem cell marker genes including *OCT4, NANOG* and *SOX2* (Figure 4.8). Which may due to a negative feedback loop mechanism activated due to the decreasing amount of Tex19 protein in NTERA2 cells that affected by the knockdown and/ or differentiation (Figure 4.9).

Unlikeness, differentiation NTERA2 cells with HMBA after *TEX19* knockdown show a decrease in expression for both stem cell marker genes and *TEX19*, which is consistence with the findings in the IPSCs experiment that suggest the hypothesized role of *TEX19* in regulation stemness (Figure 4.7). This conclusion does not contradict with negative feedback loop, were high *TEX19* expression accompanied by no protein detection in RA differentiation after *TEX19* knockdown in NTERA2 cells. This clearly seen in the Tex19 protein detected in HMBA differentiated cells after knockdown (Figure 4.9). Densitometry data reveal the significance of Oct-4 reduction after differentiating the cells using RA and HMBA p value <0.05. but, the knockdown of Tex19 with differentiation process show no significance change p value <0.899 (table 4.5).

5. Evaluation of the effect of *TEX19* depletion on transposable elements (TE) in cancer cells

5.1 Transposable Elements (TE)

Historically, repetitive genetic elements within the human genome were considered as 'junk DNA'. But after the discovery of TEs by Barbara McClintock, the importance of these elements has increasingly been recognized. TEs can modify gene structure and expression by the process of mobilization, transposition promoted ectopic rearrangements, reshuffle sequences all of which can result in conditions leading to genetic disease.

5.1.1 Introduction

On the basis of their distinct mechanism of transposition, the TEs are placed into two major classes, Class I and Class. The class I transposons are also known as retrotransposons and these elements mobilise by a 'copy and paste' mechanism, where the process of transposition involves an RNA intermediate which, after reverse transcription, is inserted at a new position in the genome. Examples include long terminal repeat (LTR) elements in the form of endogenous retroviruses (leftovers of viruses which lost their capability to be infectous) and non-LTR retrotransposons. These elements make approximately 8% of human genome and carryout reverse transcription as a cytoplasmic virus (Lander et al., 2001). Non-LTR retrotransposons adopt a different mechanism of transposition, where the RNA copies are reverse transcribed and integrated to the genomic DNA through a coupled process (O'Donnell and Burns, 2010). Class II or DNA transposons follow the mechanism of 'cut-and-paste' for their mobilization, which means the DNA part (transposon) is removed from a site and then inserted at a new location. TEs are relatively inactive in mammals, but accompanied with some exceptions such as a piggyBac element was first identified to be active in bats (Ray et al., 2008). The percentage of DNA transposons in human is as low as 3% of the genome (Lander et al., 2001).

The genome sequences of different mammals have revealed that amongst all of the TE families, the retrotransposons can be seen mobile actively in genomes. Moreover, these retrotransposons constitute a significant percentage of human genome; LINEs (long interspersed nucleotide elements) are the most abundant (18%) and autonomous amongst all the retrotransposons in humans. Whereas, the non-autonomous TEs including SINEs (short interspersed nucleotide elements) and SVAs [hybrid SINE-R-VNTR (variable number of tandem repeat)-*Alu* elements] mobilization is dependent on a protein encoded by LINE-1

(L1) encoded proteins are ~13% of the human genome (Lander et al., 2001; Cordaux and Batzer, 2009).

5.1.2 Link between CT genes in cancer and TE

There are many tumour antigens but many of those which are presented to human cytotoxic T lymphocytes (CTL) by human leukocyte antigen (HLA) class I molecules have been emerged as safe immunotherapy targets due to their absence in normal tissues. Amongst such tumour specific antigens an important category is CTAs, including; the *BAGE, CAGE, GAGE, HAGE, LAGE, MAGE, PAGE, NY-ESO-1, SCP* and *SSX* gene families (Simpson *et al.*, 2005; see introduction). Expression of CT genes in cancer cells involves a unique mechanism through epigenetic regulations. Amongst these epigenetic events DNA methylation has been found to have a crucial role in gene expression and correlating with hypomethylated CpG dinucleotides in CTA promoters. Moreover, CT gene expression has been evident in some types of cancer (Cho *et al*., 2003; Grunau *et al.*, 2005; Lim *et al*., 2005; Wang *et al*., 2006). Therefore, CT genes expressed in different tumour can be induced by DNA demethylation or by inhibiting deacetylation of histone documented for cutaneous melanoma (Sigalotti *et al*., 2004). It has also been reported that in chronic myeloid leukemia (CML) the promotor hypomethylation of CT genes result in activation of the *LINE1* retrotransposon and often related with the disease progression to the advanced phase (Roman-Gomez *et al.*, 2007). Hypomethylation is constantly related with *LINE1*. Therefore, it can tentatively be suggested that a genome-wide hypomethylation can be used to reactivate the silenced genes by DNA methylation such as CT genes in CML patients (Roman-Gomez *et al.*, 2007).

5.1.3 *TEX19* and Retrotransposons in DNA methylation

The expression profile of *TEX19* has been associate with pluripotency and fertility (Ollinger *et al*., 2008; Tarabay *et al.*, 2013). The underlaying molecular mechanism is still unknown. Knockout studies of *TEX19*.1 in mouse have revealed an over-expression of *MMERVK10C* retrotransposons and the heterogeneous spermatogenic that was initially described as *TEX19.1* deficient (Ollinger *et al*., 2008).

DNA hypomethylation can induce retrotransposon activity resulting in genome instability reported in the developing germline (Hackett et al., 2012). In addition, the DNA hypomethylation in primordial germ cells may induce the expression of genome-defence genes including *Tex19.1, Mov10l1, Piwil2, Asz1* and *Dazl* that are sensitive to

hypomethylation and protect the germline DNA from retrotransposon activity (Hackett et al., 2012). Whereas, inhibition of retrotransposons in testicular germ cells may lead to male sterility, which can be induced through mutations in some genes such as *Tex19.1*, *Mov10l1*, *Piwil2* or *Asz1* genes. This mutation results in reduction of retrotransposons in testicular germ cells. And finally cause male sterility (Reichmann et al., 2013).

Placenta cell genomes are hypomethylated in a fashion similar to primordial germ cells, and this hypomethylated condition of the placenta is related to retrotransposons (Reichmann et al., 2013). The cytosine in CpG is almost of 40–50% methylated within different classes of transposons including LTRs, LINEs and SINEs in the mouse placentas, compared with approximately 75–80% in the embryo (Popp et al., 2010). Moreover, the other specific classes of retrotransposon, including *LINE-1* have also been documented for hypomethylation in the placenta.Therefore, DNA hypomethylation of placenta cells can possibly result in retrotransposon activation (Reichmann et al., 2013).

The microarray expression profile of *TEX19.1*$^{-/-}$ mice from placentas demonstrated that an increased expression of *LINE-1* retrotransposons has been evident with the loss of *Tex19.1* in placenta tissue. In addition, a study show that *LINE-1* transposons are inhibited in trophectoderm-derived cells with hypomethylated epigenetic state, while these cells normally express *Tex19.1* (Reichmann et al., 2013).

5.2 Results

To commence investigations into the possible functional role of *TEX19* in cancer cell, we knockdown *TEX19* using HS_FLJ35767_6 one of the *TEX19* siRNA, in two cancer cell-lines including NTERA2 and A2780. Then we quantified the gene expression of human *ERVK* genes and *TEX19* using qRT-PCR analysis to determine whether the depletion of TEX19 resulted in changes to retroelements expression. The data were normalized using *TUBULIN* and *LAMIN* expression. Untreated and non-interference conditions were applied as a control for *TEX19* knockdown. In addition, no template control (NTC) and no reverse transcription (NRT) samples were applied as a control in both NTERA2 and A2780 cancer cells.

5.2.1 Effect of *TEX19* knockdown on *ERVK* genes expression in NTERA2

The knockdown of *TEX19* was successful and clear reduction of *TEX19* expression was observed in the siRNA sample compared to the untreated and non-interfering samples (Figure 5.1). The H *ERVK* family was reduced after *TEX19* knockdown. It is clearly *ERVK* genes expression was reduced including *ERVK ENV, ERVK GAG, ERVK HML2RE, ERVK POL* and *ERVK PRO.* Their expression was decreased in *TEX19* knockdown samples compared to a higher level of expression in untreated and non-interfering samples (Figure 5.1)

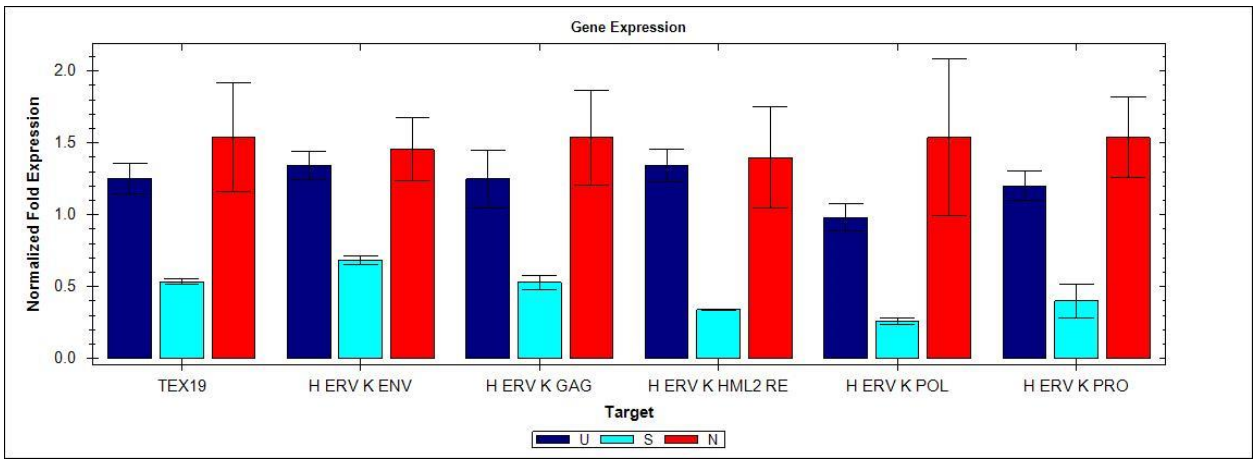

5.1 qRT PCR normalised result of *TEX19* knockdown in NTERA2 cancer cell-line show the expression of *ERVK* family TE in three different conditions including untreated, siRNA *TEX19* and non-intereferance samples.

Table 5.1 quantification cycle reading (Cq) and standard deviation reading (SEM). The reading were normalized against TUBULIN and LAMIN. siRNA sample (S), non-interference sample (N) and untreated sample (U).

Target	Sample	Expression	Expression SEM	Corrected Expression SEM	Mean Cq	Cq SEM
H ERV K ENV	N	1.45549	0.21738	0.21738	26.95	0.04595
H ERV K ENV	S	0.68597	0.03093	0.03093	27.41	0.06264
H ERV K ENV	U	1.34324	0.09669	0.09669	26.87	0.01994
H ERV K GAG	N	1.53844	0.32818	0.32818	32.03	0.22450
H ERV K GAG	S	0.52915	0.05243	0.05243	32.95	0.14188
H ERV K GAG	U	1.24837	0.20207	0.20207	32.13	0.21012
H ERV K HML2 RE	N	1.39811	0.35140	0.35140	25.28	0.25497
H ERV K HML2 RE	S	0.33935	0.00455	0.00455	26.70	0.00821
H ERV K HML2 RE	U	1.34324	0.11616	0.11616	25.14	0.07197
H ERV K POL	N	1.53844	0.54536	0.54536	26.86	0.46609
H ERV K POL	S	0.26090	0.02269	0.02269	28.80	0.12425
H ERV K POL	U	0.98122	0.09360	0.09360	27.32	0.09248
H ERV K PRO	N	1.53844	0.28206	0.28206	27.60	0.05910
H ERV K PRO	S	0.40068	0.11915	0.11915	28.92	0.42865
H ERV K PRO	U	1.20195	0.10316	0.10316	27.76	0.07032
LAMIN	N				23.16	0.28049
LAMIN	S				22.30	0.02324
LAMIN	U				23.04	0.12367
TEX19	N	1.53844	0.38095	0.38095	33.32	0.28863
TEX19	S	0.53344	0.01953	0.01953	34.22	0.04983
TEX19	U	1.25445	0.10633	0.10633	33.41	0.06758
TUBULIN	N				18.54	0.31398
TUBULIN	S				18.15	0.02620
TUBULIN	U				18.27	0.16203

5.2.2 Effect of *TEX19* knockdown on *ERVK* genes expression in A2780 cancer cells

In ovarian cancer cell-line A2780, the knockdown of *TEX19* was unsuccessful and no inhibition of *TEX19* expression was observed in the siRNA sample compared with the untreated and non-interfering samples. Human *ERVK* family gene expression were significantly increased in *TEX19* knockdown samples compared to the untreated and non-interfering samples. It is clearly shown the expression of *ERVK ENV, ERVK GAG, ERVK HML2RE, ERVK POL* and *ERVK PRO* were all highly elevated in *TEX19* knockdown sample comparing with lower level of expression in untreated and non-interfering samples regardless the failure knockdown of *TEX19* (Figure 5.2)

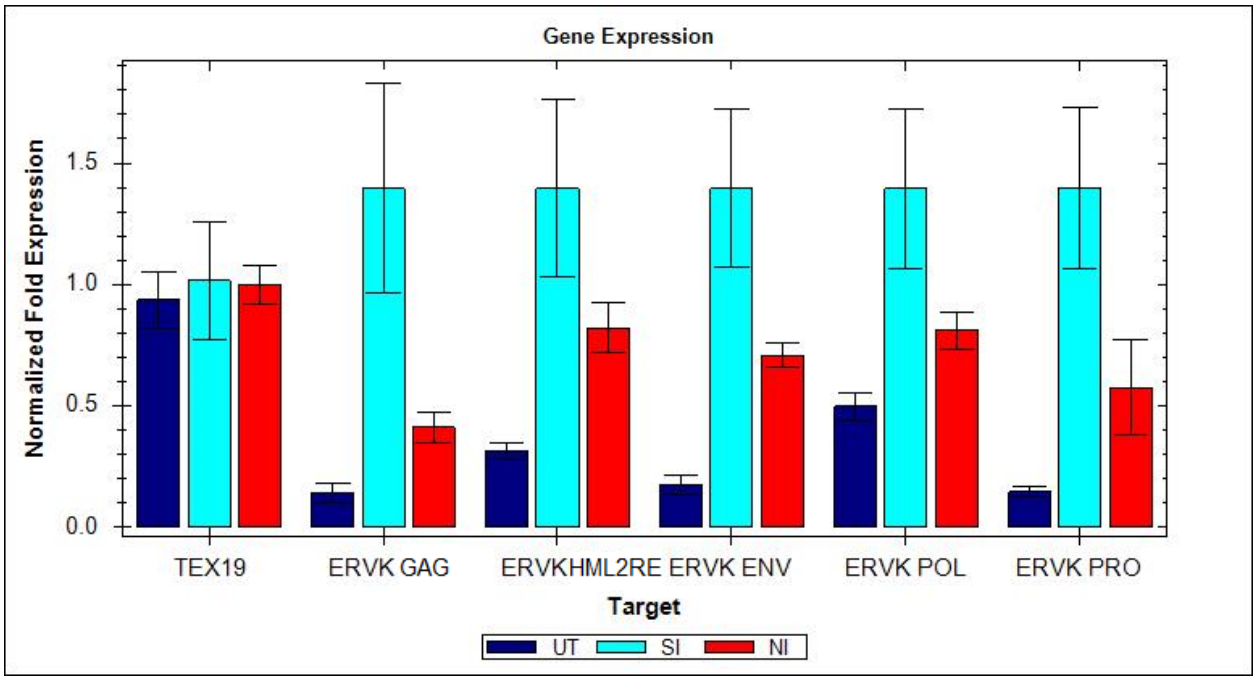

Figure 5.2 qRT PCR normalised result of *TEX19* knockdown in A2780 cancer cell-line show the expression of *ERVK* family TE in three different samples including untreated, siRNA *TEX19* and non-intereferance samples.

Table 5.2 quantification cycle reading (Cq) and standard deviation reading (SEM). The reading were normalized against TUBULIN and LAMIN. siRNA sample (S), non-interference sample (N) and untreated sample (U).

Target	Sample	Expression	Expression SEM	Corrected Expression SEM	Mean Cq	Cq SEM
ERVK GAG	NI	0.41131	0.06340	0.06340	30.02	0.19942
ERVK GAG	SI	1.39636	0.43103	0.43103	28.74	0.29033
ERVK GAG	UT	0.14197	0.03926	0.03926	31.71	0.37043
ERVK HML2RE	NI	0.82043	0.10254	0.10254	28.21	0.15107
ERVK HML2RE	SI	1.39636	0.36393	0.36393	27.92	0.16539
ERVK HML2RE	UT	0.31547	0.03354	0.03354	29.74	0.03906
ERVK ENV	NI	0.70720	0.05032	0.05032	27.14	0.02920
ERVK ENV	SI	1.39636	0.32686	0.32686	26.64	0.00443
ERVK ENV	UT	0.17473	0.03738	0.03738	29.31	0.27070
ERVK POL	NI	0.81196	0.07647	0.07647	27.99	0.09368
ERVK POL	SI	1.39636	0.32820	0.32820	27.69	0.03093
ERVK POL	UT	0.49741	0.05791	0.05791	28.85	0.07884
ERVK PRO	NI	0.57614	0.19845	0.19845	28.11	0.48708
ERVK PRO	SI	1.39636	0.33330	0.33330	27.31	0.06753
ERVK PRO	UT	0.14557	0.01926	0.01926	30.25	0.12008
LAMIN	NI				23.35	0.06471
LAMIN	SI				24.14	0.67005
LAMIN	UT				23.64	0.28996
TEX19	NI	1.00000	0.07947	0.07947	27.58	0.05880
TEX19	SI	1.01545	0.24009	0.24009	28.04	0.04831
TEX19	UT	0.93684	0.11701	0.11701	27.83	0.10231
TUBULIN	NI				17.90	0.18590
TUBULIN	SI				18.08	0.08439
TUBULIN	UT				17.92	0.06263

5.2.3 Evaluation of cancer cellular proliferation after *TEX19* knockdown using ELDA

In this study, we are trying to assess the effect of *TEX19* knockdown on the cellular proliferation of NTERA2 and A2780. The ELDA (extreme limiting dilution analysis) assay is a method for the assessment of the self-renewal potential of cells. A series of cellular dilution were applied in cell seeding including 1000, 100 and 10 cells per well for each condition. Light microscope were used to assess the morphological growth of the cells and an image were taken from each condition starting from the first day of treatment and on the tenth day from both treated cancer cell-line including NTERA2 and A2780. Knockdown *TEX19* in NTERA2 and A2780 cells were performed using four *TEX19* siRNA including HS_FLJ35767_1, HS_FLJ35767_6, HS_FLJ35767_7 and HS_FLJ35767_8. Three different conditions were applied as a control for this experiment including Hiperfect transfection, non-interferance RNA and untreated. These conditions were applied in both cancer cell-line with 12 wells repetition per condition for each cancer cell-line. The evaluation of cellular proliferation frequency were determined by ELDA web-tool (http://bioinf.wehi.edu.au/software/elda/).

5.2.3.1 ELDA assay of *TEX19* knockdown in NTERA2

The knockdown of *TEX19* using HS_FLJ35767_1 show significant reduction of cellular proliferation in NTERA2 comparing to non-interfering condition ($P < .0.01$) and the effect of transfection agent show no significant effect on cell proliferation (Figure 5.3 and Table 5.3 and 5.4) this clearly show in pairwise comparison between untreated condition versus non-interferance or Hiperfect sample which show similar cellular proliferation ($P<0.01$). In contrast, no significance difference was observed in HS_FLJ35767_6 comparing to non-interferance sample (Figure 5.4, Table 5.3 and Table 5.4). Both HS_FLJ35767_7 and HS_FLJ35767_8 show significant reduction in cellular proliferation of NTERA2 comparable to non-interfering sample conditions ($P<0.01$) (Figure 5.5, Figure 5.6, Table 5.3 and Table 5.4).

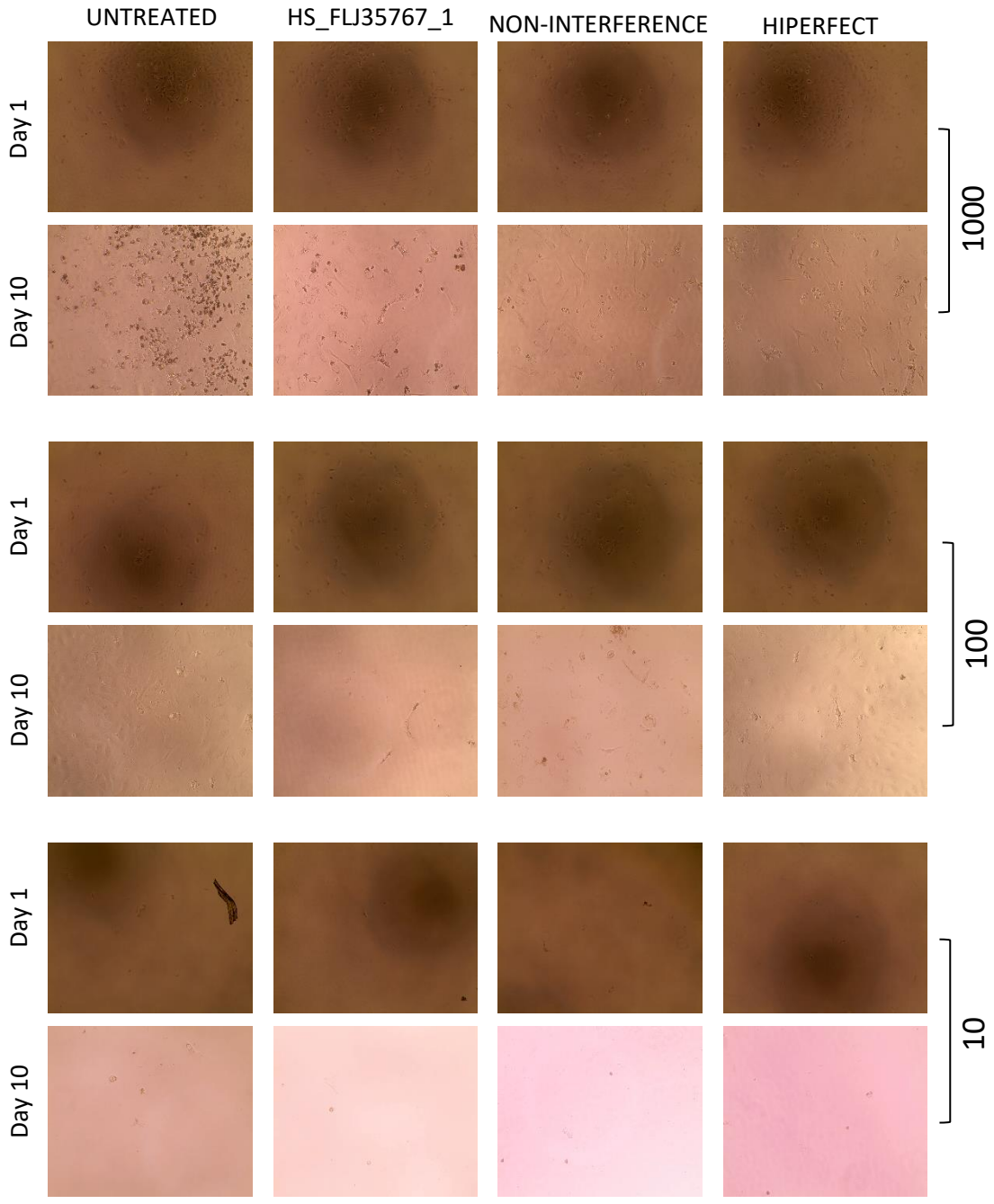

Figure 5.3. light microscopy images of NTERA2 cancer cells in four conditions including HS_FLJ35767_1, non-interferance, Hiperfect and untreated cells. Numbers on the right hand side denote cell number per well. Some images were clear during taking the image but after printing were not.

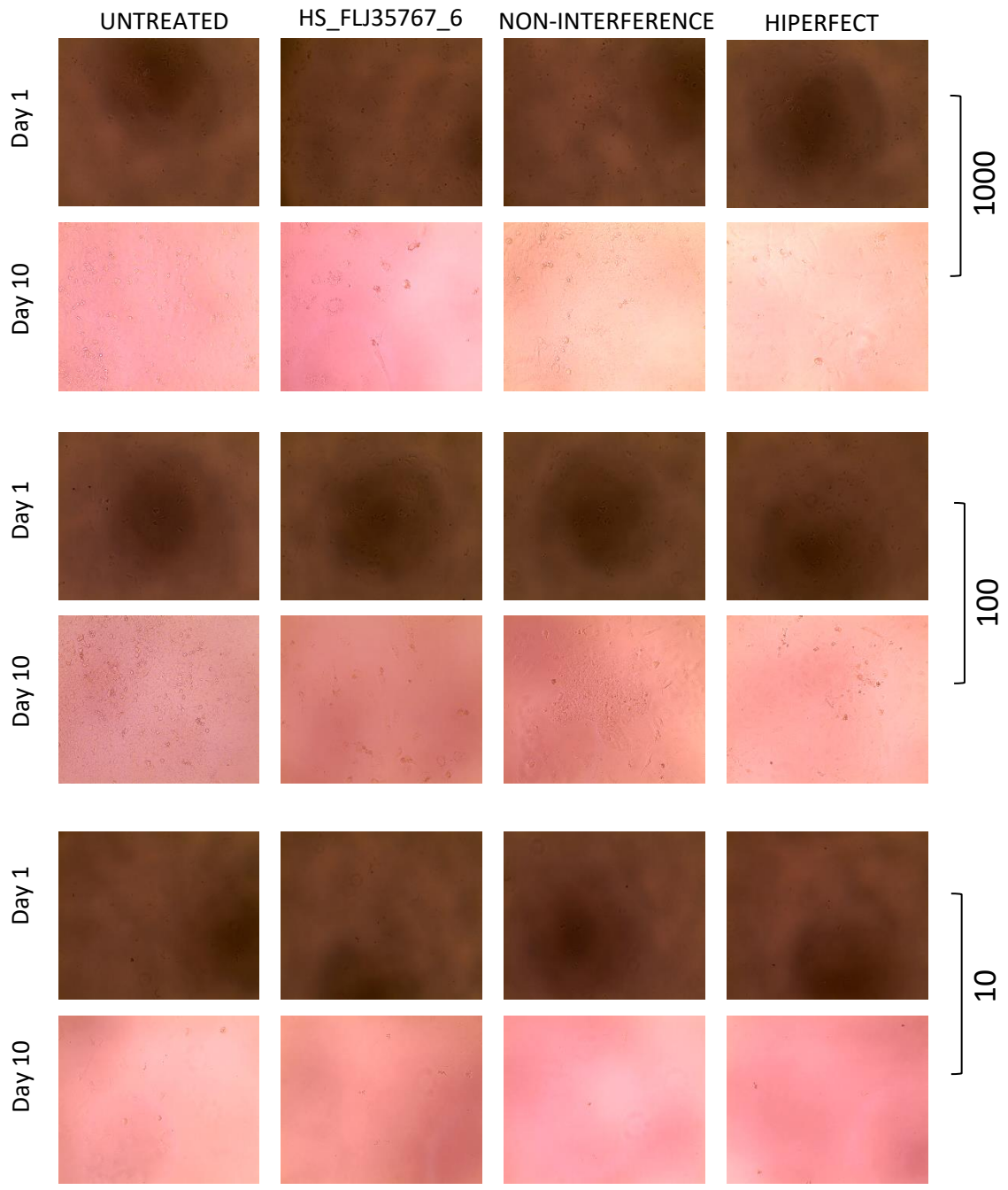

Figure 5.4. light microscopy images of NTERA2 cancer cells in four conditions including HS_FLJ35767_6, non-interferance, Hiperfect and untreated cells. Numbers on the right hand side denote cell number per well.

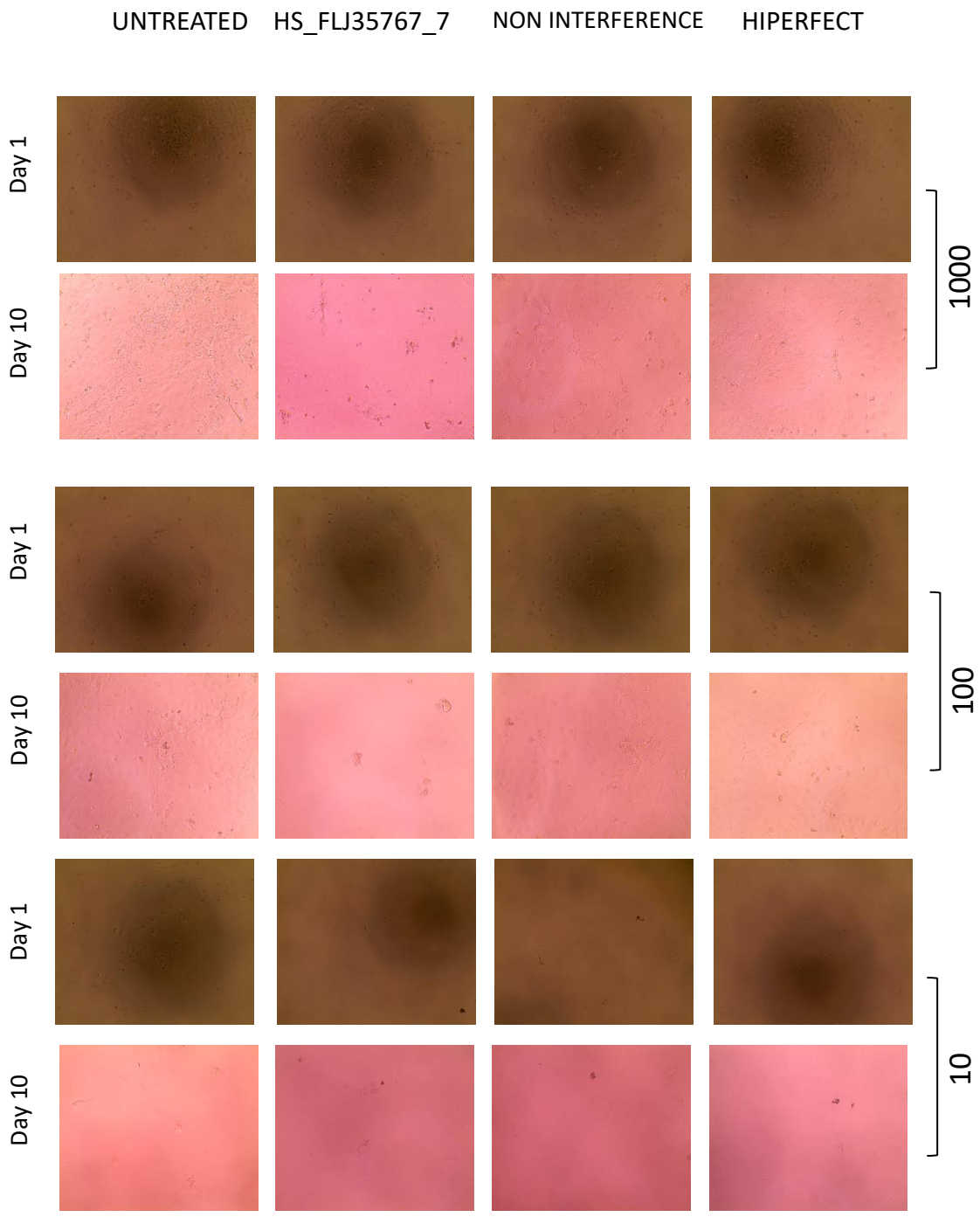

Figure 5.5. light microscopy images of NTERA2 cancer cells in four conditions including HS_FLJ35767_7, non-interferance, Hiperfect and untreated cells. Numbers on the right hand side denote cell number per well.

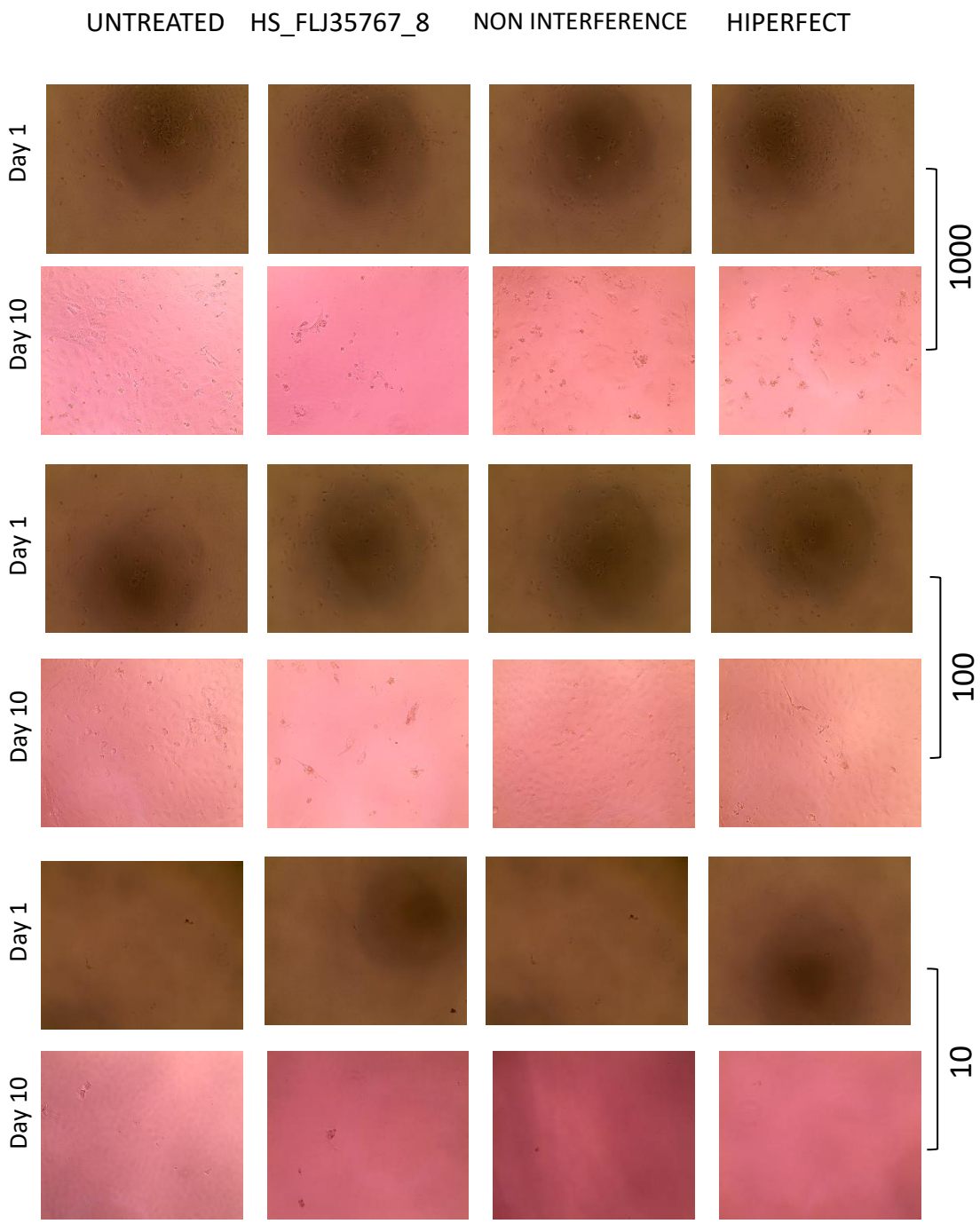

Figure 5.6. light microscopy images of NTERA2 cancer cells in four conditions including HS_FLJ35767_8, non-interferance, Hiperfect and untreated cells. Numbers on the right hand side denote cell number per well.

Table 5.3 show the effect of four TEX19 siRNA effect on NTERA2 cellular proliferation. untreated (U), siRNA TEX19 (S), non-intereferance samples (N) and Hiperfect (H)

HS_FLJ35767_1	TESTED	POSITIVE	TREATMENT	HS_FLJ35767_7	TESTED	POSITIVE	TREATMENT
1000	12	12	U	1000	12	12	U
100	12	12	U	100	12	12	U
10	12	8	U	10	12	11	U
1000	12	6	S	1000	12	10	S
100	12	2	S	100	12	6	S
10	12	0	S	10	12	0	S
1000	12	10	N	1000	12	11	N
100	12	6	N	100	12	9	N
10	12	0	N	10	12	0	N
1000	12	10	H	1000	12	11	H
100	12	6	H	100	12	8	H
10	12	0	H	10	12	0	H
HS_FLJ35767_6	**TESTED**	**POSITIVE**	**TREATMENT**	**HS_FLJ35767_8**	**TESTED**	**POSITIVE**	**TREATMENT**
1000	12	12	U	1000	12	12	U
100	12	11	U	100	12	12	U
10	12	9	U	10	12	3	U
1000	12	10	S	1000	12	8	S
100	12	8	S	100	12	4	S
10	12	0	S	10	12	0	S
1000	12	10	N	1000	12	10	N
100	12	8	N	100	12	8	N
10	12	0	N	10	12	0	N
1000	12	11	H	1000	12	10	H
100	12	9	H	100	12	5	H
10	12	0	H	10	12	0	H

Table 5.4 ELDA pairwise test for differences in NTERA2 cellular proliferation frequency. Untreated cells (U), non-interferance (N) and Hiperfect (H). degrees of freedom (DF) and the probability value (Pr)

Group 1	Group 2	Chisq	DF	Pr(>Chisq)
H	N	1.20	1	0.273
H	HS_FLJ35767_1	1.20	1	0.273
H	U	29.8	1	4.89e-08
N	HS_FLJ35767_1	0	1	1
N	U	43.7	1	3.81e-11
HS_FLJ35767_1	U	43.7	1	3.81e-11
H	N	0.0758	1	0.783
H	HS_FLJ35767_6	1.55	1	0.213
H	U	61.8	1	3.89e-15
N	HS_FLJ35767_6	2.35	1	0.125
N	U	58.7	1	1.85e-14
HS_FLJ35767_6	U	81.3	1	1.89e-19
H	N	0.0758	1	0.783
H	HS_FLJ35767_7	1.55	1	0.213
H	U	61.8	1	3.89e-15
N	HS_FLJ35767_7	2.35	1	0.125
N	U	58.7	1	1.85e-14
HS_FLJ35767_7	U	81.3	1	1.89e-19
H	N	0.498	1	0.48
H	HS_FLJ35767_8	1.36	1	0.244
H	U	33.8	1	6.02e-09
N	HS_FLJ35767_8	3.63	1	0.0568
N	U	28.1	1	1.13e-07
HS_FLJ35767_8	U	46.7	1	8.46e-12

5.2.3.2 ELDA assay of *TEX19* knockdown in A2780 cells

No significant cellular proliferation frequency of A2780 cancer cells were observed using four *TEX19* siRNA including HS_FLJ35767_1 (Figure 5.7), HS_FLJ35767_6 (Figure 5.8), HS_FLJ35767_7 (Figure 5.9) and HS_FLJ35767_8 (Figure 5.10) compared with non-interferance condition, Hiperfect transfection and untreated. The cellular proliferation of A2780 cells keep increasing regardless transfection or siRNA applied.

Relative decrease in cellular proliferation were observed only in low number of cells plated such as 10 cells per well. (Table 5.5) However, ELDA assay web-tool did not show data with statistically significant differences.

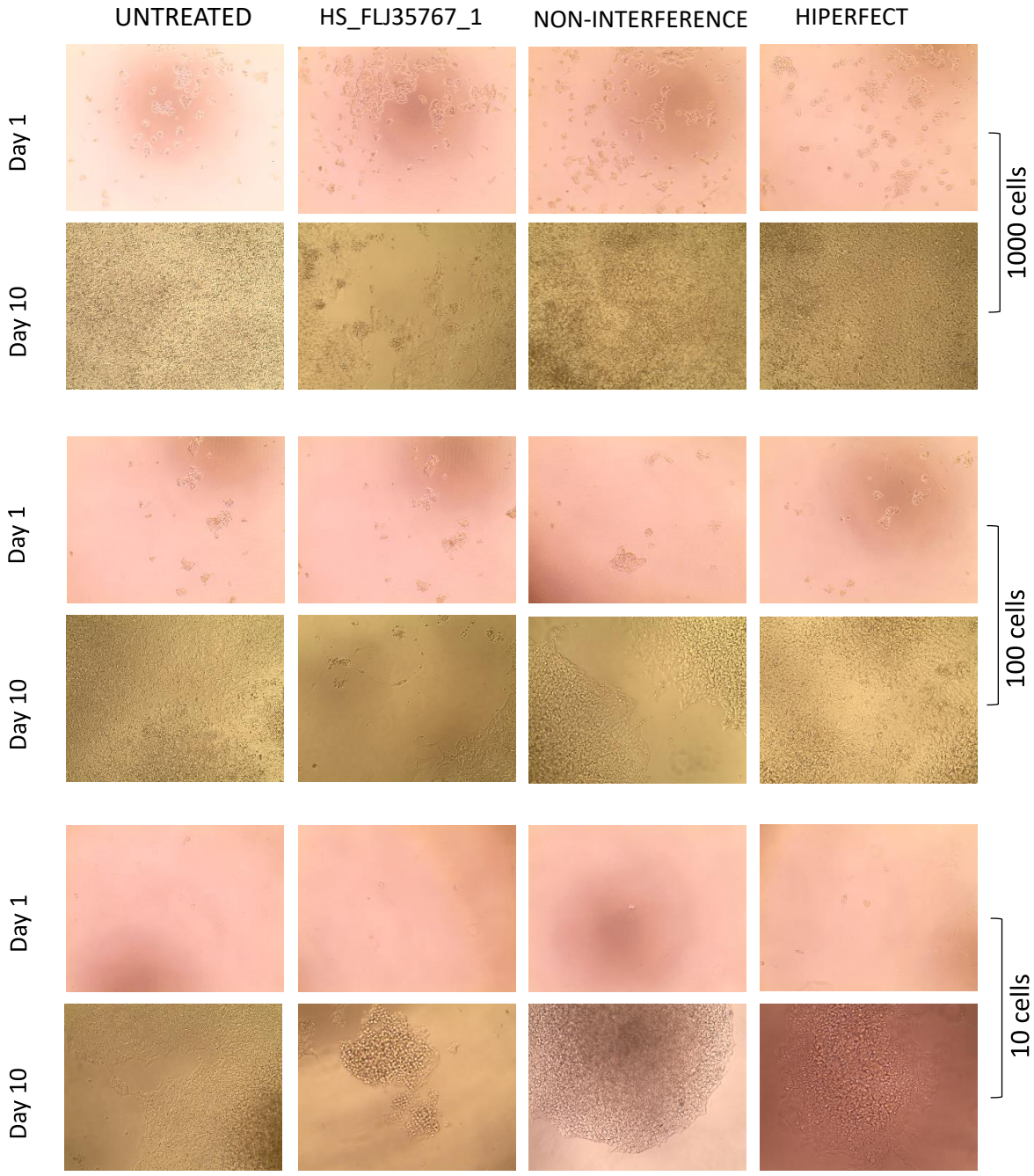

Figure 5.7. Light microscopy images of A2780 cancer cells in four conditions including HS_FLJ35767_1, non-interferance, Hiperfect and untreated cells. Numbers on the right hand side denote cell number per well.

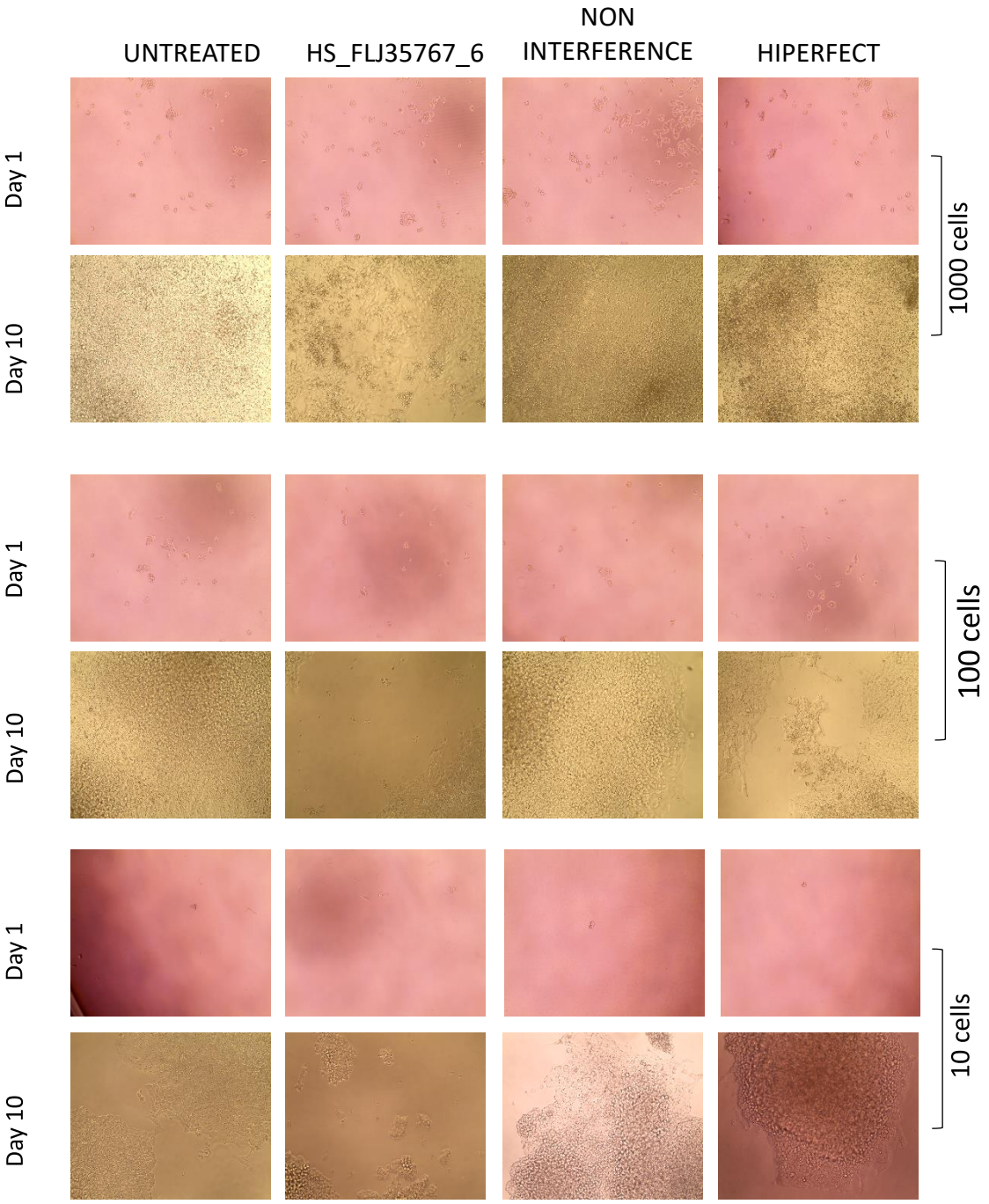

Figure 5.8. light microscopy images of A2780 cancer cells in four conditions including HS_FLJ35767_6, non-interferance, Hiperfect and untreated cells. Numbers on the right hand side denote cell number per well.

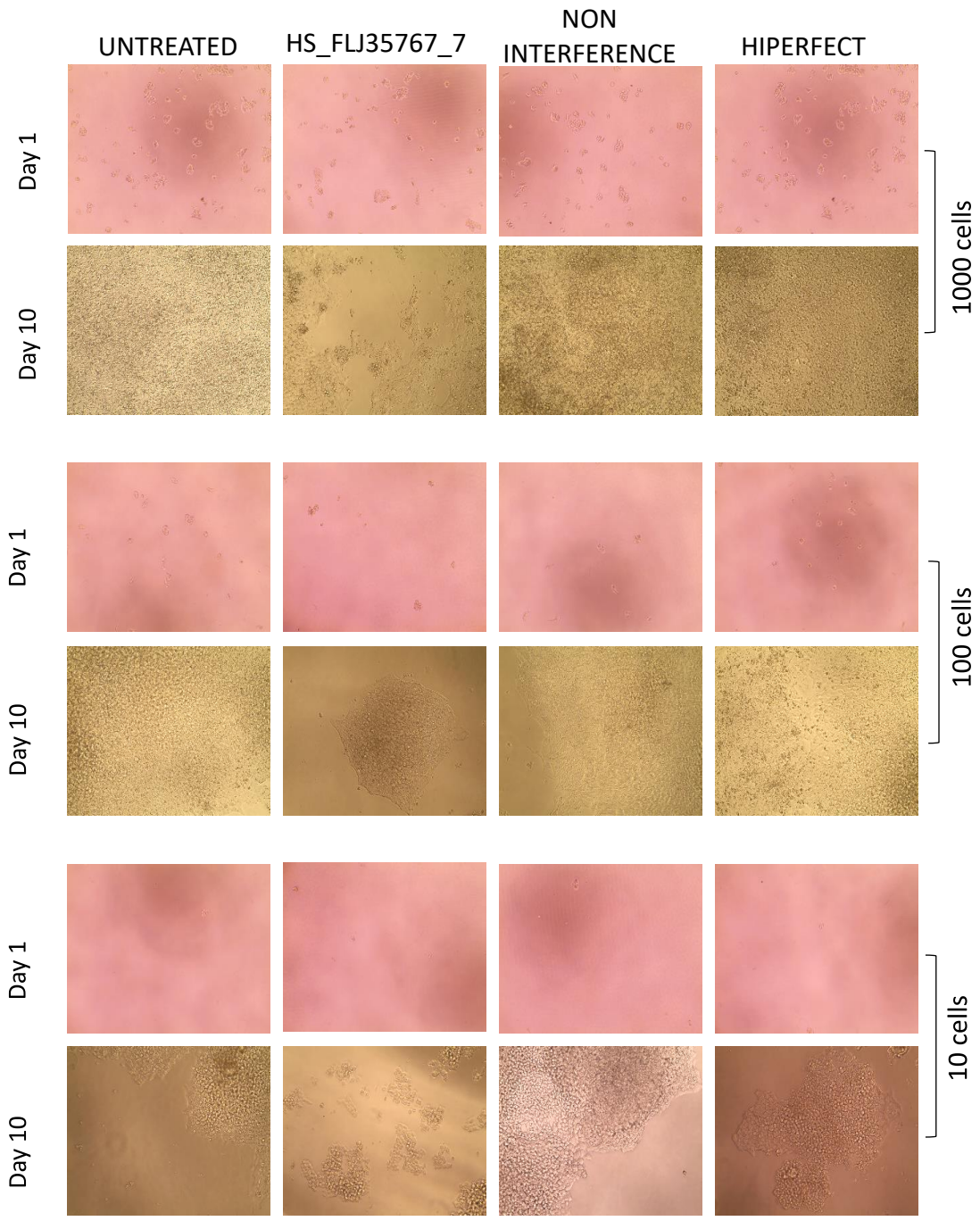

Figure 5.9. light microscopy images of A2780 cancer cells in four conditions including HS_FLJ35767_7, non-interferance, Hiperfect and untreated cells. Numbers on the right hand side denote cell number per well.

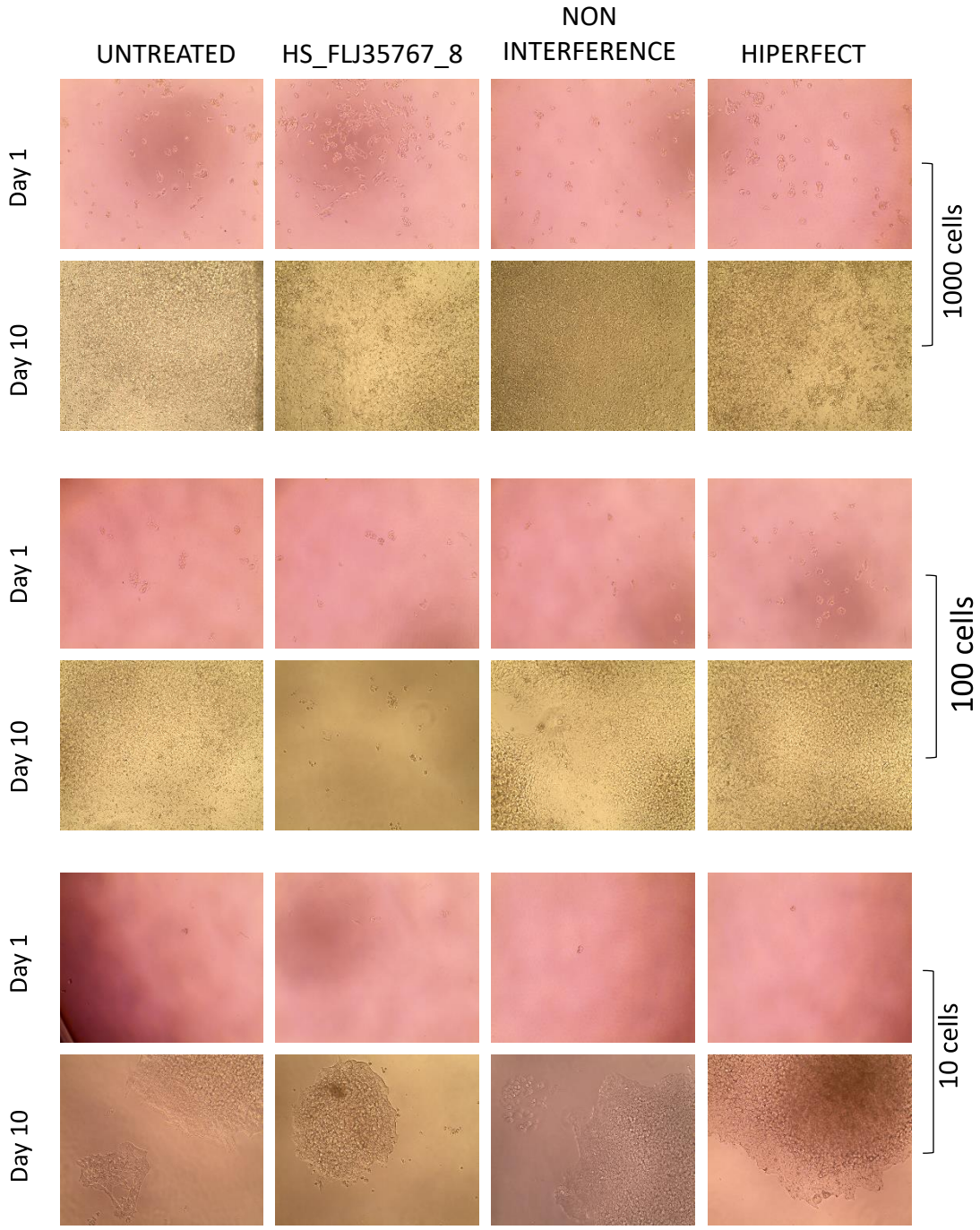

Figure 5.10 light microscopy images of A2780 cancer cells in four conditions including HS_FLJ35767_8, non-interferance, Hiperfect and untreated cells. Numbers on the right hand side denote cell number per well.

Table 5.5 show the effect of four TEX19 siRNA effect on A2780 cellular proliferation. This experiment was repeated 12 times per condition in 6 well plate from confluent A2780 cells. untreated (U), siRNA TEX19 (S), non-intereferance samples (N) and Hiperfect (H)

HS_FLJ35767_1	TESTED	POSITIVE	TREATMENT	HS_FLJ35767_7	TESTED	OPSITIVE	TREATMENT
1000	12	12	U	1000	12	12	U
100	12	12	U	1000	12	12	U
10	12	12	U	1000	12	12	U
1000	12	12	S	1000	12	12	S
100	12	10	S	1000	12	12	S
10	12	10	S	1000	12	10	S
1000	12	12	N	1000	12	12	N
100	12	12	N	1000	12	12	N
10	12	12	N	1000	12	12	N
1000	12	12	H	1000	12	12	H
100	12	12	H	1000	12	12	H
10	12	12	H	1000	12	12	H
HS_FLJ35767_6	**TESTED**	**POSITIVE**	**TREATMENT**	**HS_FLJ35767_8**	**TESTED**	**POSITIVE**	**TREATMENT**
1000	12	12	U	1000	12	12	U
100	12	12	U	1000	12	12	U
10	12	12	U	1000	12	12	U
1000	12	12	S	1000	12	12	S
100	12	10	S	1000	12	10	S
10	12	10	S	1000	12	10	S
1000	12	12	N	1000	12	12	N
100	12	12	N	1000	12	12	N
10	12	12	N	1000	12	12	N
1000	12	12	H	1000	12	12	H
100	12	12	H	1000	12	12	H
10	12	12	H	1000	12	12	H

5.3 Discussion

The correlation of expression of *ERVK* family of TEs with *TEX19* expression in the NTERA2 cancer cell line was clearly shown in this experiment. The reduction of the expression of *ERVK* family genes using *TEX19* knockdown in NTERA2 was observed, including *ERVK ENV, ERVK GAG, ERVK HML2RE, ERVK POL* and *ERVK PRO*. The expression of *ERVK* family genes are consistent with *ERVK* genes profiles, since,the *ERVK* family genes show high expression profile in ESCs (Kelley and Rinn, 2012) In addition, NTERA2 is a well-characterised cancer cell-line that is composed of pluripotent embryonal carcinoma (EC) cells capable of differentiation into neuron cells using RA induction (Andrews *et al.,* 1982). In addition, human ESCs and EC cells share some pluripotency characteristics (Abu Dawud *et al*., 2012) However, the reduction of *ERVK* genes expression after knockdown of *TEX19* expression in NTERA2 were contradictory with some other studies including activation of *LINE-1* transposonas after *TEX19.1* deletion in the mouse placenta (Reichmann et al., 2013). Moreover, deletion of *TEX19.1* in the mouse causes upregulation of retrotransposons including mouse *ERVK* genes (Ollinger *et al*., 2008). Therefore, collectively, we suggest that *TEX19* may be involve in *ERVK* genes regulation in EC cells of NTERA2 differently from its role in testis. Alternatively, this might reveal difference between the mouse and human.

In contrast, attempted *TEX19* knockdown in A2780 show an increasing expression of *ERVK* genes including *ERVK ENV, ERVK GAG, ERVK HML2RE, ERVK POL* and *ERVK PRO*. Regardless the failure of *TEX19* expression knockdown in A2780, the elevation of human *ERVK* genes after *TEX19* knockdown were consistence with some studies including the upregulation of retrotransposons in mouse after deletion *TEX19.1* gene (Ollinger *et al*., 2008). In addition, the activation of *LINE-1* transposons in placenta after *TEX19.1* deletion (Reichmann et al., 2013). Here, the activation of human *ERVK* genes in A2780 cancer cells after attempted kncockdown *TEX19* may support a hypothetical role of *TEX19* in transposons suppression.

Overall, these two opposite findings of upregulation and down-regulation of human *ERVK* genes after knockdown of *TEX19* in A2780 and NTERA2 may be related to role that *TEX19* may play in EC cells of NTERA2.

The apparent failure of *TEX19* expression reduction should be treated with caution, however, and these experiments should be repeated to confirm these findings.

The effect on cell proliferation of NTERA2 cancer cells following *TEX19* depletion was significant using *TEX19* siRNA including HS_FLJ35767_1, HS_FLJ35767_7 and HS_FLJ35767_8 compared with non-interference. This significant changes in cell proliferation of NTERA may suggest the important role of *TEX19* in NTERA2 cancer cells. In addition, the significant cell proliferation frequency of NTERA2 after knockdown *TEX19* is consistence with previous q-RT-PCR and western blot, which assume the neccecity of *TEX19* gene in NTERA2 cells. However, knockdown of *TEX19* expression in A2780 cancer cells did not show cellular proliferation frequency using four *TEX19* siRNA including HS_FLJ35767_1, HS_FLJ35767_6, HS_FLJ35767_7 and HS_FLJ35767_8. This may indicate that A2780 cells proliferation does not require *TEX19*. Moreover, morphological comparisons of A2780 cells show no significant cell proliferation frequency between untreated, siRNA, non-interference and Hiperfect.

The failure to demonstrate *TEX19* expression reduction in A2780, however, should be treated with caution and these experiment should be repeated. Moreover, the success of crispr technology developments means gene deletions could be applied to these cell systems to further explore function. The data presented here provide clues to a possible need for *TEX19* in cancer cells based on a retroelements regulation control, but further investigation is required.

Chapter 6. Evaluation the influence of *TEX19* depletion in cancer cell based on RNA sequencing data

6.1. RNA Sequencing

RNA sequencing is important for studying the transcriptome, which is the total complement of transcripts in a cell. Knowing the RNA sequence helps in understanding some mechanisms of inheritance and functional genetic regulations. Several techniques are used to characterize the cellular transcriptome including techniques based on Sanger sequencing (Bertone *et al*., 2004; David *et al.,* 2006). With the introduction of high-throughput sequencing methods the study of the genome and the transcriptome has become easier and faster. RNA sequencing is performed by direct sequencing of cDNAs, and the cDNA sequencing results are then followed by mapping of the sequencing reads to the genome. The resulting cDNA sequences are helpful to understand the eukaryotic transcriptomes. Moreover, this sequence is used to find the transcription start sites (Tsuchihara *et al*., 2009), identifying splice variants, and detecting expression. In addition, the sequence can be used for estimating the expression and splice variants of exons (Cloonan *et al*., 2008; Wang *et al*., 2009). RNA sequencing involves formation of a cDNA library using oligo (dT) or random primers. The generation of cDNA is carried out by using polyA+ RNA followed by fragmentation through DNase I and ligated to the adapters. Sequencing is usually completed using an Illumina Genome Analyzer. (Nagalakshmi *et al.*, 2010).

6.1.1 Preparation of cDNA library from hydrolyzed or fragmented RNA

RNA molecules to be sequenced are fragmented by partial hydrolysis instead of cDNA fragmentation. These fragmented RNA molecules are used to generate cDNA library using reverse transcriptase along with oligo(dT) or random hexamers primers followed by sequencing by Illumina Genome Analyzer (Nagalakshmi *et al.*, 2010).

6.1.2 DNA sequencing and data analysis

There are many sequencing methods available for DNA sequencing including Roche/454 FLX, Illumina genome analyser, Applied Biosystems SOLiD^{TM} System, the Helicos Heliscope^{TM}, Pacific Biosciences SMRT (Mardis, 2008). All these methods have some specific differences at different steps but main scheme almost the same. Here the details of Illumina genome analyser is described as RNA-Seq uses this method.

The RNA-Sequencing uses Illumina genome analyzer for DNA sequencing. Mapping of sequence reads utilises bioinformatics for analyzing the sequencing (Wang *et al.,* 2009).

cDNA sequencing reads utilising Illumina Genome Analyzer is done in two steps. The first step includes preparation of flow-cell, utilizing a cluster station, which involves loading of double-stranded template sequence to flow-cell with covalently bound oligos. The template strands are hybridized with the oligos on flow-cell surface. The second strand of template will be synthesized here. This double stranded template is again denatured and free end of separated strand again bound to oligos from complementary region and again synthesises double stranded template. In this way a second template strand is synthesized. The process is repeated to create clusters of identical DNA strands. In second step the Genome Analyzer synthesize the sequence through the process of synthesis of complementary strand by adding one nucleotide at a time to the DNA bound to fluorophore.

The software of Illumina analyser converts the fluorophore information to sequence data. The RNA-Seq data can be analysed using many tools of bioinformatics. Firstly, a combination of BLAT (Kent, 2002) and SOAP (Li *et al*., 2008) is used for mapping sequence reads. SOAP program is used as a fast mapping of sequence reads tool whereas BLAT is useful for mapping gapped reads.

6.1.3 RNA sequencing in cancer

One of important tools to explore transcriptome and identify variation of genes expression is RNA sequencing, which have been employed in cancer research. For example, identification of some microbial pathogens related to prostate cancer were achieved using RNA sequencing (Chen and Wei, 2015). In esophageal squamous cell carcinoma, RNA sequencing reveal genes that were dysregulated in this cancer. These identified genes may serve in early diagnosis and therapy (Fu *et al*., 2015). Moreover, in breast cancer, 24 newly identified fusion genes were achieved using RNA sequencing (Edgren *et al*., (2011).

Using RNA sequencing, genes affected by *CTCFL* expression were identified. *CTCFL* is a CT gene involve in dysregulation of some genes, which affect TGFP pathway in the mouse, which consequently lead to growth retardation and fatality (Sati *et al.,* 2015).

6.2 Results

Initially *TEX19* knockdown were performed, using HS_FLJ35767_6 one of *TEX19* siRNA, in SW480 cancer cells (this was carried out by a colleague in the group Vicente Planells Palop). Then, total RNA isolation were performed to synthesize cDNA. qRT-PCR was used to validate *TEX19* knockdown. Then, RNA samples of *TEX19* knockdown and non-interference control were sent for RNA sequencing. Dr. Julia Feichtinger performed the computation analysis of RNA sequencing data.

In addition, *TEX19* knockdown were performed, using HS_FLJ35767_ in another three cancer cells including H460, NTERA2 and A2780. Then, total RNA isolation were performed to synthesize cDNA. qRT-PCR was used to validate *TEX19* knockdown. Vicente Planells Palop performed the treatment and RNA isolation for SW480, A2780 and H460. Where this experiment was carried out by me and cDNA was achieved for these cells, however, our laboratory sent Mr Vincenta's samples for RNA sequencing due to cost issue and no significance to do so.

Based on RNA sequencing data analysis from SW480, we identified a cohort of 80 genes with altered expression in response to *TEX19* depletion were identified. From this list, we set out to validate these expression changes in H460, A2780, SW40 and NTERA2 to identify common gene changes in response to TEX19 depletion. I was allocated 20 of these genes including 10 upregulated genes and 10 downregulated genes (Table 6.1).

The quantification of gene expression for the 20 selected genes from RNA sequencing data were normalized against *TUBULIN* and *LAMIN*. Moreover, untreated and non-interference conditions were applied as a control for *TEX19* knockdown. No template control (NTC) and no reverse transcription (NRT) samples were also applied as a control in all qRT-PCR analysis.

6.2.1 Evaluation the genetic expression influence of *TEX19* knockdown in SW480

Knockdown of *TEX19* expression in SW480 influences some genes in this study; *GALNT2* expression was increased with *TEX19* expression knockdown compared to both untreated and non-interference sample (Figure 6.1). This elevation of expression in *TEX19* knockdown sample were observed for other genes in this study, including *ELK4, ASB2, CD22, CALB2, CPS1, LY96, SLC17A7* and *TRIM54* (Figure 6.2, Figure 6.3 and Figure 6.4). In contrast, some show correlated low expression in the *TEX19* expression knockdown sample including *NAPB, RIPA, MRP523* and *SAA2* compared to the untreated and non-interference sample

(Figure 6.1 and Figure 6.2). Some gene expression show no significant changes, however, such as *MPEP*, *PGM1*, *ATP5C1* and *ZBTB5* compared to both treated and non-interfering samples (Figure 6.1 and Figure 6.2). In addition, *NOS3* shows higher expression compared to untreated sample and no comparable significant expression changes were observed to non-interference sample (Figure 6.3). Moreover, both *TAGLN* and *ZNF367* show no expression difference compared to untreated sample. While, a clear expression inhibition were observed for *TAGLN* compared to non-interfering sample, and high expression of *ZNF367* were observed compared to non-interfering sample (Figure 6.3).

Table 6.1 RNA sequence data analysis of selected 20 genes affected by *TEX19* knockdown in SW480 cancer cells.

Gene	**Adjusted p Value**	**Average count KO**	**Average count N**	**Fold change**	**log2 fold change**	**Strand**
MIPEP	0	826	1804.666667	0.45770225	-1.1275187	-1
PGM1	0	708.6666667	1910	0.37102967	-1.430393542	1
NAPB	0	344.3333333	784	0.43920068	-1.187047806	-1
GALNT2	0	1081	2472.666667	0.43717983	-1.193701244	1
TAGLN	0	944.3333333	342	2.76120858	1.465299871	1
RPIA	0	853	2431.666667	0.35078821	-1.511327831	1
ELK4	0	721.6666667	1463.333333	0.49316629	-1.019853915	-1
NOS3	0	366	179.3333333	2.04089219	1.029199976	1
ZNF367	0	2090.666667	923.3333333	2.26425993	1.179039583	-1
ATP5C1	0	2328	6496	0.35837438	-1.480460574	1
ZBTB5	0	398.3333333	847	0.47028729	-1.088385757	-1
MRPS23	0	1460	2959.333333	0.49335436	-1.019303839	-1
SAA2	2.88E-11	138.6666667	280.3333333	0.49464923	-1.015522272	-1
CD22	1.23E-09	162.6666667	77	2.11255411	1.078988296	1
SLC17A7	2.95E-08	117	51.33333333	2.27922078	1.18854068	-1
ASB2	8.59E-07	200.6666667	81	2.47736626	1.308807173	-1
CPS1	0.0001786	57.33333333	21.66666667	2.64615385	1.403896942	1
CALB2	0.0002651	87.66666667	38.33333333	2.28695652	1.193428938	1
TEX19	0.009333	20.66666667	45	0.45925926	-1.122619287	1
TRIM54	0.02034	3	13.33333333	0.225	-2.152003093	1
LY96	0.03967	26.66666667	13	2.05128205	1.036525876	1

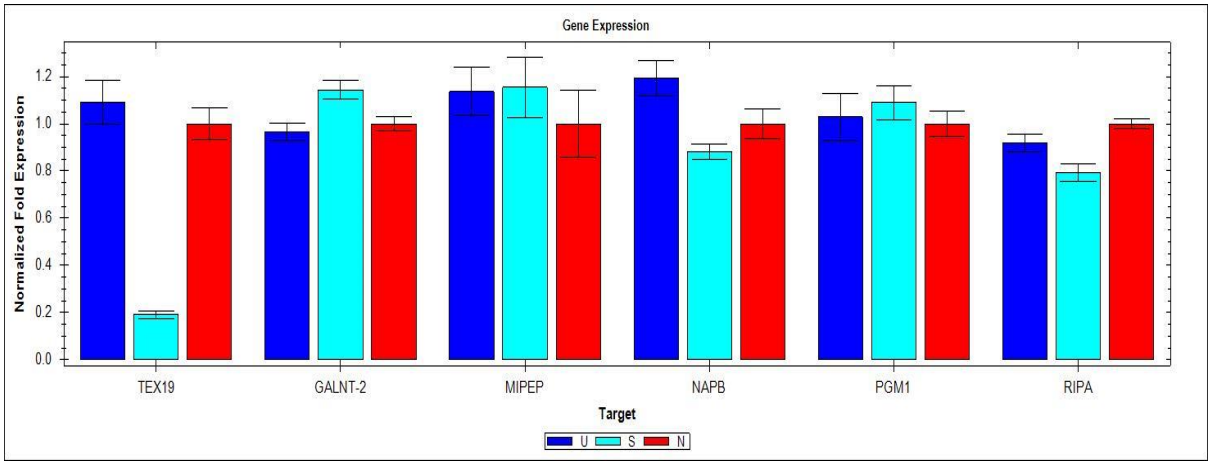

Figure 6.1 qRT PCR in SW480 cancer cell show TEX19 knockdown (S), untreated cells (U) and non-interfering sample (N).

Table 6.2 quantification cycle reading (Cq) and standard deviation reading (SEM). The reading was normalized against TUBULIN and LAMIN. siRNA sample (S), non-interference sample (N) and untreated sample (U).

Target	Sample	Expression	Expression SEM	Corrected Expression SEM	Mean Cq	Cq SEM
GALNT-2	N	1.00000	0.02829	0.02829	27.15	0.03355
GALNT-2	S	1.14351	0.04020	0.04020	27.27	0.01807
GALNT-2	U	0.96611	0.03859	0.03859	27.51	0.02497
LAMIN	N				21.58	0.02324
LAMIN	S				21.89	0.04739
LAMIN	U				21.89	0.05193
MIPEP	N	1.00000	0.14041	0.14041	26.39	0.20124
MIPEP	S	1.15421	0.12659	0.12659	26.49	0.15097
MIPEP	U	1.13716	0.10326	0.10326	26.51	0.12027
NAPB	N	1.00000	0.06205	0.06205	28.74	0.08645
NAPB	S	0.88000	0.03341	0.03341	29.24	0.02747
NAPB	U	1.19439	0.07410	0.07410	28.79	0.07290
PGM1	N	1.00000	0.05491	0.05491	26.27	0.07574
PGM1	S	1.08898	0.07362	0.07362	26.46	0.08525
PGM1	U	1.02854	0.09933	0.09933	26.54	0.12929
RIPA	N	1.00000	0.02235	0.02235	24.73	0.02236
RIPA	S	0.79208	0.03615	0.03615	25.38	0.04572
RIPA	U	0.91934	0.03586	0.03586	25.16	0.02166
TEX19	N	1.00000	0.06862	0.06862	31.89	0.09624
TEX19	S	0.19130	0.01646	0.01646	34.59	0.11475
TEX19	U	1.09067	0.09108	0.09108	32.07	0.10871

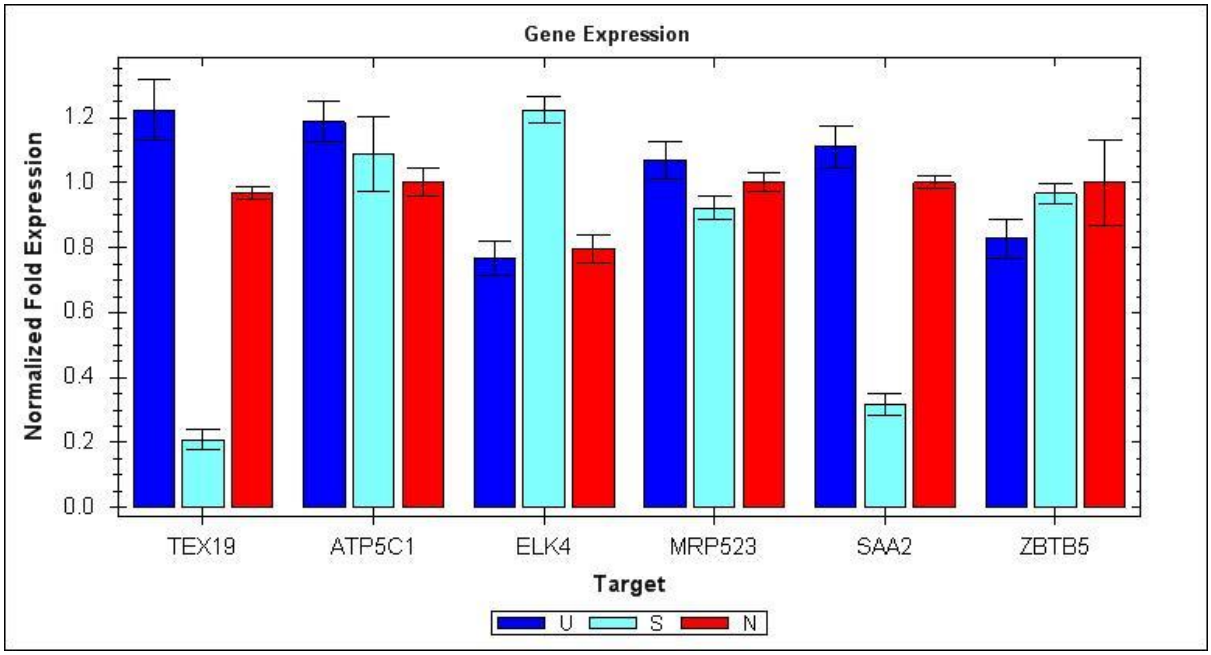

Figure 6.2 qRT PCR in SW480 cancer cell show *TEX19* knockdown (S), untreated cells (U) and non-interfering sample (N).

Table 6.3 quantification cycle reading (Cq) and standard deviation reading (SEM). The reading were normalized against TUBULIN and LAMIN. siRNA sample (S), non-interference sample (N) and untreated sample (U).

Target	Sample	Expression	Expression SEM	Corrected Expression SEM	Mean Cq	Cq SEM
ATP5C1	N	1.00000	0.04337	0.04337	22.95	0.05970
ATP5C1	S	1.08789	0.11356	0.11356	23.12	0.14435
ATP5C1	U	1.18830	0.06073	0.06073	22.99	0.03829
ELK4	N	0.79701	0.04296	0.04296	26.31	0.07547
ELK4	S	1.22273	0.04112	0.04112	25.98	0.02256
ELK4	U	0.76715	0.05251	0.05251	26.66	0.07602
LAMIN	N				21.10	0.02715
LAMIN	S				21.42	0.08371
LAMIN	U				21.34	0.02614
MRP523	N	1.00000	0.02885	0.02885	23.66	0.03716
MRP523	S	0.92216	0.03539	0.03539	24.07	0.03494
MRP523	U	1.06955	0.05841	0.05841	23.86	0.04728
SAA2	N	1.00000	0.01900	0.01900	22.76	0.02000
SAA2	S	0.31751	0.03401	0.03401	24.71	0.14843
SAA2	U	1.11093	0.06430	0.06430	22.90	0.05479
TEX19	N	0.96804	0.01873	0.01873	31.42	0.02069
TEX19	S	0.20946	0.03256	0.03256	33.92	0.22013
TEX19	U	1.22403	0.09280	0.09280	31.38	0.08940
TUBULIN	N				18.10	0.02583
TUBULIN	S				18.36	0.01929
TUBULIN	U				18.45	0.12329
ZBTB5	N	1.00000	0.13151	0.13151	28.04	0.18880
ZBTB5	S	0.96706	0.02981	0.02981	28.38	0.01150
ZBTB5	U	0.82774	0.05921	0.05921	28.60	0.08173

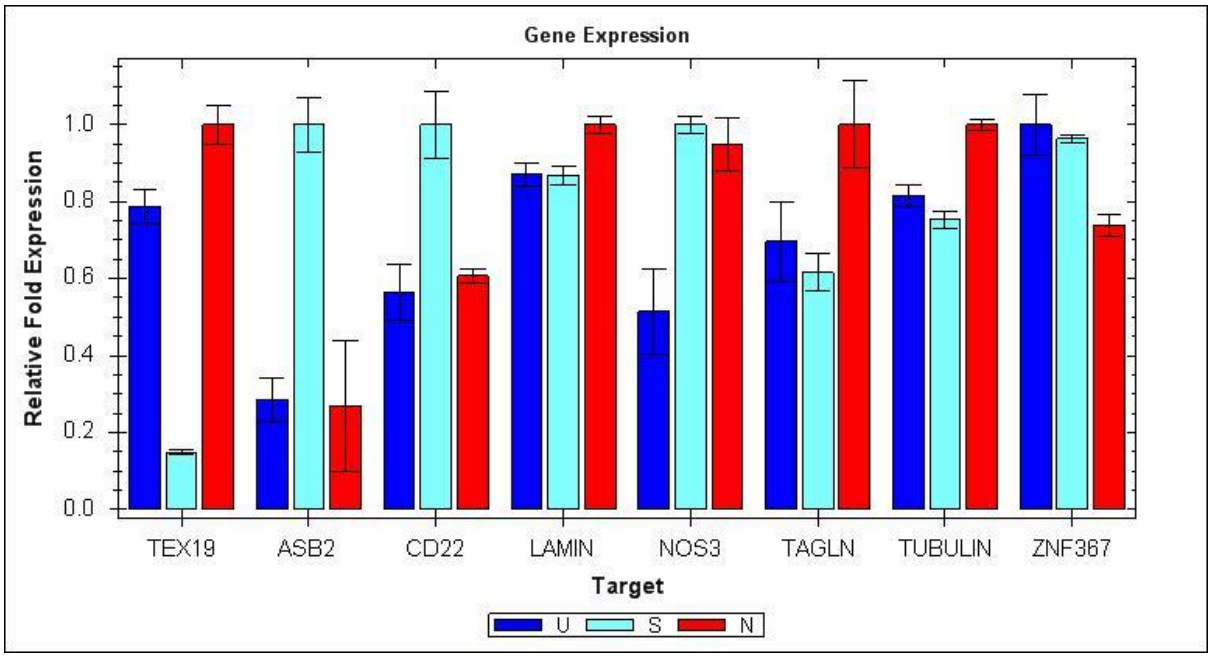

Figure 6.3 qRT PCR in SW480 cancer cell show *TEX19* knockdown (S), untreated cells (U) and non-interfering sample (N).

Table 6.4 quantification cycle reading (Cq) and standard deviation reading (SEM). The reading were normalized against TUBULIN and LAMIN. siRNA sample (S), non-interference sample (N) and untreated sample (U).

Target	Sample	Relative Quantity	Relative Quantity SEM	Corrected Relative Quantity SEM	Mean Cq	Cq SEM
ASB2	N	0.26824	0.16970	0.16970	32.41	0.91273
ASB2	S	1.00000	0.07060	0.07060	30.51	0.10185
ASB2	U	0.28554	0.05747	0.05747	32.32	0.29038
CD22	N	0.60687	0.01821	0.01821	30.01	0.04328
CD22	S	1.00000	0.08822	0.08822	29.29	0.12728
CD22	U	0.56460	0.07402	0.07402	30.12	0.18915
LAMIN	N	1.00000	0.02131	0.02131	21.20	0.03075
LAMIN	S	0.86918	0.02462	0.02462	21.40	0.04087
LAMIN	U	0.86990	0.03226	0.03226	21.40	0.05351
NOS3	N	0.95022	0.06921	0.06921	28.55	0.10508
NOS3	S	1.00000	0.02290	0.02290	28.47	0.03304
NOS3	U	0.51407	0.11194	0.11194	29.43	0.31415
TAGLN	N	1.00000	0.11390	0.11390	32.62	0.16433
TAGLN	S	0.61637	0.04799	0.04799	33.32	0.11232
TAGLN	U	0.69666	0.10389	0.10389	33.14	0.21514
TEX19	N	1.00000	0.05079	0.05079	31.36	0.07328
TEX19	S	0.14870	0.00615	0.00615	34.11	0.05966
TEX19	U	0.78798	0.04538	0.04538	31.71	0.08308
TUBULIN	N	1.00000	0.01446	0.01446	18.31	0.02086
TUBULIN	S	0.75274	0.02168	0.02168	18.72	0.04154
TUBULIN	U	0.81439	0.02915	0.02915	18.61	0.05164
ZNF367	N	0.74008	0.02848	0.02848	25.87	0.05551
ZNF367	S	0.96313	0.00909	0.00909	25.49	0.01362
ZNF367	U	1.00000	0.07998	0.07998	25.43	0.11539

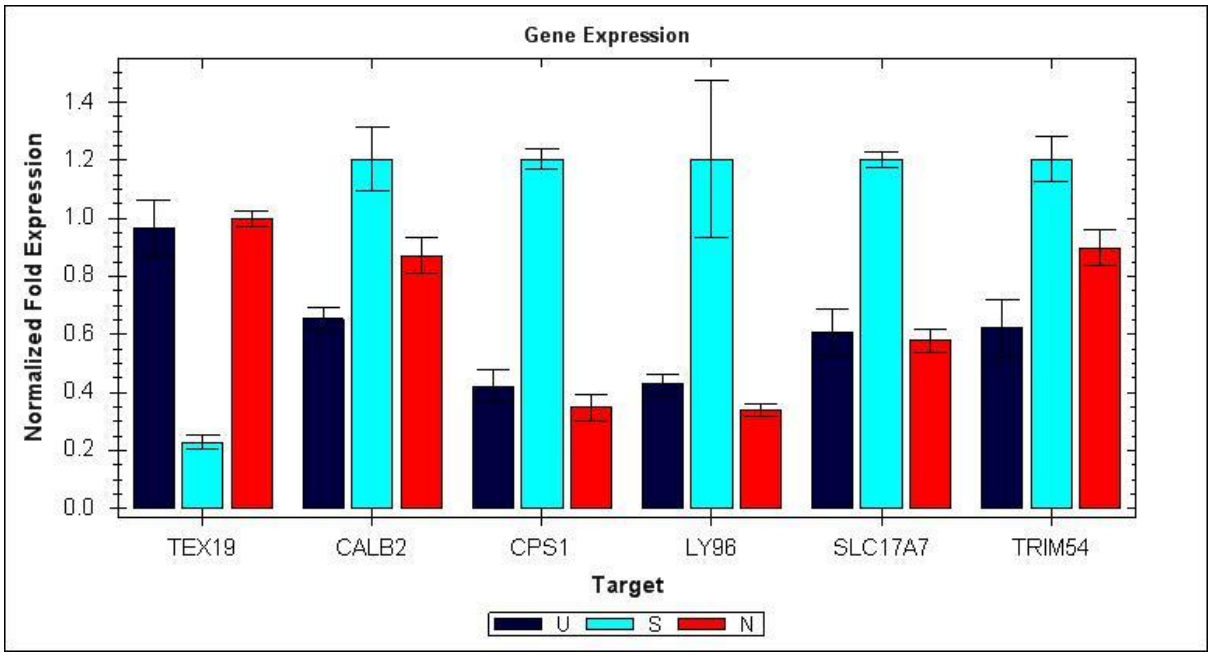

Figure 6.4 qRT PCR in SW480 cancer cell show *TEX19* knockdown (S), untreated cells (U) and non-interfering sample (N).

Table 6.5 quantification cycle reading (Cq) and standard deviation reading (SEM). The reading were normalized against TUBULIN and LAMIN. siRNA sample (S), non-interference sample (N) and untreated sample (U). p value <0.05

Target	Sample	Expression	Expression SEM	Corrected Expression SEM	Mean Cq	Cq SEM
CALB2	N	0.87144	0.06097	0.06097	32.73	0.09530
CALB2	S	1.20439	0.10933	0.10933	32.53	0.12741
CALB2	U	0.65341	0.03756	0.03756	33.42	0.07908
CPS1	N	0.34873	0.04607	0.04607	32.22	0.18766
CPS1	S	1.20439	0.03668	0.03668	30.70	0.03184
CPS1	U	0.42142	0.05605	0.05605	32.23	0.19026
LAMIN	N				21.01	0.05262
LAMIN	S				21.23	0.03476
LAMIN	U				21.28	0.03273
LY96	N	0.33747	0.02065	0.02065	30.75	0.08179
LY96	S	1.20439	0.27020	0.27020	29.18	0.32224
LY96	U	0.42905	0.03429	0.03429	30.68	0.11256
SLC17A7	N	0.57800	0.04247	0.04247	30.07	0.10067
SLC17A7	S	1.20439	0.02618	0.02618	29.28	0.00814
SLC17A7	U	0.60882	0.07680	0.07680	30.27	0.18027
TEX19	N	1.00000	0.02578	0.02578	31.15	0.01667
TEX19	S	0.22851	0.02480	0.02480	33.55	0.15364
TEX19	U	0.96837	0.09477	0.09477	31.48	0.13897
TRIM54	N	0.89928	0.05951	0.05951	32.69	0.08949
TRIM54	S	1.20439	0.07628	0.07628	32.53	0.08620
TRIM54	U	0.62160	0.09768	0.09768	33.50	0.22534
TUBULIN	N				18.14	0.04067
TUBULIN	S				18.46	0.04961
TUBULIN	U				18.43	0.03768

6.2.2 Evaluation the genetic expression influence of *TEX19* knockdown in A2780

qRT PCR results shows expression of some genes is not affected with *TEX19* knockdown in A2780 cancer cells including *MPEP, NAPB, PGM1, RIPA, ATP5C1, SLC17A7, CPS1* and *CALB2* where the expression did not changed significantly compared to both untreated and non-interference samples except *GALANT2* (Figure 6.5, Figure 6.6 and Figure 6.8). However, four genes had expression elevated in the knockdown sample compared to both untreated and non-interfering samples including *GALANT2, ZBTB5, ZNF367* and *TRIM54* (Figure 6.5, Figure 6.6, Figure 6.7 and Figure 6.8). In addition, *SAA2* show an increasing expression with *TEX19* expression knockdown in A2780 compared to untreated sample and lower expression compared to non-interference sample. Moreover, *MRP523* show lower expression with *TEX19* knockdown compared to non-interfering sample. Nevertheless, the expression changes were insignificant compared to untreated sample (Figure 6.6). Another result was observed in *ASB2* expression with *TEX19* expression knockdown, an increasing expression comparable to untreated sample and reversely low expression comparable to non-interfering sample (Figure 6.7). *SLC17A7* expression in *TEX19* knockdown sample were elevated compared to non-interference sample and low expression observed compared to untreated sample (Figure 6.8). *CD22* and *NOS3* show no difference in their expression compared to non-interfering sample and both were highly expressed compared to untreated sample (Figure 6.7). Insignificant expression change were observed in *TAGLN* compared to untreated sample, and low expression were observed compared to non-interfering sample (Figure 6.7).

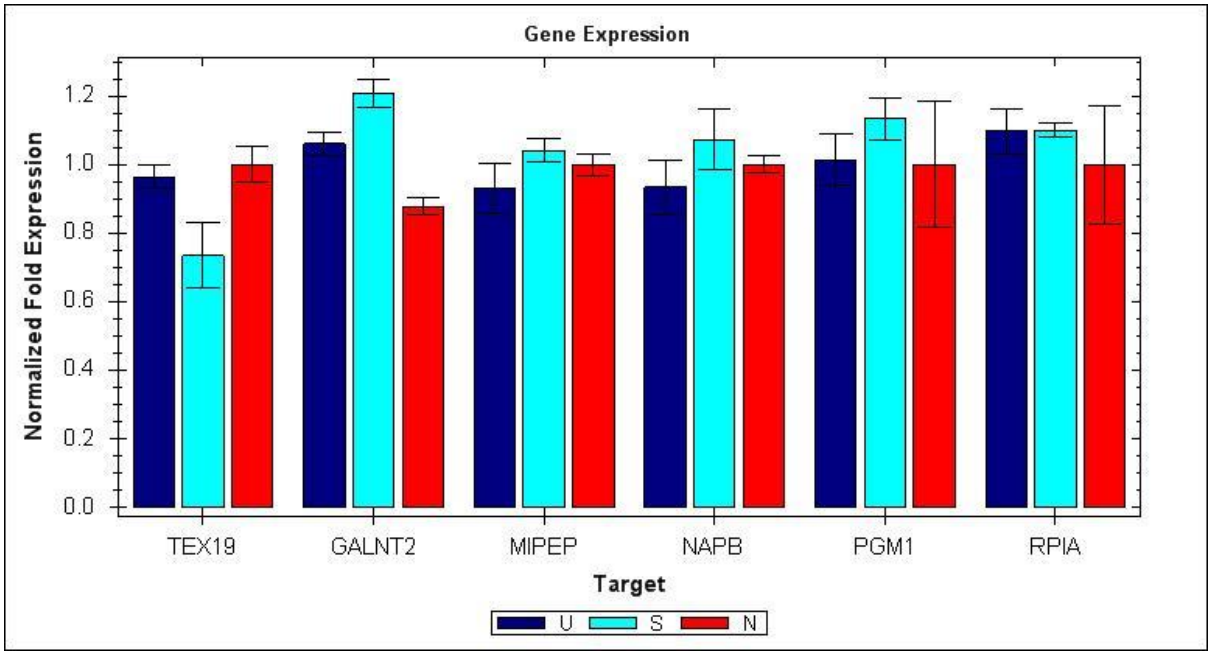

Figure 6.5 qRT PCR in A2780 cancer cell show *TEX19* knockdown (S), untreated cells (U) and non-interfering sample (N).

Table 6.6 quantification cycle reading (Cq) and standard deviation reading (SEM). The reading were normalized against TUBULIN and LAMIN. siRNA sample (S), non-interference sample (N) and untreated sample (U).

Target	Sample	Ctrl	Expression	Expression SEM	Corrected Expression SEM	Mean Cq	Cq SEM
GALNT2	N		0.87729	0.02481	0.02481	26.04	0.03390
GALNT2	S		1.20762	0.04038	0.04038	25.85	0.04362
GALNT2	U		1.06116	0.03549	0.03549	25.92	0.03866
LAMIN	N					24.39	0.03210
LAMIN	S					24.75	0.02207
LAMIN	U					24.70	0.05648
MIPEP	N		1.00148	0.03157	0.03157	26.45	0.03941
MIPEP	S		1.04258	0.03475	0.03475	26.67	0.04345
MIPEP	U		0.93295	0.07289	0.07289	26.71	0.10896
NAPB	N		1.00148	0.02401	0.02401	30.75	0.02057
NAPB	S		1.07285	0.08804	0.08804	30.92	0.11658
NAPB	U		0.93492	0.07961	0.07961	30.99	0.11941
PGM1	N		1.00148	0.18506	0.18506	25.64	0.26563
PGM1	S		1.13485	0.06084	0.06084	25.73	0.07456
PGM1	U		1.01391	0.07558	0.07558	25.77	0.10359
RPIA	N		1.00148	0.17268	0.17268	24.55	0.24771
RPIA	S		1.10139	0.02006	0.02006	24.69	0.01633
RPIA	U		1.09750	0.06742	0.06742	24.57	0.08379
TEX19	N		1.00148	0.05390	0.05390	30.99	0.07426
TEX19	S		0.73518	0.09499	0.09499	31.71	0.18527
TEX19	U		0.96540	0.03266	0.03266	31.19	0.03934
TUBULIN	N					19.39	0.03211
TUBULIN	S					19.58	0.03477
TUBULIN	U					19.39	0.01202

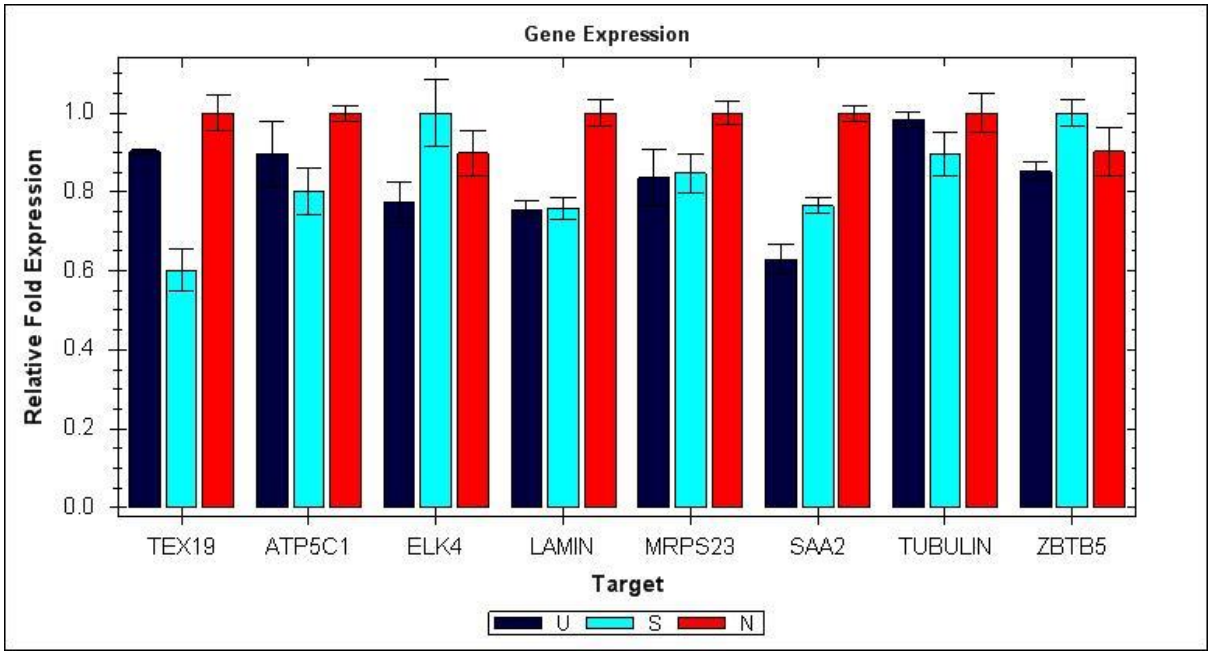

Figure 6.6 qRT PCR in A2780 cancer cell show *TEX19* knockdown (S), untreated cells (U) and non-interfering sample (N).

Table 6.7 quantification cycle reading (Cq) and standard deviation reading (SEM). The reading were normalized against TUBULIN and LAMIN. siRNA sample (S), non-interference sample (N) and untreated sample (U).

Target	Sample	Relative Quantity	Relative Quantity SEM	Corrected Relative Quantity SEM	Mean Cq	Cq SEM
ATP5C1	N	1.00000	0.01971	0.01971	22.36	0.02843
ATP5C1	S	0.80242	0.06002	0.06002	22.68	0.10791
ATP5C1	U	0.89708	0.08350	0.08350	22.52	0.13428
ELK4	N	0.89851	0.05726	0.05726	25.99	0.09194
ELK4	S	1.00000	0.08478	0.08478	25.84	0.12231
ELK4	U	0.77410	0.05216	0.05216	26.21	0.09722
LAMIN	N	1.00000	0.03434	0.03434	24.39	0.04955
LAMIN	S	0.75901	0.02793	0.02793	24.79	0.05309
LAMIN	U	0.75544	0.02249	0.02249	24.80	0.04295
MRPS23	N	1.00000	0.02946	0.02946	24.09	0.04250
MRPS23	S	0.84725	0.04899	0.04899	24.33	0.08341
MRPS23	U	0.83656	0.07051	0.07051	24.34	0.12160
SAA2	N	1.00000	0.01934	0.01934	26.82	0.02790
SAA2	S	0.76577	0.02037	0.02037	27.21	0.03837
SAA2	U	0.62928	0.03781	0.03781	27.49	0.08668
TEX19	N	1.00000	0.04568	0.04568	31.29	0.06590
TEX19	S	0.60110	0.05371	0.05371	32.02	0.12891
TEX19	U	0.90278	0.00671	0.00671	31.44	0.01072
TUBULIN	N	1.00000	0.05000	0.05000	19.36	0.07214
TUBULIN	S	0.89798	0.05511	0.05511	19.52	0.08854
TUBULIN	U	0.98442	0.02010	0.02010	19.38	0.02945
ZBTB5	N	0.90273	0.06016	0.06016	28.92	0.09614
ZBTB5	S	1.00000	0.03360	0.03360	28.77	0.04847
ZBTB5	U	0.85258	0.02337	0.02337	29.00	0.03955

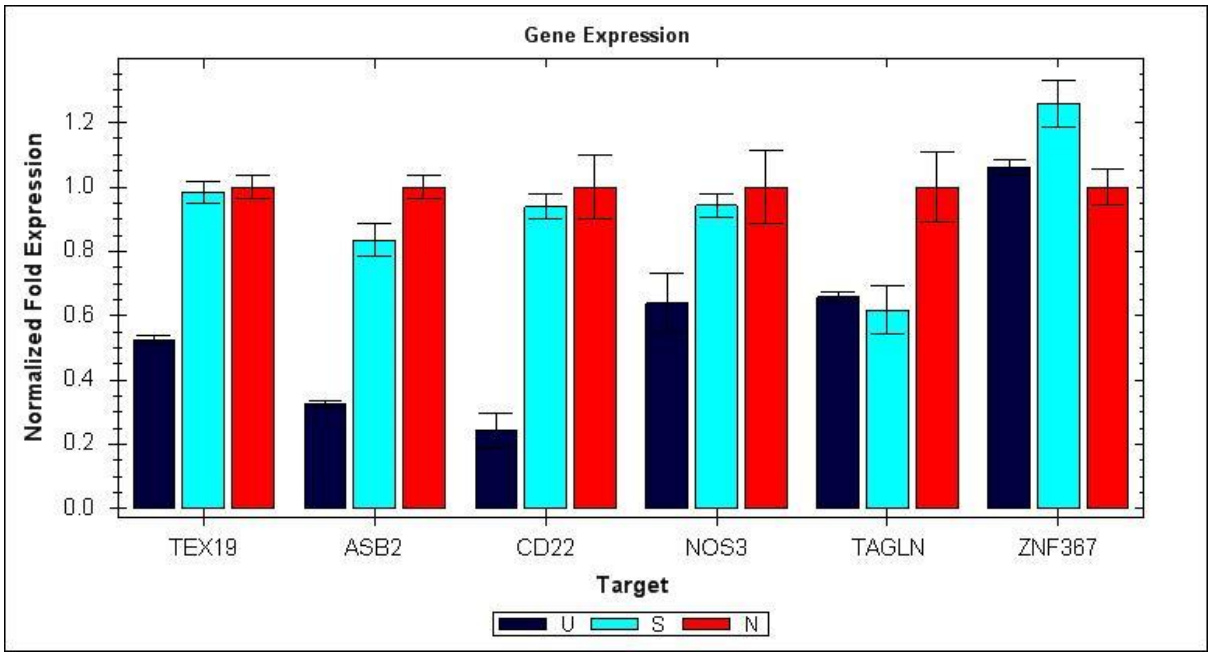

Figure 6.7 qRT PCR in A2780 cancer cell show *TEX19* knockdown (S), untreated cells (U) and non-interfering sample (N).

Table 6.8 quantification cycle reading (Cq) and standard deviation reading (SEM). The reading were normalized against TUBULIN and LAMIN. siRNA sample (S), non-interference sample (N) and untreated sample (U).

Target	Sample	Expression	Expression SEM	Corrected Expression SEM	Mean Cq	Cq SEM
ASB2	N	1.00000	0.03564	0.03564	33.61	0.02566
ASB2	S	0.83411	0.05007	0.05007	34.22	0.07515
ASB2	U	0.32588	0.00780	0.00780	35.41	0.00944
CD22	N	1.00000	0.09969	0.09969	36.89	0.13675
CD22	S	0.93884	0.03962	0.03962	37.33	0.00000
CD22	U	0.24376	0.05295	0.05295	39.11	0.31160
LAMIN	N				24.67	0.02801
LAMIN	S				25.11	0.06737
LAMIN	U				25.03	0.05348
NOS3	N	1.00000	0.11256	0.11256	31.00	0.15826
NOS3	S	0.94309	0.03618	0.03618	31.43	0.03477
NOS3	U	0.63854	0.09278	0.09278	31.83	0.20698
TAGLN	N	1.00000	0.10747	0.10747	31.71	0.15071
TAGLN	S	0.61645	0.07468	0.07468	32.76	0.17120
TAGLN	U	0.65836	0.01620	0.01620	32.50	0.01257
TEX19	N	1.00000	0.03795	0.03795	30.43	0.03183
TEX19	S	0.98446	0.03455	0.03455	30.80	0.02665
TEX19	U	0.52368	0.01409	0.01409	31.55	0.02779
TUBULIN	N				19.58	0.06715
TUBULIN	S				19.84	0.02011
TUBULIN	U				19.59	0.00899
ZNF367	N	1.00000	0.05768	0.05768	28.02	0.07484
ZNF367	S	1.25836	0.07188	0.07188	28.03	0.07453
ZNF367	U	1.06171	0.02517	0.02517	28.11	0.00822

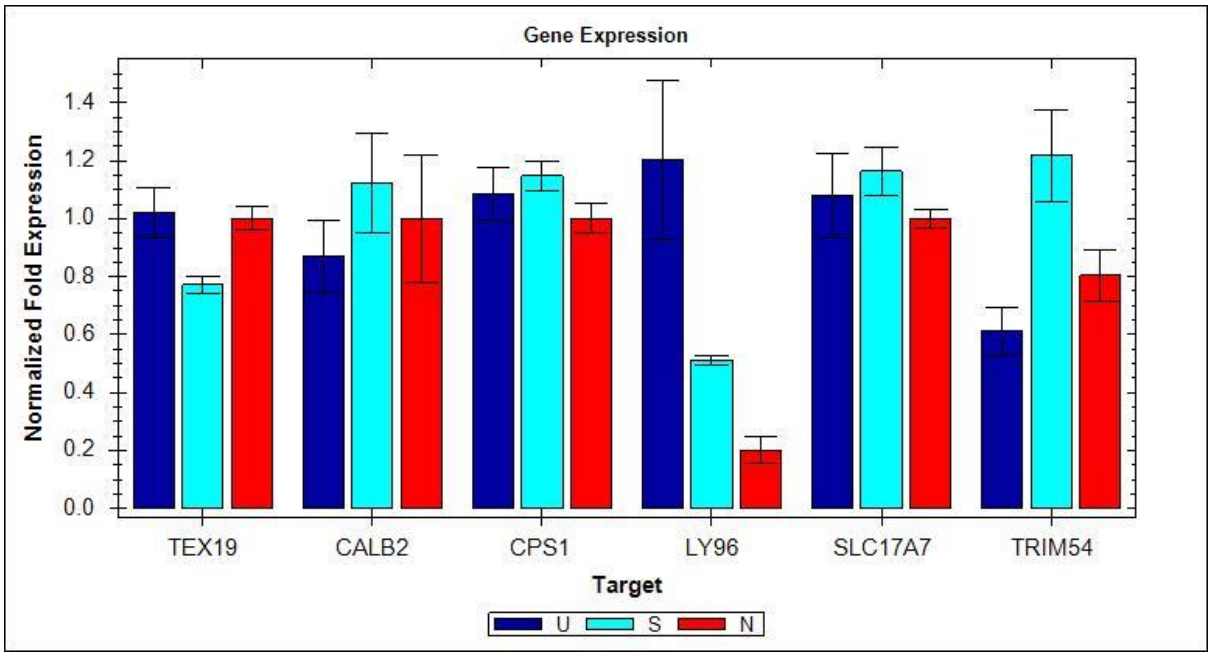

Figure 6.8 qRT PCR in A2780 cancer cell show *TEX19* knockdown (S), untreated cells (U) and non-interfering sample (N).

Table 6.9 quantification cycle reading (Cq) and standard deviation reading (SEM). The reading were normalized against TUBULIN and LAMIN. siRNA sample (S), non-interference sample (N) and untreated sample (U).

Target	**Sample**	**Expression**	**Expression SEM**	**Corrected Expression SEM**	**Mean Cq**	**Cq SEM**
CALB2	N	1.00000	0.21953	0.21953	35.71	0.31643
CALB2	S	1.12404	0.17199	0.17199	35.82	0.21946
CALB2	U	0.87093	0.12518	0.12518	36.17	0.20393
CPS1	N	1.00000	0.05049	0.05049	30.59	0.07161
CPS1	S	1.14679	0.05092	0.05092	30.67	0.05946
CPS1	U	1.08495	0.08930	0.08930	30.73	0.11264
LAMIN	N				24.18	0.01707
LAMIN	S				24.54	0.03167
LAMIN	U				24.59	0.07453
LY96	N	0.20228	0.04452	0.04452	39.68	0.31708
LY96	S	0.51099	0.01477	0.01477	38.63	0.02975
LY96	U	1.20122	0.27424	0.27424	37.38	0.32614
SLC17A7	N	1.00000	0.03138	0.03138	29.78	0.04328
SLC17A7	S	1.16437	0.08293	0.08293	29.85	0.09994
SLC17A7	U	1.07890	0.14339	0.14339	29.94	0.18802
TEX19	N	1.00000	0.04009	0.04009	30.59	0.05628
TEX19	S	0.77166	0.02928	0.02928	31.25	0.04928
TEX19	U	1.02066	0.08622	0.08622	30.82	0.11593
TRIM54	N	0.80385	0.08962	0.08962	34.58	0.16029
TRIM54	S	1.21846	0.15781	0.15781	34.27	0.18532
TRIM54	U	0.61223	0.08292	0.08292	35.24	0.19175
TUBULIN	N				19.05	0.02042
TUBULIN	S				19.26	0.03567
TUBULIN	U				19.17	0.00992

6.2.3 Evaluation the gene expression profile of *TEX19* knockdown in H460

In H460 cancer cell, knockdown *TEX19* show an increasing expression level of some genes compared with untreated and non-interference samples including *MPEP* (Figure 6.9), *ATP5C1* (Figure 6.10), *CALB2, CPS1, LY96, SLC17A7* and *TRIM54* (Figure 6.12). Inhibition of expression of *PGM1* was observed in the *TEX19* knockdown sample compared with both untreated and non-interference samples (Figure 6.9). In addition, no expression changes were quantified in *TEX19* knockdown sample compared with untreated and non-interfering samples of *RIPA* (Figure 6.9), *ASB2* and *ZNF367* (Figure 6.11). However, a significant elevation in expression of *GALNT2, MRP524* (Figure 6.10) and *CD22* (Figure 6.11) was observed in *TEX19* knockdown sample compared with untreated condition. In addition, low expression of *ELK4* and *ZBTB5* was observed in *TEX19* depleted sample compared to non-interfering sample, and insignificant expression changes compared to untreated cells was observed (Figure 6.10). In contrast, *NAPB* and *NOS3* expression were reduced relative to untreated sample and show similar expression to non-interfering sample (Figure 6.9 and Figure 6.11). Moreover, *SAA2* show low expression in *TEX19* knockdown sample compared with non-interference and high level of expression were observed compared with untreated sample (Figure 6.10). In addition, high expression in *TEX19* knockdown sample compared with non-interfering were observed in *TAGLN* and no expression difference observed compared to untreated sample (Figure 6.11).

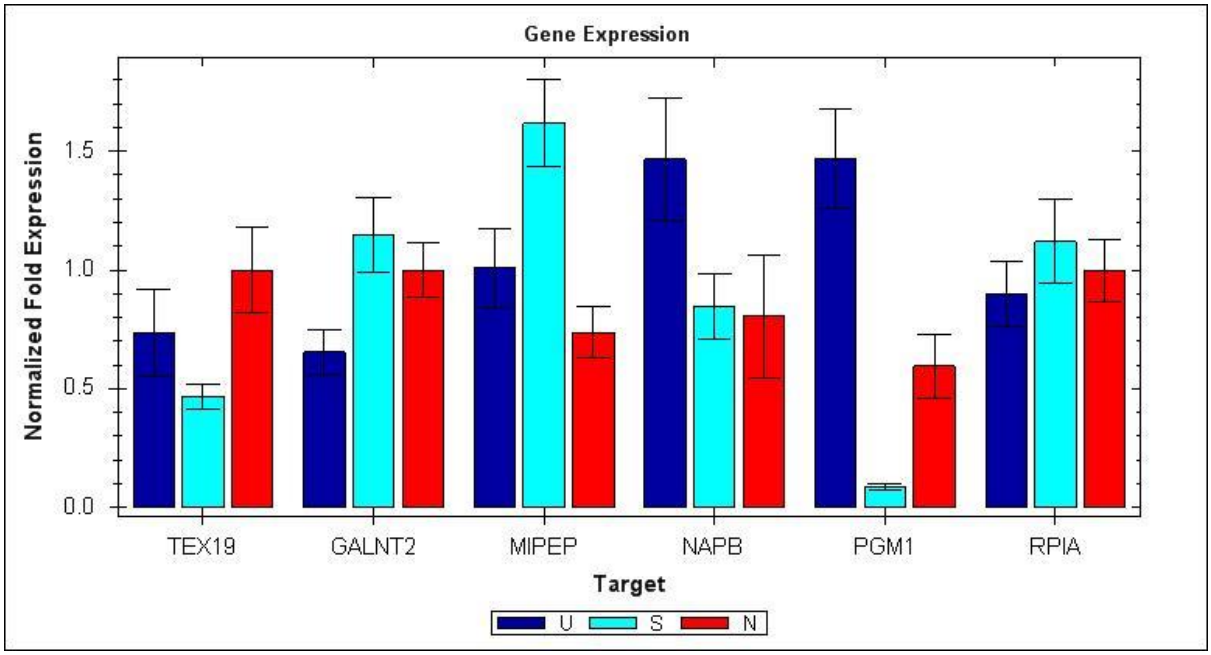

Figure 6.9 qRT PCR in H460 cancer cell show *TEX19* knockdown (S), untreated cells (U) and non-interfering sample (N).

Table 6.10 quantification cycle reading (Cq) and standard deviation reading (SEM). The reading were normalized against TUBULIN and LAMIN. siRNA sample (S), non-interference sample (N) and untreated sample (U).

Target	Sample	Expression	Expression SEM	Corrected Expression SEM	Mean Cq	Cq SEM
GALNT2	N	1.00000	0.11188	0.11188	25.40	0.01855
GALNT2	S	1.14616	0.15861	0.15861	25.90	0.15003
GALNT2	U	0.65405	0.09541	0.09541	26.57	0.13094
LAMIN	N				22.12	0.17556
LAMIN	S				22.63	0.14375
LAMIN	U				22.69	0.10944
MIPEP	N	0.73808	0.10689	0.10689	27.71	0.16284
MIPEP	S	1.61859	0.18229	0.18229	27.28	0.01942
MIPEP	U	1.00916	0.16716	0.16716	27.81	0.12800
NAPB	N	0.80516	0.25829	0.25829	31.32	0.43414
NAPB	S	0.84436	0.13864	0.13864	31.95	0.19689
NAPB	U	1.46536	0.25707	0.25707	31.01	0.15274
PGM1	N	0.59560	0.13451	0.13451	28.18	0.28363
PGM1	S	0.33193	0.45007	0.45007	29.72	1.94952
PGM1	U	1.46536	0.20941	0.20941	27.43	0.04222
RPIA	N	1.00000	0.13114	0.13114	25.87	0.13658
RPIA	S	1.11999	0.17717	0.17717	26.40	0.16143
RPIA	U	0.89856	0.13574	0.13574	26.58	0.14263
TEX19	N	1.00000	0.18300	0.18300	31.58	0.20974
TEX19	S	0.46729	0.05379	0.05379	33.37	0.03948
TEX19	U	0.73672	0.18179	0.18179	32.57	0.31557
TUBULIN	N				19.44	0.19426
TUBULIN	S				20.32	0.23583
TUBULIN	U				19.97	0.31720

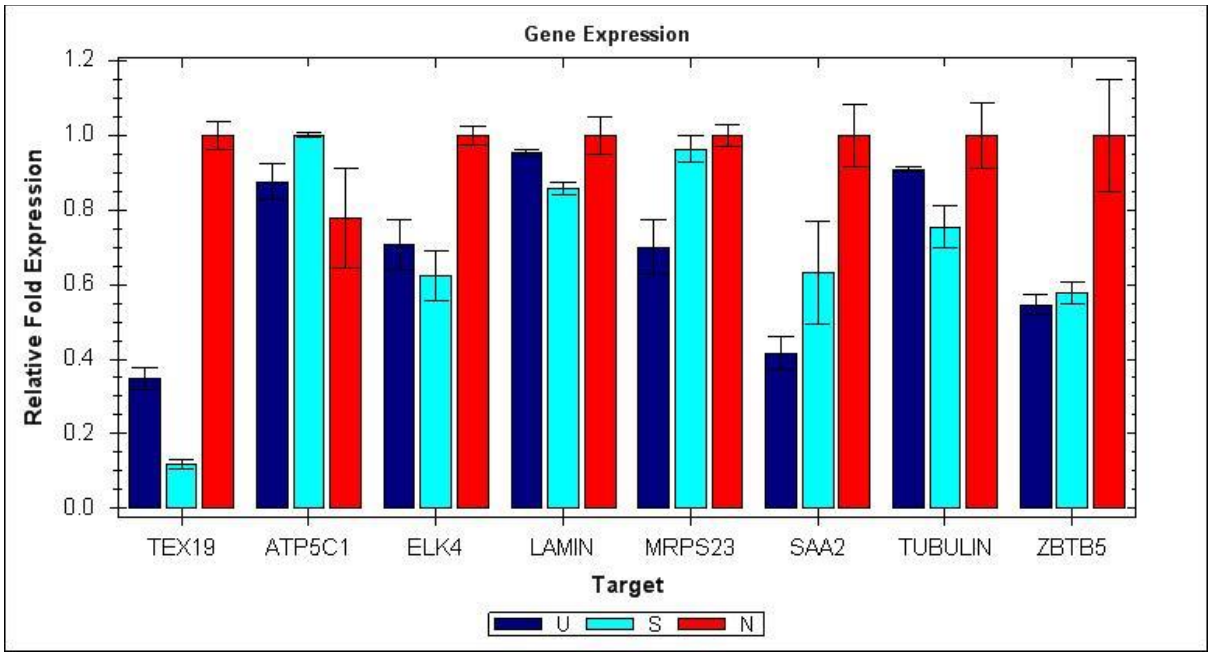

Figure 6.10 qRT PCR in H460 cancer cell show *TEX19* knockdown (S), untreated cells (U) and non-interfering sample (N).

Table 6.11 quantification cycle reading (Cq) and standard deviation reading (SEM). The reading were normalized against TUBULIN and LAMIN. siRNA sample (S), non-interference sample (N) and untreated sample (U).

Target	Sample	Relative Quantity	Relative Quantity SEM	Corrected Relative Quantity SEM	Mean Cq	Cq SEM
ATP5C1	N	0.77930	0.13422	0.13422	23.48	0.24848
ATP5C1	S	1.00000	0.00643	0.00643	23.12	0.00928
ATP5C1	U	0.87607	0.04855	0.04855	23.31	0.07995
ELK4	N	1.00000	0.02489	0.02489	25.96	0.03591
ELK4	S	0.62548	0.06670	0.06670	26.64	0.15384
ELK4	U	0.70802	0.06653	0.06653	26.46	0.13556
LAMIN	N	1.00000	0.04860	0.04860	21.55	0.07011
LAMIN	S	0.85810	0.01584	0.01584	21.77	0.02663
LAMIN	U	0.95298	0.00952	0.00952	21.62	0.01441
MRPS23	N	1.00000	0.02888	0.02888	24.42	0.04167
MRPS23	S	0.96361	0.03536	0.03536	24.47	0.05294
MRPS23	U	0.70026	0.07429	0.07429	24.93	0.15306
SAA2	N	1.00000	0.08500	0.08500	34.37	0.12263
SAA2	S	0.63300	0.13831	0.13831	35.02	0.31523
SAA2	U	0.41633	0.04376	0.04376	35.63	0.15164
TEX19	N	1.00000	0.03850	0.03850	31.93	0.05555
TEX19	S	0.11832	0.01417	0.01417	35.01	0.17275
TEX19	U	0.34814	0.02937	0.02937	33.45	0.12169
TUBULIN	N	1.00000	0.08887	0.08887	18.91	0.12821
TUBULIN	S	0.75489	0.05474	0.05474	19.32	0.10462
TUBULIN	U	0.90969	0.00626	0.00626	19.05	0.00992
ZBTB5	N	1.00000	0.14903	0.14903	28.71	0.21501
ZBTB5	S	0.57845	0.02959	0.02959	29.50	0.07379
ZBTB5	U	0.54556	0.02714	0.02714	29.58	0.07177

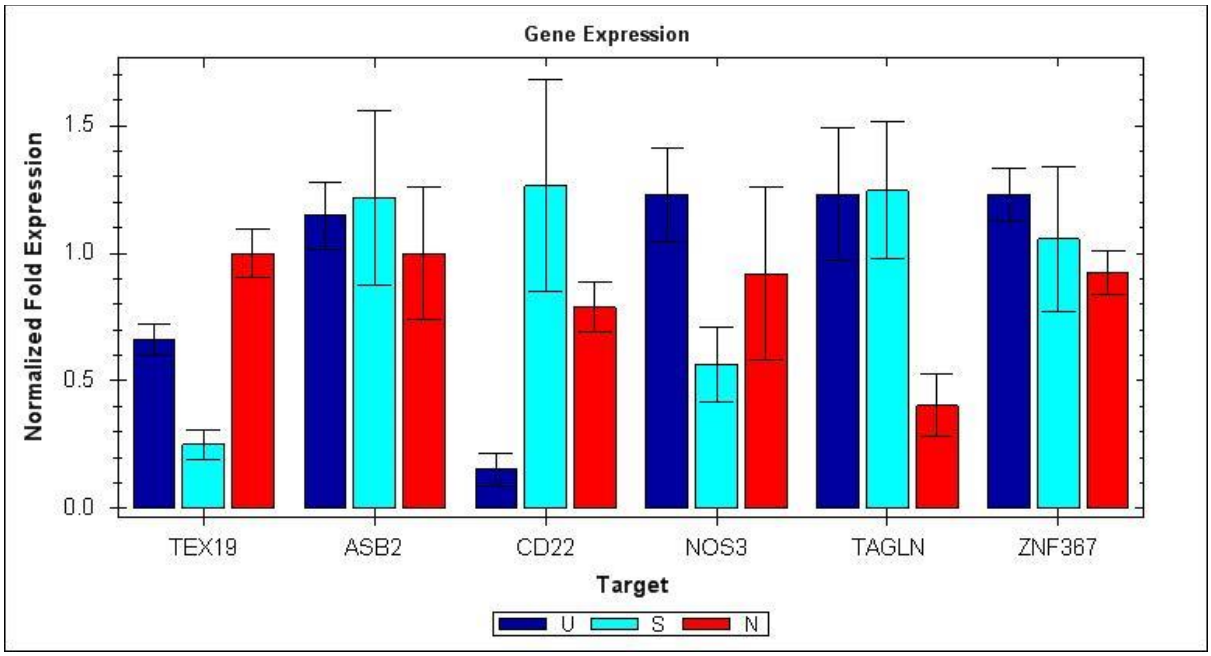

Figure 6.11 qRT PCR in H460 cancer cell show *TEX19* knockdown (S), untreated cells (U) and non-interfering sample (N).

Table 6.12 quantification cycle reading (Cq) and standard deviation reading (SEM). The reading were normalized against TUBULIN and LAMIN. siRNA sample (S), non-interference sample (N) and untreated sample (U).

Target	**Sample**	**Expression**	**Expression SEM**	**Corrected Expression SEM**	**Mean Cq**	**Cq SEM**
ASB2	N	1.00000	0.25890	0.25890	35.74	0.35002
ASB2	S	1.21754	0.34152	0.34152	35.79	0.29846
ASB2	U	1.14858	0.13233	0.13233	35.84	0.13404
CD22	N	0.78888	0.09524	0.09524	36.11	0.06961
CD22	S	1.26466	0.41492	0.41492	35.76	0.00000
CD22	U	0.15203	0.06464	0.06464	38.78	0.60147
LAMIN	N				22.31	0.06258
LAMIN	S				22.52	0.06374
LAMIN	U				22.86	0.18632
NOS3	N	0.92010	0.33870	0.33870	29.26	0.50651
NOS3	S	0.56393	0.14551	0.14551	30.30	0.16297
NOS3	U	1.23048	0.18452	0.18452	29.14	0.17977
TAGLN	N	0.40195	0.12182	0.12182	31.79	0.40706
TAGLN	S	1.24611	0.26827	0.26827	30.50	0.14759
TAGLN	U	1.23048	0.26081	0.26081	30.48	0.28111
TEX19	N	1.00000	0.09239	0.09239	31.28	0.02780
TEX19	S	0.25112	0.05755	0.05755	33.61	0.18613
TEX19	U	0.65979	0.06032	0.06032	32.17	0.08796
TUBLAIN	N				19.73	0.25310
TUBLAIN	S				20.19	0.54283
TUBLAIN	U				19.78	0.06263
ZNF367	N	0.92355	0.08542	0.08542	27.46	0.02849
ZNF367	S	1.05577	0.28481	0.28481	27.61	0.19861
ZNF367	U	1.23048	0.10433	0.10433	27.35	0.02175

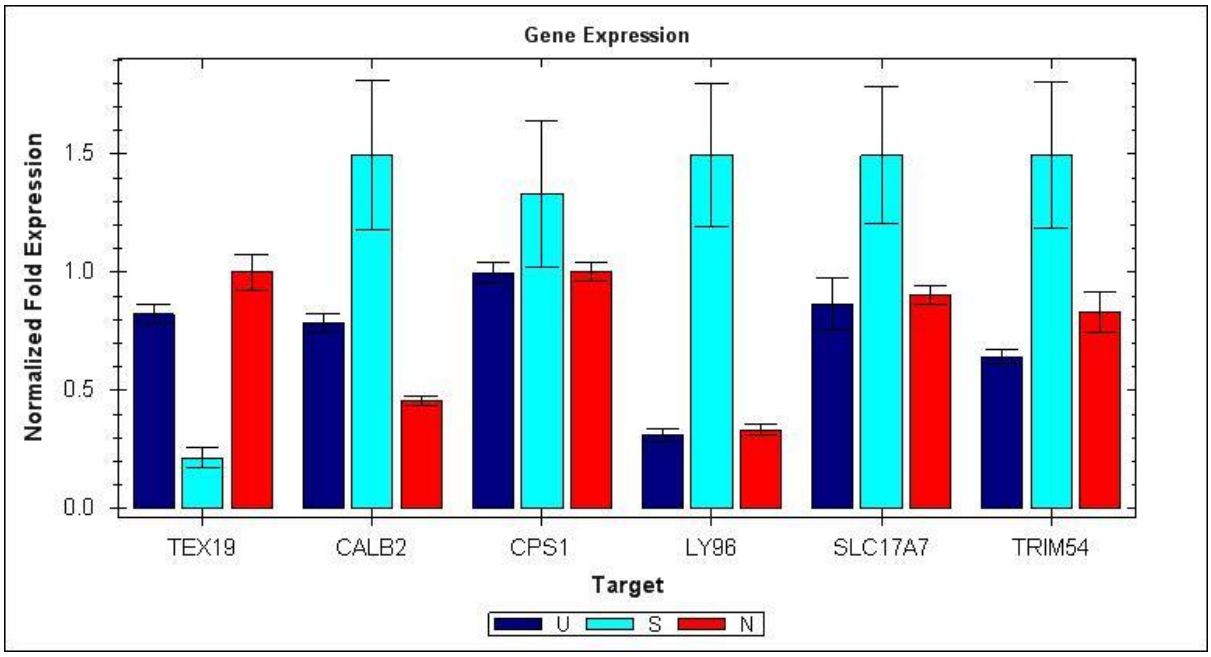

Figure 6.12 qRT PCR in H460 cancer cell show *TEX19* knockdown (S), untreated cells (U) and non-interfering sample (N).

Table 6.13 quantification cycle reading (Cq) and standard deviation reading (SEM). The reading were normalized against TUBULIN and LAMIN. siRNA sample (S), non-interference sample (N) and untreated sample (U).

Target	**Sample**	**Expression**	**Expression SEM**	**Corrected Expression SEM**	**Mean Cq**	**Cq SEM**
CALB2	N	0.45505	0.02072	0.02072	32.64	0.05708
CALB2	S	1.49575	0.31480	0.31480	31.51	0.12981
CALB2	U	0.78573	0.03836	0.03836	32.05	0.05347
CPS1	N	1.00000	0.04027	0.04027	22.04	0.04814
CPS1	S	1.33289	0.31121	0.31121	22.20	0.02113
CPS1	U	0.99863	0.04054	0.04054	22.23	0.01666
LAMIN	N				21.64	0.04815
LAMIN	S				22.42	0.54772
LAMIN	U				21.86	0.04192
LY96	N	0.33346	0.02351	0.02351	32.39	0.09356
LY96	S	1.49575	0.30508	0.30508	30.81	0.10602
LY96	U	0.31288	0.02750	0.02750	32.67	0.11371
SLC17A7	N	0.90377	0.04262	0.04262	33.07	0.05513
SLC17A7	S	1.49575	0.28767	0.28767	32.93	0.04052
SLC17A7	U	0.86691	0.10618	0.10618	33.32	0.17065
TEX19	N	1.00000	0.07415	0.07415	32.45	0.10190
TEX19	S	0.21451	0.04181	0.04181	35.25	0.06113
TEX19	U	0.82291	0.04038	0.04038	32.92	0.05394
TRIM54	N	0.83100	0.08771	0.08771	32.61	0.14875
TRIM54	S	1.49575	0.30868	0.30868	32.34	0.11533
TRIM54	U	0.64215	0.02870	0.02870	33.17	0.03168
TUBULIN	N				19.08	0.04379
TUBULIN	S				19.46	0.03714
TUBULIN	U				19.24	0.08155

6.2.4 Evaluation the genetic expression influence of TEX19 knockdown in NTERA2

TEX19 depletion in NTERA2 showed significant reduction in expression of 14 genes compared to untreated and non-interfering samples, these are *GALNT2, MPEP, NAPB, PGM1,RIPA* (Figure 6.13), *ATP5C1, ELK4, MRP523, ZBTB5* (Figure 6.14), *ASB2, NOS3, ZNF367* (Figure 6.15), *CPS1* and *SLC17A7* (Figure 6.16). However, *SAA2* showed higher expression following *TEX19* expression knockdown compared to both untreated and non-interfering samples (Figure 6.14). In addition, low expression was observed for *TAGLN* (Figure 6.15), *CALB2* and *LY96* (Figure 6.16) in *TEX19* depleted cells accompanied with high expression compared to untreated sample. Moreover, *TRIM54* showed insignificant expression change in *TEX19* knockdown sample compared to non-interfering sample and low expression were observed compared to untreated sample.

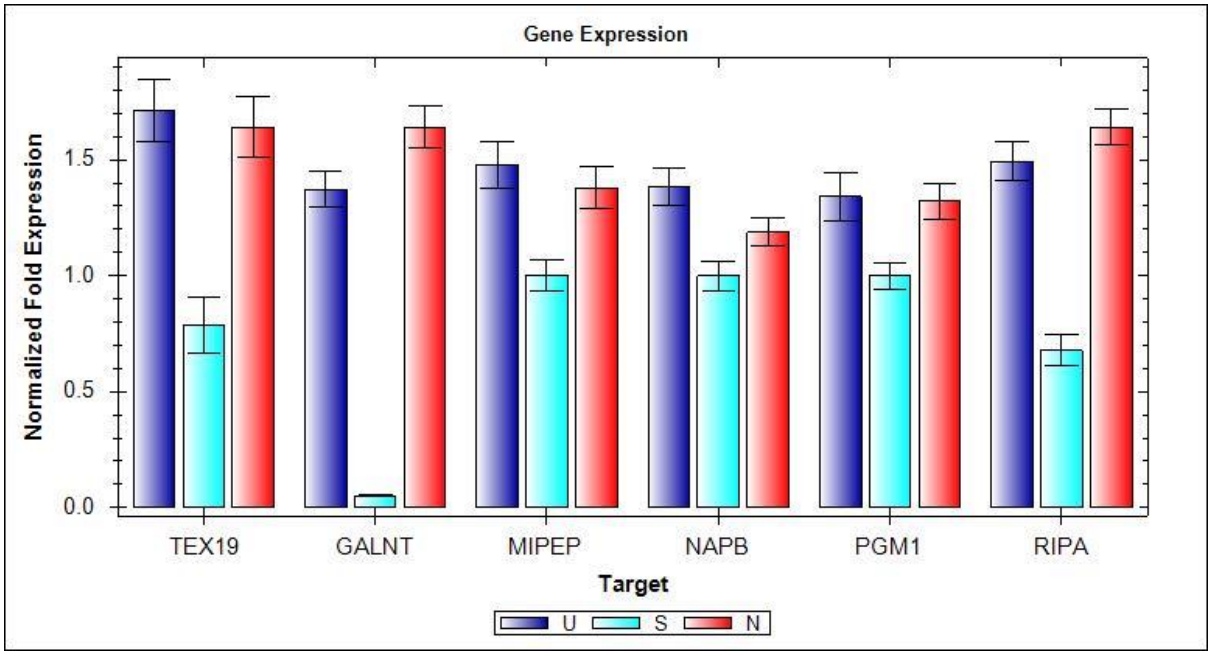

Figure 6.13 qRT PCR in NTERA2 cancer cell show *TEX19* knockdown (S), untreated cells (U) and non-interfering sample (N).

Table 6.14 quantification cycle reading (Cq) and standard deviation reading (SEM). The reading were normalized against TUBULIN and LAMIN. siRNA sample (S), non-interference sample (N) and untreated sample (U).

Target	**Sample**	**Expression**	**Expression SEM**	**Corrected Expression SEM**	**Mean Cq**	**Cq SEM**
GALNT	N	1.64139	0.09162	0.09162	24.72	0.04543
GALNT	S	0.05149	0.00387	0.00387	29.00	0.07766
GALNT	U	1.37256	0.07500	0.07500	25.58	0.05228
LAMIN	N				22.57	0.11180
LAMIN	S				21.72	0.06640
LAMIN	U				23.19	0.07363
MIPEP	N	1.37934	0.08870	0.08870	26.70	0.06470
MIPEP	S	1.00000	0.06697	0.06697	26.45	0.05996
MIPEP	U	1.47967	0.10007	0.10007	27.19	0.07770
NAPB	N	1.18774	0.06129	0.06129	30.99	0.03350
NAPB	S	1.00000	0.06276	0.06276	30.52	0.04957
NAPB	U	1.38419	0.07892	0.07892	31.37	0.05731
PGM1	N	1.32002	0.07598	0.07598	24.38	0.04975
PGM1	S	1.00000	0.05699	0.05699	24.06	0.03194
PGM1	U	1.34088	0.10275	0.10275	24.95	0.09349
RIPA	N	1.64139	0.07986	0.07986	25.23	0.02249
RIPA	S	0.67773	0.06891	0.06891	25.79	0.12562
RIPA	U	1.49210	0.08269	0.08269	25.97	0.05395
TEX19	N	1.64139	0.13265	0.13265	32.66	0.09577
TEX19	S	0.78408	0.12134	0.12134	33.01	0.21002
TEX19	U	1.71185	0.13290	0.13290	33.20	0.09520
TUBULIN	N				18.16	0.07200
TUBULIN	S				17.58	0.13620
TUBULIN	U				18.73	0.09223

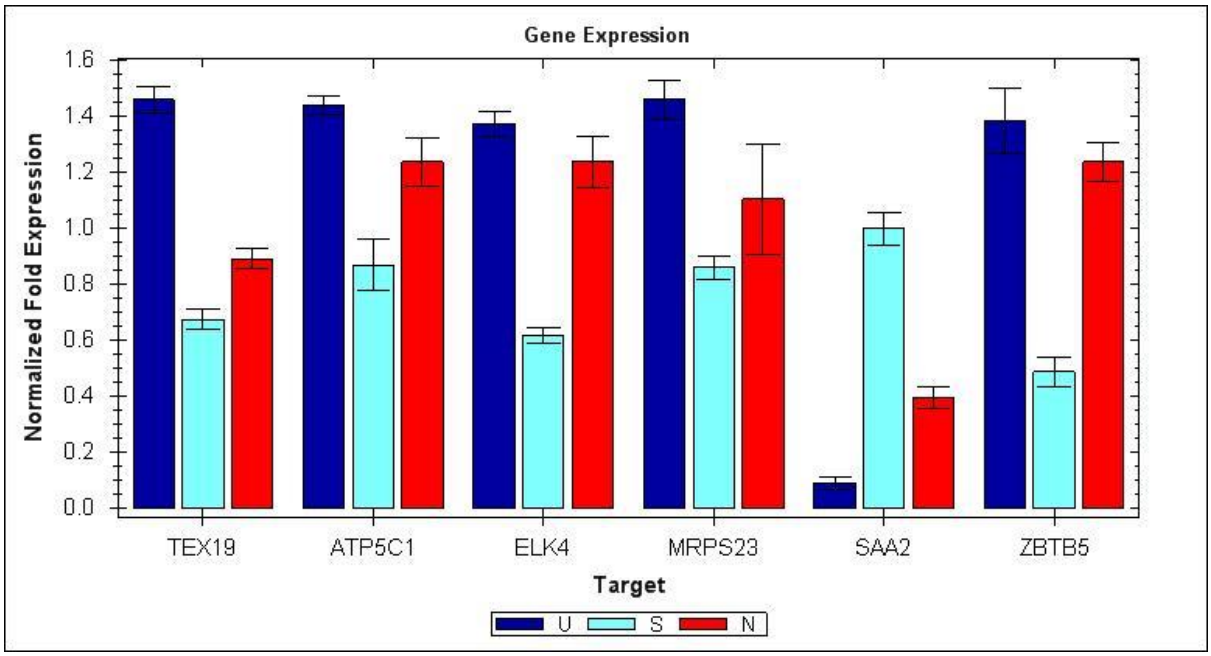

Figure 6.14 qRT PCR in NTERA2 cancer cell show *TEX19* knockdown (S), untreated cells (U) and non-interfering sample (N).

Table 6.15 quantification cycle reading (Cq) and standard deviation reading (SEM). The reading were normalized against TUBULIN and LAMIN. siRNA sample (S), non-interference sample (N) and untreated sample (U).

Target	Sample	Expression	Expression SEM	Corrected Expression SEM	Mean Cq	Cq SEM
ATP5C1	N	1.23795	0.08403	0.08403	24.39	0.09557
ATP5C1	S	0.87056	0.08960	0.08960	24.59	0.13916
ATP5C1	U	1.44119	0.03523	0.03523	24.41	0.02164
ELK4	N	1.23795	0.09005	0.09005	28.77	0.10275
ELK4	S	0.61755	0.02877	0.02877	29.47	0.04285
ELK4	U	1.37369	0.04236	0.04236	28.86	0.03470
LAMIN	N				23.05	0.02823
LAMIN	S				22.46	0.09979
LAMIN	U				23.55	0.02704
MRPS23	N	1.10511	0.19806	0.19806	26.71	0.25768
MRPS23	S	0.86097	0.04298	0.04298	26.76	0.05005
MRPS23	U	1.46043	0.06749	0.06749	26.55	0.06058
SAA2	N	0.39482	0.03859	0.03859	31.77	0.13937
SAA2	S	1.00000	0.05752	0.05752	30.12	0.06485
SAA2	U	0.09218	0.02289	0.02289	34.11	0.35714
TEX19	N	0.89145	0.03525	0.03525	33.98	0.05290
TEX19	S	0.67451	0.03604	0.03604	34.08	0.05710
TEX19	U	1.46043	0.04733	0.04733	33.51	0.03756
TUBULIN	N				20.12	0.03209
TUBULIN	S				20.09	0.02775
TUBULIN	U				20.09	0.04867
ZBTB5	N	1.23795	0.06721	0.06721	29.82	0.07535
ZBTB5	S	0.48808	0.05299	0.05299	30.85	0.14783
ZBTB5	U	1.38365	0.11652	0.11652	29.90	0.11826

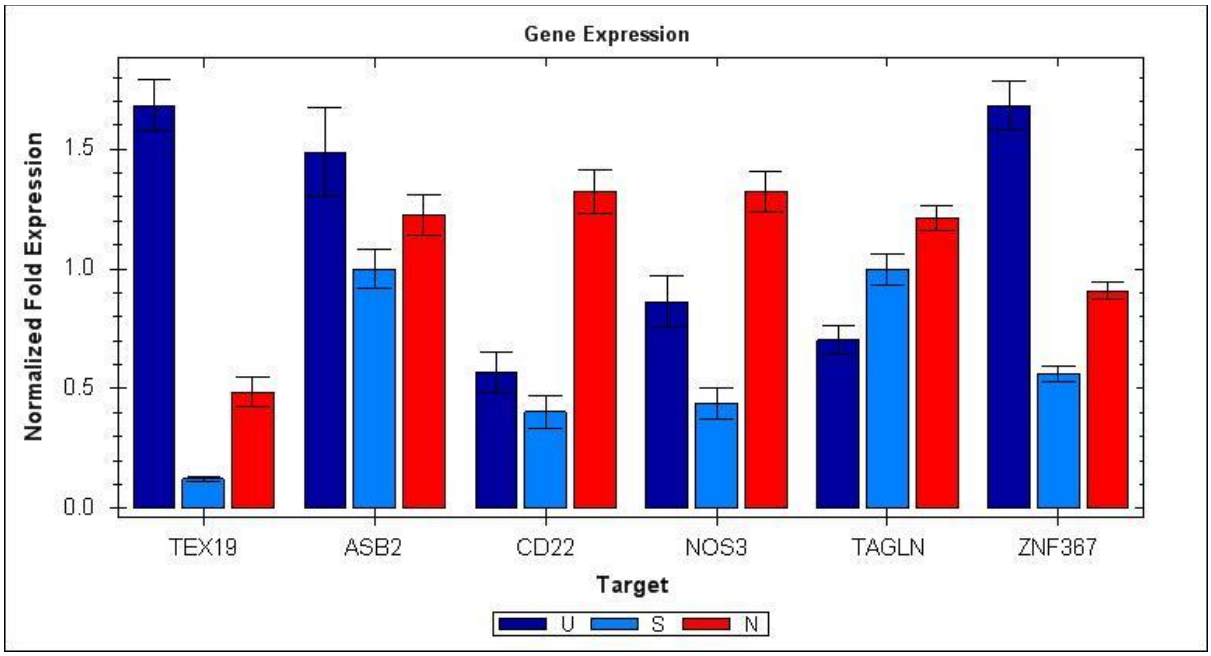

Figure 6.15 qRT PCR in NTERA2 cancer cell show *TEX19* knockdown (S), untreated cells (U) and non-interfering sample (N).

Table 6.16 quantification cycle reading (Cq) and standard deviation reading (SEM). The reading were normalized against TUBULIN and LAMIN. siRNA sample (S), non-interference sample (N) and untreated sample (U).

Target	Sample	Expression	Expression SEM	Corrected Expression SEM	Mean Cq	Cq SEM
ASB2	N	1.22499	0.08483	0.08483	35.47	0.08395
ASB2	S	1.00000	0.08444	0.08444	35.36	0.09905
ASB2	U	1.48714	0.18751	0.18751	35.54	0.16645
CD22	N	1.32258	0.08964	0.08964	32.53	0.08141
CD22	S	0.40318	0.06820	0.06820	33.84	0.23350
CD22	U	0.57126	0.08471	0.08471	34.09	0.20097
LAMIN	N				23.32	0.10321
LAMIN	S				22.53	0.02910
LAMIN	U				24.00	0.14410
NOS3	N	1.32258	0.08772	0.08772	32.77	0.07888
NOS3	S	0.43903	0.06613	0.06613	33.96	0.20541
NOS3	U	0.86530	0.10792	0.10792	33.73	0.16428
TAGLN	N	1.21167	0.05391	0.05391	30.85	0.03443
TAGLN	S	1.00000	0.06599	0.06599	30.72	0.06351
TAGLN	U	0.70573	0.05647	0.05647	31.97	0.08912
TEX19	N	0.67621	0.08385	0.08385	37.88	0.17050
TEX19	S	0.17088	0.01738	0.01738	39.46	0.12843
TEX19	U	1.68335	0.56704	0.56704	36.92	0.48040
TUBULIN	N				20.28	0.03293
TUBULIN	S				20.27	0.13881
TUBULIN	U				20.31	0.02778
ZNF367	N	0.90845	0.03829	0.03829	30.04	0.02762
ZNF367	S	0.56311	0.03297	0.03297	30.32	0.04591
ZNF367	U	1.68335	0.10123	0.10123	29.49	0.04629

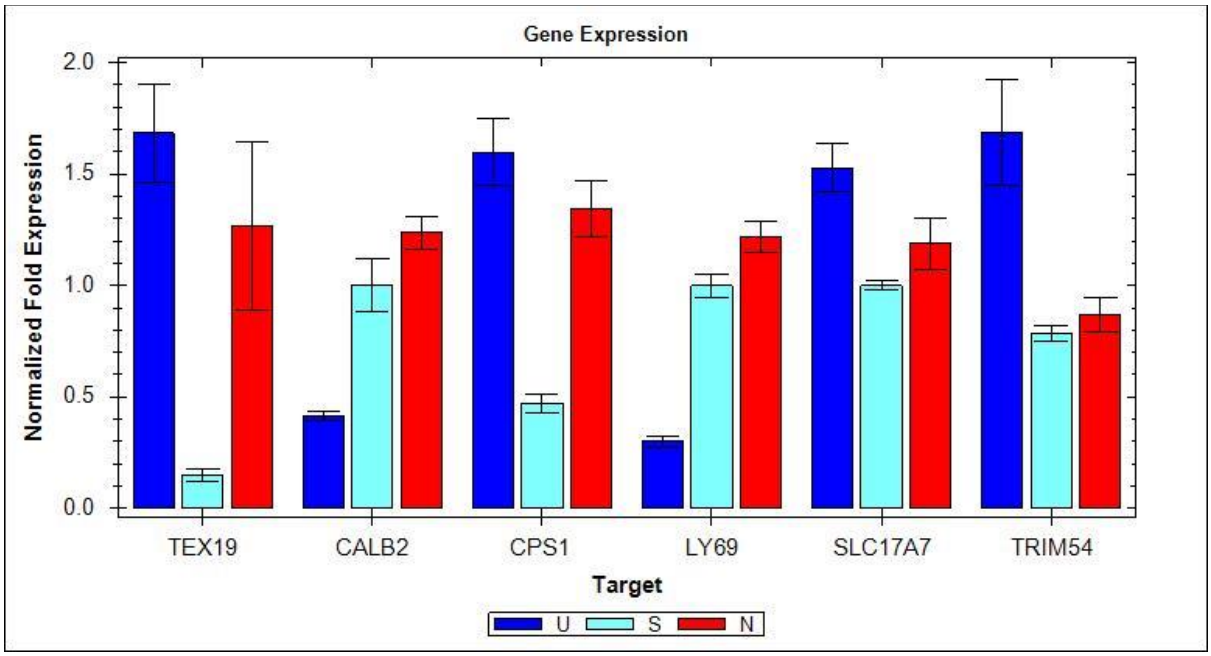

Figure 6.16 qRT PCR in NTERA2 cancer cell show *TEX19* knockdown (S), untreated cells (U) and non-interfering sample (N).

Table 6.17 quantification cycle reading (Cq) and standard deviation reading (SEM). The reading were normalized against TUBULIN and LAMIN. siRNA sample (S), non-interference sample (N) and untreated sample (U).

Target	**Sample**	**Expression**	**Expression SEM**	**Corrected Expression SEM**	**Mean Cq**	**Cq SEM**
CALB2	N	1.23913	0.07334	0.07334	28.26	0.03659
CALB2	S	1.00000	0.12076	0.12076	28.15	0.17303
CALB2	U	0.41269	0.01981	0.01981	30.18	0.06823
CPS1	N	1.34279	0.12668	0.12668	29.87	0.11212
CPS1	S	0.47072	0.04494	0.04494	30.95	0.13621
CPS1	U	1.59866	0.14885	0.14885	29.94	0.13381
LAMIN	N				23.20	0.15328
LAMIN	S				22.38	0.03724
LAMIN	U				23.75	0.00796
LY69	N	1.21834	0.07196	0.07196	30.16	0.03617
LY69	S	1.00000	0.05377	0.05377	30.02	0.07486
LY69	U	0.30026	0.02401	0.02401	32.51	0.11477
SLC17A7	N	1.18913	0.11515	0.11515	32.40	0.11647
SLC17A7	S	1.00000	0.01991	0.01991	32.22	0.02025
SLC17A7	U	1.52781	0.10993	0.10993	32.36	0.10313
TEX19	N	1.26541	0.37785	0.37785	36.80	0.42029
TEX19	S	0.14814	0.02933	0.02933	39.47	0.28450
TEX19	U	1.68444	0.22195	0.22195	36.72	0.18955
TRIM54	N	0.86912	0.07693	0.07693	32.59	0.10176
TRIM54	S	0.78589	0.03401	0.03401	32.31	0.05901
TRIM54	U	1.68444	0.23832	0.23832	31.96	0.20378
TUBULIN	N				20.09	0.01782
TUBULIN	S				20.06	0.01650
TUBULIN	U				20.20	0.02220

6.3 Discussion

The *GALNT2* gene encodes a protein which is a member of the glycosyltransferase 2 protein family, which introduce mucin-type O-glycoslation of peptides in the Golgi apparatus (Pokrovskaya *et al*., 2011).. Dysregulation of this gene has been associated with many types of cancers, and overexpression of *GALANT2* has been reported in some types of cancers particularly oral squamous cell carcinoma (Lin *et al*., 2014). *GALNT2* expression has been downregulated in hepatocellular carcinoma (Wu *et al*., 2011). Our qRT-PCR analysis show high expression of *GALNT2* in *TEX19* knockdown samples in SW480 and A2780 cancer cells. The high expression of *GALNT2* in these two-cancer cell-lines is consistence with RNA sequencing data that were performed in SW480. In contrast, low expression of *GALNT2* were observed in NTERA2 cells, this low expression may due to the origin of the tissue in which the cancer arises; it may be an interaction between *TEX19* and *GALANT2* genes; where both normally expressed in normal testis.

Another gene, *ELK4*, showed low expression with *TEX19* knockdown in NTERA2 and show high expression in SW480 cancer cells. *ELK4* is a member of E Twenty Six family (ETS), which play important roles in cell cycle, proliferation, differentiation and apoptosis (Kerr *et al*., 2010; Day *et al*., 2011). High expression of *ELK4* has been associated with some types of cancer, including prostate cancer (Shaikhibrahim *et al*., 2012).

qRT-PCR results of *SAA2* show high expression profile in NTERA2 cancer cell with *TEX19* knockdown and low expression in SW480. These inverted results recurrently observed between NTERA2 and SW480 including *GALNT2*, *ELK4*, *ASB2*, *CD22*, *SLC17A7* and *CPS1*, where high expression detected in SW480 accompanied by low expression were observed in NTERA2 cells for these genes. Saa2 protein is a member of serum amyloid A that usually responsible for amyloid deposit in chronic inflammation. In addition, this protein been upregulated in some types of malignancies (Malle *et al*., 2009). Moreover, *SAA2* may play a possible a role in tumour initiation and promotion (Vlasova and Moshkovskii, 2006).

The expression of *ZBTB5* gene in the *TEX19* knockdown sample show elevated expression in A2780 and inhibition of its expression in NTERA2. *ZBTB5* is related to cancer progression particularly thyroid cancer (Xu *et al*, 2014). However, no significant expression differences were observed in SW480 or H460.

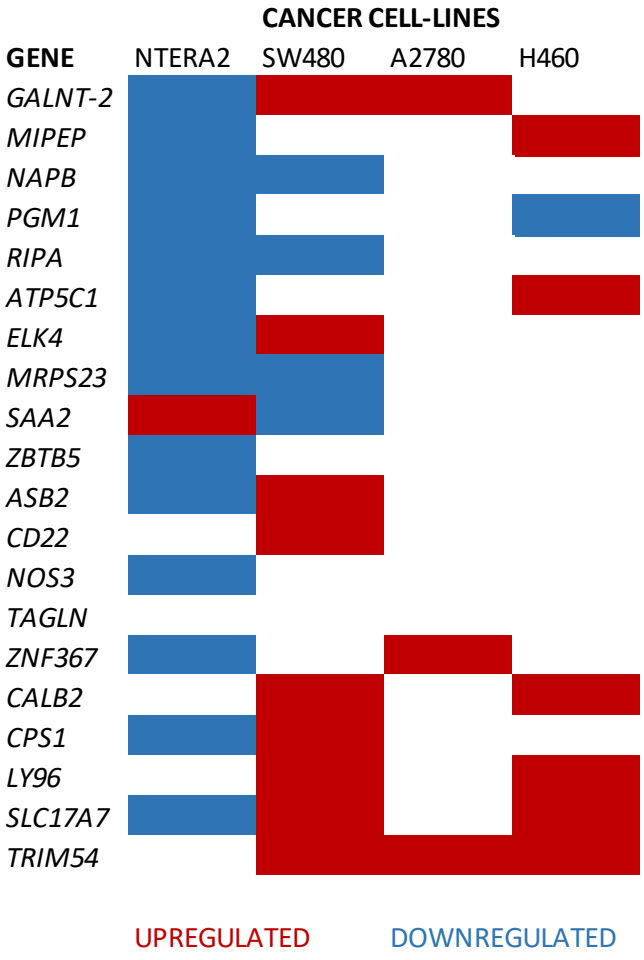

Figure 6.17 representation of 20 dysregulated genes based on RNA sequencing data. Genes shows upregulation and downregulation following *TEX19* depletion in four cancer cell-lines.

The *ASB2* gene encodes an Ankyrin repeat protein and SOCS box protein 2, the activation of this protein in acute promyelocytic leukemia consequently cause inhibition of cell growth and chromatin condensation (Guibal *et al*., 2002). In our experiment, we observe elevated *ASB2* expression in NTERA2 following *TEX19* knockdown, which is opposing the RNA sequencing data. However, *ASB2* expression was reduced in SW480 following *TEX19* knockdown, which shows complementarity with the RNA sequence data.

qRT PCR result of *CD22* show that increased expression was observed in SW480 with *TEX19* knockdown and low expression was observed in NTERA2 cells. While, our RNA sequencing analysis show down-regulation of *CD22* after knockdown *TEX19*. *CD22* is member of sialic acid-binding Ig-like lectin, which normally expressed in B-lymphocytes and associated with lung cancer (Tuscano *et al*., 2012).

Over-expression of *NOS3* (nitric oxide synthase 3) plays a role in DNA damage by inhibiting the mechanism of DNA repair (Yan *et al*., 2014). In addition, *NOS3* shown to be involved in cancer development. Moreover, *NOS3* dysregulation has been reported in some types of tumours (Ying and Hofseth, 2007). However, in our study, *NOS3* show low expression after knockdown of *TEX19* in NTERA2, which is consistent with RNA sequencing data. However, no significant gene expression changes were observed in SW480, A2780 and H460 cancer cells.

TAGLN have been associated with tumourgenesis; one study showed the influence of *TAGLN* expression indirectly causing regular cancer cells proliferation and growth in osteosarcoma (Zhao *et al*., 2014). However, in our experiment, *TAGLN* show lower expression profile in A2780, NTERA2 and SW480 following *TEX19* knockdown compared to non-interference sample. These findings are consistence with the data of RNA sequencing. In contrast, *TAGLN* show high expression in H460 after *TEX19* knockdown compared with non-interfering sample.

Consistent expression profile of five genes in SW480 and H460, this including *CALB2, CSP1, LY96, SLC17A7* and *TRIM54* were highly expressed following *TEX19* knockdown compared with untreated and non-interfering samples. These results are consistent with the RNA sequencing data, which indicate elevated expression profile after *TEX19* knockdown, with the exception *TRIM54*. This may suggest the influencing role of *TEX19* that may play in the regulation of these genes.

An interesting high expression of *TRIM54* was observed following *TEX19* depletion in SW480, A2780 and H460 compared with untreated and non-interfering samples. This high expression was inconsistent with RNA sequencing data which show approximately 80% reduction of *TRIM54* after knockdown *TEX19* in SW480 cancer cells. However, *TRIM54* expression in NTERA2 shows an insignificant expression change. The inconsistency findings of *TRIM54* expression in qRT-PCR analysis and RNA sequencing after knockdown TEX19 was previously noticed in some genes including *ELK4, GALNT2, NOS3, CD22, ZBTB5, SAA2,* and *ASB2.* In addition, the common factor or the cross point between these genes expression was NTERA2 cell-line, which is characterized by pluripotent EC cells. Moreover, in Chapter 4, we demonstrate *TEX19* knockdown down-regulation effect on some stem cell marker genes including *OCT4, NANOG* and *SOX2* in NTERA2 cells. Therefore, we suggest the down-regulation effect of *TEX19* on some stem cell marker genes may indirectly involve in the dissimilarity of genes expression in NTERA2 cells.

Some genes did not show consistence significant changes compared with untreated and non-interference samples after Tex19 depletion such as *MRPS23, SAA2, ZBTB5*and *ELK4* (figure 6.10). however, a significant reduction of some of these genes compared to non-interference samples were observed in *ELK4, SAA2* and *ZBTB5*, and elevated expression level of *MRPS23* compared to untreated sample. The inconsistence of these data of *TEX19* knockdown compared with non-interference samples might be the involvement of non-interference RNA with these genes. Moreover, ATP5C1 shows increase level of expression after TEX19 depletion compared with both untreated and non-interference samples (Figure 6.10)

7. Detection of Spo11 covalently bound to DNA in SW480 cells

7.1 Background

Meiosis is specialized cell division in sexual reproducing eukaryotes including single cell and multicellular organisms to generate haploid cells from diploid proginerator cells. This is achieved by meiotic recombination, which initiated by the programmed formation of DNA double strand breaks (DSBs), which are triggered by the conserved meiosis-specific protein Spo11 (Keeney *et al*., 2014). Then, Spo11 among other protein initiate meiotic recombination by introducing DNA DSB at specific area called recombination hotspot. The hotspot is determined by PRDM9 protein through DNA sequence-specific binding site of this hotspot (Smagulova *et al*., 2013). After DNA DSB, Spo11 is remain covalently bound to 5' of DNA strands resemble protein-DNA covalent complex. Endonuclease activity of some proteins mainly Mre11, release Spo11 bound to DNA resulting two Spo11-DNA complexes (Keeney *et al*., 2014).

Several publish work, report the presence of some CTA including Spo11 in some types of cancer including colorectal cancer (Eldai, *et al.*, 2013) and cutaneous T-cell lymphoma, (Litvinov *et al*., 2014)

Here, we are aiming to detect Spo11 covalent bound to DNA in SW480 colorectal cancer cells using modified DSB assay (Hartsuiker, 2011).

7.2 Result

In this part, we knockdown *SPO11* in SW480 cells using four *SPO11* siRNA. Then, protein lysate were extracted from nuclear and cytoplasm. In addition, western blot were performed to detect Spo11 in the extracted protein lysate of SW480 cells. Moreover, DSB assay were carried out to verify Spo11 covalently binding to DNA in DNA fractions of colorectal cancer cell SW480.

7.2.1 SPO11 knockdown in SW480

The western blot result show clear inhibition of Spo11 protein detection in nuclear fractions using four SPO11 siRNA including siRNAs 1, 2, 4 and 6 compared to the corresponding untreated nuclear fraction protein lysate of SW480 and whole protein lysate as well (Figure 7.1). In addition, no detection of Spo11 were observed in the cytoplasmic fraction of SW480 protein lysate except the untreated cytoplasmic protein lysate fraction which may due to technical error during the protein extraction process. Lamin were detected in nuclear fractions of protein lysate reflect the accuracy of the amount of protein loading (Figure 7.1).

7.1.2.2 Detection of Spo11-DNA binding

This experiment carried out using modified DSB assay (Hartsuiker, 2011). Spo11 knockdown were applied in SW480 using SPO11 siRNA 4. Then, DNA gradient fractions were achieved after ultracentrifugation which mainly concentrated in gradient 3 and 4 in the slot blot. Western blot were performed and labelling the membrane using Spo11 antibody. Spo11 were detected in untreated fraction number 3, 4 and 5. In addition, Spo11 were also detected in siRNA and non-interference fractions number 3 and 4. However, re-labelling the membrane using α-Tubulin antibody were detected in untreated fraction in number 9 and 10. While, Tubulin were detected in fraction number 10 of siRNA fraction. Moreover, α-tubulin were detected in non-interference fraction number 8 and 9 of our membrane.

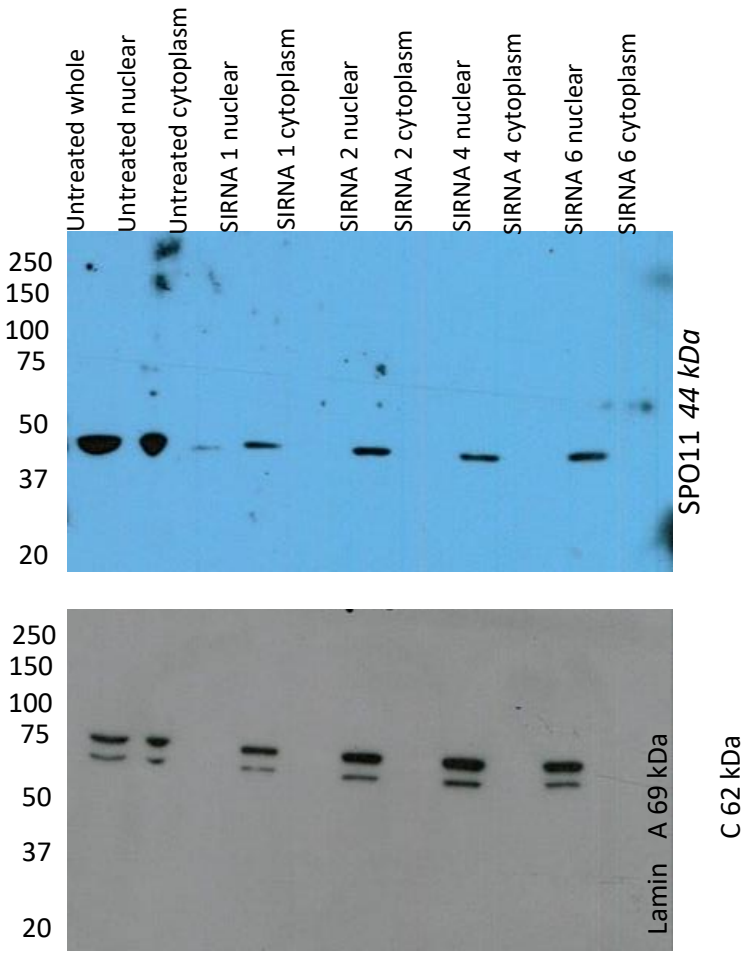

Figure 7.1 Western blot result show Spo11 in nuclear protein lysate fractions of SW480 were detected in whole and nuclear protein lysate after Spo11 knockdown using four SPO11 siRNA. Lamin was used as control for loading and fraction protein lysate accuracy.

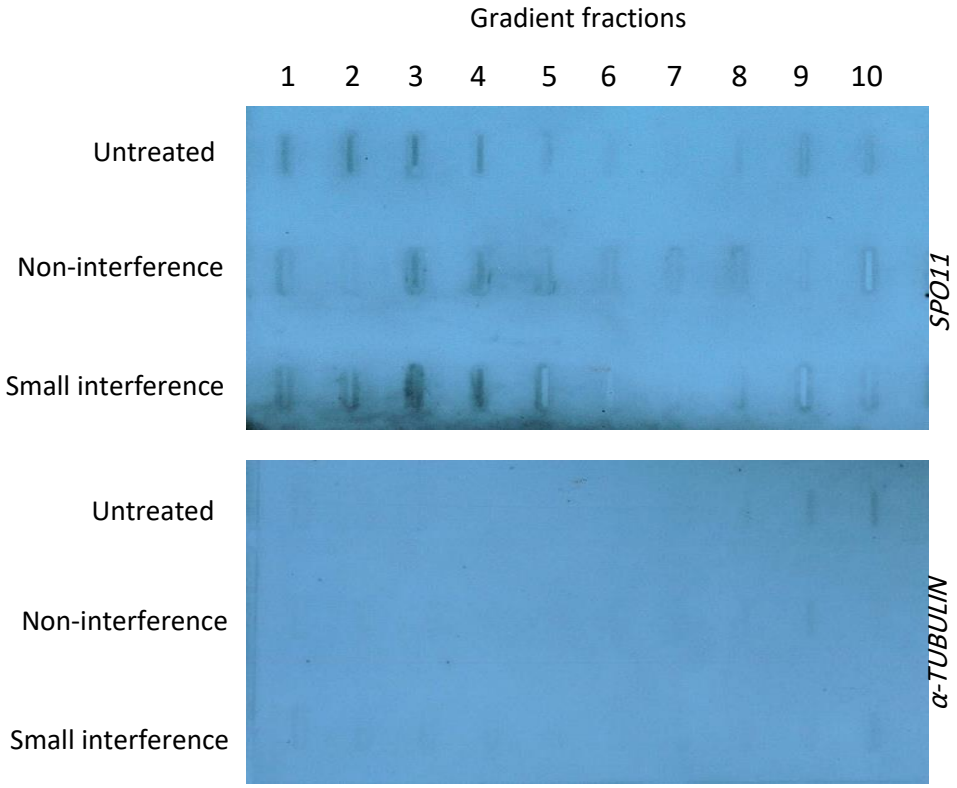

Figure 7.2 Spo11-DNA binding detection. Spo11 was detected in untreated fraction number 3, 4 and 5. Spo11 was also detected in siRNA and non-interference fractions number 3 and 4 which indicate Spo11 bound to DNA. In contrast, Tubulin was observed in the last fractions number 8, 9 or 10 which confirm presence of protein within these fractions.

7.1.3 Discussion

Validation of Spo11 antibody were achieved by knockdown *SPO11* in SW480 cells using four *SPO11* siRNA. Western blot result show Spo11 detection in the extracted protein lysate of SW480 cells. In addition, detection of Spo11 in DNA fractions of SW480 cancer cells reflect protein-DNA binding of Spo11. This may suggest the possible mitotic role of *SPO11* in SW480 cells. The observation of Spo11 in SW480 cancer cells were correlated with many studies shows its detection in some cancer including colorectal cancer (Eldai, *et al.*, 2013) and cutaneous T-cell lymphoma, (Litvinov *et al*., 2014). Spo11 association with some types of cancer may suggest its involvement in DSB in somatic tissue. In addition, escalating the question of its oncogenic activity in somatic tissue, this has been reported especially the expression of some CTA genes been correlated with poor prognosis in hepatocellular carcinoma (Wang *et al.,* 2015).

8. Discussion

8.1 Identification and validation potential CT genes using bioinformatics tools and RT-PCR analysis

Significant mortality are encounter in cancer, due to cancer cells uncontrolled cell division leading to invasion and metastasis (Cancer Research UK, 2014). Therefore, early detection of neoplastic changes is crucial to treat cancer patient. In addition, tumour antigens have been used to target cancer via immunotherapy and cancer vaccination (Sharpeand and Mount, 2015). CT genes are recognised for their confined expression in testis and limited expression in somatic tissue, and their abnormal activation in cancer including melanoma, liver, breast, ovarian, and lung cancer (Caballero and Chen, 2009; Wang *et al*., 2015; Whitehurst, 2014). This aberrant activation of CT genes in cancer emphasise their oncogenic involvement. Upregulation of CT gene *MAGE-A4* in kidney tumour were associated with inhibition of apoptosis (Peikert *et al.,* 2006). Also, in another study, reveal the inactivation of tumour suppressor gene P53 were related to CT gene *MAGE-A2* (Monte et al., 2006). The oncogenic activity of CT genes lead to use them as cancer biomarkers for early diagnosis and prognosis of cancer. In solid tumours, some CT genes expression were used to predict the outcome of cancer (Wang *et al*., 2015). The significance of CT genes is their confined expression in testis supported by blood-testis barrier (BTB), where sertoli cells control and prevent immune cells and antibodies entry into testis (Mital *et al*., 2011). Therefore, the possible use of testis-restricted genes to target some types of cancer through immunotherapy are achievable due to testicular immune-privilege and could be used as cancer biomarkers for cancer diagnosis and prognosis (Seoane and De Mattos-Arruda, 2014; Whitehurst, 2014).

In our screening to identify and validate potential CT genes, two approaches were applied and show promising results. Both approaches including the manual search and *in-silico* pipeline provide us adequate data to identify novel CT genes. Bioinformatics were useful tool to identify novel CTA genes, and the validation of these novel cancer biomarkers by RT-PCR in in normal and cancer tissue reveal CT gene *TEX19* expression in normal testis and many types of human tumours including colon cancer, lung cancer, breast cancer, ovarian cancer, leukaemia, melanoma and liver carcinoma (Feichtinger et al., 2012). These results questioning the possible functions of these genes that might play in cancer, and suggest the unknown role of some identified genes that might contribute in oncogenesis.

In a study on mouse, *TEX19.1* expression were detected in germ and pluripotent cells, and show high expression in mitotic spermatogonia and gradually decreased expression through meiotic differentiation. In addition, *TEX19.1* show low expression in differentiated pluripotent stem cells (Öllinger et al., 2008). Based on several studies, these germline genes normally involve in spermatogenesis functions such as differentiation, and maintaining the mitotic spermatogonia. In addition, according to CT genes classification, many of CT gene were located in X chromosome. They exhibit active expression in spermatogonia, and throughout the meiotic differentiation to spermatocyte become inactivated. Moreover, these germline genes are associated with many types of cancer and may contributes in carcinogenesis (McFarlane *et al.,* 2015). Moreover, recent study show cancer cells using telomere maintenance pathway known as alternative lengthening of telomeres (ALT) to maintain telomere synthesis. This process is require two elements, the first one is Rad51 which involve in DNA DSB repair, and secondly is Hop2-Mnd1 which are meiosis-specific factors required for pairing of homologous chromosomes in meiotic recombination (Cho et al., 2014). This discovery emphasise the importance to comprehend the underlying mechanisms, that cause the activation of meiosis-specific genes and their interaction with variety of catalytic factors involved in oncogenesis, including meiotic mechanism (McFarlane *et al.,* 2015).

The successful production of T-cells specific to tumour-associated antigens open the door to target these tumours by immunotherapy. The development of CD4+ T-cells to target CTA gene *NY-ESO-1* were expressed in melanoma patient, show positive result and trigger the immune system to produce T-cells specific to target the tumour (Hunder *et al.*, 2008). Recently, study suggest that CT gene *SLLP1* could be used to target multiple myeloma (Yousef, *et al*., 2015).

Another CT gene we descried as testis-CNS selective gene *CXorf27* were detected in the testis and spinal cord, whole brain, foetal brain and uterus of the normal tissue. In addition, this gene was expressed in many cancer tissues such as testicular, lung, breast, ovarian and melanoma cancer cells. This expression pattern suggests the possible use of *CXorf27* as biomarker for cancer early detection, and immunotherapy applications due to its confined expression in the testis and CNS which characterised by their immune-privilege through blood brain barrier (BBB) of the CNS (Neuwelt *et al*., 2011).

8.2 Potential role of *TEX19* in regulation of stemness

In chapter 3, *TEX19* exhibit interesting expression profile in many cancer tissues. However, not well known about *TEX19* function in testis and cancer. *TEX19* play an important role in spermatogenesis, this explain the impairment of spermatogenesis in mouse after knockout *TEX19.1* (Zeng *et al.*, 2009).

We demonstrate in chapter 4 the effect of *TEX19* knockdown on some stem cell marker genes including *OCT4, SOX2 and NANOG* in NTERA2 cancer cells. Which show down-regulation of these gene expression after the knockdown of *TEX19*. This finding might be related to a study in mouse pluripotent stem cells show the similar expression profile between Tex19.1 and stem cell marker Oct4 (Kuntz *et al.*, 2008). Therefore, to study the possible role of *TEX19* that may contributes in regulation of stem cell markers in NTERA2, which represent a human cancer cell-line model that got stem cell-like features; is important to understand this relationship.

In addition, our experiment in chapter 4, after the differentiation of NTERA2 using HMBA and RA show inhibition of stem cell markers including Oct4, Sox-2 and Nanog. However, Tex19 did not affected by the differentiation of NTERA2 cells. In contrast, *TEX19* knockdown in IPSc reveal the gene expression of *OCT4, NANOG* and *SOX2* were unaffected. These results suggest that some stem cell marker genes expression is requires *TEX19* in NTERA2 cells. Because, the expression of stem cell marker genes including *OCT4, NANOG* and *SOX2* were unaffected after *TEX19* knockdown in IPSc. This explained by *TEX19.1* deletion in mouse did not influence on the ability of unaffected ES cells to grow, and the stem cell marker genes were unaffected with *TEX19.1* deletion including Oct4, Nanog and Sox2 (Tarabay, *et al*., 2013).

8.3 Influence of *TEX19* depletion on TE in cancer cells

We demonstrate the inhibition of *ERVK* family genes after *TEX19* knockdown in NTERA2, down regulation of human *ERVK* genes were clear including *ERVK ENV, ERVK GAG, ERVK HML2RE, ERVK POL* and *ERVK PRO*. However, other study show activation of *LINE-1* transposons in placenta after deletion *TEX19.1* (Reichmann et al., 2013). In addition, it was reported that deletion of *TEX19.1* in mouse cause upregulation of retrotransposons including mouse *ERVK* genes (Ollinger *et al*., 2008). In addition, a study on TEs on mouse long intergenic noncoding RNAs (lincRNAs) show *ERVK* genes high expression profile and

strong effect in ESCs (Kelley and Rinn, 2012) compared with NTERA2 that composed of pluripotent embryonal carcinoma (EC) cells that differentiate into neuron cells using RA (Andrews *et al.*, 1982). In addition, human ESCs and EC cells share some pluripotency characteristics (Abu Dawud *et al*., 2012). However, *TEX19* knockdown in A2780 were unsuccessful, due to time limitation we could not repeat this experiment. The up-regulation of *ERVK* family genes are difficult to explain. Nevertheless, may *TEX19* siRNA influence the overexpression of *ERVK* genes, while, non-interference RNA did not interfere with *ERVK* genes expression.

Collectively, the effect of *TEX19* depletion on NTERA2 cells were obvious compared to A2780. ELDA results show significant cell proliferation frequency when treated with *TEX19* in NTERA2 compared with unaffected cellular proliferation in A2780 cells after *TEX19* knockdown. Which may suggest that *TEX19* may play a role in cell proliferation in NTERA2 embryonic cancer cells, and not needed in A2780 cells.

8.4 Influence of TEX19 depletion on differential gene expression based on RNA sequencing

RNA Seq. were significant tool to explore the differential gene expression in NTERA2, H460, A2780 and SW480 cancer cells in response to *TEX19* depletion. Here, we validate 20 genes expression using qRT-PCR and reveal some significant upregulated and downregulated gene expression in response to knockdown *TEX19* in these cancer cell-lines. We summarise the consistence and significant gene expression in four cancer cell-lines after knockdown *TEX19*.

TRIM54 upregulated expression after *TEX19* knockdown were observed in SW480, A2780 and H460. This observation oppose the RNA sequencing data, which indicate approximately 80% inhibition of *TRIM54* after *TEX19* depletion in SW480 cancer cells. However, *TRIM54* expression in NTERA2 show insignificant expression change. In addition, differential gene expression in NTERA2 after *TEX19* depletion show downregulation of most of genes expression except *SAA2* were upregulated. The conflicting results of *TRIM54* gene expression in qRT-PCR analysis and RNA sequencing after *TEX19* depletion were observed in some genes may be related to NTERA2 cell-line, which is characterized by pluripotent EC cells. suggest the down-regulation effect of *TEX19* on some stem cell marker genes may indirectly involve in the dissimilarity of genes expression in NTERA2 cells.

The depletion of *TEX19* in H460 cancer cells show upregulation in most of the genes including *MIPEP, ATP5C1, SLC17A7, CPS1, CALB2, TRIM54* and *LY96*. This high expression were correlated with high expression of *SLC17A7, CPS1, CALB2, TRIM54* and *LY96* in SW480 cancer cells. In addition, except *TRIM54*, the upregulation in these genes are consistence with our data from RNA sequencing. Therefore, we suggest that *TEX19* may involve in suppress regulation of these genes in H460 cancer cells. However, two genes including *PGM1* and *ELK4* were downregulated after depletion *TEX19* in H460, and this downregulation of these two genes were observed also in NTERA2 cancer cells. In addition, the down regulation of *PGM1* and *ELK4* in H460 and NTERA2 were consistence with the RNA sequencing data. Moreover, the downregulation of *PGM1* were only observed in NTERA2 cells, which suggest this gene expression requires *TEX19* in these cancer cells.

In A2780 cancer cells, we noticed that most of the genes were not affected by *TEX19* depletion. Out of 20 genes in our list, only 3 genes were upregulated in response to the knockdown of *TEX19* including *GALNT2, ZNF367* and *TRIM54*. Previously in Chapter 5, we evaluate the effect of *TEX19* depletion on TE in A2780 and ELDA assay. In addition, we demonstrate the cell proliferation frequency after depletion *TEX19* in A2780 were insignificant compared to NTERA2. In addition, the insignificant TE expression after knockdown *TEX19* in A2780 compared to NTERA2. Moreover, based on RNA sequencing data, *GALNT2* and *TRIM54* were downregulated in SW480 cancer cells in response to *TEX19* depletion. Therefore, we suggest that depletion of *TEX19* in A2780 cancer cells is not influencing cellular proliferation frequency changes, and no significant effect on the genes expression in A2780.

In SW480 cancer cells, we observed that approximately half of the genes in our study show high expression upon *TEX19* depletion. Out of 20 genes in our list, only 9 genes were upregulated in response to the knockdown of *TEX19* including *CD22, ASB2, SLC17A7, CPS1, GALNT2, CALB2, ELK4, TRIM54* and *LY96.* In addition, the expression of these genes were compatible with our RNA sequencing data with exception in *ELK4, TRIM54* and *GALNT2.* Moreover, some of these upregulated genes were also exhibit similar expression in H460 cancer cells including *SLC17A7, CPS1, CALB2, TRIM54* and *LY96.* In contrast, four genes were downregulated after *TEX19* knockdown including *NAPB, RIPA, MRPS23* and *SAA2* in SW480 cells. In addition, *NAPB* and *MRPS23* were downregulated only in SW480 cancer cells and their expression were not affected in NTERA2, H460 and A2780 after

TEX19 depletion. Moreover, the expression of those two genes were consistence with RNA sequencing data.

Out of 20 genes in our RNA sequencing, only *TAGLN* were not dysregulated after the depletion of *TEX19* in four cell-lines including NTERA2, H460, A2780 and SW480. However, based on RNA sequencing, *TAGLN* were upregulated after *TEX19* depletion in SW480.

9. References

Abdolhosseini, M., Nandula, S. R., Song, J., Hirt, H., & Gorr, S. U. (2012). Lysine substitutions convert a bacterial-agglutinating peptide into a bactericidal peptide that retains anti-lipopolysaccharide activity and low hemolytic activity. *Peptides*, *35*(2), 231-238.

Ackerman, S. L., Knowles, B. B., & Andrews, P. W. (1994). Gene regulation during neuronal and non-neuronal differentiation of NTERA2 human teratocarcinoma-derived stem cells. *Molecular brain research*, *25*(1), 157-162.

Adelmann, M., Köllner, B., Bergmann, S. M., Fischer, U., Lange, B., Weitschies, W., ... & Fichtner, D. (2008). Development of an oral vaccine for immunisation of rainbow trout (Oncorhynchus mykiss) against viral haemorrhagic septicaemia. *Vaccine*, *26*(6), 837-844.

Ali, S. H., & DeCaprio, J. A. (2001, February). Cellular transformation by SV40 large T antigen: interaction with host proteins. In *Seminars in cancer biology* (Vol. 11, No. 1, pp. 15-22). Academic Press.

Andrews PW, Goodfellow PN, Shevinsky L, Bronson DL, Knowles BB (1982) Cell surface antigens of a clonal human embryonal carcinoma cell line: Morphological and antigenic differentiation in culture. Int. J. Cancer.;29:523–531.

Andrews, P.W. (1984) Retinoic acid induces neuronal differentiation of a cloned human embryonal carcinoma cell line *in vitro*. *Dev. Biol*., 103: 285–293.

Andrews, P.W., Banting, G.S., Damjanov, I., Arnaud, D.and Avner P. (1984b) Three monoclonal antibodies defining distinct differentiation antigens associated with different high molecular weight polypeptides on the surface of human embryonal carcinoma cells. *Hybridoma*, 3: 347–361.

Andrews, P.W., Casper, J., Damjanov, I., Duggan-Keen, M., Giwercman, A., Hata, J. von Keitz, A., Looijenga, L.H., Millán, J.L., Oosterhuis, J.W., Pera, M., Sawada, M., Schmoll, H.J., Skakkebaek, N.E., van Putten, W. and Stern, P. (1996) Comparative analysis of cell surface antigens expressed by cell lines derived from human germ cell tumours. *Int. J. Cancer*, 66: 806–816.

Andrews, P.W., Meyer, L.J., Bednarz, K.L. and Harris, H. (1984c) Two monoclonal antibodies recognizing determinants on human embryonal carcinoma cells react specifically with the liver isozyme of human alkaline phosphatase. *Hybridoma*, 3: 33–39.

Andrews, P.W., Nudelman, E., Hakomori, S-I. and Fenderson, B.A. (1990) Different patterns of glycolipid antigens are expressed following differentiation of TERA-2 human embryonal carcinoma cells induced by retinoic acid, hexamtehylene bisacetamide (HMBA) or bromodeoxyuridine (BUdR). *Differentiation*., 43:131–138.

Ayarpadikannan, S., & Kim, H. S. (2014). The impact of transposable elements in genome evolution and genetic instability and their implications in various diseases. *Genomics & informatics*, *12*(3), 98-104.

Ayton, P.M., and Cleary, M.L. (2001). Molecular mechanisms of leukemogenesis mediated by MLL fusion proteins. Oncogene *20*, 5695-5707

Badcock, G., Pigott, C., Goepel, J. and Andrews, P.W. (1999) The Human Embryonal Carcinoma Marker Antigen TRA-1-60 Is A Sialylated Keratan Sulphate Proteoglycan. *Cancer Res*., 59: 4715–4719.

Bader, S., Walker, M., McQueen, H.A., Sellar, R., Oei, E., Wopereis, S., Zhu, Y., Peter, A., Bird, A.P., and Harrison, D.J. (2003). MBD1, MBD2 and CGBP genes at chromosome 18q21 are infrequently mutated in human colon and lung cancers. Oncogene *22*, 3506-3510.

Bai S, He B, Wilson EM. (2005) Melanoma antigen gene protein MAGE-11 regulates androgen receptor function by modulating the interdomain interaction. Mol Cell Biol; 25: 1238–57.

Bakin, A., and Curran, T. (1999). Role of DNA 5-methylcytosine transferase in cell transformation by fos. Science *283*, 387-390.

Bart J, Groen HJ, van der Graaf WT, Hollema H, Hendrikse NH, Vaalburg W, Sleijfer DT, de Vries EG. (2002). An oncological view on the blood-testis barrier. Lancet Oncol 3:357–363.

Baudat F. and Nicolas A. (1997) Clustering of meiotic double-strand breaks on yeast chromosome III, Proc. Natl. Acad. Sci. USA 94 5213–5218.

Beaulieu, N., Morin, S., Chute, I.C., Robert, M.-F., Nguyen, H., and MacLeod, A.R. (2002). An essential role for DNA methyltransferase DNMT3B in cancer cell survival. Journal of Biological Chemistry *277*, 28176-28181.

Beck, C. R., Garcia-Perez, J. L., Badge, R. M., & Moran, J. V. (2011). LINE-1 Elements in Structural Variation and Disease. *Annual Review of Genomics and Human Genetics*, *12*, 187–215.

Belancio VP, Hedges DJ, Deininger P. (2008) Mammalian non-LTR retrotransposons: for better or worse, in sickness and in health. Genome Res;18:343-358.

Bernstein BE, Meissner A, Lander ES. (2007) The mammalian epigenome. Cell; 128:669–681.

Berrong, Z. J. (2016). *Combinational immunotherapy of anti-OX40 antibody and IDO inhibitor synergistically enhances anti-tumor immune T cell-mediated response* (Doctoral dissertation).

Bertone, P., Stolc, V., Royce, T.E., Rozowsky, J.S., Urban, A.E., Zhu, X., Rinn, J.L., Tongprasit, W., Samanta, M., Weissman, S., Gerstein, M. and Snyder, M. (2004) Global identification of human transcribed sequences with genome tiling arrays. *Science*, 306: 2242-2246.

Bhaskara, S., Chyla, B.J., Amann, J.M., Knutson, S.K., Cortez, D., Sun, Z.-W., and Hiebert, S.W. (2008). Deletion of histone deacetylase 3 reveals critical roles in S phase progression and DNA damage control. Molecular cell *30*, 61-72.

Bird, A. (2002). DNA methylation patterns and epigenetic memory. Genes & development *16*, 6-21.

Bogdanovic O, Veenstra GJ. (2009) DNA methylation and methyl-CpG binding proteins: developmental requirements and function. Chromosoma;118:549–565.

Bolden, J.E., Peart, M.J., and Johnstone, R.W. (2006). Anticancer activities of histone deacetylase inhibitors. Nature reviews Drug discovery *5*, 769-784.

Boon T, Cerottini JC, van den Eynde B, van der Bruggen P, van Pel A. (1994) Tumor antigens recognized by T lymphocytes. Annu Rev Immunol 12:337–365.

Borde V, Goldman AS, Lichten M. (2000) Direct coupling between meiotic DNA replication and recombination initiation. Science; 290:806-9.

Borde V. (2007) The multiple roles of the Mre11 complex for meiotic recombination, Chromosome Res. 15:551–563.

Brimble SN, Eric S. Sherrer, Elizabeth W. Uhl, Elaine Wang, Samuel Kelly, Alfred H. Merrill Jr., Allan J. Robins, Thomas C. Schulz (2007) The cell surface glycosphingolipids SSEA-3 and SSEA-4 are not essential for human ESC pluripotency. Stem Cells; 25(1):54–62.

Brinkmann, U., Vasmatzis, G., Lee, B., Yerushalmi, N., Essand, M., & Pastan, I. (1998). PAGE-1, an X chromosome-linked GAGE-like gene that is expressed in normal and neoplastic prostate, testis, and uterus. *Proceedings of the National Academy of Sciences*, *95*(18), 10757-10762.

Butland SL, Sanders SS, Schmidt ME, Riechers SP, Lin DT, Martin DD, Vaid K, Graham RK, Singaraja RR, Wanker EE, (2014) The palmitoyl acyltransferase HIP14 shares a high proportion of interactors with huntingtin: implications for a role in the pathogenesis of Huntington's disease. Hum Mol Genet.;23:4142–4160.

Caballero OL, Chen YT, (2009) Cancer/testis (CT) antigens: potential targets for immunotherapy. Cancer Sci**.;** 100:2014**–**2021.

Caballero, J. N., Frenette, G., Belleannée, C., & Sullivan, R. (2013). CD9-Positive Microvesicles Mediate the Transfer of Molecules to Bovine Spermatozoa during Epididymal Maturation. *PLoS ONE*, *8*(6), e65364.

Cairns, B.R. (2001). Emerging roles for chromatin remodeling in cancer biology. Trends in Cell biology *11*, S15-S21.

Cancer Research UK (2014), Cancer Statistics for the UK, Cancer Research UK.

Castro A. and Lorca T. (2005) Exploring meiotic division in Cargèse. Meeting on meiotic divisions and checkpoints. EMBO Rep. Sep; 6(9):821-5.

Cebrian, A., Pharoah, P.D., Ahmed, S., Ropero, S., Fraga, M.F., Smith, P.L., Conroy, D., Luben, R., Perkins, B., and Easton, D.F. (2006). Genetic variants in epigenetic genes and breast cancer risk. Carcinogenesis *27*, 1661-1669.

Cedar H, Bergman Y. (2009) Linking DNA methylation and histone modification: patterns and paradigms. Nat Rev Genet;10:295–304

Chalmel F, Rolland AD, Niederhauser-Wiederkehr C, Chung SS, Demougin P, Gattiker A, Moore J, Patard JJ, Wolgemuth DJ, Jéqou B, Primig M (2007) The conserved transcriptome in human and rodent male gametogenesis.Proc Natl Acad Sci USA;104:8346–8351.

Chambers, C. A., Kuhns, M. S., Egen, J. G., & Allison, J. P. (2001). CTLA-4-mediated inhibition in regulation of T cell responses: mechanisms and manipulation in tumor immunotherapy. *Annual review of immunology*, *19*(1), 565-594.

Chen ME, Lin SH, Chung LW, Sikes RA. (1998). Isolation and characterization of PAGE-1 and GAGE-7. New genes expressed in the LNCaP prostate cancer

progression model that share homology with melanoma-associated antigens. J Biol Chem 273:17618–17625.

Chen YT, Scanlan MJ, Sahin U, Tureci O, Gure AO, Tsang S, Williamson B, Stockert E, Pfreundschuh M, Old LJ. (1997). A testicular antigen aberrantly expressed in human cancers detected by autologous antibody screening. Proc Natl Acad Sci USA 94:1914–1918.

Chen YT, Scanlan MJ, Venditti CA, Chua R, Theiler G, Stevenson BJ, Iseli C, Gure AO, Vasicek T, Strausberg RL, Jongeneel CV, Old LJ, Simpson AJ (2005) Identification of cancer/testis-antigen genes by massive parallel signature sequencing. Proc Natl Acad Sci USA;102:7940–7945.

Chen, Y., & Wei, J. (2015). Identification of Pathogen Signatures in Prostate Cancer Using RNA-seq. *PLoS ONE*, *10*(6), e0128955.

Cho N.W., Dilley R.L., Lampson M.A., Greenberg R.A (2014) Interchromosomal homology searches drive directional ALT telomere movement and synapsis Cell;159:108–121.

Cho, B., Lee, H., Jeong, S., Lee, H.J., Hwang, K.S., Kim, H.Y., Lee, Y.S., Kang, G.H. and Jeoung, D.I. (2003) Promoter hypomethylation of a novel cancer/testis antigen gene CAGE is correlated with its aberrant expression and is seen in premalignant stage of gastric carcinoma. *Biochem Biophys Res Commun*., 307: 52-63.

Choi, J.H., Kwon, H.J., Yoon, B.I., Kim, J.H., Han, S.U., Joo, H.J., and Kim, D.Y. (2001). Expression profile of histone deacetylase 1 in gastric cancer tissues. Cancer science *92*, 1300-1304.

Cilensek ZM, Yehiely F, Kular RK, Deiss LP. (2002) A member of the GAGE family of tumor antigens is an anti-apoptotic gene that confers resistance to Fas／CD95／APO-1, Interferon-gamma, taxol and gamma-irradiation. Cancer Biol Ther; 1: 380–7.

Cloonan, N., Forrest, A.R., Kolle, G., Gardiner, B.B., Faulkner, G.J., Brown, M.K., Taylor, D.F., Steptoe, A.L., Wani, S., Bethel, G., Roberstson, A.J., Perkins, A.C., Bruce, S.J., Lee, C.C., Ranade, S.S., Peckham, H.E., Manning, J.M., McKernan, K.J. and Grimmond, S.M. (2008) Stem cell transcriptome profiling via massivescale mRNA sequencing. *Nat. Methods*, 5: 585- 587.

Colombo, M., Mirandola, L., Reidy, A., Suvorava, N., Konala, V., Chiaramonte, R., Grizzi, F., Rahman, R.L., Jenkins, M.R., Nugyen, D.D., Dalhbeck, S., Cobos,

E., Figueroa, J.A., Chiriva-Internati, M. (2015) Targeting Tumor Initiating Cells through Inhibition of Cancer Testis Antigens and Notch Signaling: A Hypothesis. *Int Rev Immunol*. 34: 188-99.

Craig NL, Craigie R, Gellert M, Lambowitz AM (2002) Mobile DNA II. Washington, DC: ASM Press.

Cress, W.D., and Seto, E. (2000). Histone deacetylases, transcriptional control, and cancer. Journal of cellular physiology *184*, 1-16.

Dalerba P, Ricci A, Russo V, Rigatti D, Nicotra MR, Mottolese M, Bordignon C, Natali PG, Traversari C. (1998). High homogeneity of MAGE, BAGE, GAGE, tyrosinase and Melan-A/MART-1 gene expression in clusters of multiple simultaneous metastases of human melanoma: Implications for protocol design of therapeutic antigenspecific vaccination strategies. Int J Cancer 77:200–204.

David, L., Huber,W., Granovskaia, M., Toedling, J., Palm, C.J., Bofkin, L., Jones, T., Davis, R.W. and Steinmetz, L.M. (2006) A high-resolution map of transcription in the yeast genome. *Proc. Natl. Acad. Sci. USA*, 103: 5320-5325.

Davis, P.K., and Brachmann, R.K. (2003). Chromatin remodeling and cancer. Cancer biology & therapy *2*, 23-30.

Dawud, R. A., Schreiber, K., Schomburg, D., & Adjaye, J. (2012). Human embryonic stem cells and embryonal carcinoma cells have overlapping and distinct metabolic signatures. *PloS one*, *7*(6), e39896.

Day, B. W., Stringer, B. W., Spanevello, M. D., Charmsaz, S., Jamieson, P. R., Ensbey, K. S., Boyd, A. W. (2011). ELK4 neutralization sensitizes glioblastoma to apoptosis through downregulation of the anti-apoptotic protein Mcl-1. *Neuro-Oncology*, *13*(11), 1202–1212

Dianatpour, M., Mehdipour, P., Nayernia, K., Mobasheri, M.B., Ghafouri-Fard, S., Savad, S. and Modarressi, M.H. (2012). Expression of testis specific Genes TSGA10, TEX101 and ODF3 in breast cancer. *Iran Red Crescent Med J*, 14: 722-726.

Djureinovic, D., Hallström, B. M., Horie, M., Mattsson, J. S. M., La Fleur, L., Fagerberg, L., & Ekman, S. (2016). Profiling cancer testis antigens in non–small-cell lung cancer. *JCI Insight*, *1*(10).

Donovan, P.J. and Gearhart, J. (2001) The end of the beginning for pluripotent stem cells. *Nature*: 41492- 41497.

Dougan M, Dranoff G. (2009) Immune therapy for cancer. Annu Rev Immunol.;27:83–117.doi:10.1146/annurev.immunol.021908.132544.

Dunn GP, Old LJ, Schreiber RD (2004b). The immunobiology of cancer immunosurveillance and immunoediting. Immunity. ; 21:137-48.

Eads, C.A., Nickel, A.E., and Laird, P.W. (2002). Complete genetic suppression of polyp formation and reduction of CpG-island hypermethylation in ApcMin/+ Dnmt1-hypomorphic mice. Cancer research *62*, 1296-1299.

Eckhardt, F., Lewin, J., Cortese, R., Rakyan, V.K., Attwood, J., Burger, M., Burton, J., Cox, T.V., Davies, R., and Down, T.A. (2006). DNA methylation profiling of human chromosomes 6, 20 and 22. Nature genetics *38*, 1378-1385.

Eckner, R., Ewen, M.E., Newsome, D., Gerdes, M., DeCaprio, J.A., Lawrence, J.B., and Livingston, D.M. (1994). Molecular cloning and functional analysis of the adenovirus E1A-associated 300-kD protein (p300) reveals a protein with properties of a transcriptional adaptor. Genes & development *8*, 869-884.

Eden, A., Gaudet, F., Waghmare, A., and Jaenisch, R. (2003). Chromosomal instability and tumors promoted by DNA hypomethylation. Science *300*, 455-455.

Edgren, H., Murumagi, A., Kangaspeska, S., Nicorici, D., Hongisto, V., Kleivi, K., Kallioniemi, O. (2011). Identification of fusion genes in breast cancer by paired-end RNA-sequencing. *Genome Biology*, *12*(1), R6. doi:10.1186/gb-2011-12-1-r6

Eijpe M, Heyting C, Gross B, Jessberger R. (2000) Association of mammalian SMC1 and SMC3 proteins with meiotic chromosomes and synaptonemal complexes. J Cell Sci.;113:673–682.

Eldai, H., Periyasamy, S., Al Qarni, S., Al Rodayyan, M., Muhammed Mustafa, S., Deeb, A., Aziz, M. A. (2013). Novel Genes Associated with Colorectal Cancer Are Revealed by High Resolution Cytogenetic Analysis in a Patient Specific Manner. *PLoS ONE*, *8*(10), e76251. doi:10.1371/journal.pone.0076251.

Ellis, L., Atadja, P.W., and Johnstone, R.W. (2009). Epigenetics in cancer: targeting chromatin modifications. Molecular cancer therapeutics *8*, 1409-1420.

Feichtinger, J., Aldeailej, I., Anderson, R., Almutairi, M., Almatrafi, A., Alsiwiehri, N., … McFarlane, R. J. (2012). Meta-analysis of clinical data using human meiotic genes identifies a novel cohort of highly restricted cancer-specific marker genes. *Oncotarget*, *3*(8), 843–853.

Feichtinger, J., McFarlane, R. J., & Larcombe, L. D. (2014). CancerEST: a web-based tool for automatic meta-analysis of public EST data. *Database: The Journal of Biological Databases and Curation*, *2014*, bau024. doi:10.1093/database/bau024

Fenderson, B.A., Andrews, P.W., Nudelman, E., Clausen, H. and Hakomori, S-i. (1987) Glycolipid core structure switching from globo- to lacto- and ganglio-series during retinoic acid-induced differentiation of TERA-2-derived human embryonal carcinoma cells. *Dev. Biol*., 122: 21–34.

Ferrari, R., Pellegrini, M., Horwitz, G.A., Xie, W., Berk, A.J., and Kurdistani, S.K. (2008). Epigenetic reprogramming by adenovirus e1a. Science *321*, 1086-1088.

Fledel-Alon A, Wilson DJ, Broman K, Wen X, Ober C, Coop G, Przeworski M. (2009) Broad-scale recombination patterns underlying proper disjunction in humans. PLoS Genet. ;5:e1000658.

Fonseca, S. A. S., Costas, R. M., & Pereira, L. V. (2015). Searching for naïve human pluripotent stem cells. *World Journal of Stem Cells*, *7*(3), 649–656.

Fraga, M.F., Ballestar, E., Villar-Garea, A., Boix-Chornet, M., Espada, J., Schotta, G., Bonaldi, T., Haydon, C., Ropero, S., and Petrie, K. (2005). Loss of acetylation at Lys16 and trimethylation at Lys20 of histone H4 is a common hallmark of human cancer. Nature genetics *37*, 391-400.

Frank M. Burnet (1957) Cancer—a Biological Approach. BMJ, 1 pp. 841–847

Friedman, R. C., Farh, K. K. H., Burge, C. B., & Bartel, D. P. (2009). Most mammalian mRNAs are conserved targets of microRNAs. *Genome research*, *19*(1), 92-105.

Frigola, J., Song, J., Stirzaker, C., Hinshelwood, R.A., Peinado, M.A., and Clark, S.J. (2006). Epigenetic remodeling in colorectal cancer results in coordinate gene suppression across an entire chromosome band. Nature genetics *38*, 540-549.

Fu JH, Wang LQ, Li T, Ma GJ (2015) RNA-sequencing based identification of crucial genes for esophageal squamous cell carcinoma. J Cancer Res Ther.; 11(2):420-5.

Fuks F, Deplus R, Brenner C, Burgers WA, Putmans P, Kouzarides T, de Launoit Y (2002). Dnmt3L is a transcriptional repressor that recruits histone deacetylase.Nucleic Acids Res.;30:3831–3838.

Fyodorov DV, Kadonaga JT. (2001) The many faces of chromatin remodeling: SWItching beyond transcription. Cell; 106:523-5.

G.P. Dunn, A.T. Bruce, H. Ikeda, L.J. Old, R.D. Schreiber (2002) Cancer immunoediting: from immunosurveillance to tumor escape. Nat. Immunol., 3, pp. 991–998

G.P. Dunn, L.J. Old, R.D. Schreiber (2004a) The Three Es of Cancer Immunoediting. Annu. Rev. Immunol., 22 pp. 329–360.

Gaudet, F., Hodgson, J.G., Eden, A., Jackson-Grusby, L., Dausman, J., Gray, J.W., Leonhardt, H., and Jaenisch, R. (2003). Induction of tumors in mice by genomic hypomethylation. Science *300*, 489-492.

Gayther, S.A., Batley, S.J., Linger, L., Bannister, A., Thorpe, K., Chin, S.-F., Daigo, Y., Russell, P., Wilson, A., and Sowter, H.M. (2000). Mutations truncating the EP300 acetylase in human cancers. Nature genetics *24*, 300-303.

Ghafouri-Fard, S. (2015) Expression of Cancer-Testis Antigens in Stem Cells: Is it a Potential Drawback or an Advantage in Cancer Immunotherapy. *Asian Pacific Journal of Cancer Prevention*, 16: 3079-3081.

Ghafouri-Fard, S. and Modarressi, M.H. (2012). Expression of cancer-testis genes in brain tumours: implications for cancer immunotherapy. *Immunotherapy*, 4: 59-75.

Ghafouri-Fard, S., Abbasi, A., Moslehi, H., Faramarzi, N., Taba Taba Vakili, S., Mobasheri, M.B. and Modarressi, M.H. (2010) Elevated expression levels of testis-specific genes TEX101 and SPATA19 in basal cell carcinoma and their correlation with clinical and pathological features. *Br J Dermatol*, 162: 772-779.

Ghafouri-Fard, S., Modarressi, M.H. and Yazarloo, F. (2012b). Expression of testis-specific genes, TEX101 and ODF4, in chronic myeloid leukemia and evaluation of TEX101 immunogenicity. *Ann Saudi Med*, 32: 256-261.

Ghafouri-Fard, S., Ousati A.Z., Sabah G.B, Hasheminasab, S.M. and Modarressi, M.H. (2010b). Expression of two testis-specific genes, SPATA19 and LEMD1, in prostate cancer. *Arch Med Res*, 41, 195-200.

Glozak, M., and Seto, E. (2007). Histone deacetylases and cancer. Oncogene *26*, 5420-5432.

Glozak, M.A., Sengupta, N., Zhang, X., and Seto, E. (2005). Acetylation and deacetylation of non-histone proteins. gene *363*, 15-23.

Gorrini, C., Squatrito, M., Luise, C., Syed, N., Perna, D., Wark, L., Martinato, F., Sardella, D., Verrecchia, A., and Bennett, S. (2007). Tip60 is a haplo-

insufficient tumour suppressor required for an oncogene-induced DNA damage response. Nature *448*, 1063-1067.

Grunau, C., Sanchez, C., Ehrlich, M., van der Bruggen, P., Hindermann, W., Rodriguez, C., Krieger, S., Dubeau, L., Fiala, E. and De Sario, A. (2005) Frequent DNA hypomethylation of human juxtacentromeric BAGE loci in cancer. *Genes Chromosomes Cancer*, **43**: 11-24.

Grunstein, M. (1997). Histone acetylation in chromatin structure and transcription. Nature *389*, 349-352.

Guibal F. C., Moog-Lutz C., Smolewski P., Di Gioia Y., Darzynkiewicz Z., Lutz P. G., Cayre Y. E. (2002) ASB-2 inhibits growth and promotes commitment in myeloid leukemia cells. J. Biol. Chem. 277, 218–224.

Gure AO, Tureci O, Sahin U, Tsang S, Scanlan MJ, Jager E, Knuth A, Pfreundschuh M, Old LJ, Chen YT. (1997). SSX: A multigene family with several members transcribed in normal testis and human cancer. Int J Cancer 72:965–971.

Hackett, J.A., Reddington, J.P., Nestor, C.E., Dunican, D.S., Branco, M.R., Reichmann, J., Reik, W., Surani, M.A., Adams, I. and Meehan R.R. (2012) Promoter DNA methylation couples genome-defence mechanisms to epigenetic reprogramming in the mouse germline. Development, 139: 3623-3632.

Haig, D. (2012) Retroviruses and the placenta. *Curr. Biol*., 22: R609-R613.

Hainaut P and Hollstein M (2000). p53 and human cancer: the first ten thousand mutations. Adv Cancer Res 77: 81-137

Halkidou, K., Gaughan, L., Cook, S., Leung, H.Y., Neal, D.E., and Robson, C.N. (2004). Upregulation and nuclear recruitment of HDAC1 in hormone refractory prostate cancer. The Prostate *59*, 177-189.

Hamer G, Gell K, Kouznetsova A, Novak I, Benavente R, Hoog C. (2006) Characterization of a novel meiosis-specific protein within the central element of the synaptonemal complex. J Cell Sci; 119: 4025–32.

Hamer G, Wang H, Bolcun-Filas E, Cooke HJ, Benavente R, Hoog C. (2008) Progression of meiotic recombination requires structural maturation of the central element of the synaptonemal complex. J Cell Sci; 121:2445-51.

Hanahan, Douglas, and Robert A. Weinberg. "Hallmarks of cancer: the next generation." *cell* 144.5 (2011): 646-674.

Hansen, R.S., Wijmenga, C., Luo, P., Stanek, A.M., Canfield, T.K., Weemaes, C.M., and Gartler, S.M. (1999). The DNMT3B DNA methyltransferase gene is mutated in the ICF immunodeficiency syndrome. Proceedings of the National Academy of Sciences *96*, 14412-14417.

Hao, B., Wang, H., Zhou, K., Li, Y., Chen, X., Zhou, G., Zhu, Y., Miao, X., Tan, W., and Wei,Q. (2004). Identification of genetic variants in base excision repair pathway and their associations with risk of esophageal squamous cell carcinoma. Cancer research *64*, 4378-4384.

Hao, J., Sawyer, D. B., Hatzopoulos, A. K., & Hong, C. C. (2011). Recent Progress on Chemical Biology of Pluripotent Stem Cell Self-renewal, Reprogramming and Cardiomyogenesis. *Recent Patents on Regenerative Medicine, 1*(3), 263–274.

Harrison, A., Olds-Clarke, P., & King, S. M. (1998). Identification of the *t*Complex–encoded Cytoplasmic Dynein Light Chain Tctex1 in Inner Arm I1 Supports the Involvement of Flagellar Dyneins in Meiotic Drive . *The Journal of Cell Biology*, *140*(5), 1137–1147.

Hartsuiker E. 2011. Detection of covalent DNA-bound Spo11 and topoisomerase complexes. Methods Mol. Biol. 745:65–77

Henzler, C. M., Li, Z., Dang, J., Arcila, M. L., Zhou, H., Liu, J., Kosik, K. S. (2013). Staged miRNA re-regulation patterns during reprogramming. *Genome Biology*, *14*(12), R149. doi:10.1186/gb-2013-14-12-r149

Hodi FS, O'Day SJ, McDermott DF, Weber RW, Sosman JA, Haanen JB, Gonzalez R, Robert C, Schadendorf D, Hassel JC, Akerley W, van den Eertwegh AJ, Lutzky J, Lorigan P, Vaubel JM, Linette GP, Hogg D, Ottensmeier CH, Lebbé C, Peschel C, Quirt I, Clark JI, Wolchok JD, Weber JS, Tian J, Yellin MJ, Nichol GM, Hoos A, Urba WJ. (2010) Improved survival with ipilimumab in patients with metastatic melanoma. N Engl J Med;363:711–723. doi:10.1056/NEJMoa1003466.

Hofmann O, Cabellero OL, Stevenson BJ, Chen YT, Cohen T, Chua R, Maher CA, Panji S, Schaefer U, Kruger A, Lehvaslaiho M, Carninci P, Hayashizaki Y, Jongeneel CV, Simpson AJ, Old LJ, et al. (2008) Genome-wide analysis of cancer/testis gene expression. Proc Natl Acad Sci USA;105:20422–20427.

Huang, B., Laban, M., Leung, C.H., Lee, L., Lee, C., Salto-Tellez, M., Raju, G., and Hooi, S. (2005). Inhibition of histone deacetylase 2 increases apoptosis and

p21Cip1/WAF1 expression, independent of histone deacetylase 1. Cell Death & Differentiation *12*, 395-404.

Huang, Y., Liang, P., Liu, D., Huang, J., & Songyang, Z. (2014). Telomere regulation in pluripotent stem cells. *Protein & Cell*, *5*(3), 194–202.

Hunder NN, Wallen H, Cao J, Hendricks DW, Reilly JZ, Rodmyre R, Jungbluth A, Gnjatic S, Thompson JA, Yee C, (2008) Treatment of metastatic melanoma with autologous CD4+ T cells against NY-ESO-1. N Engl J Med.; 358:2698–2703.

Hunter N. and Kleckner N. (2001) The single-end invasion: an asymmetric intermediate at the double-strand break to double-Holliday junction transition of meiotic recombination, Cell 106: 59–70.

IARC (1986). Preamble. In: IARC monographs on the evaluation of the carcinogenic risk of chemicals to humans, Volume 39, Some chemicals used in plastics and elastomers. Lyon, France: International Agency for Research on Cancer 13-32.

IARC (1999). Hexachlorobutadiene. In: IARC monographs on the evaluation of carcinogenic risks to humans, Volume 73, Some chemicals that cause tumours of the kidney or urinary bladder in rodents and some other substances. Lyon, France: International Agency for Research on Cancer 277-294

Illingworth, R., Kerr, A., DeSousa, D., Jørgensen, H., Ellis, P., Stalker, J., Jackson, D., Clee,C., Plumb, R., and Rogers, J. (2008). A novel CpG island set identifies tissue-specific methylation at developmental gene loci. PLoS biology *6*, e22.

Inche, A.G., and La Thangue, N.B. (2006). Keynote review: Chromatin control and cancer-drug discovery: realizing the promise. Drug discovery today *11*, 97-109.

Inoue, S., Mai, A., Dyer, M.J., and Cohen, G.M. (2006). Inhibition of histone deacetylase class I but not class II is critical for the sensitization of leukemic cells to tumor necrosis factor–related apoptosis-inducing ligand–induced apoptosis. Cancer Research *66*, 6785-6792.

Issa, J. (2000). CpG-island methylation in aging and cancer. Current topics in microbiology and immunology *249*, 101.

Jaenisch, R., and Bird, A. (2003). Epigenetic regulation of gene expression: how the genome integrates intrinsic and environmental signals. Nature genetics *33*, 245-254.

Jang, J.-S., Lee, S.J., Choi, J.E., Cha, S.I., Lee, E.B., Park, T.I., Kim, C.H., Lee, W.K., Kam, S., and Choi, J.-Y. (2005). Methyl-CpG binding domain 1 gene

polymorphisms and risk of primary lung cancer. Cancer Epidemiology Biomarkers & Prevention *14*, 2474-2480.

Jones, P.A., and Baylin, S.B. (2002). The fundamental role of epigenetic events in cancer. Nature reviews genetics *3*, 415-428.

Jones, P.A., and Baylin, S.B. (2007). The epigenomics of cancer. Cell *128*, 683-692.

Jungbluth AA, Chen YT, Stockert E, Busam KJ, Kolb D, Iversen K, Coplan K, Williamson B, Altorki N, Old LJ. (2001) Immunohistochemical analysis of NY-ESO-1 antigen expression in normal and malignant human tissues. *Int J Cancer*, 92:856-860.

Kanai, Y., Ushijima, S., Nakanishi, Y., Sakamoto, M., and Hirohashi, S. (2003). Mutation of the DNA methyltransferase (DNMT) 1 gene in human colorectal cancers. Cancer letters *192*, 75-82.

Kanwal, R., & Gupta, S. (2012). Epigenetic modifications in cancer. *Clinical Genetics*, *81*(4), 303–311.

Karlic R, Chung HR, Lasserre J, Vlahovicek K, Vingron M (2010) Histone modification levels are predictive for gene expression. Proc Natl Acad Sci U S A. ;107:2926–2931.

Keeney S and Kleckner N. (1995) covalent protein-DNA complexes at the 5' strand termini of meiosis-specific double-strand breaks in yeast. Proc Natl Acad Sci USA. ;92:11274–11278.

Keeney S. (2001) Mechanism and control of meiotic recombination initiation, Curr. Top Dev. Biol. 52:1–53.

Keeney, S. (2008). Spo11 and the Formation of DNA Double-Strand Breaks in Meiosis. *Genome Dynamics and Stability*, *2*, 81–123.

Keeney, S., Lange, J., & Mohibullah, N. (2014). Self-Organization of Meiotic Recombination Initiation: General Principles and Molecular Pathways. *Annual Review of Genetics*, *48*, 187–214.

Kelley D and Rinn J. (2012) Transposable elements reveal a stem cell-specific class of long noncoding RNAs. Genome Biol.; 13:R107.

Kent, W.J. (2002) BLAT- the BLAST-Like Alignment Tool. *Genome Res*., 12: 656-664.

Kerr, N., Pintzas, A., Holmes, F., Hobson, S.-A., Pope, R., Wallace, M., … Wynick, D. (2010). The expression of ELK transcription factors in adult DRG: novel

isoforms, antisense transcripts and upregulation by nerve damage.*Molecular and Cellular Neurosciences*, *44*(2), 165–177.

Kim, B.-D. (2014). Foldback Intercoil DNA and the Mechanism of DNA Transposition. *Genomics & Informatics*, *12*(3), 80–86.

Klapholz S., Waddell CS., Esposito RE (1985). The role of the *SPO11*gene in meiotic recombination in yeast. Genetics; 110:187-216.

Klein F, Mahr P, Galova M, Buonomo S B C, Michaelis C, Nairz K, Nasmyth K. (1999) A central role for cohesins in sister chromatid cohesin, formation of axial elements, and recombination during yeast meiosis. Cell.;98:91–103.

Kouzarides, T. (2007). Chromatin modifications and their function. Cell *128*, 693-705.

Kulkarni, P., Shiraishi, T., Rajagopalan, K., Kim, R., Mooney, S. M., & Getzenberg, R. H. (2012). Cancer/testis antigens and urological malignancies. *Nature Reviews. Urology*, *9*(7), 386–396.

Kuntz S., Kieffer E., Bianchetti L., Lamoureux N., Fuhrmann G., Viville S.(2008).Te x19, a mammalian-specific protein with a restricted expression in pluripotent stem cells and germ line. Stem Cells 26, 734–744.

Lai AY, Wade PA. (2011) Cancer biology and NuRD: a multifaceted chromatin remodelling complex. Nat Rev Cancer;11:588–596.

Lamarche, B. J., Orazio, N. I., & Weitzman, M. D. (2010). The MRN complex in Double-Strand Break Repair and Telomere Maintenance. *FEBS Letters*,*584*(17), 3682–3695.

Lan, F., Nottke, A.C., and Shi, Y. (2008). Mechanisms involved in the regulation of histone lysine demethylases. Current opinion in cell biology *20*, 316-325.

Lander ES, Linton LM, Birren B, Nusbaum C, Zody MC, Baldwin J, et al. (2001) Initial sequencing and analysis of the human genome. Nature;409:860-921.

Lee, S.J., Jeon, H.-S., Jang, J.-S., Park, S.H., Lee, G.Y., Lee, B.-H., Kim, C.H., Kang, Y.M., Lee, W.K., and Kam, S. (2005). DNMT3B polymorphisms and risk of primary lung cancer. Carcinogenesis *26*, 403-409.

Lethe B, Lucas S, Michaux L, de Smet C, Godelaine D, Serrano A, de Plaen E, Boon T. (1998). LAGE-1, a new gene with tumor specificity. Int J Cancer 76:903–908.

Li R, Yerganian G, Duesberg P, Kraemer A, Willer A, Rausch C, Hehlmann R. (1997) Aneuploidy correlated 100% with chemical transformation of Chinese hamster cells. Proc Natl Acad Sci USA. 94: 14506-11.

Li, E., Bestor, T.H., and Jaenisch, R. (1992). Targeted mutation of the DNA methyltransferase gene results in embryonic lethality. Cell *69*, 915-926.

Li, R., Li, Y., Kristiansen, K. and Wang, J. (2008) SOAP: Short oligonucleotide alignment program. *Bioinformatics*, 24: 713-714.

Li, S.Y., Rong, M., and Iacopetta, B. (2006). Germ-line variants in methyl-group metabolism genes and susceptibility to DNA methylation in human breast cancer. Oncology reports *15*, 221-225.

Liang, J., Prouty, L., Williams, B.J., Dayton, M.A., and Blanchard, K.L. (1998). Acute mixed lineage leukemia with an inv (8)(p11q13) resulting in fusion of the genes for MOZ and TIF2. Blood *92*, 2118-2122.

Lim JH, Kim SP, Gabrielson E Park YB, Park JW, Kwon TK. (2005) Activation of human cancer/testis antigen gene, XAGE-1, in tumor cells is correlated with CpG island hypomethylation. Int J Cancer; 2:200–206.

Lin MC, Huang MJ, Liu CH, Yang TL, Huang MC (2014). GALNT2 enhances migration and invasion of oral squamous cell carcinoma by regulating EGFR glycosylation and activity. Oral Oncol;50:478–484.

Lin, R.J., Sternsdorf, T., Tini, M., and Evans, R.M. (2001). Transcriptional regulation in acute promyelocytic leukemia. Oncogene *20*, 7204-7215.

Litvinov IV, Cordeiro B, Huang Y, Zargham H, Pehr K, Dore MA, Gilbert M, Zhou Y, Kupper TS, Sasseville D (2014) Ectopic expression of cancer-testis antigens in cutaneous T-cell lymphoma patients. Clin Cancer Res;20:3799–3808.

Liu M, Shi X, Bi Y, Qi L, Guo X (2014) SHCBP1L, a conserved protein in mammals, is predominantly expressed in male germ cells and maintains spindle stability during meiosis in testis. *Mol Hum Reprod*; 20: 463-75.

Loidl J (1990) The initiation of meiotic chromosome pairing: the cytological view. Genome 33, 759–778.

Longhese MP, Bonetti D, Guerini I, Manfrini N, Clerici M. (2009) DNA double-strand breaks in meiosis: checking their formation, processing and repair. DNA Repair (Amst); 8(9):1127–1138.

Lovell-Badge, R. (2001) The future for stem cell research. *Nature*: 41488- 41491.

Lucas S, de Smet C, Arden KC, Viars CS, Lethe B, Lurquin C, Boon T. (1998). Identification of a new MAGE gene with tumor-specific expression by representational difference analysis. Cancer Res 58: 743–752.

Luger K, Mäder AW, Richmond RK, Sargent DF, Richmond TJ. (1997) Crystal structure of the nucleosome core particle at 2.8A resolution. Nature; 389:251–260.

Magdinier, F., and Wolffe, A.P. (2001). Selective association of the methyl-CpG binding protein MBD2 with the silent p14/p16 locus in human neoplasia. Proceedings of the National Academy of Sciences *98*, 4990-4995.

Mahadevaiah SK, Turner JM, Baudat F, Rogakou EP, de Boer P, Blanco-Rodriguez J, Jasin M, Keeney S, Bonner WM, Burgoyne PS (2001). Recombinational DNA double-strand breaks in mice precede synapsis. Nat Genet; 27:271-6.

Maherali, N., Sridharan, R., Xie, W., Utikal, J., Eminli, S., Arnold, K., ... & Plath, K. (2007). Directly reprogrammed fibroblasts show global epigenetic remodeling and widespread tissue contribution. *Cell stem cell*, *1*(1), 55-70.

Malle E, Sodin-Semrl S, Kovacevic A (2009). Serum amyloid A: an acute-phase protein involved in tumour pathogenesis. Cellular and Molecular Life Sciences;66(1):9–26.

Manning AT, Garvin JT, Shahbazi RI, Miller N, McNeill RE, Kerin MJ. (2007) Molecular profiling techniques and bioinformatics in cancer research. *Eur J Surg Oncol*.; 33: 255 – 265.

Mardis, E. (2008) The impact of next generation sequencing technology on genetics. *Trends Genet*. 24: 133-141.

Marguerat, S., Wilhelm, T. and Bahler, J. (2008) ® Next-generation sequencing: Applications beyond genomes. *Biochem. Soc. Trans*, 36: 1091- 1096.

Margueron R, Trojer P, Reinberg D (2005). The key to development: Interpreting the histone code? Curr Opin Genet Dev; 15:163-76.

Mariano, E. D., Teixeira, M. J., Marie, S. K. N., & Lepski, G. (2015). Adult stem cells in neural repair: Current options, limitations and perspectives. *World Journal of Stem Cells*, *7*(2), 477–482.

Marín, I. (2012). Origin and Diversification of TRIM Ubiquitin Ligases. *PLoS ONE*, *7*(11), e50030.

Matzuk, M. M., McKeown, M. R., Filippakopoulos, P., Li, Q., Ma, L., Agno, J. E., Bradner, J. E. (2012). Small-Molecule Inhibition of BRDT for Male Contraception. *Cell*, *150*(4), 673–684.

McClintock B. CB (1950) The origin and behavior of mutable loci in maize. Proc Natl Acad Sci U S A;36:344-355.

McFarlane Ramsay J, Feichtinger Julia , Larcombe Lee (2015) Germline/meiotic genes in cancer: new dimensions. Cell Cycle Vol. 14, Iss. 6.

McKim K.S. and Hayashi-Hagihara A. (1998) mei-W68 in *Drosophila melanogaster* encodes a Spo11 homolog: evidence that the mechanism for initiating meiotic recombination is conserved, Genes Dev. 12:2932–2942.

Mellman, I., Coukos, G., & Dranoff, G. (2011). Cancer immunotherapy comes of age. *Nature*, *480*(7378), 480.

Miremadi, A., Oestergaard, M.Z., Pharoah, P.D., and Caldas, C. (2007). Cancer genetics of epigenetic genes. Human molecular genetics *16*, R28-R49.

Mital P, Hinton BT, Dufour JM (2011) The blood-testis and blood-epididymis barriers are more than just their tight junctions. *Biol Reprod* ; 84:851–858.

Monte M, Simonatto M, Peche LY Bublik DR, Gobessi S, Pierotti MA, Rodolfo M, Schneider C. (2006) MAGE-A tumor antigens target p53 transactivation function through histone deacetylase recruitment and confer resistance to chemotherapeutic agents. Proc Natl Acad Sci U S A; 103: 11160–5.

Morin, R., Bainbridge, M., Fejes, A., Hirst, M., Krzywinski, M., Pugh, T., McDonald, H., Varhol, R., Jones, S. and Marra, M. (2008) Pro- filing the Hela S3 transcriptome using randomly primed cDNA and massively parallel short-read sequencing. Biotechniques 45:81-94. Wang, Z., Gerstein, M., and Snyder, M. 2009. RNASeq: A revolutionary tool for transcriptomics. *Nat. Rev. Genet*., 10: 57-63.

Mottet, D., Bellahcène, A., Pirotte, S., Waltregny, D., Deroanne, C., Lamour, V., Lidereau, R., and Castronovo, V. (2007). Histone deacetylase 7 silencing alters endothelial cell migration, a key step in angiogenesis. Circulation research *101*, 1237-1246.

Mueller JL, Mahadevaiah SK, Park PJ, Warburton PE, Page DC, Turner JM. (2008) The mouse X chromosome is enriched for multicopy testis genes showing postmeiotic expression. Nat Genet; 40: 794–9.

Muldoon, L. L., Alvarez, J. I., Begley, D. J., Boado, R. J., del Zoppo, G. J., Doolittle, N. D., … Neuwelt, E. A. (2013). Immunologic privilege in the central nervous system and the blood–brain barrier. *Journal of Cerebral Blood Flow & Metabolism*, *33*(1), 13–21. doi:10.1038/jcbfm.2012.153

Müller, H., Fiegl, H., Goebel, G., Hubalek, M., Widschwendter, A., Müller-Holzner, E., Marth, C., and Widschwendter, M. (2003). MeCP2 and MBD2 expression

in human neoplastic and non-neoplastic breast tissue and its association with oestrogen receptor status. British journal of cancer *89*, 1934-1939.

Nagalakshmi, U., Waern, K. and Snyder, M. (2008) RNA-Seq: A Method for Comprehensive UNIT 4.11 Transcriptome Analysis. *Curr. Protoc. Mol. Biol*., 89: 4.11.1-4.11.13.

Nakagawachi, T., Soejima, H., Urano, T., Zhao, W., Higashimoto, K., Satoh, Y., Matsukura, S., Kudo, S., Kitajima, Y., and Harada, H. (2003). Silencing effect of CpG island hypermethylation and histone modifications on O6-methylguanine-DNA methyltransferase (MGMT) gene expression in human cancer. Oncogene *22*, 8835-8844.

Nettersheim, D., Arndt, I., Sharma, R., Riesenberg, S., Jostes, S., Schneider, S., ... & Schorle, H. (2016). The cancer/testis-antigen PRAME supports the pluripotency network and represses somatic and germ cell differentiation programs in seminomas. *British Journal of Cancer*.

Neuwelt EA, Bauer B, Fahlke C, Fricker G, Iadecola C, Janigro D, et al (2011). Engaging neuroscience to advance translational research in brain barrier biology. Nat Rev Neurosci;12:169–182.

Nguyen, C.T., Gonzales, F.A., and Jones, P.A. (2001). Altered chromatin structure associated with methylation-induced gene silencing in cancer cells: correlation of accessibility, methylation, MeCP2 binding and acetylation. Nucleic acids research *29*, 4598-4606.

Ohm, J.E., McGarvey, K.M., Yu, X., Cheng, L., Schuebel, K.E., Cope, L., Mohammad, H.P., Chen, W., Daniel, V.C., and Yu, W. (2007). A stem cell–like chromatin pattern may predispose tumor suppressor genes to DNA hypermethylation and heritable silencing. Nature genetics *39*, 237-242.

Okano, M., Bell, D.W., Haber, D.A., and Li, E. (1999). DNA methyltransferases Dnmt3a and Dnmt3b are essential for de novo methylation and mammalian development. Cell *99*, 247-257.

Okita, K., Ichisaka, T. and Yamanaka, S. (2007) Generation of germline-competent induced pluripotent stem cells. *Nature*, 448: 313–317.

Öllinger, R., Childs, A. J., Burgess, H. M., Speed, R. M., Lundegaard, P. R., Reynolds, N., … Adams, I. R. (2008). Deletion of the Pluripotency-Associated*Tex19.1* Gene Causes Activation of Endogenous Retroviruses and Defective Spermatogenesis in Mice. *PLoS Genetics*, *4*(9), e1000199.

Pace JK 2nd, Feschotte C (2007). The evolutionary history of human DNA transposons: evidence for intense activity in the primate lineage. Genome Res;17:422-432.

Panagopoulos, I., Fioretos, T., Isaksson, M., Samuelsson, U., Billström, R., Strömbeck, B., Mitelman, F., and Johansson, B. (2001). Fusion of the MORF and CBP genes in acute myeloid leukemia with the t (10; 16)(q22; p13). Human molecular genetics *10*, 395-404.

Pandolfi, P.P. (2001). Transcription therapy for cancer. Oncogene *20*, 3116-3127.

Pasierbek, P., Jantsch, M., Melcher, M., Schleiffer, A., Schweizer, D., and Loidl, J. (2001). A Caenorhabditis elegans cohesin protein with functions in meiotic chromosome pairing and disjunction. Genes Dev. *15*, 1349–1360.

Peikert T, Specks U, Farver C, Erzurum SC, Comhair SA. (2006) Melanoma antigen A4 is expressed in non-small cell lung cancers and promotes apoptosis. Cancer Res; 66: 4693–700.

Peters, A.H., O'Carroll, D., Scherthan, H., Mechtler, K., Sauer, S., Schöfer, C., Weipoltshammer, K., Pagani, M., Lachner, M., and Kohlmaier, A. (2001). Loss of the Suv39h histone methyltransferases impairs mammalian heterochromatin and genome stability. Cell *107*, 323-337.

Peterson CL and Cote J. (2004) Cellular machineries for chromosomal *DNA* repair. Genes Dev; 18:602-16.

Petrovic, N. (2016). Targeting Angiogenesis in Cancer Treatments: Where do we Stand?. *Journal of Pharmacy & Pharmaceutical Sciences*, *19*(2), 226-238.

Pezzi N, Prieto I, Kremer L, Perez Jurado L A, Valero C, Del Mazo J, Martinez A C, Barbero J L. (2000) STAG3, a novel gene encoding a protein involved in meiotic chromosome pairing and location of STAG3-related genes flanking the Williams-Beuren syndrome deletion. FASEB J.;14:581–592.

Pitot HC. (2002) Fundamentals of Oncology; 4th ed. New York: Marcel Dekker, Inc.

Pleasure, S.J., Page, C. and Lee, V.M-Y. (1992) Pure, post-mitotic, polarized human neurons derived from Ntera2 cells provide a system for expressing exogenous proteins in terminally differentiated neurons. *J. Neurosci*., **12**: 1802–1815.

Pokrovskaya, I. D., Willett, R., Smith, R. D., Morelle, W., Kudlyk, T., & Lupashin, V. V. (2011). Conserved oligomeric Golgi complex specifically regulates the maintenance of Golgi glycosylation machinery. *Glycobiology*,*21*(12), 1554–1569.

Popp, C., Dean, W., Feng, S., Cokus, S.J., Andrews, S., Pellegrini, M., Jacobsen, S.E. and Reik, W. (2010) Genome-wide erasure of DNA methylation in mouse primordial germ cells is affected by AID deficiency. *Nature*, **463**: 1101-1105.

Pradhan S, Kim JK, Samaranayake M. (2009) Epigenetic mechanisms in mammals. Cell Mol Life Sci. ;66:596–612

Prieto, I., Suja, J.A., Pezzi, N., Kremer, L.,Martinez, A.C., Rufas, J.S. and Barbero, J.L. (2001). Mammalian STAG3 is a cohesin specific to sister chromatid arms in meiosis I. Nat. Cell Biol. *3*, 761–766.

Prowse, A.B., McQuade, L.R., Bryant, K.J., Marcal, H. and Gray, P.P. (2007) Identification of potential pluripotency determinants for human embryonic stem cells following proteomic analysis of human and mouse fibroblast conditioned media. *J. Proteome Res.*, **6**: 3796–3807.

Ramesh, T., Lee, S.-H., Lee, C.-S., Kwon, Y.-W., & Cho, H.-J. (2009). Somatic Cell Dedifferentiation/Reprogramming for Regenerative Medicine. *International Journal of Stem Cells*, *2*(1), 18–27.

Rasti, M., Grand, R.J., Mymryk, J.S., Gallimore, P.H., and Turnell, A.S. (2005). Recruitment of CBP/p300, TATA-binding protein, and S8 to distinct regions at the N terminus of adenovirus E1A. Journal of virology *79*, 5594-5605.

Ray, D.A., Feschotte, C., Pagan, H.J., Smith, J.D., Pritham, E.J., Arensburger, P., Atkinson, P.W. and Craig, N.L. (2008) Multiple waves of recent DNA transposon activity in the bat, *Myotis lucifugus*. *Genome Res*., **18**: 717–728.

Reichmann, J., Reddington, J. P., Best, D., Read, D., Öllinger, R., Meehan, R. R., & Adams, I. R. (2013). The genome-defence gene *Tex19.1* suppresses *LINE-1* retrotransposons in the placenta and prevents intra-uterine growth retardation in mice. *Human Molecular Genetics*, *22*(9), 1791–1806.

Rendt, J., Erulkar, S. and Andrews, P.W. (1989) Presumptive neurons derived by differentiation of a human embryonal carcinoma cell line exhibit tetrodotoxin-sensitive sodium currents and the capacity for regenerative responses. *Exp. Cell Res*., **180**: 580–584.

Revenkova, E., Eijpe, M., Heyting, C., Gross, B., and Jessberger, R. (2001). Novel meiosis-specific isoform of mammalian SMC1. Mol. Cell. Biol. *21*, 6984–6998.

Robert, M.-F., Morin, S., Beaulieu, N., Gauthier, F., Chute, I.C., Barsalou, A., and MacLeod, A.R. (2003). DNMT1 is required to maintain CpG methylation and aberrant gene silencing in human cancer cells. Nature genetics *33*, 61-65.

Robertson KD. (2005) DNA methylation and human disease. Nat Rev Genet. ;6:597–610

Rodriguez-Paredes M, Esteller M. (2011) Cancer epigenetics reaches mainstream oncology. Nat Med;17:330–339.

Román-Gómez, J., Cordeu, L., Agirre, X., Jiménez-Velasco, A., San José-Eneriz, E., Garate, L., Calasanz, M. J., Heiniger, A., Torres, A., & Prosper, F. (2007). Epigenetic regulation of Wnt-signaling pathway in acute lymphoblastic leukemia. Blood, 109(8), 3462-3469.

Romanienko PJ, Camerini-Otero RD. (1999) Cloning, characterization, and localization of mouse and human SPO11. *Genomics*, 61:156-169.

Romanienko PJ, Camerini-Otero RD. (2000) The mouse *Spo11* gene is required for meiotic chromosome synapsis. Mol Cell; 6:975-987.

Ross MT, Grafham DV, Coffey AJ, Scherer S, McLay K, Muzny D, Platzer M, Howell GR, Burrows C, Bird CP (2005). The DNA sequence of the human X chromosome. Nature;434:325–337.

SanMiguel P, Tikhonov A, Jin YK, Motchoulskaia N, Zakharov D, Melake-Berhan A, et al. (1996) Nested retrotransposons in the intergenic regions of the maize genome. Science;274:765- 768.

Sansom, O.J., Berger, J., Bishop, S.M., Hendrich, B., Bird, A., and Clarke, A.R. (2003). Deficiency of Mbd2 suppresses intestinal tumorigenesis. Nature genetics *34*, 145-147.

Sati L, Zeiss C, Yekkala K, Demir R, McGrath J (2015) Expression of the CTCFL Gene during Mouse Embryogenesis Causes Growth Retardation, P ostnatal Lethalityand Dysregulation of the TGFB Pathway. Mol Cell Biol.. pii: MCB.00381-15

Scanlan MJ, Altorki NK, Gure AO, Williamson B, Jungbluth A, Chen YT, Old LJ. 2000. Expression of cancer-testis antigens in lung cancer: Definition of bromodomain testis-specific gene (BRDT) as a new CT gene, CT9. Cancer Lett 150:155–164.

Scanlan MJ, Simpson AJ, Old LJ. (2004) The cancer/testis genes: Review, standardization and commentary. Cancer Immunity; 4:1–15.

Schlesinger, Y., Straussman, R., Keshet, I., Farkash, S., Hecht, M., Zimmerman, J., Eden, E., Yakhini, Z., Ben-Shushan, E., and Reubinoff, B.E. (2007). Polycomb-mediated methylation on Lys27 of histone H3 pre-marks genes for de novo methylation in cancer. Nature genetics *39*, 232-236.

Scott, S. P., & Pandita, T. K. (2006). The Cellular Control of DNA Double-Strand Breaks. *Journal of Cellular Biochemistry*, *99*(6), 1463–1475.

Ségurel, L. (2013). The complex binding of PRDM9. *Genome Biology*, *14*(4), 112.

Seligson, D.B., Horvath, S., Shi, T., Yu, H., Tze, S., Grunstein, M., and Kurdistani, S.K. (2005). Global histone modification patterns predict risk of prostate cancer recurrence. Nature *435*, 1262-1266.

Seoane J, De Mattos-Arruda L (2014) The challenge of intratumour heterogeneity in precision medicine. J Intern Med. 276: 41–51.

Shah, M., & Allegrucci, C. (2013). Stem cell plasticity in development and cancer: epigenetic origin of cancer stem cells. In *Epigenetics: Development and Disease* (pp. 545-565). Springer Netherlands.

Shaikhibrahim Z, Braun M, Nikolov P, Boehm D, Scheble V, Menon R, Fend F, Kristiansen G, Perner S, Wernert N. (2012) Rearrangement of the ETS genes ETV-1, ETV-4, ETV-5, and ELK-4 is a clonal event during prostate cancer progression. Human pathology; 43:1910–1916.

Shamblott, M.J., Axelman, J., Wang, S. (1998) Derivation of pluripotent stem cells from cultured human primordial germ cells. *Proc Natl Acad Sci USA,* **95**:13726–13731.

Shankaran V., H. Ikeda, A.T. Bruce, J.M. White, P.E. Swanson, L.J. Old, R.D. Schreiber (2001)IFNγ and lymphocytes prevent primary tumour development and shape tumour immunogenicity. Nature, 410, pp. 1107–1111

Sharif WD, Glick GG, Davidson MK, *et al*. (2002) Distinct functions of *S. pombe* Rec12 (Spo11) protein and Rec12-dependent crossover recombination (chiasmata) in meiosis I; and a requirement for Rec12 in meiosis II. Cell Chromosome; 1:1.

Sharma, S., Kelly, T.K., and Jones, P.A. (2010). Epigenetics in cancer. Carcinogenesis *31*, 27-36.

Sharpe, M., and Mount, N. (2015). Genetically modified T cells in cancer therapy: opportunities and challenges. *Disease Models & Mechanisms*, *8*(4), 337–350.

Shen, H., Wang, L., Spitz, M.R., Hong, W.K., Mao, L., and Wei, Q. (2002). A novel polymorphism in human cytosine DNA-methyltransferase-3B promoter is associated with an increased risk of lung cancer. Cancer research *62*, 4992-4995.

Sigalotti, L., Fratta, E., Coral, S., Tanzarella, S., Danielli, R., Colizzi, F., Fonsatti, E., Traversari, C., Altomonte, M. and Maio, M. (2004) Intratumor heterogeneity of cancer/testis antigens expression in human cutaneous melanoma is methylation-regulated and functionally reverted by 5-aza-2'-deoxycytidine. *Cancer Res*, **64**: 9167-9171.

Simpson AJ, Caballero OL, Jungbluth A, Chen YT, Old LJ, (2005) Cancer/testis antigens, gametogenesis and cancer. Nat Rev Cancer; 5: 615–25.

Sincic N and Herceg Z. (2011) DNA methylation and cancer: ghosts and angels above the genes. Curr Opin Oncol.;23:69–76.

Smagulova, F., Brick, K., Pu, Y., Sengupta, U., Camerini-Otero, R. D., & Petukhova, G. V. (2013). Suppression of genetic recombination in the pseudoautosomal region and at subtelomeres in mice with a hypomorphic*Spo11* allele. *BMC Genomics*, *14*, 493.

Soejima, K., Fang, W., and Rollins, B.J. (2003). DNA methyltransferase 3b contributes to oncogenic transformation induced by SV40T antigen and activated Ras. Oncogene *22*, 4723-4733.

Song, J., Noh, J.H., Lee, J.H., Eun, J.W., Ahn, Y.M., Kim, S.Y., Lee, S.H., Park, W.S., Yoo, N.J., and Lee, J.Y. (2005). Increased expression of histone deacetylase 2 is found in human gastric cancer. Apmis *113*, 264-268.

Spike, C. A., Coetzee, D., Eichten, C., Wang, X., Hansen, D., & Greenstein, D. (2014). The TRIM-NHL Protein LIN-41 and the OMA RNA-Binding Proteins Antagonistically Control the Prophase-to-Metaphase Transition and Growth of*Caenorhabditis elegans* Oocytes. *Genetics*, *198*(4), 1535–1558.

Spradling, A., Drummond-Barbosa, D., Kai, T. (2001) Stem cells find their niche. *Nature.* **2001**: 41498- 41504.

Squires, P.E., Wakeman, J.A., Chapman, H., Kumpf, S., Fidock, M.D., Andrews, P.W. and Dunne, M.J. (1996) Regulation of intracellular Ca^{2+} in response to muscarinic and glutamate receptor agonists during the differentiation of NTERA2 human embryonal carcinoma cells into neurons. *Eur. J. Neurosci.*, **8**: 783–793.

Surani, M.A. (2001) Reprogramming of genome function through epigenetic inheritance. *Nature*, inheritance. *Nature.* **2001**: 414122- 414128.

Suzuki, M.M., and Bird, A. (2008). DNA methylation landscapes: provocative insights from epigenomics. Nature Reviews Genetics *9*, 465-476.

Takahashi, K., Yamanaka, S. (2006) Induction of pluripotent stem cells from mouse embryonic and adult fibroblast cultures by defined factors. *Cell*, **126**: 663–676.

Takai, D., and Jones, P.A. (2003). The CpG island searcher: a new WWW resource. In silico biology *3*, 235-240.

Tani, S., Blyth, B. J., Shang, Y., Morioka, T., Kakinuma, S., & Shimada, Y. (2016). A Multi-stage Carcinogenesis Model to Investigate Caloric Restriction as a Potential Tool for Post-irradiation Mitigation of Cancer Risk. *Journal of Cancer Prevention*, *21*(2), 115–120.

Tarabay, Y. Kieffer E, Teletin M, Celebi C, Van Montfoort A, Zamudio N, Achour M, El Ramy R, Gazdag E, Tropel P, Mark M, Bourc'his D, Viville S. (2013) The mammalian-specific Tex19.1 gene plays an essential role in spermatogenesis and placenta-supported development. *Hum. Reprod.* 28, 2201–2214.

Tay, S. K. (2012). Cervical cancer in the human papillomavirus vaccination era. *Current Opinion in Obstetrics and Gynecology* 24 (1): 3–7.

Theodoraki, M. N., Lorenz, K. J., Schneider, J., Thierauf, J. C., Spagnoli, G., Schuler, P. J., & Laban, S. (2016). Influence of Photodynamic Therapy on the Expression of Cancer/Testis Antigens in Squamous Cell Carcinoma of the Head and Neck. *Anticancer Research*,*36*(8), 3973-3982.

Thomson, J.A., Itskovitz-Eldor, J., Shapiro, S.S. et al. Embryonic stem cell lines derived from human blastocysts. *Science* 1998;**282**:1145–1147.

Tsuchihara, K., Suzuki, Y., Wakaguri, H., Irie, T., Tanimoto, K., Hashimoto, S.I., Matsushima, K., Sugano, J.M., Yamashita, R., Nakai, K., Bentley, D., Esumi, H. and Sugano, S. (2009) Massive transcriptional start site analysis of human genes in hypoxia cells. *Nucleic Acid Res.*, **37**: 2249- 2263.

Tuch, B.E. (2006). Stem cells—a clinical update. *Australian Family Physician*, **35**: 719–721.

Tureci O, Sahin U, Zwick C, Koslowski M, Seitz G, Pfreundschuh M. (1998). Identification of a meiosis-specific protein as a member of the class of cancer/testis antigens. Proc Natl Acad Sci USA 95:5211–5216.

Tuscano JM., Kato J, Pearson D, Xiong C, Newell L, Ma Y, Gandara DR, O'Donnell RT. (2012) CD22 antigen is broadly expressed on lung cancer cells and is a target for antibody-based therapy. Cancer Res; 72:5556-65.

Uroz L, Templado C (2012) Meiotic non-disjunction mechanisms in human fertile males. Hum. Reprod;27:1518–1524.

Van der Bruggen P, Traversari C, Chomez P et al. (1991) A gene encoding an antigen recognized by cytolytic T lymphocytes on a human melanoma. Science;254: 1643–7.

Van Gent DC, Hoeijmakers JH, Kanaar R. (2001) Chromosomal stability and the DNA double-stranded break connection. Nat Rev Genet 2: 196–206.

Vlasova MA and Moshkovskii SA (2006). Molecular interactions of acute phase serum amyloid A: possible involvement in carcinogenesis. Biochemistry;71(10):1051–1059.

Walker MY. and Hawley RS. (2000) Hanging on to your homolog: the roles of pairing, synapsis and recombination in the maintenance of homolog adhesion. Chromosoma; 109:3-9.

Wang, G.G., Allis, C.D., and Chi, P. (2007). Chromatin remodeling and cancer, Part I: Covalent histone modifications. Trends in molecular medicine *13*, 363-372.

Wang, M., Li, J., Wang, L., Chen, X., Zhang, Z., Yue, D., Zhang, Y. (2015). Combined cancer testis antigens enhanced prediction accuracy for prognosis of patients with hepatocellular carcinoma. *International Journal of Clinical and Experimental Pathology*, *8*(4), 3513–3528.

Wang, Z., Gerstein, M., and Snyder, M. (2009) RNASeq: A revolutionary tool for transcriptomics. *Nat. Rev. Genet*., **10**: 57-63.

Wang, Z., Zhang, J., Zhang, Y. and Lim, S.H. (2006) SPAN-Xb expression in myeloma cells is dependent on promoter hypomethylation and can be upregulated pharmacologically. *Int J Cancer*, **118**: 1436-1444.

Wang, P.J., McCarrey, J.R., Yang, F., and Page, D.C. (2001) An abundance of X-linked genes expressed in spermatogonia. *Nat Genet*, **27**: 422-426.

Watanabe, Y. and Nurse, P. (1999). Cohesin Rec8 is required for reductional chromosome segregation at meiosis. Nature *400*, 461–464.

Waterhouse P, Penninger JM, Timms E, Wakeham A, Shahinian A, Lee KP, Thompson CB, Griesser H, Mak TW (1995). Lymphoproliferative disorders with early lethality in mice deficient in Ctla-4. Science.;270:985–988.

Weichert, W., Röske, A., Niesporek, S., Noske, A., Buckendahl, A.-C., Dietel, M., Gekeler,V., Boehm, M., Beckers, T., and Denkert, C. (2008). Class I histone deacetylase expression has independent prognostic impact in human colorectal cancer: specific role of class I histone deacetylases in vitro and in vivo. Clinical Cancer Research *14*, 1669-1677.

Wernig, M., Meissner, A. and Foreman, R. (2007) In vitro reprogramming of fibroblasts into a pluripotent ES-cell-like state. *Nature*, 448:318–324

Whitehurst AW (2014) Cause and consequence of cancer/testis antigen activation in cancer. Annu Rev Pharmacol Toxicol 54:251–72.10.1146/annurev-pharmtox-011112-140326

Widschwendter, M., Fiegl, H., Egle, D., Mueller-Holzner, E., Spizzo, G., Marth, C., Weisenberger, D.J., Campan, M., Young, J., and Jacobs, I. (2007). Epigenetic stem cell signature in cancer. Nature genetics *39*, 157-158.

Wilson, A.J., Byun, D.-S., Nasser, S., Murray, L.B., Ayyanar, K., Arango, D., Figueroa, M., Melnick, A., Kao, G.D., and Augenlicht, L.H. (2008). HDAC4 promotes growth of colon cancer cells via repression of p21. Molecular biology of the cell *19*, 4062-4075.

Wilson, A.J., Byun, D.-S., Popova, N., Murray, L.B., L'Italien, K., Sowa, Y., Arango, D., Velcich, A., Augenlicht, L.H., and Mariadason, J.M. (2006). Histone deacetylase 3 (HDAC3) and other class I HDACs regulate colon cell maturation and p21 expression and are deregulated in human colon cancer. Journal of Biological Chemistry *281*, 13548-13558.

Winkler, E. A., Bell, R. D., & Zlokovic, B. V. (2011). Central nervous system pericytes in health and disease. *Nature Neuroscience*, *14*(11), 1398–1405.

Winters, T., McNicoll, F., & Jessberger, R. (2014). Meiotic cohesin STAG3 is required for chromosome axis formation and sister chromatid cohesion. *The EMBO Journal*, *33*(11), 1256–1270.

Witt, O., Deubzer, H.E., Milde, T., and Oehme, I. (2009). HDAC family: What are the cancer relevant targets? Cancer letters *277*, 8-21.

Wu SC, Zhang Y. (2010) Active DNA demethylation: many roads lead to Rome. Nat Rev Mol Cell Biol.;11:607–620.

Wu YM, Liu CH, Hu RH, Huang MJ, Lee JJ, Chen CH, Huang J, Lai HS, Lee PH, Hsu WM, Huang HC, Huang MC (2011) Mucin glycosylating enzyme

GALNT2 regulates the malignant character of hepatocellular carcinoma by modifying the EGF receptor. Cancer research. 71:7270–7279.

Xu, G.-L., Bestor, T.H., Bourc'his, D., Hsieh, C.-L., Tommerup, N., Bugge, M., Hulten, M., Qu, X., Russo, J.J., and Viegas-Péquignot, E. (1999). Chromosome instability and immunodeficiency syndrome caused by mutations in a DNA methyltransferase gene. Nature *402*, 187-191.

Xu, Y., Deng, Y., Ji, Z., Liu, H., Liu, Y., Peng, H. … Fan, J. (2014). Identification of Thyroid Carcinoma Related Genes with mRMR and Shortest Path Approaches. *PLoS ONE*, *9*(4), e94022. doi:10.1371/journal.pone.0094022

Yamanaka, S. (2007) Strategies and new developments in the generation of patient-specific pluripotent stem cells. *Cell Stem Cell*, **1**: 39–49.

Yamane, K., Toumazou, C., Tsukada, Y.-i., Erdjument-Bromage, H., Tempst, P., Wong, J., and Zhang, Y. (2006). JHDM2A, a JmjC-containing H3K9 demethylase, facilitates transcription activation by androgen receptor. Cell *125*, 483-495.

Yamashita K, Shinohara M, Shinohara A. (2004) Rad6-Bre1-mediated histone H2B ubiquitylation modulates the formation of double-strand breaks during meiosis. Proc Natl Acad Sci USA; 101:11380-5.

Yan, L., Guo, W., Wu, S., Liu, J., Zhang, S., Shi, L. Gu, A. (2014). Genetic Variants in Nitric Oxide Synthase Genes and the Risk of Male Infertility in a Chinese Population: A Case-Control Study. *PLoS ONE*, *9*(12), e115190. doi:10.1371/journal.pone.0115190

Yang, P., Huo, Z., Liao, H., Zhou, Q. (2015) Cancer/testis antigens trigger epithelial-mesenchymal transition and genesis of cancer stem-like cells. *Curr Pharm Des*. **21**: 1292-300.

Ying L, Hofseth LJ (2007). An emerging role for endothelial nitric oxide synthase in chronic inflammation and cancer. Cancer Res, 67, 1407-10.

Yoder, J.A., Walsh, C.P., and Bestor, T.H. (1997). Cytosine methylation and the ecology of intragenomic parasites. Trends in genetics *13*, 335-340.

Yousef, S., Heise, J., Lajmi, N., Bartels, K., Kröger, N., Luetkens, T., & Atanackovic, D. (2015). Cancer-testis antigen SLLP1 represents a promising target for the immunotherapy of multiple myeloma. *Journal of translational medicine*, *13*(1), 197.

Yuasa T, Okamoto K, Kawakami T, Mishina M, Ogawa O, Okada Y. (2001) Expression patterns of cancer testis antigens in testicular germ cell tumours and adjacent testicular tissue. *J Urol*, 165:1790-1794.

Zelent, A. (1994). Translocation of the RARα locus to the PML or PLZF gene in acute promyelocytic leukaemia. British journal of haematology *86*, 451-460.

Zeng M., Lu Y., Liao X., Li D., Sun H., Liang S., Zhang S., Ma Y., Yang Z (2009)DAZL binds to 3'UTR of Tex19.1 mRNAs and regulates Tex19.1 expression. Mol. Biol.Rep;36:2399–2403.

Zhang, Q., Putheti, P., Zhou, Q., Liu, Q., & Gao, W. (2008). Structures and biological functions of IL-31 and IL-31 receptors. *Cytokine & Growth Factor Reviews*, *19*(5-6), 347–356.

Zhang, Z., Yamashita, H., Toyama, T., Sugiura, H., Ando, Y., Mita, K., Hamaguchi, M., Hara, Y.,Kobayashi, S., and Iwase, H. (2005). Quantitation of HDAC1 mRNA expression in invasive carcinoma of the breast*. Breast cancer research and treatment *94*, 11-16.

Zhang, Z., Yamashita, H., Toyama, T., Sugiura, H., Omoto, Y., Ando, Y., Mita, K., Hamaguchi, M., Hayashi, S.-i., and Iwase, H. (2004). HDAC6 expression is correlated with better survival in breast cancer. Clinical Cancer Research *10*, 6962-6968.

Zhao, M., Huang, J., Gui, K., Xiong, M., Cai, G., Xu, J., Wang, K., Liu, D., Zhang, X., Yin, W. (2014) The downregulation of miR-144 is associated with the growth and invasion of osteosarcoma cells through the regulation of TAGLN expression". International Journal of Molecular Medicine 34.6 :1565-1572.

Zhao, W., Ji, X., Zhang, F., Li, L. and Ma, L. (2012) Embryonic stem cell markers. *Molecules***,** 17: 6196-6236.

Zhou JX, Li Y, Chen SX, Deng AM. (2011) Expression and prognostic significance of cancer-testis antigens (CTA) in intrahepatic cholagiocarcinoma. J Exp Clin Cancer Res.6;30:2.

Zhu, P., Martin, E., Mengwasser, J., Schlag, P., Janssen, K.-P., and Göttlicher, M. (2004). Induction of HDAC2 expression upon loss of APC in colorectal tumorigenesis. Cancer cell *5*, 455-463.